https://doi.org/10.1070/RCR5025

Conjugated nitroxides

Evgeny V. Tretyakov,[a]* Victor I. Ovcharenko,[b] Alexander O. Terent'ev,[a] Igor B. Krylov,[a] Tatiana V. Magdesieva,[c] Dmitrii G. Mazhukin,[d] Nina P. Gritsan[e]

[a] *N.D.Zelinsky Institute of Organic Chemistry, Russian Academy of Sciences, Leninsky prosp. 47, 119991 Moscow, Russian Federation*
[b] *International Tomography Centre, Siberian Branch, Russian Academy of Sciences, ul. Institutskaya 3A, 630090 Novosibirsk, Russian Federation*
[c] *Department of Chemistry, Lomonosov Moscow State University, Leninskie Gory 1, stroenie 3 119991 Moscow, Russian Federation*
[d] *N.N.Vorozhtsov Novosibirsk Institute of Organic Chemistry, Siberian Branch of the Russian Academy of Sciences, prosp. Akademica Lavrentieva 9, 630090 Novosibirsk, Russian Federation*
[e] *V.V.Voevodsky Institute of Chemical Kinetics and Combustion, Siberian Branch of the Russian Academy of Sciences, ul. Institutskaya 3, 630090 Novosibirsk, Russian Federation*

In recent years, research dealing with organic paramagnetic compounds such as stable radicals and high-spin systems has been focused on applied aspects. Several key trends have formed in the application and, hence, in the function-oriented synthesis of organic radicals and polyradicals. This review addresses one of such trends in which the dominant role is played by so-called conjugated nitroxides. Their specific feature is the presence of any unsaturated moiety (C=C, C=N or C=O multiple bond; aromatic or heteroaromatic ring; fused polyaromatic system) adjacent to the nitroxide group. The achievements of the chemistry of conjugated nitroxides are presented, and their physicochemical properties, magneto-structural correlations and practical applications are discussed.
The bibliography includes 641 references.

Contents

1. Introduction 2
2. Acyclic nitroxides 3
2.1. Vinyl nitroxides 3
2.2. Aryl- and heteroaryl-substituted nitroxides 4
2.3. Carbonyl nitroxides 12
3. Cyclic nitroxides 15
3.1. Heterocyclic vinyl nitroxides with *endo*- and *exo*-methylene bonds 15
3.2. (Hetero)arene-annulated cyclic nitroxides 16
3.3. Hybrid phenoxyl nitroxides 19
3.4. Classical nitronyl nitroxide and imino nitroxides 21
3.5. Phthalimide-*N*-oxyl radicals 40
3.6. Pyrrole- and benzimidazole-based aromatic nitroxides 46
4. Quantum chemistry of nitroxide radicals and biradicals 47
4.1. Parameters of the EPR spectra of nitroxides 47
4.1.1. Alkyl aryl and diaryl nitroxides 47
4.1.2. Nitronyl nitroxide and imino nitroxides 48
4.2. Electronic absorption spectra of nitroxides 49
4.2.1. Electronic absorption spectra of aliphatic nitroxides 49
4.3. Vibrational spectra of nitroxides 51
4.4. Quantum chemical calculations of the properties of nitroxide bi- and triradicals 51
5. Potential of practical application of conjugated nitroxides 53
5.1. Redox switchable molecular systems based on unsaturated nitroxides 54
5.2. Complex formation of metal ions with conjugated nitroxides: an approach to the molecular design of magnets 57
5.3. Photoswitchable molecular systems based on nitroxides 62
5.4. Nitroxide radicals as ambipolar redox-active materials 63
6. Conclusion 66
7. List of acronyms and designations 67
8. References 67

Received 13 March 2021
© 2022 Uspekhi Khimii, ZIOC RAS, Russian Academy of Sciences and IOP Publishing Limited

1. Introduction

The vast majority of organic compounds created by nature and humans are diamagnetic. The molecules of such compounds have closed electron shell in the ground state and a large energy gap between this state and the nearest excited state.[1] Meanwhile, of different nature are organic molecules with one or more unpaired electrons (radicals and polyradicals) and those with the singlet ground state, but thermally populated high-spin excited state (biradicaloids). These molecules have a paramagnetic nature, which endows them with specific chemical and physicochemical properties.

The pioneer in the study of stable organic paramagnets was Mozes Gomberg,[2] who proved the formation of the triphenylmethyl radical in 1900. Since then, a multitude of organic radicals of various types have been synthesized and studied, including localized and delocalized (conjugated) radicals with either one or several unpaired electrons.[3] The progress of synthetic chemistry and investigations of stable organic radicals and elucidation of structure – property relationships culminated in the gradual formation of fundamental principles for the design of functional paramagnetic and high-spin systems. The application of these principles resulted in the synthesis of organic paramagnetic compounds with diverse functions, which served as reagents, efficient catalysts, tools for the control of chemical reactions, analytical and diagnostic means, building blocks for assembling magnetic and redox-active systems and as single-molecule actuators in electronic and spintronic devices. For example, organic radicals have been actively used as scavengers for radical intermediates,[4] redox catalysts[5,6] and for controlled radical polymerization.[7–9] Organic paramagnets have found use in magnetic resonance imaging,[10,11] molecular design of magnetic materials[12–17] and chemical biology and medicine;[18–22] they proved to be in demand for the fabrication of working parts of electric batteries[23,24] and molecular spintronic devices.[25,26]

Among organic radicals of each class, primary attention is always paid to their stable representatives. Paramagnetic molecules are stabilized by delocalization of spin density, introduction of heteroatoms into the paramagnetic moiety and/or the spatial shielding of paramagnetic centres. An additional kinetic stabilization of radicals can be attained by encapsulation of the radicals into hydrocarbon cages, dendrimers and hybrid structures. The best known examples of neutral and charged C-, N-, NO- and O-centred mono- and biradicals and structurally diverse organometallic derivatives that were isolated in a pure state (Structures **1** – **24**) are depicted in Fig. 1.[27–54]

The synthesis of stable representatives of some class of paramagnets has always been a common challenge for physicists and chemists, who could jointly tackle complicated problems in this field and attained practically significant results. The studies concerning nitroxides, including conjugated derivatives, have a long successful history. At the end of the 20th century, they reached the level of systematic research directed towards solution of fundamental problems of physics and chemistry, including the development of new materials and the synthesis of functional single molecules.[17,55] During 10 years after publication of a review[16] devoted to conjugated (or unsaturated) nitroxides, considerable progress has been made in this field. New approaches to estimation of the stability of nitroxide radicals were proposed;[56,57] known methods for the synthesis of stable conjugated nitroxides were optimized and new methods were developed; new structural classes of nitroxides were created; polyfluorinated substrates and stable and superstable high-spin paramagnets were obtained; multiple structure – property relationships were elucidated; a number of practical applications were proposed, using these species in various fields of chemistry, molecular design of magnets, physics of magnetism and spintronics.[58–62] This review analyzes the key achievements related to conjugated nitroxides, demonstrates the current trends in the development of this field and recently initiated points of growth and formulates relevant problems that are still to be solved. The material is arranged, as previously,[16] in the order from development of synthetic methods to chemical applications.

E.V.Tretyakov. Doctor of Chemical Sciences, Deputy Director for Science of ZIOC RAS.
E-mail: tretyakov@ioc.ac.ru
Current research interests: function-oriented synthesis, chemistry of heterocyclic compounds, including fluorinated derivatives; stable organic radicals, heterospin systems, molecular design of magnets.
V.I.Ovcharenko. Academician, Doctor of Chemical Sciences, Chief Researcher at ITC SB RAS.
E-mail: Victor.Ovcharenko@tomo.nsc.ru; ovcharenko@ioc.ac.ru
Current research interests: design of molecular magnets, stable organic radicals, chemistry of heterospin compounds.
A.O.Terent'ev. Corresponding Member of the RAS, Doctor of Chemical Sciences, Professor, Head of Laboratory and Deputy Director for Science of ZIOC RAS.
E-mail: terentev@ioc.ac.ru
Current research interests: organic chemistry, medicinal chemistry, agrochemistry, chemical engineering, manufacture of biologically active compounds and composite materials.
I.B.Krylov. Candidate of Chemical Sciences, Senior Researcher at ZIOC RAS.
E-mail: krylovigor@yandex.ru
Current research interests: organic synthesis methodology, chemistry of organic peroxides, medicinal chemistry, free radical organic chemistry, photochemistry, electrochemistry, chemical crop protection
T.V.Magdesieva. Doctor of Chemical Sciences, Professor at the Faculty of Chemistry of MSU.
E-mail: tvm@org.chem.msu.ru
Current research interests: molecular electrochemistry, ambipolar redox-active compounds; stable organic radicals; electron transfer-activated reactions.
D.G.Mazhukin. Candidate of Chemical Sciences, Senior Researcher at NIOC SB RAS.
E-mail: d-mazhukin@yandex.ru
Current research interests: synthesis and reactions of polyfunctional nitrogenous nucleophiles, chemistry of nitrogen-containing heterocycles including biologically active derivatives, stable organic radicals, paramagnetic liquid crystals, heterodiradicals, molecular design of magnets.
N.P.Gritsan. Doctor of Chemical Sciences, Professor, Head of Laboratory of ICKC SB RAS.
E-mail: gritsan@kinetics.nsc.ru
Current research interests: high-level quantum chemical calculations, density functional theory, electronic spectroscopy, stable organic radicals, heterospin systems, single-molecule magnets.

Translation: Z.P.Svitanko

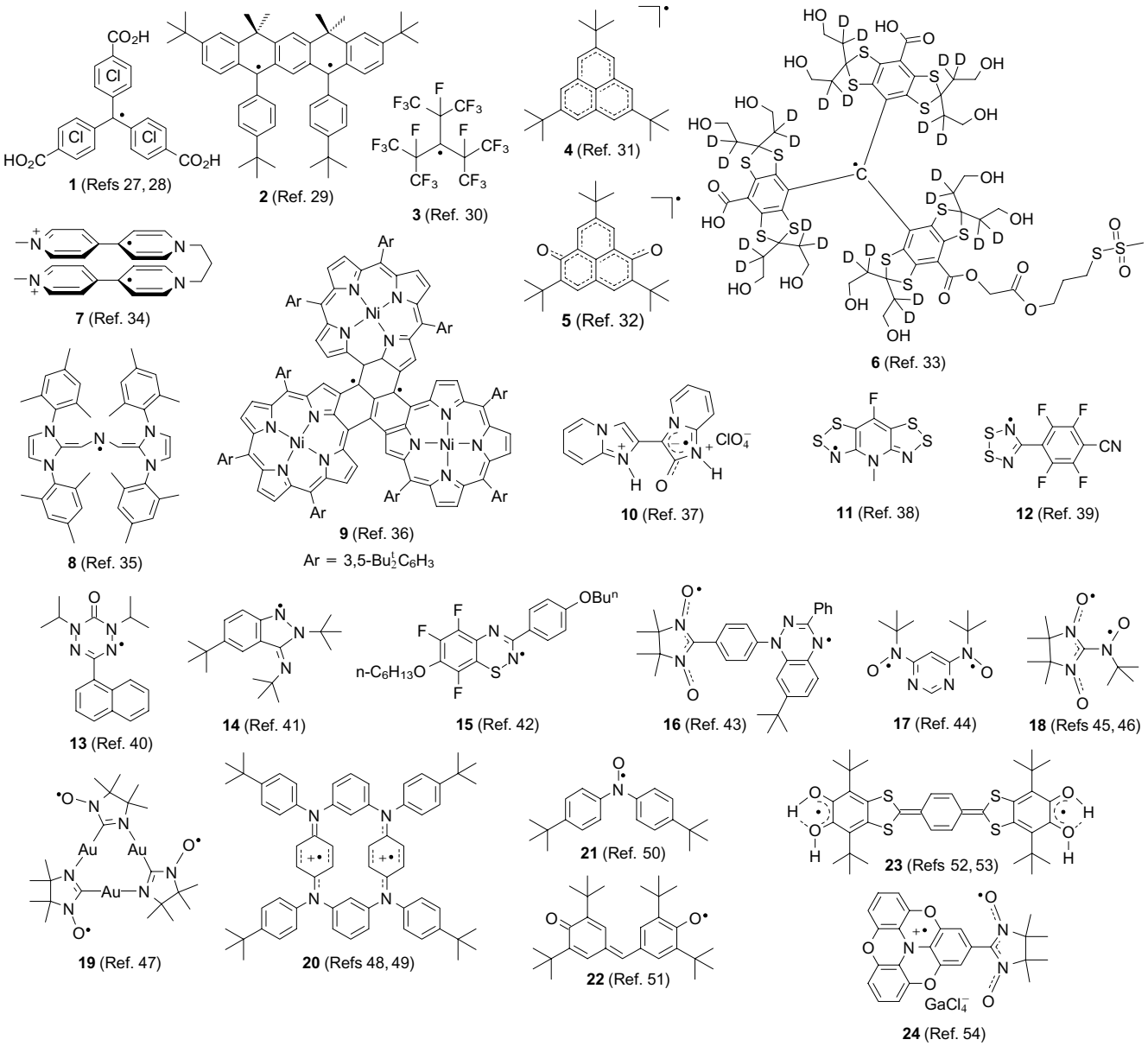


Figure 1. Structures of organic mono-, bi- and polyradicals of various classes, biradicals with various spin carriers and organometalic derivatives with references to literature sources. A halogen atom (Cl or F) inside a benzene ring stands for a perhalogenated phenyl group.[27,28]

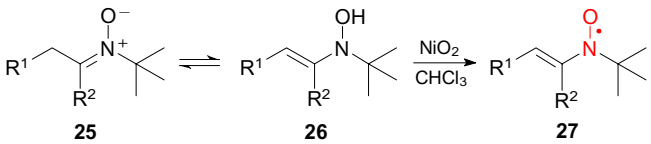
2. Acyclic nitroxides

This part of the review addresses methods of synthesis and properties of acyclic nitroxides in which the nitroxide group is bound to any unsaturated moiety: carbon–carbon or carbon–heteroatom double bond, conjugated multiple bonds, aromatic ring, a system of fused aromatic rings and so on. The attention is focused on paramagnetic stable radicals that have been isolated in a free state and characterized by X-ray diffraction. Apart from the synthetic aspects, the purpose of obtaining particular paramagnetic molecules is mentioned in brief. The main body of data about practical applications of conjugated nitroxides, including acyclic ones, is given in Section 5.

2.1. Vinyl nitroxides

A pronounced stabilization of the nitroxide group is attained when this group is conjugated with a C=C double bond substituted with one or two electron-withdrawing groups. For example, the oxidation of nitrones **25**, the ene-hydroxylamine tautomer of which (**26**) is stabilized by the −M-effect of the R^1 group, gives radicals **27**, called vinyl nitroxides (Scheme 1).[63] Vinyl nitroxides reported in the literature are highly reactive: in particular, they are able to recombine to give C−C- or C−O-bound dimers.[64] The half-life of known vinyl nitroxides does not exceed 2 h.

Scheme 1



25 **26** **27**

R^1 = SO$_2$Ph, CO$_2$Me; R^2 = H, Ph, CO$_2$Me

The vinyl nitroxide chemistry is still waiting for its renaissance, which should start with solving the problem of synthesis of stable paramagnetic compounds of this type. Quite probably, this will be done by introducing one or several cyano groups into their molecules. This will enable the use of acyclic vinyl nitroxides as structural blocks for the fabrication of extended organic high-spin systems and heterospin coordination polymers.

2.2. Aryl- and heteroaryl-substituted nitroxides

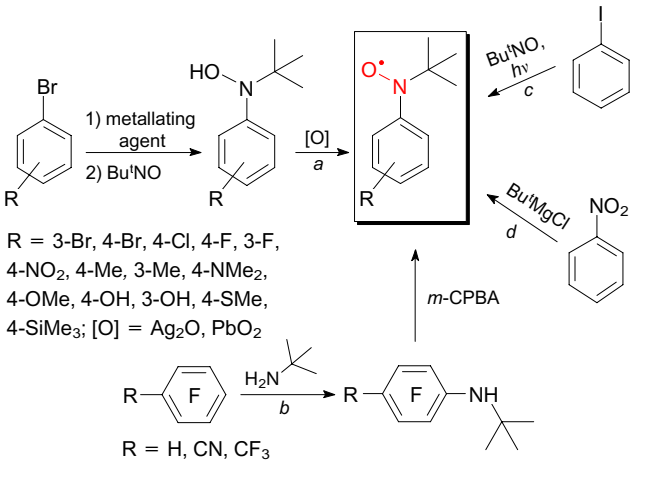
Unlike vinyl nitroxides, aryl- and heteroaryl-substituted nitroxide radicals have recently been at the focus of attention of many research groups. The synthetic chemistry of paramagnets of this class is actively developing, which includes both modification of known methods and the elaboration of new approaches. A general synthetic route to *tert*-butyl aryl nitroxides, which is used most often, is the oxidation of arylhydroxylamines (Scheme 2). The first step is usually the reaction of an appropriate aromatic organometallic compound with 2-methyl-2-nitrosopropane to give *tert*-butyl(aryl)hydroxylamine, which is then oxidized to the target paramagnetic compound (pathway *a*); in each case, the most appropriate oxidant is selected. The second approach is oxidation of secondary amines, in particular those obtained by reactions of polyfluorinated aromatic compounds with *tert*-butylamine (pathway *b*).[65] Another approach to generation of target radicals, mentioned in the literature, uses UV irradiation of appropriate iodoarenes or organic bismuth derivatives such as $Ph_3Bi(O_2CCH{=}CHMe)_2$ or $Ph_3Bi(O_2CEt)_2$[66,67] in the presence of 2-methyl-2-nitrosopropane as a radical trap (pathway *c*). In addition, the reactions of nitroaromatic compounds with *tert*-butylmagnesium chloride (pathway *d*) has been reported.[67,68] Note that pathways *c* and *d* serve only for generation of nitroxide radicals in solutions; the synthetic potential of these methods has not yet been investigated.

Pathway *a*, which implies treatment of aromatic metal derivatives with 2-methyl-2-nitrosopropane followed by oxidation of the resulting hydroxylamines, was used to obtain structurally diverse aryl *tert*-butyl nitroxides.[69–73] Many of them decomposed on attempted isolation to give substituted quinone imines and *tert*-butylanilines.[74] However, a representative series of aryl *tert*-butyl nitroxide mono- and biradicals, including chiral compounds,[75] were fairly thermally stable.[76,77] They were isolated in a free or coordinated state as parts of metal complexes and were fully characterized, in particular compounds **28**–**36** were studied by X-ray diffraction.[78–87] X-Ray diffraction data are of paramount importance for verification of theoretically calculated exchange couplings and efficiency of intra- and intermolecular exchange channels and for identification of reliable magneto-structural correlations.[88–95] In addition, it was shown that some *tert*-butyl nitroxides can be deposited on specially pretreated surfaces where spin carriers are retained for a few years.[96]

Consider a number of examples of function-oriented synthesis of *tert*-butyl aryl nitroxides, which includes the step of lithiation of aromatic bromo derivative and subsequent treatment with 2-methyl-2-nitrosopropane (see pathway *a* in Scheme 2). This route was used to prepare isomeric (9-anthryl)phenyl *tert*-butyl nitroxides **37**, **38** with the goal to elucidate the effect of π-topology of the conjugated system on the coupling of spins (*S*) in photoexcited states. According to time-resolved electron paramagnetic resonance (TREPR) data, *meta*-isomer **38** switched to the quartet excited state ($S = 3/2$) upon irradiation, whereas *para*-isomer **37** behaved in a different way, giving rise to a weak signal from the doublet state ($S = 1/2$).[97]

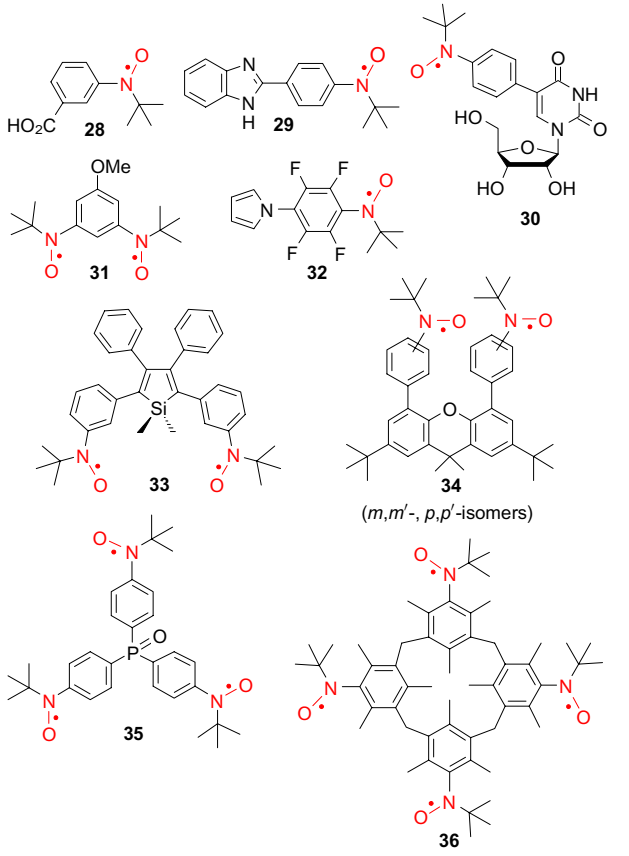
Isomeric nitroxides **39** were prepared in order to study the effect of paramagnetic substituent on the evolution of spins in metal porphyrins in the photoexcited state. It was shown that the presence of radical groups increased the rate of intersystem crossing by a factor of 10–500. Time-resolved EPR spectra of photoexcited nitroxides **39** exhibited signals for a three-spin system in the doublet and quartet excited states and signals for spin-polarized doublet state after system relaxation. All signals in the TREPR

Scheme 2

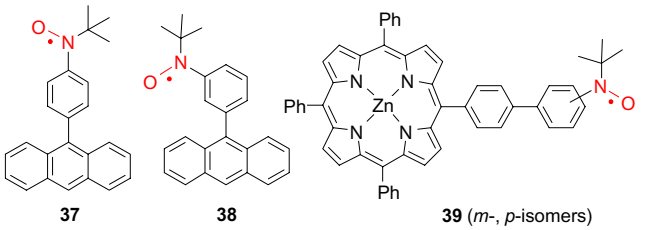


m-CPBA is *m*-chlorobenzoic acid

Structures 28–36



Structures 37 – 39

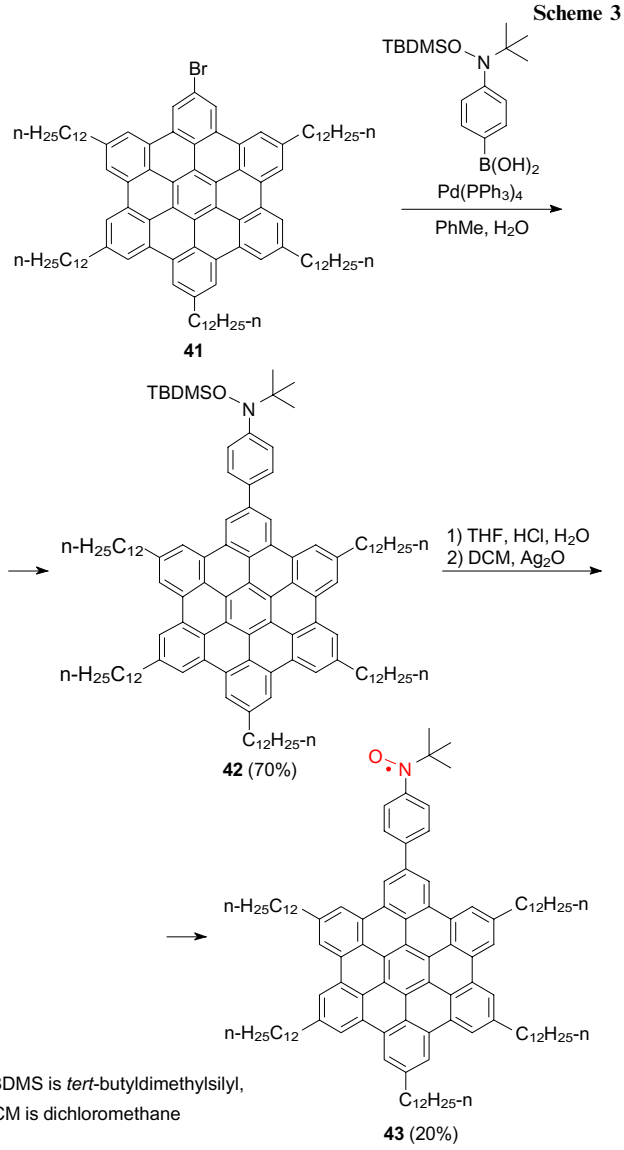


spectrum of the *para*-isomer corresponded to absorption of microwave radiation, whereas the signals of the *meta*-isomer were due to emission. In the latter case, the inversion of polarization of the quartet state occured within tens of nanoseconds, whereas in the case of *para*-isomer, no inversion of polarization took place due to higher energy of exchange coupling.[98]

Stable *tert*-butyl nitroxide **40** was obtained in order to study the details of interaction of the spin carrier with the π-system of corannulene. The use of magnetic resonance spectroscopy and calculation methods revealed a considerable (0.706) and non-uniform delocalization of spin density to the corannulene ring (Fig. 2) and thermally induced conformational dynamics of the nitroxide group in solution.[99]

The sequence of reactions consisting of cross-coupling of bromo derivative **41** with the corresponding arylboronic acid, hydrolysis of product **42** and oxidation of hydroxylamine afforded conjugated spin-labelled hexabenzocoronene **43** (Scheme 3, Fig. 3).[100] The synthesized paramagnetic compound was stable and had a higher conductivity than unsubstituted diamagnetic analogue owing to high-lying singly occupied molecular orbital (SOMO), which not only included the nitroxide moiety, but was also delocalized throughout the aromatic system; this was confirmed by density functional theory (DFT) calculations and voltammetric measurements. Using differential scanning calorimetry and wide-angle X-ray scattering, it was shown that, on heating above 368 K, nitroxide **43** is converted from a hexagonal crystalline to a columnar liquid-crystalline phase. The back transition takes place on cooling in the temperature range of 320 – 310 K and is accompanied by enhancement of magnetic interactions within the columnar stacks (see Fig. 3). This is manifested, in particular, as a signal at half field ($\Delta m_s = 2$) typical of biradicals that appears in the EPR spectrum recorded at 140 K. Thus, on the one hand, nitroxide **43** can serve as a sort of probe for EPR analysis of the phase transition, while on the other

Scheme 3



hand, thermally initiated phase transition endows this radical with unusual magnetic properties.

The synthesis of structurally complex paramagnetic compounds (D – C – A – R$^{\bullet}$) consisting of several func-

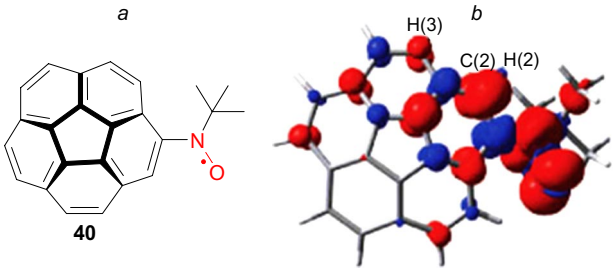


Figure 2. Structure of nitroxide **40** (*a*) and positive (red areas) and negative (blue areas) spin density (*b*) distribution in it.[99] Published with permission from CSIRO Publishing.

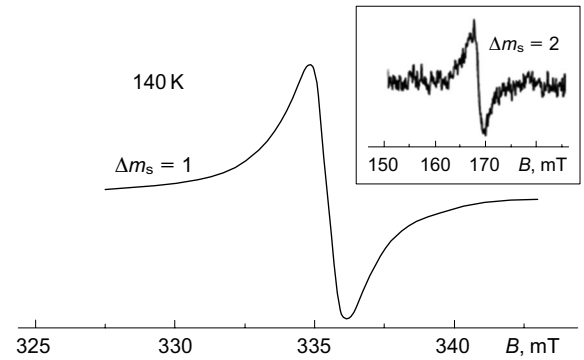
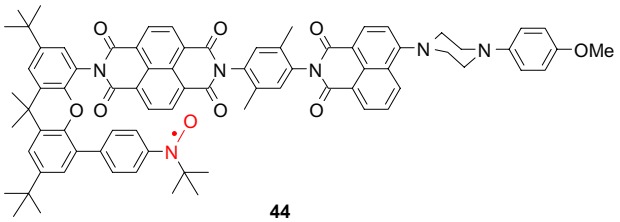


Figure 3. EPR spectrum of the crystalline phase of nitroxide **43** at 140 K (*B* is magnetic induction, m_s is the spin quantum number).[100] Published with permission from American Chemical Society.

Structure 44



44

tional blocks, donor (D), chromophore (C), acceptor (A) and nitroxide as the spin carrier was aimed to study the details of relaxation of photoinduced excited states in spin-labelled chromophores.[101, 102] A specific feature of nitroxide **44** (Fig. 4) is that the spin carrier (R$^{\bullet}$) is attached to the chromophore system *via* a xanthene bridge ensuring a U-shaped geometry of the molecule and the spatial proximity of the radical group and the acceptor moiety (~3.2 Å). Upon irradiation, the paramagnetic compound D–C–A–R$^{\bullet}$ is converted to the triradical system D$^{+\bullet}$–C–A$^{-\bullet}$–R$^{\bullet}$, which is characterized by strong dipole–dipole interaction (see Fig. 4). The anisotropic nature of this interaction was identified by experiments in 4-cyano-4′-n-pentylbiphenyl, which is a specific solvent with liquid-crystalline properties.

Among deliberately synthesized triplet aryl *tert*-butyl nitroxide biradicals **45a–d** (Scheme 4),[103, 104] some compounds were found to undergo structural phase transitions, which result in a change in the product of the molar magnetic susceptibility by temperature ($\chi_{mol}T$), similarly to this change observed in the complexes with spin transitions. It is noteworthy that the character and temperature of transitions depend on the nature of substituents in the benzene ring remote from paramagnetic centres (Fig. 5).

Biradical **45a** was isolated as two polymorphs stable at room temperature, diamagnetic and paramagnetic ones. The irreversible transition between the first and second polymorphs occurred at 350 K and was accompanied by a sharp increase in the distance between the paramagnetic centres and, as a consequence, a change in $\chi_{mol}T$ from nearly zero to 0.99 cm^3 K mol^{-1} (see Fig. 5).[103]

The dependence $\chi_{mol}T(T)$ for 3′-Me- (**45b**) and 2′,5′-difluoro derivatives (**45d**) also resembled that for spin-crossover compounds (see Fig. 5). For these biradicals, the $\chi_{mol}T$ values of high-temperature phases are close to

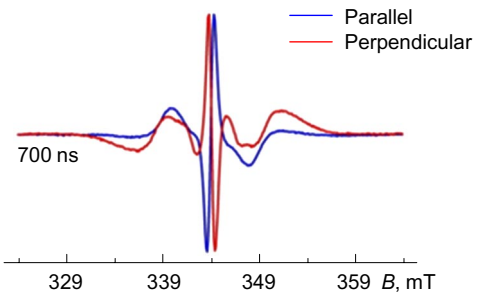
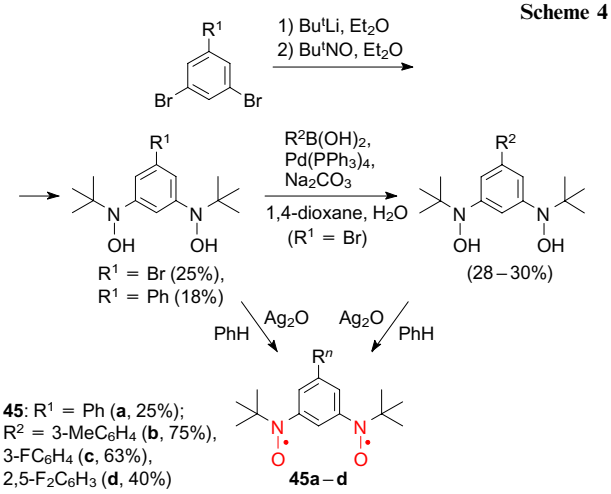


Figure 4. Central part of the TREPR spectrum of spin-labelled chromophore **44** in 4-n-pentyl-4′-cyanobiphenyl at 85 K recorded 700 ns after photoexcitation with a 7 ns laser pulse at 416 nm (for parallel and perpendicular orientation of the liquid crystals relative to the magnetic field).[102] Published with permission from American Chemical Society.

Scheme 4



0.375 cm^3 K mol^{-1}, which corresponds to half of the whole number of paramagnetic centres. After the phase transition, a quarter of paramagnetic centres remained in difluoro derivative **45d**, whereas in methyl derivative **45b**, they completely disappeared. According to X-ray diffraction data, the anomalous magnetic behaviour of these biradicals is due to partial and reversible dimerization of the neighbouring nitroxide groups, accompanied by hysteresis in the dependences $\chi_{mol}T(T)$.[104, 105]

Water-soluble biradical **46** with $S = 1$ meant for biological assays was synthesized by the same method supplemented by intermediate steps of aromatic ring functionali-

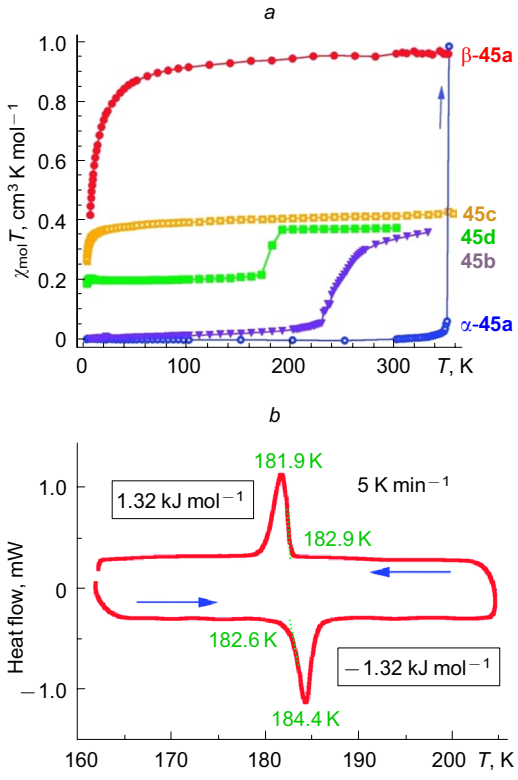
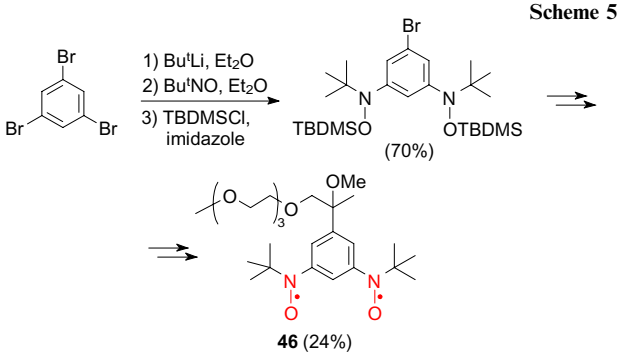


Figure 5. Dependences $\chi_{mol}T(T)$ for a series of 3,5-bis(*tert*-butyl nitroxide)biphenyls **45a–d** (*a*) and observed hysteresis for 2′,5′-difluoro derivative **45d** (*b*).[105] Published with permission from Royal Society of Chemistry.

zation with polyethylene glycol (Scheme 5).[106] Solvation in water increases the effective volume of polyethylene glycol, which results in a greater rotation angle of nitroxide groups relative to the aromatic ring and, as a consequence, in a decrease in the energy difference between the triplet and singlet states.

Scheme 5



In order to study the effect of complex formation on the exchange between paramagnetic centres, *tert*-butyl nitroxide biradical **47** (Fig. 6 *a*) with a polyether bridge was prepared.[107] The reaction of $Ca(hfac)_2$ or $Ba(hfac)_2$ (hfac is hexafluoroacetylacetonate) with biradical **47** gave complexes $[M(hfac)_2(\mathbf{47})]$ in which both the ether and nitroxide oxygen atoms were coordinated to the metal ion. According to X-ray diffraction data, the distances between the O atoms of paramagnetic centres in the obtained complexes were 4.460(3) and 4.382(4) Å for M = Ca and Ba, respectively. Unexpectedly, it was found that the EPR spectrum of the starting biradical consisting of five lines changed upon coordination: the spectrum of the complex exhibited three lines (see Fig. 6 *b*). Thus, alkaline earth metal ion, first, rigidly fixed the ligand geometry and ensured proximate positions of the paramagnetic centres and, second, acted as a magnetic insulator suppressing exchange couplings.

The use of *tert*-butyl nitroxides facilitated marked progress in the design of high-spin organic systems, studies of stable analogues of canonical hydrocarbon radicals and the design of magnetic switches and sensors. A series of *tert*-butyl nitroxide biradicals **48a–c** were prepared for studying the magneto-structural correlations inherent in stable analogues of the Chichibabin s biradical. It was shown that the elongation of the conjugated system leads to considerable decrease in the energy of antiferromagnetic exchange between the paramagnetic centres, which induces biradical transition from quinoid (**48a**) and semiquinoid (**48b**) states to the biradical form(**48c**) (Fig. 7).[108]

Significant correlations were identified in a study of *tert*-butyl nitroxide biradicals **49a–d** with regularly varying

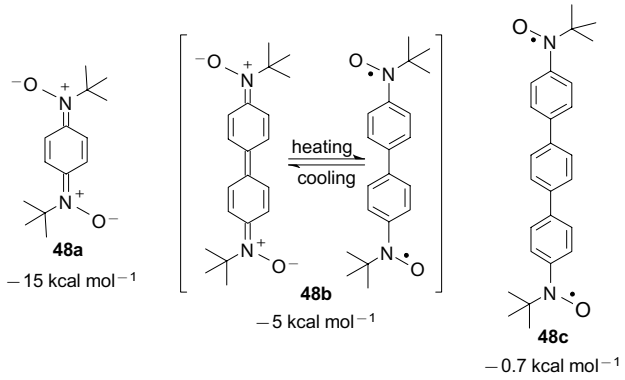
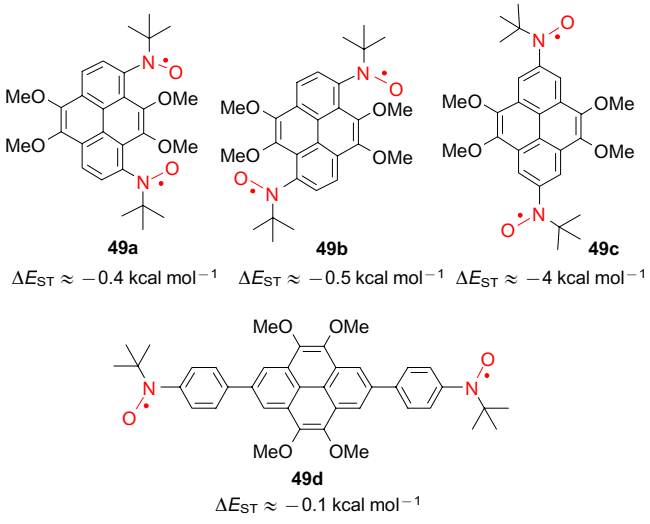


Figure 7. Weakening of the antiferromagnetic exchange coupling in the *para*-substituted *tert*-butyl nitroxide biradicals **48a–c**. The values below the structures are exchange coupling energies, or singlet–triplet splitting energies (ΔE_{ST}).

structure, containing the tetramethoxy-substituted pyrene core.[108–110] Quantum chemical calculations [UBLYP/6-31g(d)] showed that exchange coupling energies in isomeric singlet biradicals **49a–c** differ by an order of magnitude. The highest ΔE_{ST} value ($\Delta E_{ST} = -4$ kcal mol^{-1}) was found for dinitroxide **49c**; this accounts for its semiquinoid structure.

A variety of mono-, bi-, tetra- and octaradicals with rigid calix[4]arene core were prepared by lithiation of the corresponding bromo derivatives followed by treatment with 2-methyl-2-nitrosopropane and PbO_2.[72,111–114] Study

Structures 49



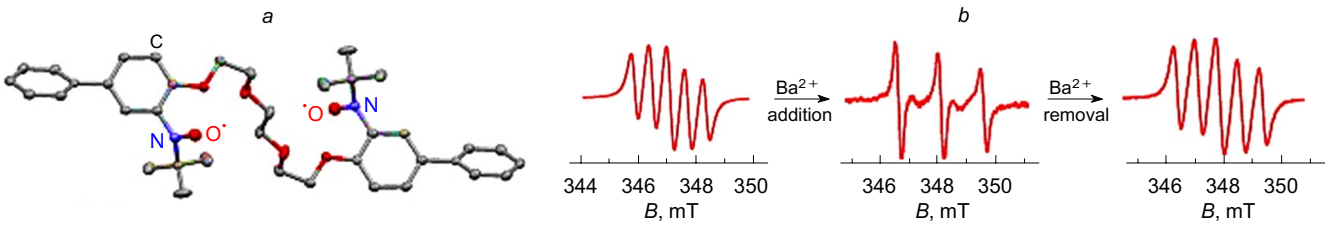


Figure 6. Molecular structure of biradical **47** (*a*) and change in its EPR spectrum upon binding to the Ba^{2+} ion and subsequent removal of the complex-forming ion (*b*).[107] Published with permission from Elsevier.

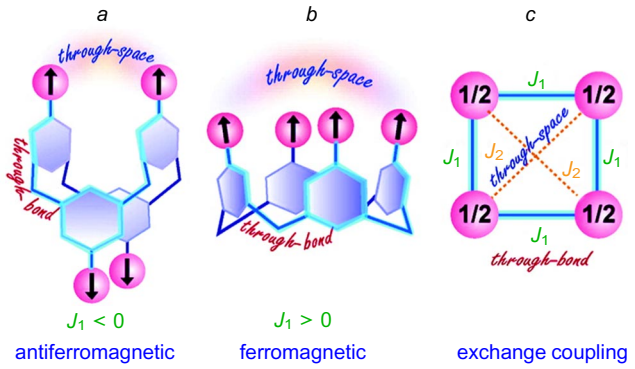


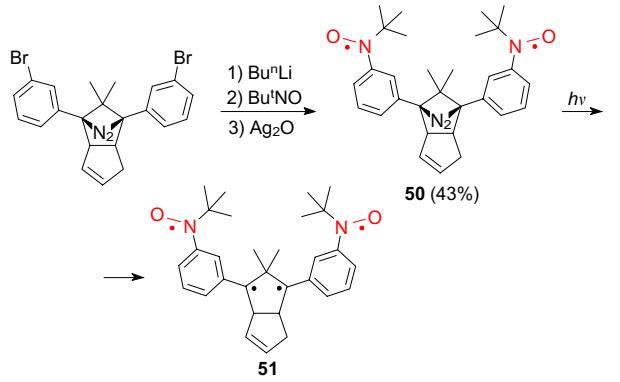
Figure 8. Exchange coupling in calix[4]arenes with 1,3-alternate (*a*) and cone (*b*) configurations functionalized at the upper rim with nitroxides (highlighted in pink) and schematic of intramolecular exchange channels (*c*) (J_n are exchange coupling parameters; the arrows show the direction of spins).[116] Published with permission from American Chemical Society.

of the magnetic properties of these spin-labelled calix[4]arenes showed that the energy and type of the intramolecular exchange couplings in them depend on many factors such as structure, conformational mobility, steric hindrance, temperature, nature of the solvent and the presence of metal ions (Fig. 8).[115,116] Furthermore, it was shown that variation of the nature of the linker between the calix[4]arene core and spin carriers ($S = 1/2$ or 1) has a considerable effect on the relaxation rate. This opens up the way towards multispin systems applicable for magnetic resonance imaging and dynamic nuclear polarization.[117]

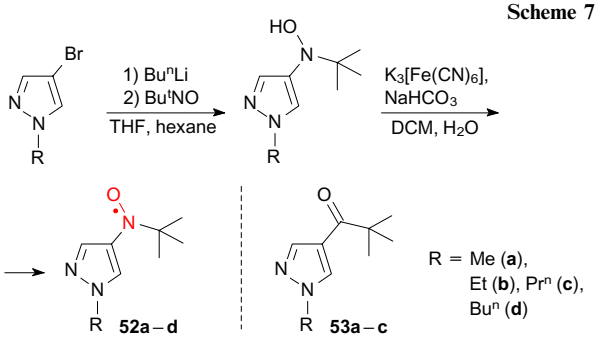
One more example of using principles for the design of high-spin systems is the synthesis of azo biradical **50**, which undergoes photodecomposition to give quintet tetraradical **51** (Scheme 6).[118]

The synthetic route to nitroxide radicals considered above (see pathway *a* in Scheme 2) is also actively used to prepare their diverse heterocyclic analogues — *tert*-butyl heteroaryl nitroxides. Many organic paramagnets synthesized in this way were converted to heterospin metal complexes of various architecture and for various purposes.[119–125] Owing to the presence of heterocyclic substituents, some macrocyclic heterospin complexes could be isolated[126,127] and, which is more important, their dimensionality increased, *i.e.*, coordination compounds

Scheme 6



Scheme 7



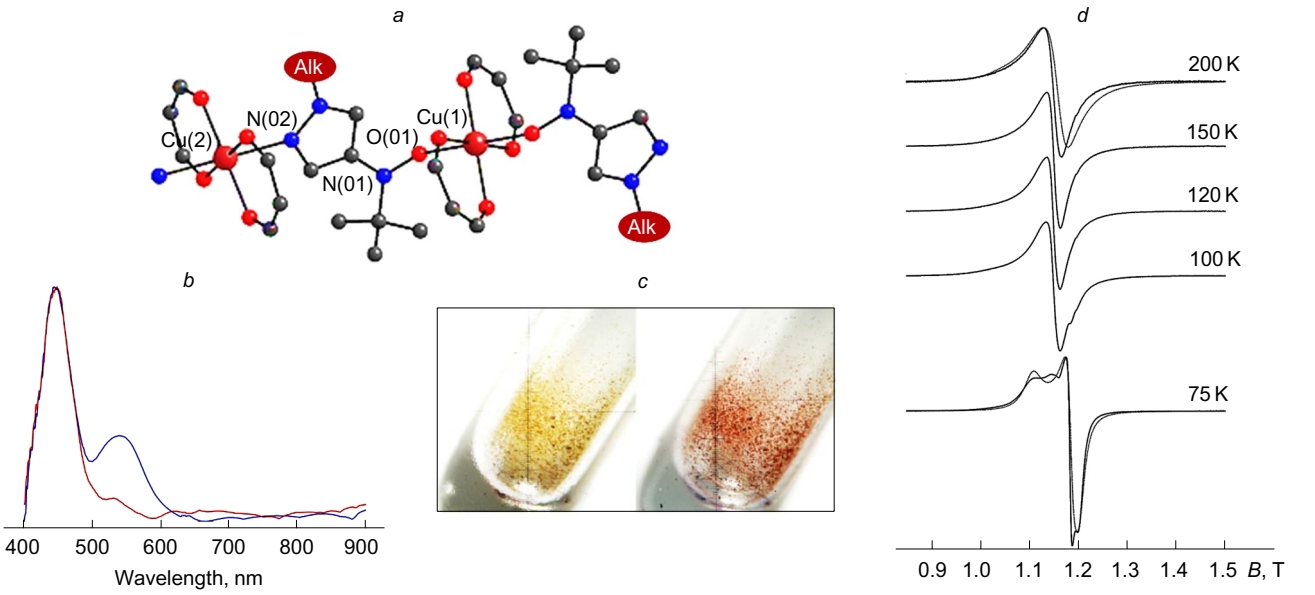
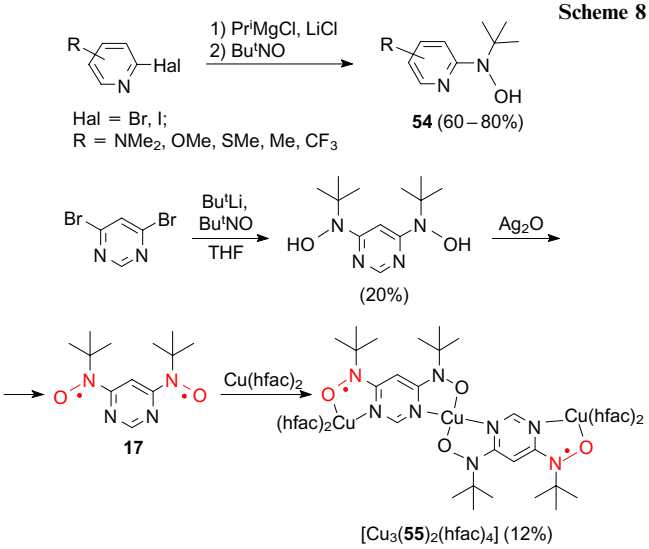


Figure 9. Molecular structure of Cu(hfac)$_2$ complexes with nitroxides **52a–d** (*a*), electronic absorption spectra of [Cu(hfac)$_2$(**52a**)]$_n$ at 80 (blue line) and 150 K (red line) (*b*), external appearance of polycrystalline [Cu(hfac)$_2$(**52a**)]$_n$ sample at room temperature (on the left) and at 77 K (on the right) (*c*), and temperature dynamics of its EPR spectrum (*d*).[132,133] Published with permission from American Chemical Society (Fig. 9 *b*,*c*) and Springer Nature (Fig. 9 *d*).

with one-, two- and even three-dimensional architectures were obtained.[128–131] This can be exemplified by *tert*-butyl pyrazolyl nitroxides **52a–d** (Scheme 7), which are coordinated to $Cu(hfac)_2$ to yield polymer chain heterospin complexes $[Cu(hfac)_2(\mathbf{52})]_n$ (called breathing crystals). The complexes can undergo temperature- and photo-induced spin transitions (Fig. 9, see also Section 5).[132,133] No such transitions were observed in polymer chain complexes with diamagnetic structural analogues of *tert*-butyl pyrazolyl nitroxides — pivaloylpyrazoles **53a–c**. This points to the key role of ligand paramagnetism in the abnormal magnetic behaviour of the 'breathing crystals'.[134]

The transformation of 2-halo-substituted pyridines into the corresponding nitroxide radicals in the presence of Bu^nLi did not always proceed smoothly; in some cases, alkylation of the pyridine ring took place instead of metallation. Analysis of the published data showed that the highest yields of hydroxylamines **54**, precursors of pyridyl-substituted paramagnets, were attained in those cases where an activated Grignard reagent, that is, lithium chloride complex with isopropylmagnesium chloride, is used to obtain 2-metallated pyridine derivatives (Scheme 8, first reaction).[135] However, this method for the synthesis of heteroaryl hydroxylamines was not widely used; instead, in the vast majority of cases, the required metal derivatives were generated by treatment with n-butyllithium.

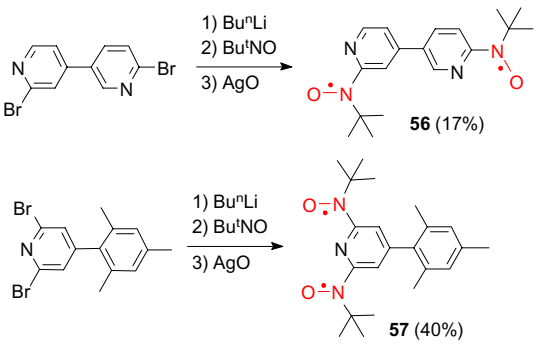
Scheme 8



For example, Ishida and co-workers[44,136] used this procedure to prepare triplet *tert*-butyl nitroxide biradicals with pyridine-2,6-diyl and pyrimidine-4,6-diyl linkers (see the synthesis of biradical **17** in Scheme 8). The attempts to isolate these biradicals showed that they differed from benzene analogues by markedly lower stability. This actually ruled out the possibility of using these biradicals in the molecular design of magnets. For example, from compound **17**, it was possible to obtain and characterize only the trinuclear copper complex $[Cu_3(\mathbf{55})_2(hfac)_4]$ incorporating paramagnetic anion **55**, resulting from reduction of the biradical.

It is necessary to give credit to Japanese chemists whose persistence and systematic effort towards stable high-spin systems finally met with success. They obtained stable heterocyclic *tert*-butyl nitroxide biradicals with the triplet ground state and strong exchange coupling. An example is

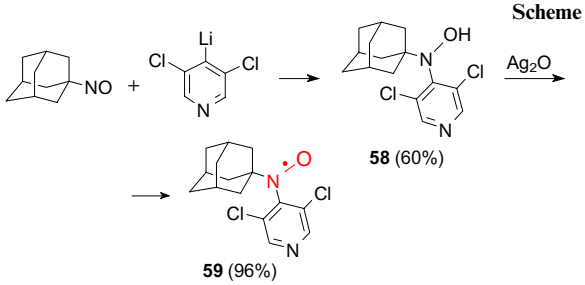
Scheme 9



3,4′-bipyridyl biradical **56** (Scheme 9), which has two chelating moieties, relatively high stability and strong intramolecular ferromagnetic exchange: the energy of exchange coupling between the paramagnetic centres $2J/k_B \approx +170$ K,† where J is the exchange coupling parameter, k_B is the Boltzmann constant.[137] In addition, stable biradical **57**, in which the triplet–singlet splitting was so high that it could not be detected by magnetometry techniques, was obtained and fully characterized. According to quantum chemical calculations, the intramolecular exchange in biradical **57** was $2J/k_B = +710$ K; therefore, even at room temperature, the population of its singlet excited state was negligibly low.[138]

Besides *tert*-butyl-substituted nitroxides, other paramagnets containing a bulky alkyl substituent can also be obtained *via* addition of organometallic compounds to nitroso derivatives. For instance, the reaction of 3,5-dichloropyridyllithium with nitrosoadamantane yielded hydroxylamine **58**, which was oxidized with Ag_2O to give stable nitroxide **59** in 96% yield (Scheme 10). According to X-ray diffraction data, the crystals of compound **59** had two crystallographically independent molecules; the N–O distances were 1.291 and 1.278 Å, and the angles between the planes of the NO group and the pyridine ring were ~76° and 87°, respectively.[139]

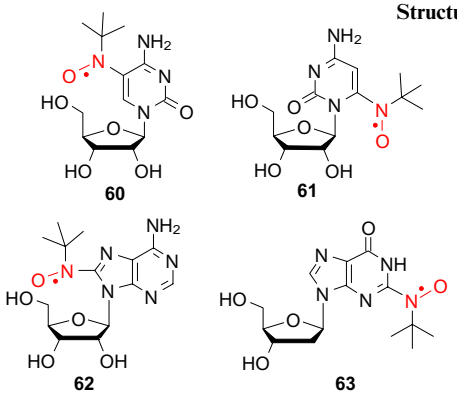
Scheme 10



Using various protecting groups, a family of nucleic acids with the *tert*-butyl nitroxide moiety, including compounds **30** and **60–63**, was obtained.[140–143] It was shown that the EPR spectral parameters of spin-labelled nucleic bases are sensitive to the viscosity and pH of the medium and to the complex formation with complementary nucleotides. Generally, the idea of complementary binding of spin-

† Note that in this review, Heisenberg exchange coupling Hamiltonian is used in the form $\hat{H} = -2J_{12}\hat{\vec{S}}_1\hat{\vec{S}}_2$, where $\hat{\vec{S}}_1$ and $\hat{\vec{S}}_2$ are spin operators of the paramagnetic centres, J_{12} is the parameter of the exchange coupling between them.

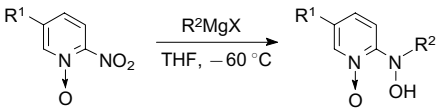
Structures 60 – 63



labelled substrates for the assembly of multispin systems *via* the formation of numerous hydrogen bonds is being developed rather actively, using spin carriers of various structural types.[144 – 146]

It was noted above that pathway *d* in Scheme 2 did not gain popularity for the preparative synthesis of aryl *tert*-butyl nitroxides. Meanwhile, this method proved to be efficient in one specific case: synthesis of 2-[*N*-(*tert*-butyl)-hydroxylamino]pyridine *N*-oxides **64** by the reaction of 2-nitropyridine *N*-oxides **65** with Grignard reagents (Scheme 11).[147] Since the authors did not oxidize the obtained hydroxylamines to nitroxide radicals, this pathway fell out of sight of specialists in nitroxide chemistry. Meanwhile, this method should be borne in mind, because unlike pathway *a* (see Scheme 2), in this case, nitroaromatic derivative served as the electrophiles, while the organometallic reagent with the alkyl group was the nucleophile. This fact may be useful for synthetic purposes and provided route to new organic radicals with previously inaccessible combinations of functional groups.

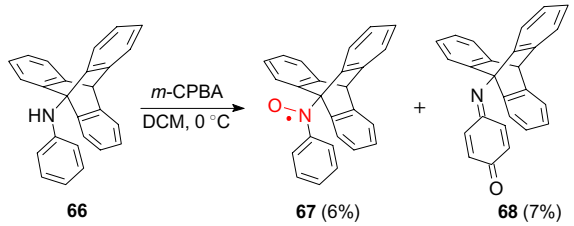
Scheme 11



R^1 = H, Me; R^2 = Bu^t, CMe_2Et

The oxidation of amines (see pathway *b* in Scheme 2) is a successful approach for the synthesis of nitroxides, including conjugated derivatives. For evaluating the potential of this approach, mention should be made of the oxidation of *N*-(9-triptycyl)aniline **66**, which gives rise to a mixture of 9-triptycyl nitroxide **67** (6% yield) and *N*-(9-triptycyl)-1,4-benzoquinone imine **68** (7%), but a large amount of the starting amine **66** (41%) remains unreacted (Scheme 12).[148]

Scheme 12

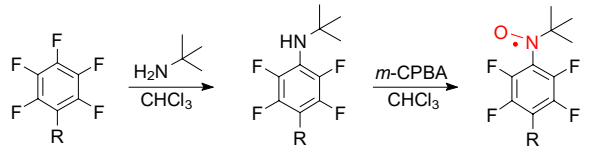


According to X-ray diffraction data, the nitrogen atom in paramagnetic compound **67** somewhat deviates from the plane of atoms bound to it, as indicated by the sum of the corresponding bond angles (358°). It is noteworthy that previously, Yamamoto *et al.*[149] attempted to synthesize the corresponding hydroxylamine, precursor of radical **67**, by addition of phenyllithium to 9-nitrosotriptycene (actually by pathway *a*, see Scheme 2); however, the reaction gave only *O*-phenyl-*N*-(9-triptycyl)hydroxylamine. This fact illustrates the possibility of reaction between organometallic compounds and nitroso derivatives *via* electron transfer followed by recombination of the resulting radicals.

Tretyakov *et al.*[150] proposed a new two-step synthesis of aryl *tert*-butyl nitroxides, which was actually a modified method *b* (see Scheme 2) and was meant for the preparation of polyfluorinated nitroxide radicals. In the first step, polyfluoroarenes reacted with *tert*-butylamine to give aminodefluorination products, while in the second step, the resulting *tert*-butylarylamines were oxidized to nitroxides. The conditions of conducting the first step depend on the polyfluoroarene reactivity towards the nucleophile (in this case, *tert*-butylamine).

Polyfluorinated substrates activated towards aromatic nucleophilic substitution such as octafluorotoluene and pentafluorobenzonitrile reacted with *tert*-butylamine in $CHCl_3$ at room temperature to afford substitution products **69a**,**b** in quantitative yields. The oxidation of the obtained anilines **69** with *m*-chloroperoxybenzoic acid furnished the target radicals **70a**,**b** in high yields (Scheme 13).[150]

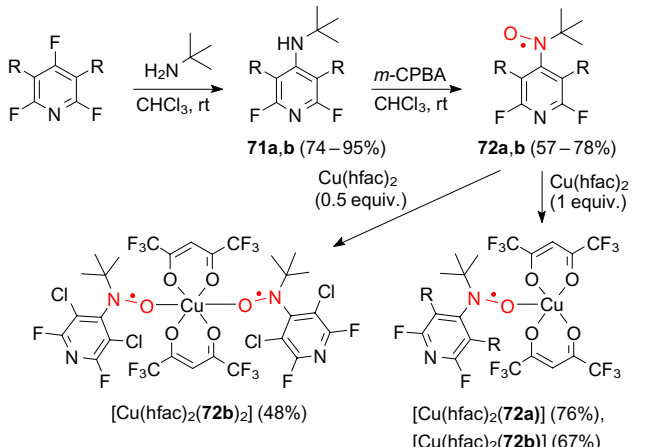
Scheme 13



R = CF_3 (**a**), CN (**b**) **69a**,**b** (99%) **70a**,**b** (> 90%)

The developed method is also applicable for the synthesis of polyfluorinated heteroaryl-substituted nitroxides. The reaction of perfluoropyridine or 3,5-dichloro-2,4,6-trifluoropyridine with *tert*-butylamine leads to *para*-substitution products **71a**,**b**, which are oxidized to give nitroxide radicals **72a**,**b** (Scheme 14). The latter react with $Cu(hfac)_2$

Scheme 14

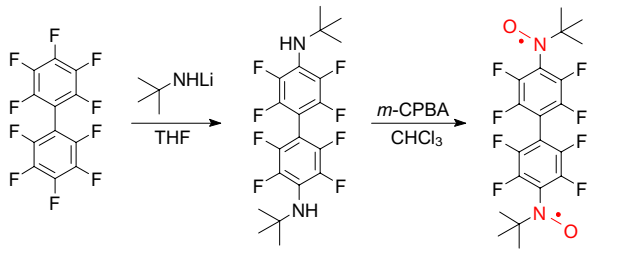


R = F (**a**), Cl (**b**)

to give stable 1 : 2 or 1 : 1 molecular complexes — $[Cu(hfac)_2(\mathbf{72b})_2]$, $[Cu(hfac)_2(\mathbf{72a})]$ and $[Cu(hfac)_2(\mathbf{72b})]$, in which the nitroxide group rather than the pyridine nitrogen atom is axially coordinated.[151]

If the reactivity of polyfluoroarenes is low, or if it is necessary to introduce two or more *tert*-butylamino groups into the polyfluorinated substrate, two other methods are used. One of them is illustrated by the synthesis of polyfluorinated biradical depicted in Scheme 15. The method consists in the reaction of perfluorobiphenyl with an excess of lithium *tert*-butoxide and subsequent oxidation of the resulting diamine **73** to biradical **74** (~90% yield).[152]

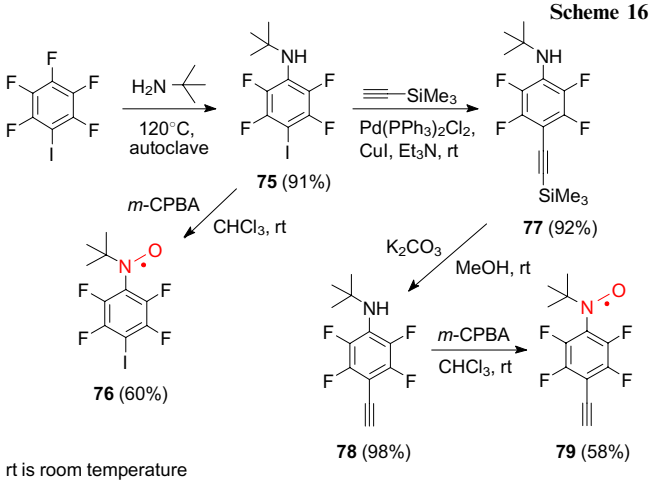
Scheme 15



73 **74** (90%)

The second method for the replacement of the fluorine atom in polyfluoroarenes by a *tert*-butylamino group is more experimentally facile and versatile. The process includes heating a mixture of polyfluoroarene with an excess of *tert*-butylamine in an autoclave. For example, the key tetrafluoroiodoaniline derivative **75** — precursor of nitroxide **76** — was obtained in this way (Scheme 16).[153] Iodoaniline **75** was also used to synthesize *p*-trimethylsilylethynylaniline **77**, which was subjected to silyl deprotection (to give terminal alkyne **78**) followed by oxidation to radical **79**. Nitroxides **76** and **79** can serve as paramagnetic building blocks for the synthesis of spin-labelled compounds.

Scheme 16

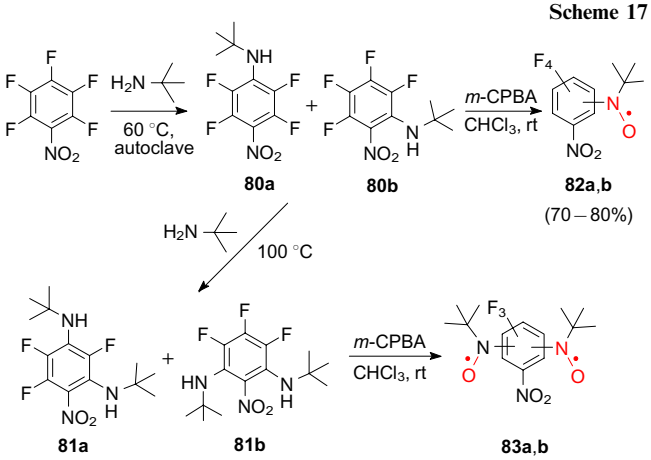


75 (91%) **77** (92%) **76** (60%) **78** (98%) **79** (58%)

rt is room temperature

One more benefit of the autoclaving of polyfluorinated arenes with *tert*-butylamine is the fact that by increasing the temperature of the reaction mixture, it is possible to successively replace one, two or more fluorine atoms in the aromatic substrate. For example, keeping perfluoronitrobenzene with *tert*-butylamine at different temperatures provides for the synthesis of mono- (**80a**,**b**; 76% yield) and

Scheme 17



80a **80b** **82a**,**b** (70–80%)

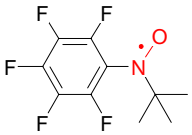
81a **81b** **83a**,**b**

Isomers: 4 (**82a**), 2 (**82b**), 2,4 (**83a**), 2,6 (**83b**)

di(*tert*-butylamino)nitrobenzenes (**81a**,**b**; 46% yield), which are oxidized with *m*-chloroperoxybenzoic acid giving mono- (**82a**,**b**) and biradicals (**83a**,**b**), respectively (Scheme 17) (our unpublished data). It is noteworthy that this process affords exclusively *meta*-substituted diamines, which are oxidized to triplet biradicals.

It is worth paying attention to the fact that *tert*-butyl polyfluoroaryl nitroxides are more stable than their non-fluorinated analogues; these radicals are stable in air and under isolation conditions and can be characterized by spectral methods. For example, pentafluorophenyl derivative **84** is isolated in a pure state after long-term refluxing in benzene, which is indicative of exceptional stability of this radical. Meanwhile, the non-fluorinated analogue is known[154,155] to disproportionate under the same conditions to give amine and quinone derivative. In the case of fluorinated derivative **84**, this reaction is thermodynamically unfavourable due to greater strength of the C–F bond compared to the C–H bond.

Structure 84

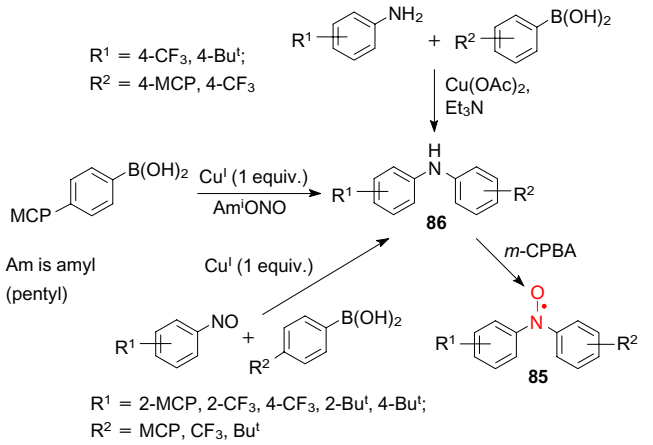


84

On treatment with $Cu(hfac)_2$, polyfluorinated radicals form heterospin complexes, which withstand heating to 100–115 °C, according to thermogravimetry and differential scanning calorimetry data. In addition, these complexes are highly volatile: they sublime at a temperature of 85–90 °C and a pressure of 30 Torr to be quantitatively converted to crystals structurally identical to the crystals before sublimation.[150,151] Generally, the approach proposed for the synthesis of polyfluorinated *tert*-butyl nitroxides, with allowance for the high volatility and stability of their metal complexes, is promising for the design and practical application of molecular magnets.

The synthetic routes to aryl *tert*-butyl nitroxides listed above resemble, to a large extent, methods for the synthesis of diaryl nitroxides. The latter are covered in a review[156] published in 2018, which presents, in particular, the general view on the synthetic chemistry of paramagnetic molecules

Scheme 18



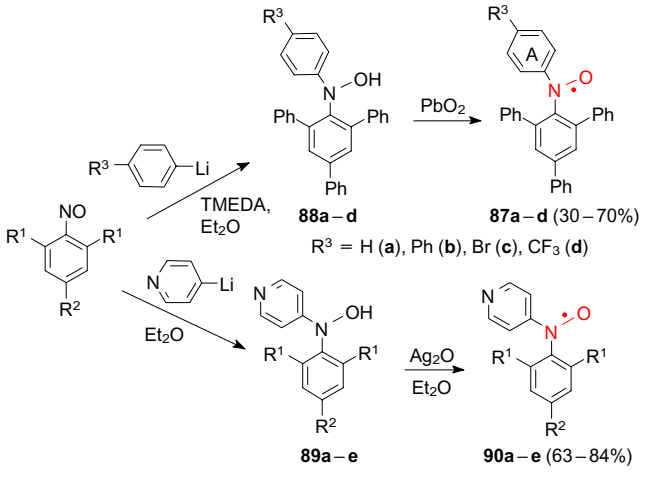
of this type. We will supplement the data of this review by a number of interesting examples.

A broad range of substituted diaryl nitroxides **85** containing α-methylcyclopropyl (MCP), trifluoromethyl and *tert*-butyl groups in various combinations were synthesized by Levitskiy *et al.*[50, 157] Diarylamines **86**, which served as precursors, were prepared by amination of substituted arylboronic acids using various approaches (Scheme 18).

According to kinetic studies, nitroxide radicals **85** are stable not only in the solid state, but also in solution. Moreover, currently 2-trifluoromethylphenyl 4′-(α-methylcyclopropyl)phenyl nitroxide is considered to be the most stable among diaryl nitroxides: the half-life of this compound in a benzene solution at room temperature is 2310 h (> 3 months).[157]

An organometallic approach similar to pathway *a* in Scheme 2 was used to synthesize a series of diaryl nitroxides **87a–d** (Scheme 19).[158] The reaction of aryllithium derivatives with 2,4,6-triphenylnitrosobenzene in ether in the presence of tetramethylethylenediamine (TMEDA) is followed by oxidation of the intermediate hydroxylamines **88a–d** with PbO_2. The authors specially emphasized that the use of THF as the solvent leads to the formation of the target compounds in very low yields. According to X-ray diffraction data, the nitroxide group is arranged virtually in the plane of aromatic ring A, being rotated, together with

Scheme 19



this ring, by ~70° relative to the 2,4,6-triphenyl-substituted benzene ring.

Pyridyl nitroxides **90a–e** were prepared in a similar way from lithiated pyridine and substituted nitrosobenzenes *via* the step of formation of hydroxylamines **89a–e** (see Scheme 19).[159] In this series, the radicals that contained both *ortho*- and *para*-substituents proved to be kinetically more stable. They were isolated as high-quality crystals, which enabled molecular and crystal structure determination. The reactions of $Co(NCS)_2$ with nitroxides **90a–e** or the reaction of a mixture of $Co(NO_3)_2$ and KNCO with tri-*tert*-butyl-substituted nitroxide **90e** afforded stable 1 : 4 complexes as dark-red crystals, which showed different magnetic behaviours depending on the structure of the paramagnetic ligand. Among the complexes, antiferromagnetic behaviour with T_N = 22 K (T_N is Néel temperature) was found for $[Co(NCS)_2(\mathbf{90a})_4]$; weak antiferromagnetic behaviour with T_N = 2.9 K was inherent in $[Co(NCS)_2(\mathbf{90b})_4]$; weak ferromagnetic properties with T_N = 4.8 K were observed for $[Co(NCS)_2(\mathbf{90c})_4]$; and $[Co(NCS)_2(\mathbf{90d})_4]$, $[Co(NCS)_2(\mathbf{90e})_4]$ and $[Co(NCO)_2(\mathbf{90e})_4]$ were single-molecule magnets with an effective activation barrier (U_{eff}) reaching 48 K in a frozen solution.[159]

Thus, several approaches for the synthesis of alkyl aryl nitroxides and diaryl nitroxides with various functional groups have been developed. In recent years, new lines of research related to this type of paramagnetic species appeared. First of all, this is the synthesis of stable polyfluorinated aryl *tert*-butyl nitroxides by the reaction of polyfluoroarenes with *tert*-butylamine, which results in the formation of aminodefluorination products, followed by oxidation of intermediate *tert*-butylarylamines. The simplicity of the method, good yields of polyfluorinated aryl *tert*-butyl nitroxides, high volatility and stability and also π-acceptor properties of the aromatic substituent will obviously draw attention of researchers. In the future, it is necessary to make the next step: to extend this approach to diaryl heteroaryl nitroxides and prepare their polyfluorinated derivatives, which would give impetus to the development of many interdisciplinary fields related to magnetic materials.

2.3. Carbonyl nitroxides

Recent years have seen avalanche-like growth of the number of studies of nitroxide radicals containing carbonyl groups at the nitrogen atom. The carbonyl group increases the reactivity of nitroxide group; therefore, mono- and especially dicarbonyl nitroxide radicals exhibit clearly defined oxidative properties; they can eliminate a hydrogen atom from organic molecules with C–H bond cleavage and add to C=C double bonds. This increase in the reactivity is correlated with increasing degree of localization of the unpaired electron on oxygen of the >N–O group, which is reflected as a decrease in the hyperfine coupling constants [$a(^{14}N)$] in mono- [$a(^{14}N) \approx 0.5–0.8$ mT][5, 160, 161] and diacyl nitroxides [$a(^{14}N) \approx 0.4–0.5$ mT][161–164] compared to those of dialkyl nitroxides [$a(^{14}N) \approx 1.5$ mT] (Fig. 10).

The main method for the synthesis of acyl nitroxide radicals is the oxidation of the corresponding NOH derivatives — N-substituted hydroxamic acids (*N*-hydroxyamides) or *N*-hydroxyimides. The oxidants used for conversion of *N*-hydroxyamides to amide-*N*-oxyl radicals include the $K_3[Fe(CN)_6]–HO^-$ system,[165–167] NiO_2,[166] $Pb(OAc)_4$ (Ref. 168) and di-*tert*-butyl peroxide under UV irradiation.[168, 169] *N*-Arylamide-*N*-oxyl radicals can be gen-

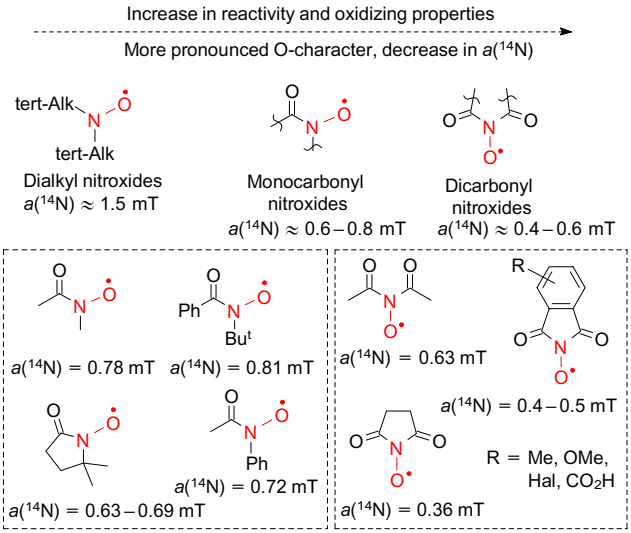


Figure 10. Correlations between the hyperfine coupling constants and the structure of nitroxide radicals. The figure was created by the authors using published data.[160–164]

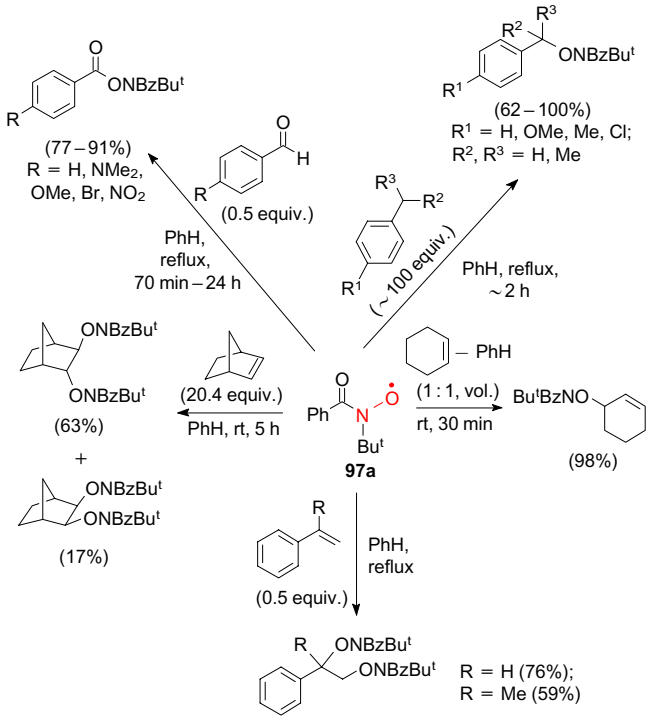
erated from the corresponding *N*-hydroxyamides by enzymatic reaction in the presence of oxidoreductases.[170]

A number of chiral imide-*N*-oxyl[171,172] and amide-*N*-oxyl[168,173] radicals **91**–**96**, which perform enantioselective elimination of a hydrogen atom from one of the enantiomers in a racemic mixture, have been studied. The enantiomeric excess (*ee*) considerably depended on the nature of the substrate and varied over a broad range: from 0 to 89%. The radicals gradually decompose in solution, but they can be generated *in situ* and used as catalysts for the oxidation of substrates with weak C–H bonds such as oxazolidines,[171] benzyl alcohols and ethers,[168,172] benzylamines,[168] *etc*.

Several acyl, alkoxycarbonyl and carbamoyl *tert*-butyl nitroxides were isolated in a pure state.[165,166] Amide-*N*-oxyl radicals containing a primary or secondary alkyl group at the nitrogen atom, instead of the *tert*-butyl group, are less stable due to the possibility of disproportionation.[169,174] Diacyl nitroxides are insufficiently stable to be isolated in a pure state, but they can be generated in an organic solvent. In this medium at room temperature, diacyl nitroxides are present for several minutes in a sufficiently high concentration and, hence, they can be used for synthetic purposes.[175,176]

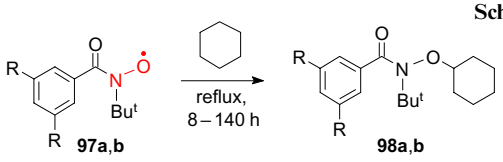
Benzoyl *tert*-butyl nitroxide (**97a**) reacts with alkylarenes, aldehydes, cyclohexene and other substrates with weak C–H bonds according to a hydrogen replacement pathway (Scheme 20).[174,177] One equivalent of the radical serves for elimination of the hydrogen atom from the substrate to give *N*-benzoyl-*N*-*tert*-butylhydroxylamine, while the other equivalent recombines with the C-centred radical thus formed. A similar reactivity was described for other acyl *tert*-butyl nitroxides.[165,174] They add to the C=C double bond of vinylarenes or norbornene containing no allylic hydrogen atoms.[177]

Scheme 20



The reactions of acyl nitroxides with non-activated alkanes are hampered due to high energy of the C–H bond. The refluxing of nitroxide **97a** in cyclohexane gives the hydrogen substitution product **98a** in a yield of not more than 30% (Scheme 21).[177] The yield of compound **98b** increases to 70% when more reactive 3,5-dinitrobenzoyl *tert*-butyl nitroxide (**97b**) is used.

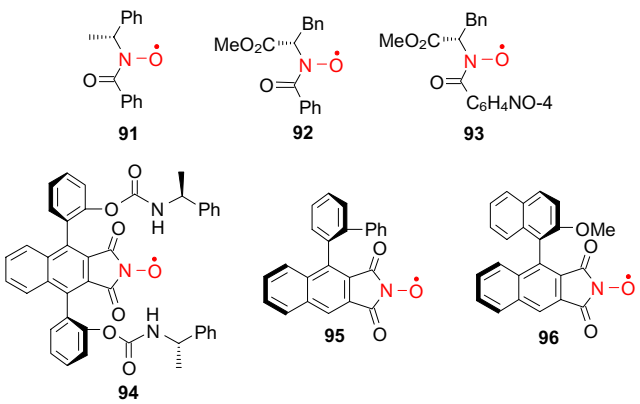
Scheme 21



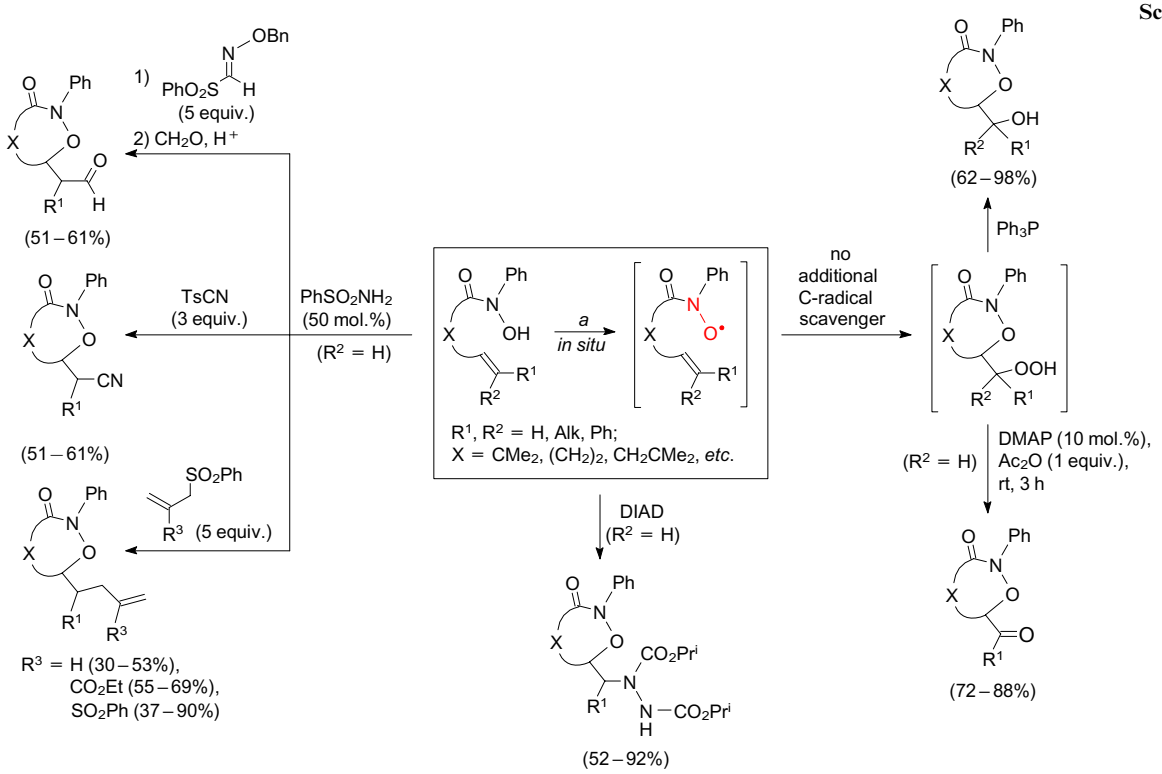
R = H (**a**, ⩽30%), NO_2 (**b**, 70%)

Most of acyl nitroxides are less stable than the above acyclic acyl *tert*-butyl nitroxides and cannot be isolated in a pure state. Nevertheless, owing to their high reactivity, they are widely used in organic synthesis as catalysts and reactants generated *in situ* for oxidative functionalization of various organic substrates.

Structures 91–96



Scheme 22



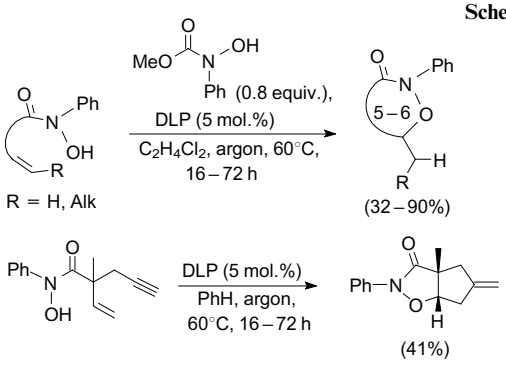
(*a*) O_2 (1 atm), DLP or azo-initiator (0–10 mol.%), AcOH, DMSO or Bu^nOAc, 40–90 °C, 2–48 h; DLP is dilauroyl peroxide, DMAP is 4-dimethylaminopyridine

Unsaturated amide-*N*-oxyl radicals generated in an oxygen atmosphere in the presence or in the absence of radical initiators undergo intramolecular addition to the C=C bond to give a five- or six-membered ring (Scheme 22).[178–181] In the absence of additional radical scavengers, the C-centred radical reacts with molecular oxygen to give hydroperoxide,[178, 179] which can be subsequently converted to the corresponding alcohol[178] or carbonyl compound.[179] When radical scavengers are added, such as diisopropyl azodicarboxylate (DIAD),[180] *O*-benzyl(phenylsulfonyl)formaldoxime, TsCN [Ts is *p*-toluenesulfonyl (tosyl)] or allyl phenyl sulfone,[181] this C-centred radical undergoes a variety of selective reactions giving new C–N (Ref. 180) or C–C bonds (see Scheme 22).[181]

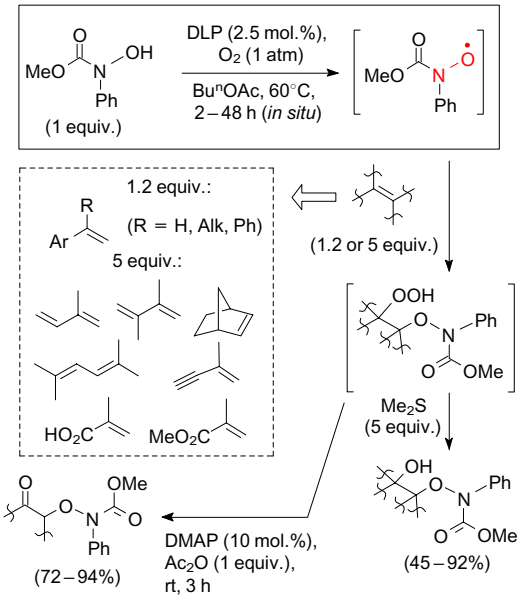
When a similar reaction is carried out in an oxygen-free atmosphere using dilauroyl peroxide as a radical initiator, cyclization of unsaturated hydroxamic acids is accompanied by addition of the amide-*N*-oxyl oxygen atom and a hydrogen atom to the C=C bond.[182] The hydrogen atom comes from methyl *N*-hydroxy-*N*-phenyl carbamate. The carbonyl nitroxide thus formed abstracts a hydrogen atom from the unsaturated hydroxamic acid molecule, thus triggering the next cycle of chain cyclization reaction (Scheme 23). A number of cascade cyclizations of unsaturated hydroxamic acids with successive closure of two rings was implemented under modified conditions without the addition of methyl *N*-hydroxy-*N*-phenyl carbamate, as exemplified in Scheme 23.[182]

Carbonyl nitroxide generated *in situ* from methyl *N*-hydroxy-*N*-phenyl carbamate under similar conditions was used for the intermolecular addition to double C=C bonds (Scheme 24).[179, 182, 183] In all of the substrates, except

Scheme 23



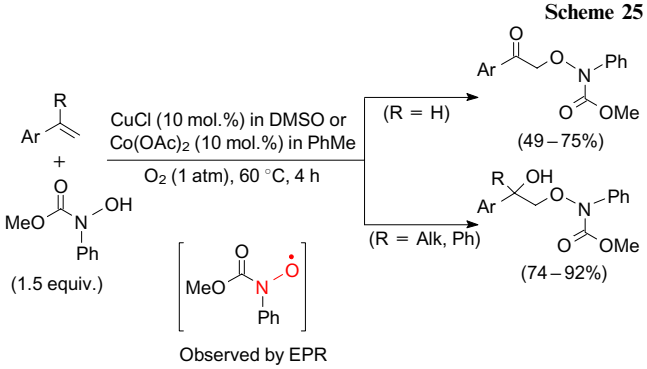
Scheme 24



for norbornene, the double bond was conjugated, which facilitated the radical addition. This reactions proceeded most readily with styrenes; in the case of dienes, mixtures of 1,2- and 1,4-addition products were formed.[183] The initially formed hydroperoxides can be reduced to alcohols[183] or converted to ketones[179] (when a hydrogen atom is present in the α-position to the OOH group).

Similar successive addition of carbonyl nitroxide generated *in situ* and molecular oxygen to styrenes was accomplished in the presence of catalytic amounts of CuCl and $Co(OAc)_2$, taken instead of the DLP radical initiator (Scheme 25).[184] In this case, α-unsubstituted vinylarenes were converted to ketones, while α-substituted derivatives were converted to alcohols.

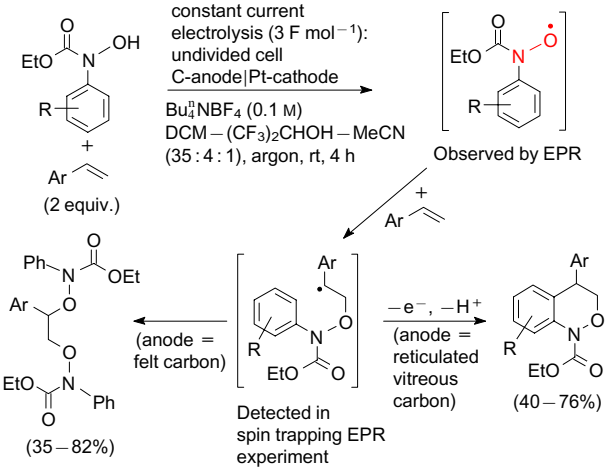
Scheme 25



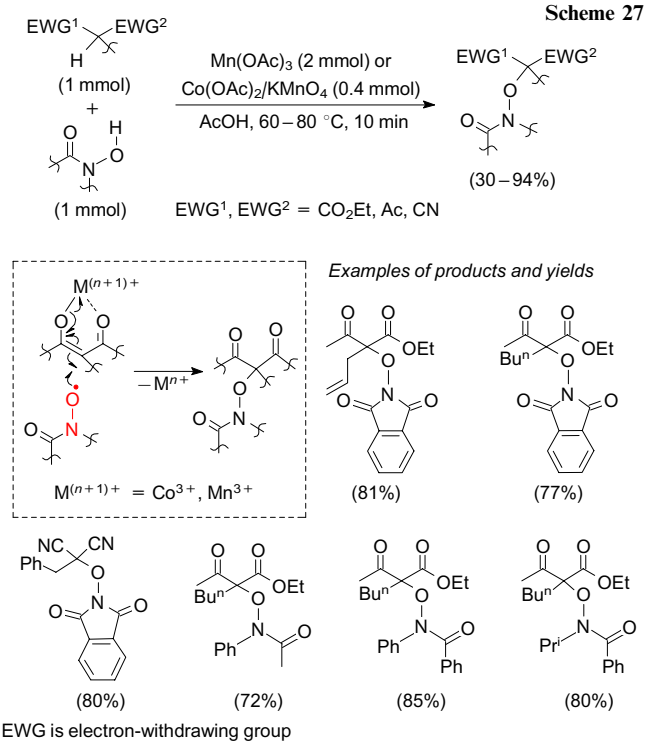
When carbonyl nitroxides are generated by anodic oxidation of hydroxamic acids, other products can be obtained.[185] In this case, the addition of carbonyl nitroxide to the C=C bond of vinylarene giving benzyl radical is followed, depending on the anode material, by either further oxidation and cyclization (formal oxidative [4 + 2]-addition of carbonyl nitroxide to the double bond) or addition of a second carbonyl nitroxide molecule (Scheme 26). Wei *et al.*[185] demonstrated the applicability of the method they developed for functionalization of not only vinylarenes, but also norbornene, its analogues and indoles.

For most amide-*N*-oxyl radicals, no efficient methods for oxidative C–O coupling with CH reagents are known, because these radicals are not sufficiently reactive to cleave C–H bonds and more rapidly self-decompose. An exception is C–O coupling involving β-dicarbonyl compounds. Apparently, in this reaction, the CH reactant is oxidized by a metal-containing single-electron oxidant rather than by the *N*-oxyl radical (Scheme 27).[186]

Scheme 26



Scheme 27



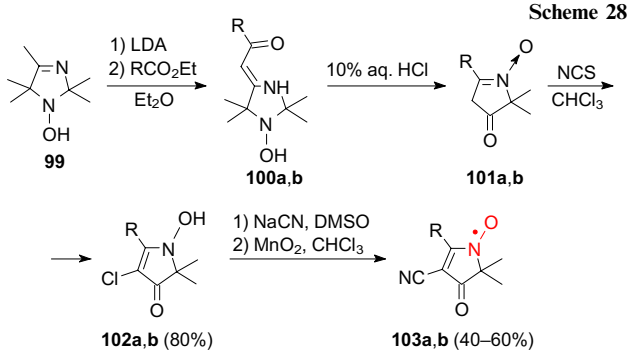
3. Cyclic nitroxides

A variety of cyclic nitroxides containing an unsaturated moiety adjacent to the NO group have been reported in the literature. Organic paramagnetic compounds characterized only by an EPR spectrum because of their low stability are mostly beyond the scope of this review. Conversely, cyclic conjugated nitroxides that have been isolated in a free state and fully characterized, in particular by X-ray diffraction, are described in detail. In addition, considerable attention is paid to new preparation methods and function-oriented synthesis of the radicals.

3.1. Heterocyclic vinyl nitroxides with *endo*- and *exo*-methylene bonds

Unlike acyclic vinyl nitroxide radicals, for which the preparation of stable representatives is still an unsolved problem, a number of their heterocyclic analogues have been isolated in a pure state. The double bond in these radicals is substituted with electron-withdrawing groups having –M effect, which actively participate in spin density delocalization. This can be exemplified by pyrroline type radicals, which are obtained beginning with functionalization of the methyl group in 1-hydroxypentamethylimidazoline **99** to give enamino ketones **100a**,**b**; the latter are subjected to ring transformation to give cyclic β-oxonitrones **101a**,**b**. These products react with NCS to afford chloro derivatives **102a**,**b**, which are converted to the corresponding nitriles

Scheme 28

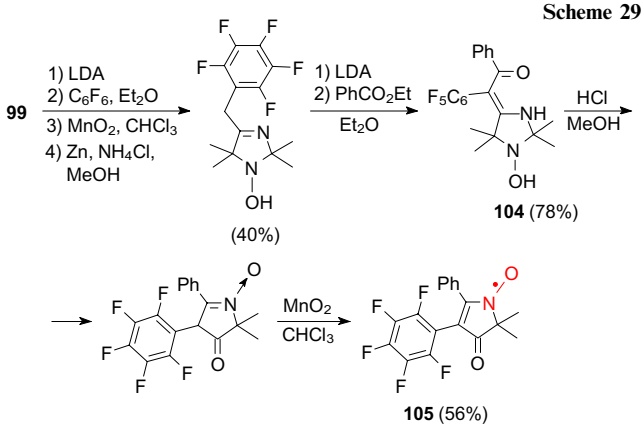


R = Ph (**a**), 3-Py (**b**); LDA is lithium diisopropylamide, Py is pyridyl

and oxidized to stable radicals **103a**,**b** (Scheme 28).[187, 188] Paramagnetic product **103a** crystallizes from hexane as a solid phase composed of two polymorphs differing in the magnetic properties.

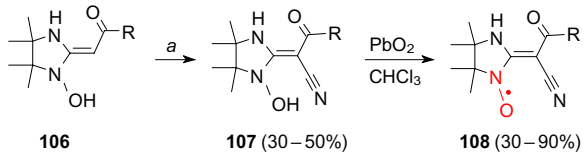
A similar synthetic route was used to prepare a stable nitroxide containing a pentafluorophenyl group in place of the nitrile group (Scheme 29). This group was introduced at early stage of the process *via* two successive functionalizations of the methyl group in compound **99**, resulting in the formation of key enamino ketone **104**, which underwent ring transformation to afford the desired heterocyclic skeleton of radical **105**.[189]

Scheme 29



One more type of heterocyclic vinyl nitroxides with an exocyclic double bond is represented by a series of stable cyano derivatives of imidazolidine. They are prepared from accessible enamino ketones **106** (Refs 190–193) in three steps: successive replacement of the hydrogen atom at the double bond by chlorine atom and CN group and oxidation of the resulting hydroxylamine **107** (Scheme 30). Paramagnetic compounds **108** thus formed are stable when stored in the crystalline state at 0 °C; they form stable salts on

Scheme 30



(*a*) 1) NCS, $CHCl_3$; 2) NaCN, DMSO; R = Ph, Me, CF_3, CO_2Et, 2-Py, 4-Py, Bu^t

deprotonation and stable coordination compounds when react with Ni^{2+}, Co^{2+}, Cu^{2+} and Pd^{2+} ions.[194]

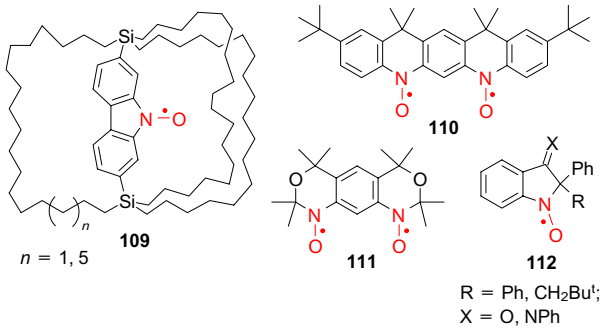
The developed synthetic routes to stable heterocyclic vinyl nitroxides can be used in the design of various high-spin systems, including derivatives with different types of spin carriers. Here it may be appropriate to carry out a preliminary quantum chemical study to identify configurations characterized by the strongest exchange coupling, including ferromagnetic ones.

3.2. (Hetero)arene-annulated cyclic nitroxides

Cyclic nitroxides in which the NO group is bound to the aromatic ring are actively used in the design of paramagnetic systems. This is due to the ease of synthesis and high stability of polyfunctional cyclic nitroxides. Furthermore, these radicals have a rigid skeleton, which may ensure a planar structure of the (di)aryl nitroxide moiety and, hence, high spin density injected into the aromatic ring. While analyzing structures of nitroxides isolated in a pure state, it is possible to identify the boundary separating stable and unstable nitroxides and to determine the stabilizing effect of substituents. The role of substituents is mainly to generate steric hindrance preventing the access to aromatic ring positions with an increased spin density from the outside or to provide for additional spin density delocalization. For example, if carbazole-*N*-oxyl, which is a relatively unstable paramagnetic compound, is placed into an artificially created cage of polymethylene units (Structures **109**), the stability of the resulting paramagnetic derivatives considerably increases and they at least can be studied by mass spectrometry.[195]

A greater stabilization effect, as compared with the environment of the whole paramagnetic molecule, is provided by introduction of bulky *tert*-butyl (or similar) groups into positions with high spin density. This prevents degradation of these radicals to give quinoid type structures and enables isolation of the radicals in a free state (Structures **110** and **111**).[196, 197] Finally, it was noticed that elongation of the conjugated system by introducing unsaturated heteroatomic substituents such as cyano, imino, keto and analogous groups leads to a substantial gain in stability of nitroxide radicals (Structures **112**).[198, 199]

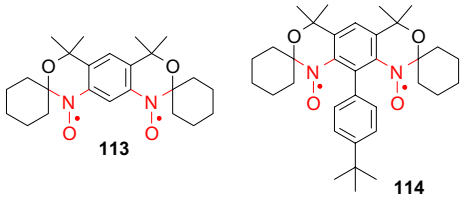
Structures 109 – 112



The main synthetic routes to cyclic conjugated nitroxides are the same as used for the preparation of acyclic alkyl aryl and diaryl nitroxides: oxidation of hydroxylamines and amines.[200] The former can be transformed into the paramagnetic state under relatively mild conditions, whereas the latter have become more accessible with the development of metal-catalyzed amination. The two above

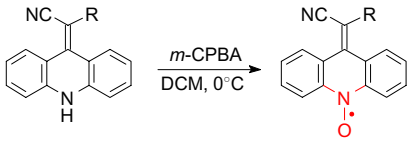
circumstances actually determine the choice of the sequence for the synthesis of one or another organic radical. In the absence of groups susceptible to the action of strong oxidants, it is convenient to use amines as the starting compounds. The oxidation of cyclic diamines with *m*-CPBA gives rise to stable benzobis(oxazine-*N*-oxyl) biradicals **111**, **113** and **114** in good yields (30–70%).[196] In these biradicals, strong intramolecular exchange of ferromagnetic nature takes place ($2J/k_B > 400$ K); the maximum exchange was found for octamethyl derivative **111** with a planar structure of the paramagnetic moiety. In the solid phase, biradical **111** ($S = 1$) forms highly isotropic exchange-coupled antiferromagnetic chains, as the zero-field splitting parameter (D) for this biradical is considerably lower than the exchange coupling parameter ($|D/2J| \approx 3 \times 10^{-3}$).

Structures 113, 114



The *m*-CPBA oxidation of secondary amines **115a**,**b** gave 2-(10-yloxy-9-acridin-9(10*H*)-ylidene)malononitrile (**116a**) and ethyl 2-cyano-2-(10-yloxyacridin-9(10*H*)-ylidene)acetate (**116b**), in which the nitroxide group was stabilized by conjugation with two aromatic rings and by cyano-substituted 1,1′-ethylene bridge. The products were isolated in a free state (Scheme 31).[201]

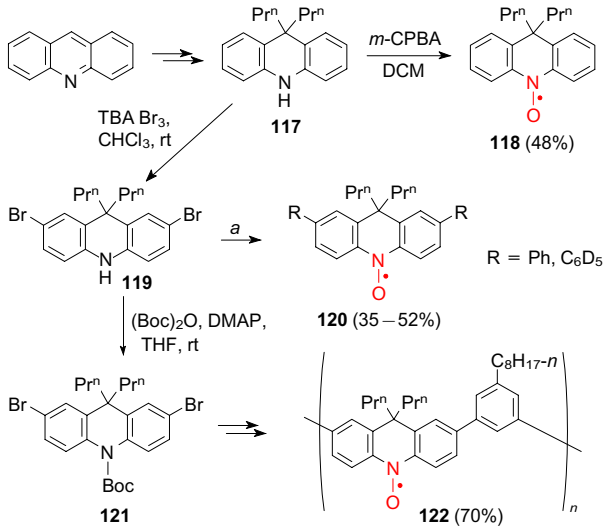
Scheme 31



The photochemical alkylation of acridine with butanoic acid to give 9,9-di-n-propyldihydroacridine **117** and subsequent oxidation with *m*-CPBA afforded cyclic diaryl nitroxide **118** (Scheme 32).[202] Analysis of the magnetic properties of paramagnet **118** showed predominance of ferromagnetic exchange coupling in the solid state; the coupling occurs through the short intermolecular contact of the nitroxide group with the hydrogen atom in the *meta*-position relative to the NO group.

The bromination of acridine derivative **117** (synthesized by a different method[203] from methyl *N*-phenylanthranilate) yielded dibromide **119**, which was subjected to Suzuki cross-coupling with boronic acid, giving rise to substituted dihydroacridines in ~23% yields. The intermediates were oxidized by usual methods to obtain nitroxide radicals **120**, in particular a radical deuterated into the lateral benzene rings. By carrying out cross-coupling of compound **121** with the protected amino group, Oka *et al.*[203] were able to implement an efficient synthesis of polyradical **122** ($n \approx 9$). The concentration of spins in the obtained polymer reached

Scheme 32

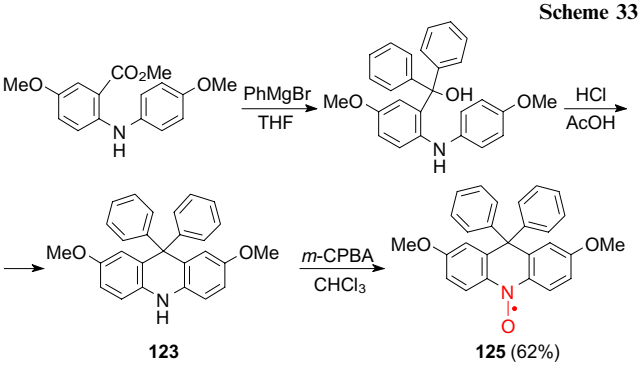


(*a*) 1) $RB(OH)_2$, $Pd(PPh_3)_4$, K_2CO_3, THF, H_2O; 2) *m*-CPBA, DCM; Boc is *tert*-butyloxycarbonyl, TBA is tetra-n-butylammonium

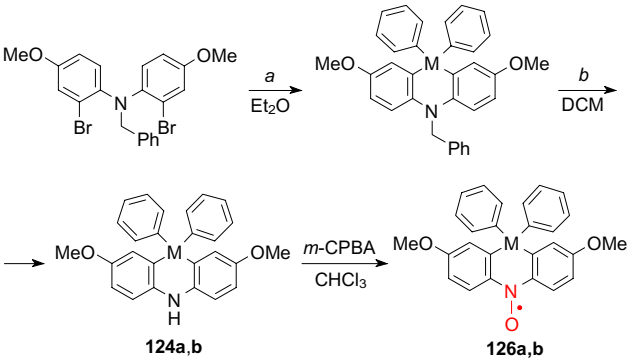
0.7; the exhange coupling was mainly ferromagnetic ($J/k_B = 8.6$ K).

The synthesis of a number of stable diaryl nitroxides with organic and organoelement bridges was reported by Professor Yoshioka and co-workers[204] (Schemes 33 and 34). In the final step, disubstituted amines **123** and **124a**,**b** were successfully oxidized with *m*-CPBA to give radicals **125** and **126a**,**b**. The molecular and crystal structures of the products were determined by X-ray diffraction. According to cyclic voltammetry data, the obtained para-

Scheme 33



Scheme 34

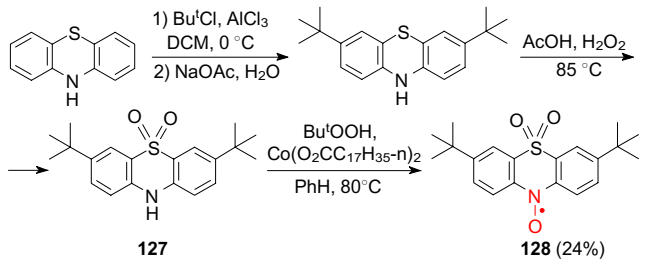


(*a*) 1) Bu^nLi, 2) MPh_2Cl_2; (*b*) H_2, Pd-sponge; M = Si (**a**, 47%), Ge (**b**, 65%)

magnets were reversibly oxidized, with organoelement derivatives **126a**,**b** being oxidized at higher potentials than nitroxide **125**, namely, 0.19, 0.17 and 0.10 V, respectively, *versus* the Fc/Fc^+ ferrocene redox pair.

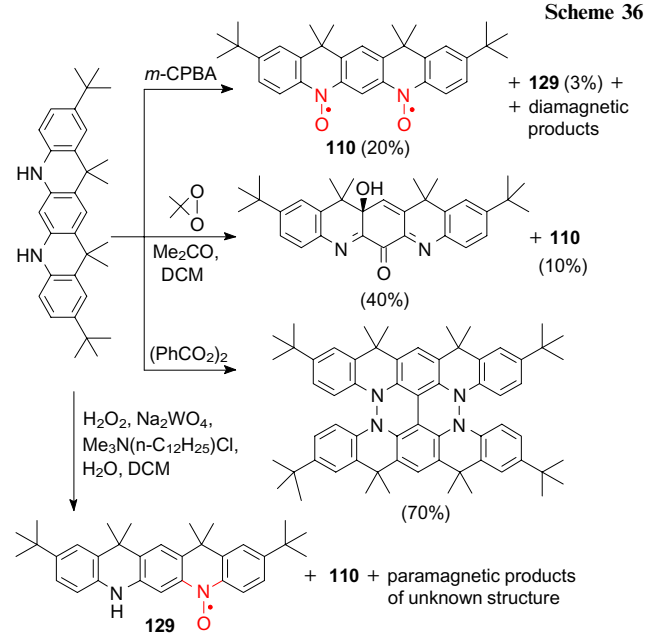
In some cases, the use of *m*-CPBA for the oxidation of disubstituted amines led to unsatisfactory results. For example, the conversion of diarylamine **127** with an SO_2 bridge to the corresponding nitroxide proved to be the problematic step in the whole sequence of transformations. Among the tested reagents, which included *m*-CPBA, H_2O_2 in the presence of $NaWO_4$ and $Bu^tOOH + Co(O_2CC_{17}H_{35}\text{-n})_2$, only the last-mentioned system made it possible to obtain highly stable diaryl nitroxide **128** in 24% yield (Scheme 35). This nitroxide had a reversible and record-high oxidation potential of 1.33 V (*versus* Ag/AgCl, KCl electrode).[205]

Scheme 35



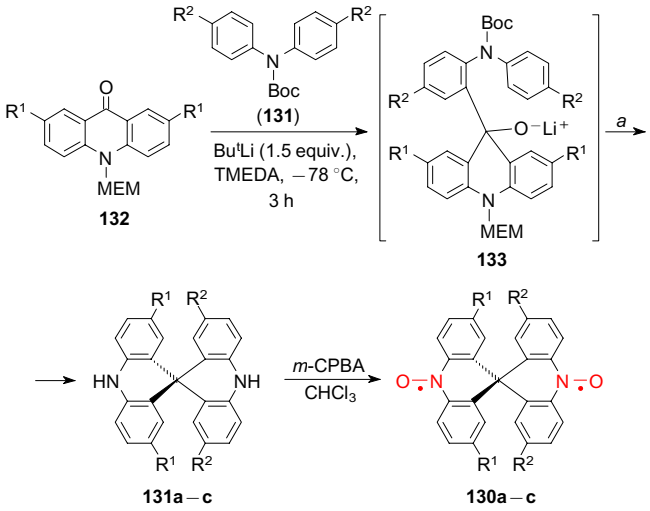
The increase in the number of nitroxide groups with the goal to obtain bi- and polyradicals with extended conjugated systems complicates not only the whole synthetic route, but also the key oxidation step. An example of painstaking search for the optimal conditions for the preparation of triplet biradical **110**, investigation of the reactions involved in the oxidation step and isolation and characterization of side products (for example, radical **129**) is provided by the study of Rajca *et al.*[206] (Scheme 36). The authors demonstrated, in particular, that the preparation of target biradical **110** is accompanied by the formation of numerous diamagnetic side products as a result of oxidation of aromatic moieties of the initial molecule.

Scheme 36



It took approximately 20 years for Ishida and co-workers[207–210] to develop a method for the synthesis of triplet biradicals **130a–c** with spiro coupled diaryl nitroxide moieties. According to X-ray diffraction data, strong intermolecular antiferromagnetic exchange coupling ($2J/k_B \approx -140$ K), caused by proximate positions of nitroxide groups, occurred in radical **130a** [the shortest distances between the oxygen atoms of the paramagnetic moieties were 3.176(2) and 3.184(2) Å]. In order to reduce the tendency of the radical to dimerization, its derivatives **130b**,**c**, containing two or four *tert*-butyl groups, were obtained. The key step of the synthesis of spirobiacridines **131a–c** was one-pot process including the addition of heteroaromatic ketone **132** to *ortho*-lithiated protected diarylamine **133**, subsequent acid-catalyzed intramolecular Friedel–Crafts reaction and final deprotection (Scheme 37). Analysis of magneto-structure correlations inherent in alkyl-substituted biradicals **130b**,**c** revealed pronounced intramolecular exchange ($2J/k_B \approx 22-23$ K) caused by the proximity and virtually orthogonal positions of the paramagnetic moieties.

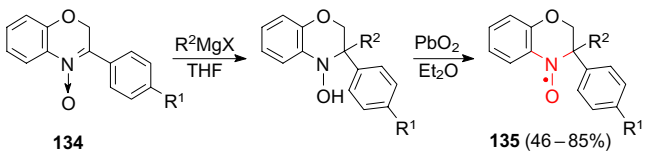
Scheme 37



(*a*) 1) AcOH, 0 °C, 1 day; 2) 1 M HCl, 12 h;
$R^1 = R^2 = H$ (**a**), Bu^t (**b**); $R^1 = H$, $R^2 = Bu^t$ (**c**);
MEM is 2-methoxyethoxymethyl

As noted in the beginning of this Section, cyclic nitroxides can also be obtained by oxidation of hydroxylamines; in some cases, it is sufficient to expose hydroxylamines in air. Hydroxylamines are traditionally synthesized by addition of Grignard reagents or organolithium compounds to nitrones. For example, nitrones **134** were converted in this

Scheme 38

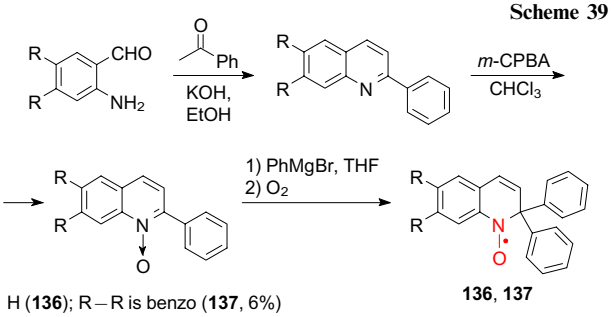


R^1 = H, Cl, OMe; R^2 = Ph, Bn, Me, Et, Bu^t

way to nitroxide radicals **135** with the benzoxazine skeleton, which were stable under ambient conditions (Scheme 38).[211]

2,2-Diphenyl-1,2-dihydroquinoline-*N*-oxyl (**136**) and 2,2-diphenyl-1,2-dihydrobenzo[*g*]quinoline-*N*-oxyl (**137**) were obtained by a similar route (Scheme 39).[212] According to X-ray diffraction data, no short contacts involving atoms of the NO group are present in the solid radical **136**, whereas analogous compound **137** with a more extended aromatic system has such contacts within the centrosymmetric dimers (Fig. 11). Remarkably, they serve as a channel providing the predominance of ferromagnetic exchange coupling ($2J/k_B$ = 6.6 K).

Scheme 39



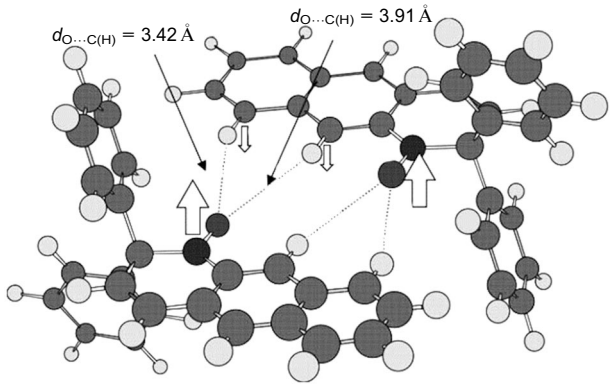
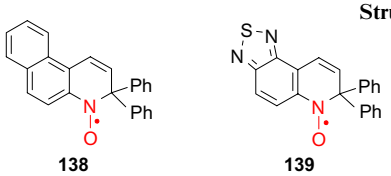


Figure 11. Short contacts within dimers {**137**···**137**} responsible for ferromagnetic exchange.[212] Published with permission from Elsevier.

It is noteworthy that modification of nitroxide **137** by changing the site of conjugation of the aromatic moieties (compound **138**) or by replacing the annulated benzene ring by a thiadiazole ring (compound **139**) may bring about unexpected magnetic consequences. Indeed, 3,3-diphenyl-3,4-dihydrobenzo[*f*]quinoline-4-oxyl (**138**) form a dimer packing in crystals; however, the distance between the radical centres is large and the exchange coupling is low. Therefore, radicals **138** behave as isolated spin doublet over a broad temperature range, whereas thiadiazole nitroxides **139** isoelectronic to them form a one-dimensional columnar structure consisting of skewed π-stacks, with rather strong antiferromagnetic exchange within the stack (J/k_B = −67 K).[213]

Structures 138, 139

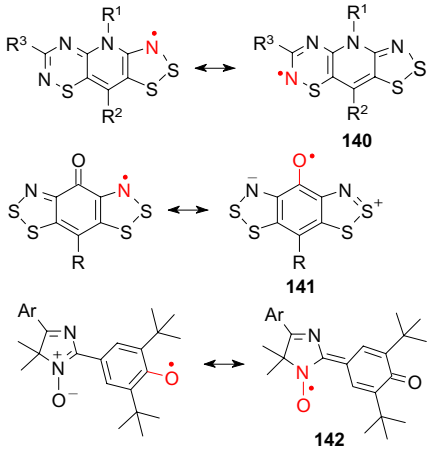


To summarize, one can state that systematic development of methods for the synthesis of (hetero)arene-annulated cyclic nitroxides generated a fundamental base that was used to prepare stable organic radicals and high-spin systems for a variety of applications. It is beyond doubt that this class of paramagnets is in most demand for the molecular design of magnetic materials.

3.3. Hybrid phenoxyl nitroxides

The active development of the chemistry of so-called hybrid radicals started in the second decade of the 21st century. In these resonance-stabilized paramagnetic organic compounds, the unpaired electron can formally be located on one of the two paramagnetic moieties that correspond to a certain class. Examples of such species are planar 1,2,3-dithiazolo-1,2,4-thiadiazinyl radicals **140** and hybrid systems **141** and **142** (Scheme 40),[214–216] the resonance forms of which are well-known paramagnets.

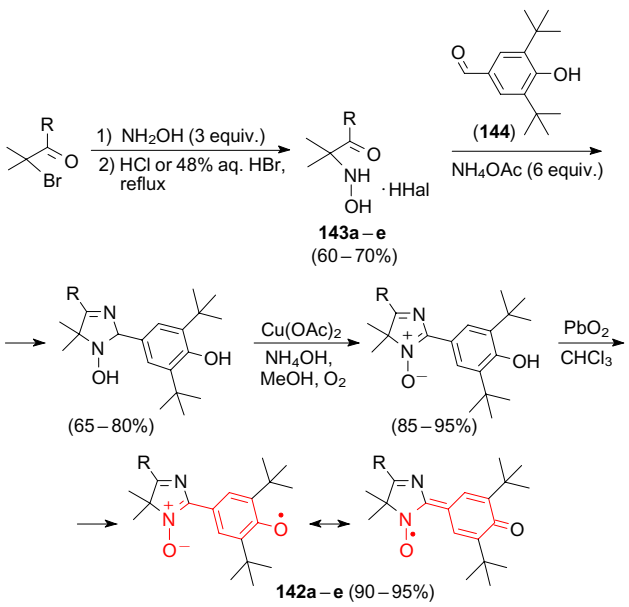
Scheme 40



A new group of hybrid radicals, phenoxyl nitroxides **142a–e**, were characterized in detail in 2020. These compounds are obtained by successive oxidation of the products formed upon condensation of 2-hydroxylamino ketones **143a–e** with sterically hindered 2,6-di-*tert*-butyl-4-formylphenol (**144**) (Scheme 41).[217] The resulting hybrid paramagnets are high-melting crystalline compounds. In the solid state, they can be stored for infinite time at room temperature. In solutions with concentrations of 10^{-4}–10^{-3} mol L^{-1}, radicals **142** slowly decompose, with their half-lives ranging from 24 h to 10 days.

A characteristic feature of hybrid radicals of this class is that their structural parameters in the crystalline state are similar to those for phenoxyl radicals, while in solutions, they behave as conjugated nitroxides according to EPR data. The molecular structure of radical **142d** is characterized by peculiar C–O [1.246(3) Å) and C–C (1.409(3) Å] bond lengths between the cyclic moieties (Fig. 12). The length of the former bond is close to that in 2,4,6-tri-*tert*-butylphenoxyl and differs considerably from the C=O bond length in diamagnetic 3,3,5,5-tetra-*tert*-butyl-4,4-diphenoquinone (1.228 Å). The latter bond is a typical sesquialteral bond with a length similar to the length of the bridging C=C bond (1.409 Å) in the conjugated phenoxyl radical of galvinoxyl. The molecules of **142a–e** are virtually planar; the torsion angles between the imidazole

Scheme 41



R = Me (**a**), Et (**b**), Ph (**c**), 4-PhC$_6$H$_4$ (**d**), 5-bromothienyl (**e**)

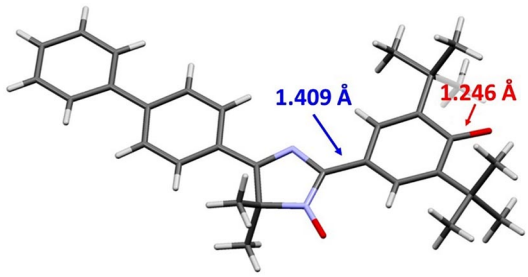


Figure 12. Molecular structure of hybrid radical **142d**. The figure was created by the authors.

moiety and the phenoxyl ring are in the range of 0.5–9° for all radicals.

The EPR spectra of hybrid radicals **142a–e** are complex multiplets in which one can clearly detect the main triplet signal, which splits due to coupling of the unpaired electron with the nitroxide nitrogen atom [$a(^{14}N) \approx 0.56$ mT and $g_{iso} = 2.0056$, where g_{iso} is the isotropic *g*-factor]. It is noteworthy that g_{iso} is between ~2.0044, which is typical of conjugated phenoxyl radicals, and ~2.0065, which is typical of nitroxides. A satisfactory simulation of multiplet signals is attained by taking account of the HFC of the unpaired electron with the nuclei of two nitrogen atoms and two hydrogen atoms connected by a system of conjugated bonds (Fig. 13).

It was shown that the radical stability is mainly affected by the nature of substituent R at the C(5) atom of the heterocyle. Indeed, derivatives **142** with *para*-X-substituted (X = Alk, Hal, Ar, OAlk) (hetero)aryl moiety in position 5 are stable in solutions and can be purified by chromatography, whereas radicals with R = Alk or X = H can be only recrystallized. A study of the effect of steric factors on the stability of compounds **142** showed that the most stable radicals are those having a *tert*-butyl group at the α,α′-carbon atoms of the phenoxyl centre. It was found that even methyl-substituted phenoxyls can be preserved in solutions for long periods of time.[218] This fact points to the possibility

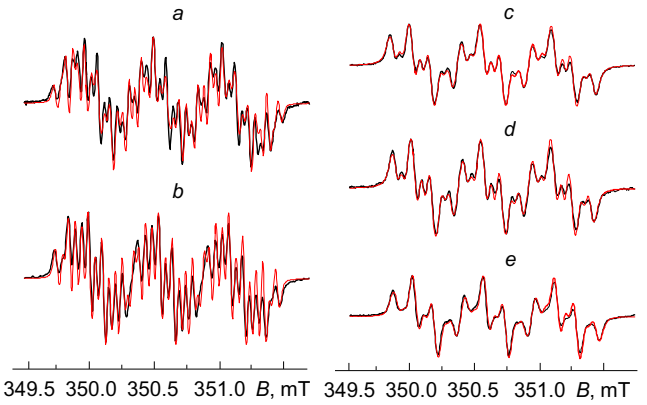


Figure 13. Experimental (blue line) and simulated (red line) EPR spectra of dilute (10^{-4} mol L^{-1}) oxygen-free toluene solutions of radicals **142a–e** (Figs *a–e*, respectively) at 295 K.[217] Published with permission from American Chemical Society.

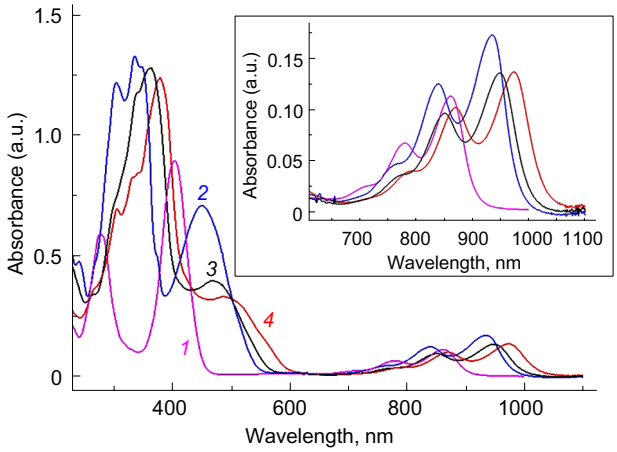


Figure 14. UV/Vis absorption spectra (in the inset, near-IR spectra) for **142b** (*1*), **142c** (*2*), **142d** (*3*) and **142e** (*4*). The figure was created by the authors using Supplementary Information of Ref. 217.

of further modification of the phenol moiety of the hybrid radicals in order to flatten the molecule and provide for π-stacking interactions in the crystal.

The electronic absorption spectra of radicals **142a–d** exhibit quite noticeable bands in the near-IR range, at 780–870 and 870–980 nm, in addition to the strong bands in the ranges of 330–390 and 400–500 nm (Fig. 14).

The magnetic properties of radicals **142** were studied by DFT at the UB3LYP/cc-pVDZ level of theory using the single crystal geometry as the starting point to optimize the molecular structure. An example of the calculated SOMO orbital and electron density distribution map for hybrid radical **142c** is shown in Fig. 15. It can be seen that the major part of the electron density of the unpaired electron is concentrated around the conjugated nitroxide-phenoxyl moiety and the spin densities on heteroatoms have positive sign.

According to Zaytseva *et al.*,[217] the magnetic properties of hybrid radicals **142** depend on the nature of substituent R in the heterocycle. The dependences $\chi T(T)$ for radicals **142a**,**b**,**d** attest to the predominance of weak antiferromag-

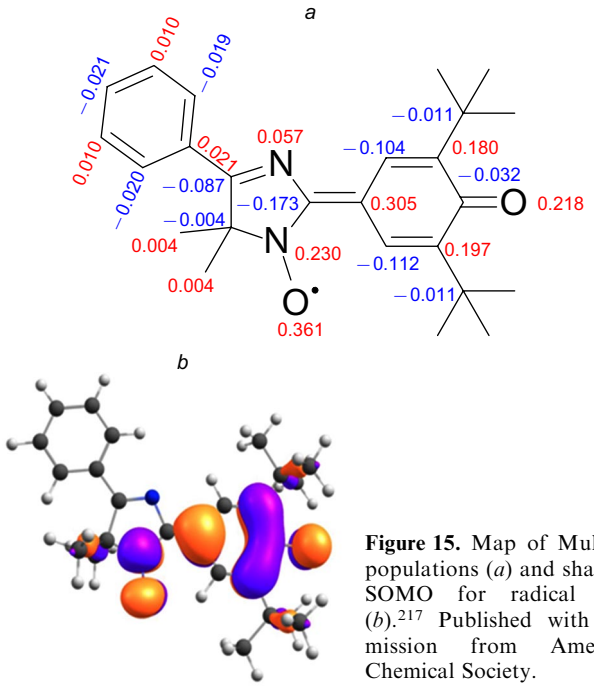
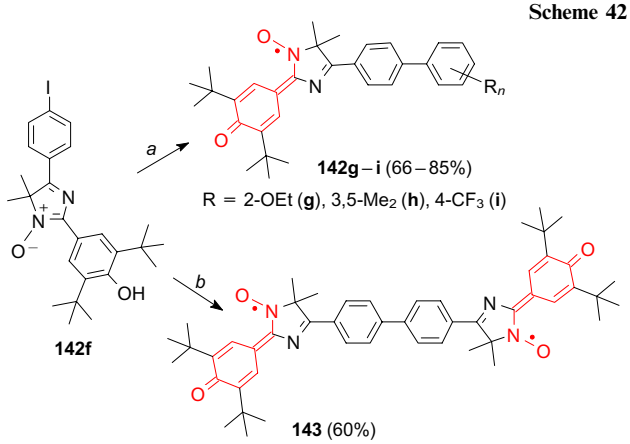


Figure 15. Map of Mullican populations (*a*) and shape of SOMO for radical **142c** (*b*).[217] Published with permission from American Chemical Society.

netic exchange couplings, whereas in the case of radical **142c**, weak ferromagnetic exchange predominates. A relatively strong antiferromagnetic exchange was detected for radical **142e** ($2J/k_B = -52$ K), which forms dimer packing.

Phenoxyl-nitroxide radicals **142** are more thermodynamically stable than galvinoxyl and, furthermore, they can be subjected to chemical modification *via* introduction of additional functional groups. Thus, compounds like **142** can be considered as new building blocks convenient for the design of multispin exchange-coupled systems. In 2018, it was shown[219] that 5-(4-iodophenyl) 4*H*-imidazole derivative **142f** can undergo cross-coupling reactions with arylboronic acids to give the corresponding biphenyls, which are readily oxidized by air oxygen or PbO_2 to give target phenoxyl-nitroxides **142g**–**i**. The reaction of radical **142f** with $B_2(pin)_2$ (pin is pinacolate) in the presence of $PdCl_2(PPh_3)_2$ proceeds *via* the 1,3,2-dioxoborolane intermediate to give biphenyl-bis(imidazole) as the homocoupling product. This product is oxidized to stable conjugated biradical **143** in a quantitative yield (Scheme 42).[219]

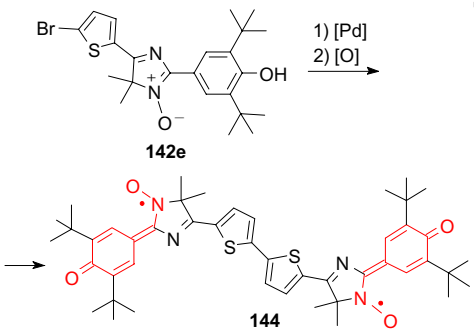
Scheme 42



(*a*) 1) $ArB(OH)_2$, $Pd(PPh_3)_4$, K_2CO_3, PhMe, Δ; 2) PbO_2, $CHCl_3$;
(*b*) 1) $B_2(pin)_2$ (0.5 equiv.), $Pd(PPh_3)_2Cl_2$, KOAc, DMF, Δ;
2) PbO_2 (20 equiv.), $CHCl_3$, 1 h

A similar approach was utilized to convert bromo derivative **142e** to dithienyl biradical **144** (Scheme 43).[220]

Scheme 43



In general, the principles developed for the design of hybrid paramagnets can be applied to obtain extended singlet biradicals possessing high stability. These biradicals, containing an electron-donating π-linker, are of interest as switchable electroactive A–D–A triads for the design of magnetic materials that respond to external stimuli.

3.4. Classical nitronyl nitroxide and imino nitroxides

Nitronyl nitroxides and related imino nitroxides contain a conjugated paramagnetic moiety (ONCNO and ONCN, respectively) in which the spin density is mainly concentrated on nitrogen and oxygen atoms. The spin density on the carbon atom is negative and is approximately two times lower in magnitude than that on any of heteroatoms.[221, 222] The pattern of distribution of spin density inherent in nitronyl nitroxides and imino nitroxides provides for ferromagnetic intermolecular exchange in their solid phases and for magnetic ordering effects in the crystals.[223, 224]

Depending on the heterocyclic skeleton, nitronyl nitroxides and imino nitroxides can be classified into several structural types (Fig. 16). The best studied compounds are 2-imidazoline nitroxides including an extensive series of

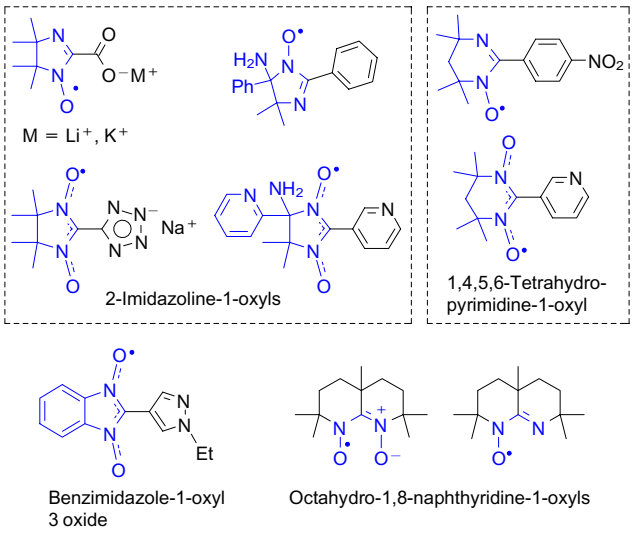
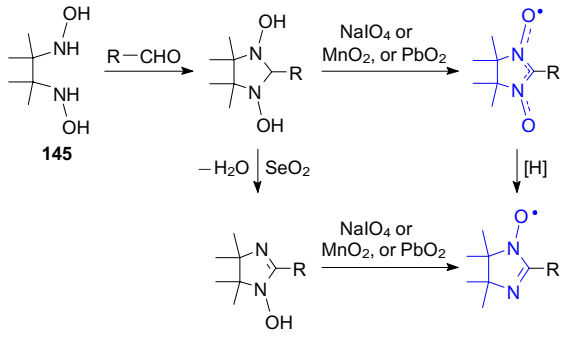


Figure 16. Examples of nitronyl nitroxides and imino nitroxids isolated in a free state.

functional derivatives with a broad range of practical applications. Some applications are associated with specific structural features of nitronyl nitroxide-substituted fused polyaromatic compounds and their higher homologues — graphene nanostructures, which are the subject of a review published in 2020.[17]

There are several known approaches for the synthesis of 2-imidazoline nitronyl nitroxides and their reduced derivatives — the corresponding imino nitroxides (Scheme 44). The classical Ullman method[225–227] implies the condensation of 2,3-bis(hydroxylamino)-2,3-dimethylbutane (**145**) with aldehydes and the subsequent oxidation of intermediate 1,3-dihydroxyimidazolidines. The reactions that result in substitution or substituent transformation are used to expand the range of polyfunctional nitronyl nitroxides. These reactions are of synthetic value not only for the nitronyl nitroxide series, but also for their diamagnetic precursors, dihydroxyimidazolidines. This makes it possible, for example, to prepare 2-aminophenyl-substituted nitronyl nitroxide from 2-nitrobenzaldehyde.[228]

Scheme 44



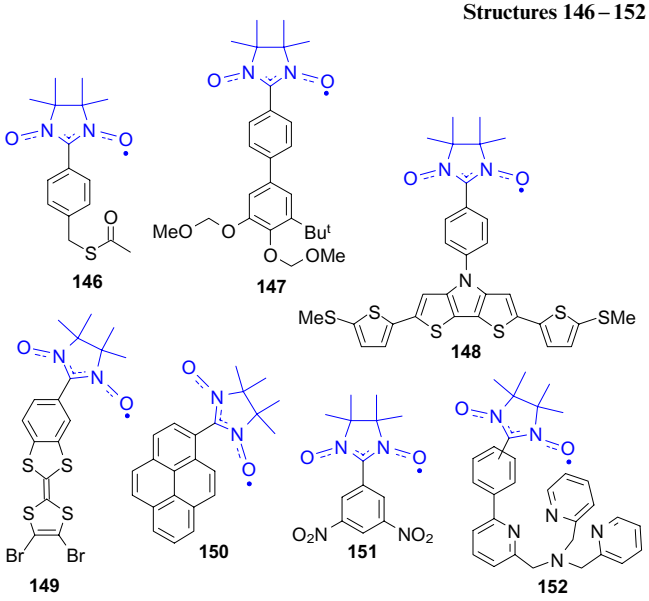
Imino nitroxides are formed upon the reduction of nitronyl nitroxides with the $NaNO_2$–AcOH system or PPh_3. An alternative approach is dehydration of dihydroxyimidazolidines, which, in some cases, proceeds spontaneously,[229] but heating of reactants in MeOH in the presence of catalytic amounts of SeO_2 is more often required (see Scheme 44).

The choice of synthetic strategy towards polyfunctional nitronyl nitroxides usually implies a balance of known approaches and researcher's own experience and intuition.[230,231] Most often, preference is given to the Ullman method, the scope of which is limited in rare cases by availability of the required aldehydes. The first step is carried out in water, if the aldehydes are water-soluble, and sulfuric acid salt **145**·H_2SO_4·H_2O is used as the substrate. Water-insoluble aldehydes can be introduced in the condensation with free **145** in MeOH, EtOH or DMF. The reaction proceeds at room temperature, but for some substrates, *e.g.*, for porphyrin or phthalocyanine derivatives, the reaction mixture must be kept for a long time or even refluxed in a MeOH–toluene mixture[232] or in THF.[16] If the reaction is carried out in the presence of TsOH, dehydration of the adduct takes place to give 1-hydroxyimidazoline derivative.[233]

The oxidation of 1,3-dihydroxyimidazolidines is performed, most often, by treatment with PbO_2 in DCM or $NaIO_4$ in the $CHCl_3$–H_2O or DCM–H_2O two-phase system. According to our experience, the highest yields of nitronyl nitroxides are obtained with MnO_2 in EtOH. Under specific conditions where it is necessary to preserve sensitive functional groups, mild oxidants are chosen such as tetra-n-propylammonium perrhutenate (TPAP)–*N*-methylmorpholine *N*-oxide (NMO)[234] or oxygen in the presence of Et_3N.[43]

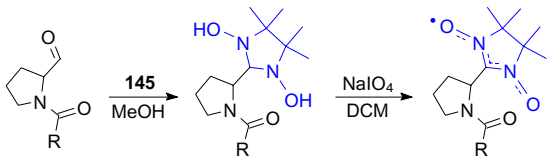
Quite an extensive series of nitronyl nitroxide radicals, meant for various applications, have been obtained by the Ullman method from available or specially prepared aldehydes. Examples are provided by paramagnets **146**–**152**, which were designed and implemented according to their functional purpose: to study chemisorption on the surface of various materials (**146**);[235–237] to fabricate memory storage devices (**147**),[238] high-spin cations (**148**),[239] magnetically active current conductors (**149**)[240] and fluorescent chemosensors (**150**);[241] to study transitions to the ferromagnetically ordered state in optically active crystals (**151**);[242] and to form heterospin complexes (**152**).[243]

Structures 146–152



Special mention should be made of chiral paramagnets,[244] especially those in which the paramagnetic moiety is directly bound to the chiral centre.[245–247] For example, two pairs of optically active nitronyl nitroxides **153** (Scheme 45),[246] demonstrating a strong Cotton effect in the 200–400 nm range, were prepared.

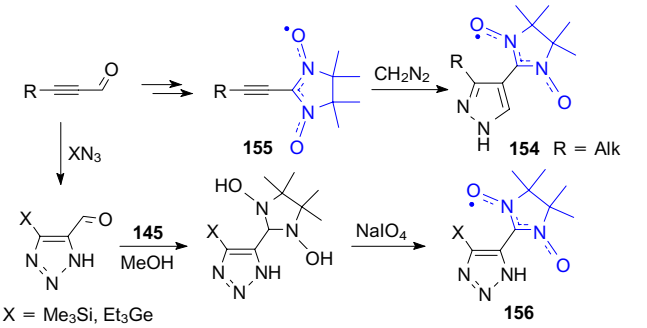
Scheme 45



R = OBu^t, $C_6H_4NO_2$-4

An example of using combined approach to the synthesis of nitronyl nitroxides is the preparation of organoelement derivatives of spin-labelled azoles. It was shown that pyrazoles **154** can be conveniently obtained by the reaction of paramagnetic acetylene derivatives **155** with diazomethane. Meanwhile, the synthesis of 2-(4-trimethylsilyl-1*H*-1,2,3-triazol-5-yl)- and 2-(4-triethylgermyl-1*H*-

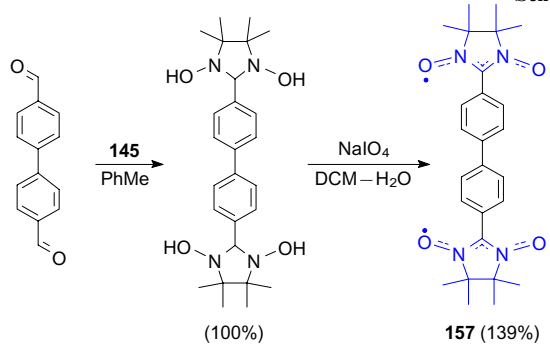
Scheme 46



1,2,3-triazol-5-yl)-substituted nitronyl nitroxides **156** is, conversely, started with the assembly of triazolecarbaldehydes (Scheme 46).[248]

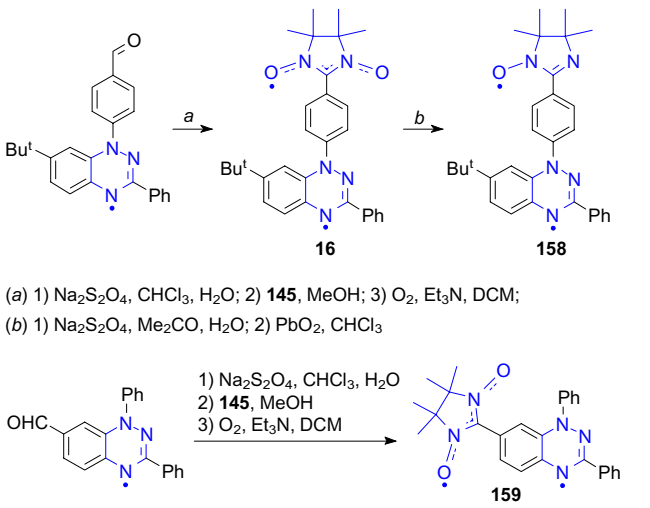
Symmetrical biradicals are synthesized by the Ullman method, provided that the corresponding dialdehyde are available. It is only necessary to select the conditions of condensation and oxidation steps. For example, condensation of biphenyl-4,4′-dicarbaldehyde with 2 equiv. of compound **145** in toluene and the subsequent oxidation of the obtained bis(dihydroxyimidazolidine) by treatment with $NaIO_4$ in the DCM – H_2O two-phase system give biphenyl-4,4′-bis(nitronyl nitroxide) **157** in a moderate yield (Scheme 47).[249] A similar procedure with slightly varied experimental conditions was used to prepare nitronyl nitroxide biradicals with both carbo-[250–253] and heterocyclic[254–256] bridging groups; the products were structurally characterized. These compounds represent a valuable systematic series to reveal magneto-structural correlations. The classical synthetic route was also used to prepare a variety of spin-labelled luminophores,[257] which are necessary to study the relaxation dynamics of photoexcited multispin systems, and biradicals with long flexible linkers, such as *p*-phenylene – $O(CH_2CH_2O)_6$ – *p*-phenylene, meant for studying the dynamic behaviour of two-spin structures in various solvents.[258]

Scheme 47



Similarly, the corresponding formyl derivatives of triazinyl radicals were converted to heterobiradicals **16**, **158** and **159** with the triplet ground state containing nitronyl nitroxide or imino nitroxide and benzotriazinyl moiety (Scheme 48). Biradical **16** is characterized by a large singlet – triplet splitting ($2J/k_B = +234 \pm 36$ K) and high thermal stability, sufficient for its quantitative sublimation in vacuum at a temperature of 140 °C and a pressure of $\sim 6 \times 10^{-6}$ mbar.[256] Even a greater singlet – triplet splitting ($2J/k_B = +876 \pm 36$ K) was found for biradical **159**. Like

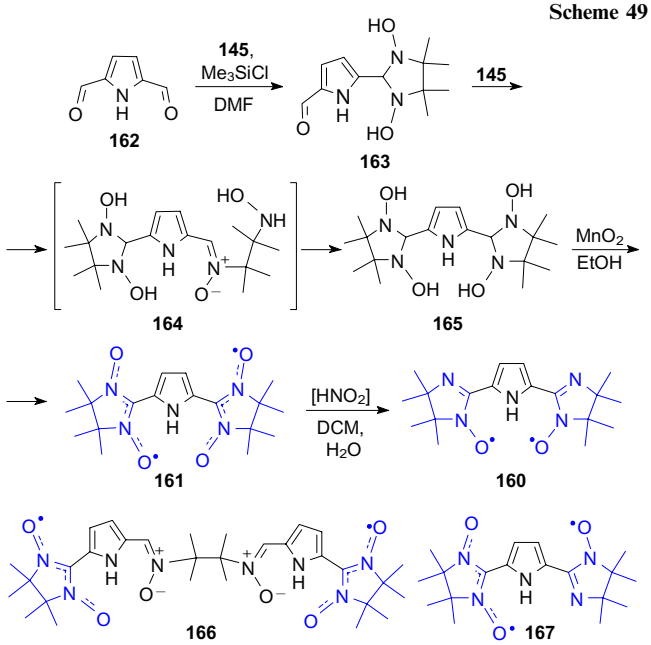
Scheme 48



compound **16**, this biradical has a high thermal stability and a sufficient volatility, which allows its deposition on, for example, $SiO_2/Si(111)$ surface by molecular beam epitaxy.[259]

Biradicals **160** and **161** were prepared by the reaction of pyrroledicarbaldehyde **162** with 2 equiv. of compound **145** (*via* the step of formation of intermediate **163**) followed by oxidation of product **164**.[260] It was noted that if the condensation was carried out in DMF in the presence of 4 equiv. of Me_3SiCl, diadduct **165**, which precipitated as the solid phase, virtually did not contain impurities and, after oxidation, afforded biradical **161** in an overall yield of 12% (Scheme 49). The reduction of compound **161** resulted in the generation of imino nitroxide diradical **160** in a yield exceeding 80%. If the condensation was carried out in the absence of Me_3SiCl, the oxidation of the reaction product furnished a complex mixture, from which biradicals **161** (16% yield) and **166** (20% yield) and traces of mixed biradical **167** were isolated. The formation of compound **166** is a rather unusual fact; this is caused by intermolecular

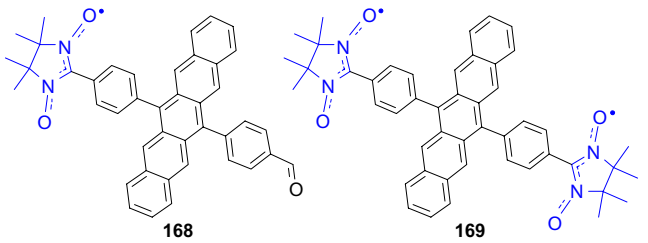
Scheme 49



condensation of hydroxylamine and aldehyde groups, giving rise to the dinitrone bridge between the pyrrole rings.[260] According to X-ray diffraction data, biradicals **160** and **161** are planar. In these molecules, the pyrrole-2,5-diyl moiety is topologically similar to a *p*-phenylene bridge, which accounts for the observed intramolecular antiferromagnetic exchange coupling with $2J/k_B = -44$ and -155 K, respectively.

Special efforts were required for the synthesis of spin-labelled pentacene derivatives **168** and **169**. Shimizu *et al.*[261] reported the synthesis of these derivatives from pentacene-6,13-dione *via* the formation of the corresponding dialdehyde in the dark to prevent photodecomposition of the pentacene core. Interestingly, biradical derivative **169** proved to be much more stable to degradation than the pristine pentacene and even 6,13-bis(triisopropylsilylethynyl)pentacene. This is due to the appearance of multiple fast relaxation pathways for the photoexcited states in the spin-labelled derivative.

Structures 168, 169

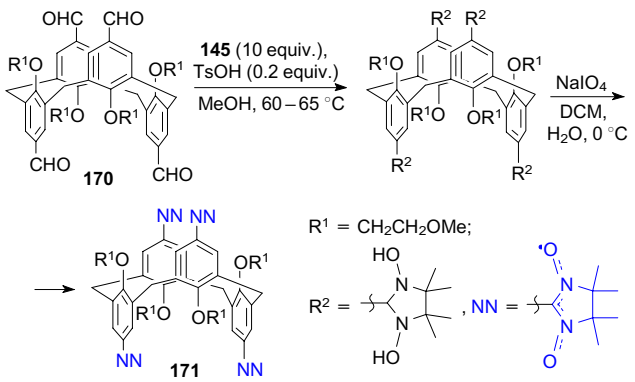


168 **169**

The condensation of di- and tetra-aldehydes with the calix[4]arene core, for example compound **170**, with bis(hydroxylamine) **145** in MeOH in the presence of *p*-toluenesulfonic acid gave the corresponding tetra(1,3-dihydroxyimidazoline) in ~90% yield. The oxidation of the resulting adduct by $NaIO_4$ (1 equiv. per 1,3-dihydroxyimidazoline moiety) in aqueous DCM at 0 °C produced tetraradical **171** in 28% yield (Scheme 50).[262] The transformation of analogous tetraformyl calix[4]arene derivative with $R^1 = Pr^n$ into the corresponding nitronyl nitroxide polyradical was carried out under somewhat different conditions: the first step was the condensation of carbonyl compound with bis(hydroxylamine) **145** in DMF, and the adduct thus formed was oxidized by treatment with MnO_2 in EtOH. In this case, the overall yield of the target paramagnet reached 30%.[263]

Hexaradical **172** was the record-setting compound regarding the number of paramagnetic groups introduced

Scheme 50



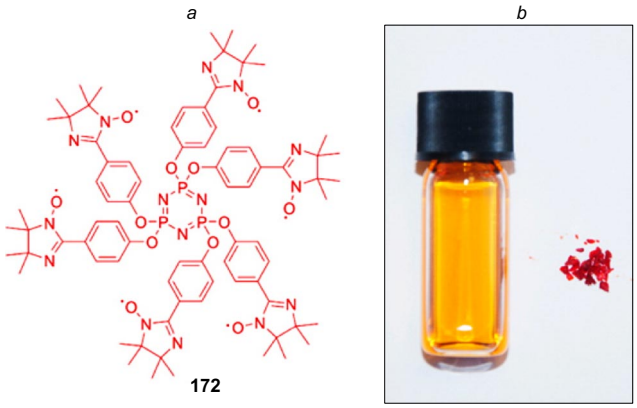
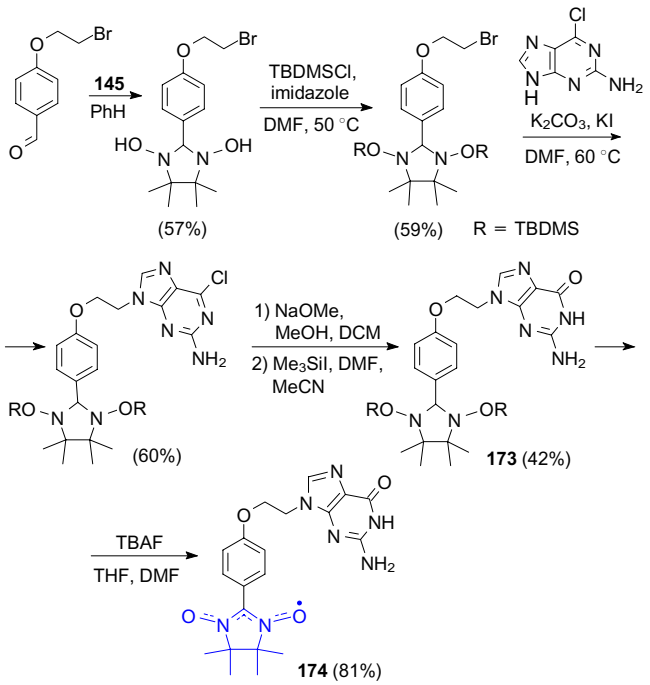


Figure 17. Structure of hexaradical **172** (*a*), its solution in chloroform and crystals (*b*).[264] Published with permission from American Chemical Society.

in the molecule by the Ullman method (Fig. 17). It was synthesized in 42% yield by the reaction of the corresponding hexa-aldehyde with bis(hydroxylamine) **145** in the presence of TsOH in MeOH followed by the oxidation by sodium periodate in the DCM – H_2O two-phase mixture in the presence of phosphate buffered saline at pH 7.[264] Surprisingly, the authors succeeded in obtaining crystals of hexaradical **172** suitable for X-ray diffraction; this was done by slow diffusion of heptane into a solution of hexaradical in a mixture of ethyl acetate with toluene and heptane.

If necessary, the OH groups in the intermediate 1,3-dihydroxyimidazoline can be protected, for example, by treatment with TBDMSCl in the presence of imidazole. The use of protectiing group made it possible to implement the whole sequence of transformations of 4-(2-bromoethoxy)benzaldehyde into guanine derivative **173**. The deprotection carried out by treatment of product **173** with

Scheme 51

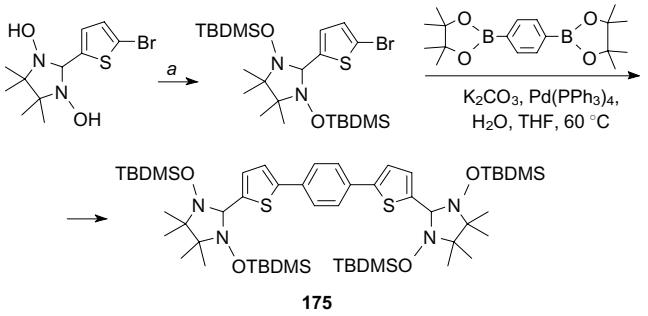


tetra-n-butylammonium fluoride in a THF – DMF mixture gave the target nitronyl nitroxide **174** (Scheme 51).[265]

The approach implying the use of protecting groups proved to be efficient in the synthesis of a number of nitronyl nitroxide biradicals with the oligoaromatic linker (Schemes 52 – 56).[266] In the first step, 5-bromothiophene-2-carboxaldehyde or 4-bromobenzaldehyde reacted with compound **145** in MeOH to give the corresponding 1,3-dihydroxyimidazolidines in > 80% yields (see Schemes 52, 53). After introduction of protecting groups, 1,3-dihydroxyimidazolidines were subjected to Suzuki cross-coupling with benzene-1,4-diboronic acid bis(pinacol) ester to give biradical precursors **175** and **176** (> 60% yields).

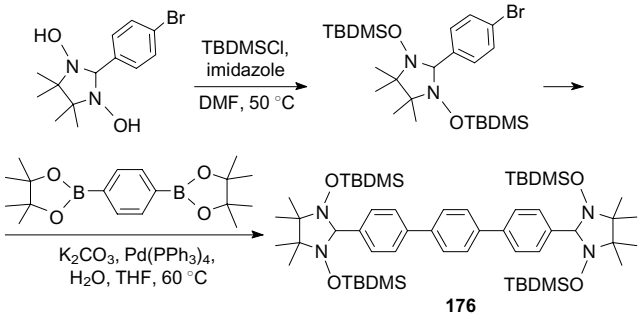
It should be noted that 2-(5-bromothienyl)-1,3-dihydroxyimidazolidine with protected OH groups did not react with the bis(pinacol) ester of thiophene-2,5-diboronic acid under these conditions. The target product **177** was obtained in 66% yield by another method: cross-coupling of

Scheme 52

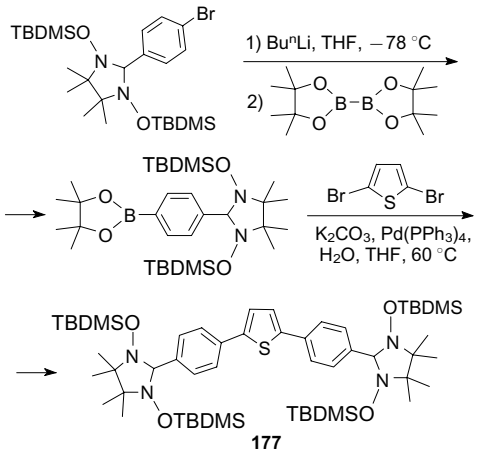


(*a*) TBDMSCl, imidazole, DMF, 50 °C

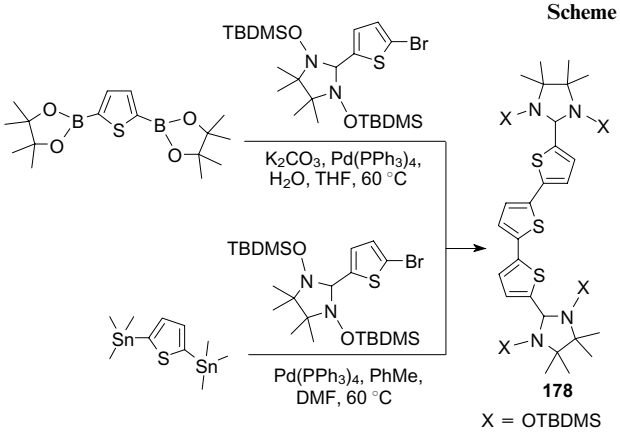
Scheme 53



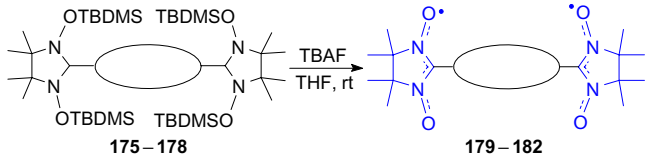
Scheme 54



Scheme 55



Scheme 56

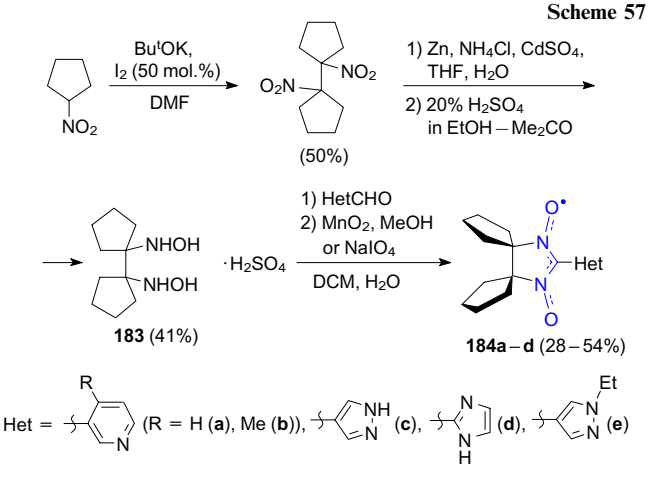


1,3-bis[(*tert*-butyldimethylsilyl)oxyl]-4,4,5,5-tetramethyl-2-[4-(4,4,5,5-tetramethyl-1,3,2-dioxaborolan-2-yl)phenyl]imidazoline with 2,5-dibromothiophene (see Scheme 54). Finally, the cross-coupling of protected 2-(5-bromothienyl)-1,3-dihydroxyimidazolidine with thiophene-2,5-diboronic acid bis(pinacol) ester afforded product **178** in 16% yield. The same compound **178** was formed in a substantially higher yield (74%) upon the Stille cross-coupling involving protected 2-(5-bromothienyl)-1,3-dihydroxyimidazolidine and 2,5-bis(trimethylstannyl)thiophene (see Scheme 55).[266]

The deprotection of compounds **175** – **178** was carried out under mild conditions on treatment with tetra-n-butylammonium fluoride in THF, which directly gave final biradicals **179** – **182** in 68 – 83% yields (see Scheme 56).

The attention is drawn by the fact that virtually all 2-imidazoline nitroxides obtained in the last decade contain methyl groups in positions 4 and 5. Exceptions are spirocyclic derivatives **184a** – **d** synthesized from bis(hydroxylamine) sulfate **183** (Scheme 57).[267] It is of interest that imidazol-2-yl-substituted nitronyl nitroxide **184d** is stable

Scheme 57



for a long time only in water, unlike the 4,4,5,5-tetramethyl analogues, while in organic solutions (for example, during growth of crystals), it is spontaneously converted to the corresponding imino nitroxide within several hours.

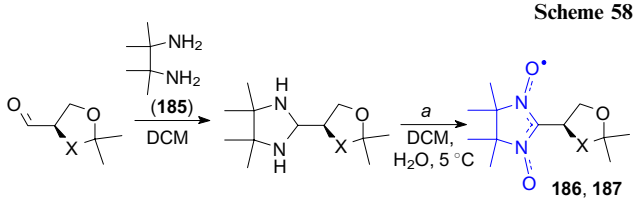
The reaction of $Cu(hfac)_2$ with nitronyl nitroxides **184a**,**b** or with *N*-ethyl derivative **184e**, obtained by alkylation of radical **184c**, leads to copper complexes of various architectures, including mono-, bi- and tetranuclear and polymer chain complexes, depending on the the paramagnetic ligand structure and conditions. It was shown[267–269] that varying the temperature induces single crystal–single crystal phase transitions in some complexes, which modify the spin state in exchange clusters and are manifested as thermochromism and changes in the magnetic susceptibility (Fig. 18). The spin transition temperature in the obtained complexes was found to considerably depend on the external pressure. For example, in the case of head-to-tail polymer chain complex [$Cu(hfac)_2$(**184e**)], a pressure increase from ambient level to 0.48 GPa induces an increase in the spin transition temperature from 110 to 325 K, which corresponds to the specific value of $\sim 290 \pm 15$ K GPa^{-1}. This is 5–10 times higher than this characteristic for classical iron complexes with spin transitions.[269]

The above examples indicate that the condensation of aldehydes with bis(hydroxylamines) followed by oxidation is a facile and convenient method for the preparation of diverse nitronyl and imino nitroxides. Bis(hydroxylamines) are usually synthesized by the reduction of vicinal dinitro compounds by zinc powder in the presence of NH_4Cl.[267, 270]

Anoter method for the preparation of nitronyl nitroxides differs from that considered above by the facts that aldehydes are condensed in the first step with 2,3-diamino-2,3-dimethylbutane (**185**), and the resulting imidazolidines are oxidized to form the desired radicals.[271] The condensation of aldehydes with diamine **185** is, most often, conducted in Et_2O or $CHCl_3$ on cooling ($\sim$0 °C), which affords intermediate imidazolidines in high yields (80–99%). Carrying out the next step giving radicals requires combined use of two oxidants: *m*-chloroperoxybenzoic acid, which efficiently converts imidazolidines to cyclic 1,3-dihydroxy derivatives, and $NaIO_4$ to oxidize these products to nitronyl nitroxides.

Using this method, chiral nitronyl nitroxides **186** and **187** were obtained from D-mannitol and L-serine, respectively (Scheme 58, the two last steps are shown). The condensation was carried out by refluxing a mixture of aldehyde with diamine **185** for 20 h, with reflux condenser being filled by 4 Å sieves; imidazolidines were formed in >90% yields. The intermediates were oxidized to target paramagnets **186** and **187** in 48–54% yields (see Scheme 58).[245] The pentapeptide Boc-(*R*)-Aic(NN)-(Ala)$_2$-(*R*)-Aic(NN)-Ala-OMe and the hexapeptide Boc-[Ala-(*R*)-Aic(NN)-Ala]$_2$-OMe, where Aic(NN) stands for 5-nitronyl nitroxide-substituted 2-aminoindan-2-carboxylic acid, were synthesized by a similar procedure.[244] Using a set of spectral methods, it was shown that these spin-labelled peptides have a dextrorotatory 3_{10}-helical structure in which both nitronyl nitroxides are located on one side of the helix.

Scheme 58



(*a*) 1) *m*-CPBA, $NaHCO_3$; 2) $NaIO_4$; X = O (**186**), N-Boc (**187**)

The considered method was also utilized to prepare a series of nitronyl nitroxide mono- and biradicals **188** bound to a 2,6-bis(pyrazolyl)pyridine moiety.[272] The condensation of mono- and dialdehydes with diamine **185** was carried out at 60 °C under inert atmosphere; the subsequent oxidation of the imidazolidines thus formed afforded mono- and dinitronyl nitroxides in moderate yields (Scheme 59).

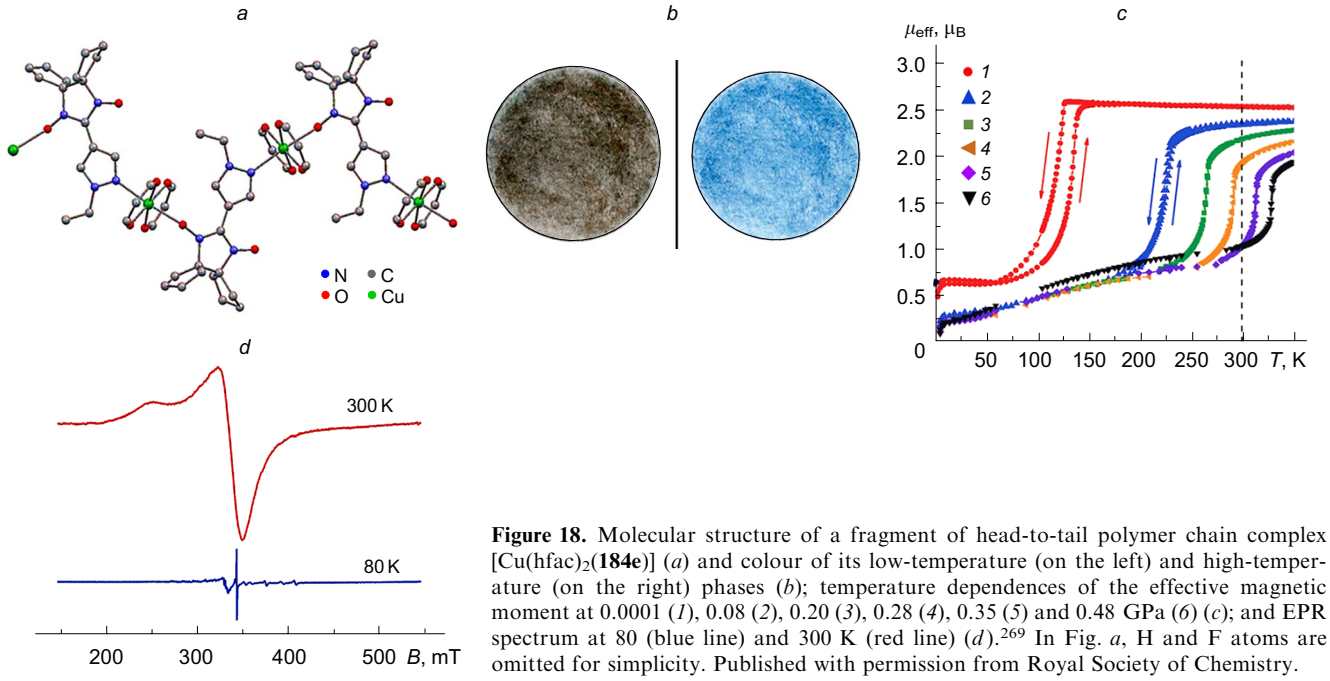
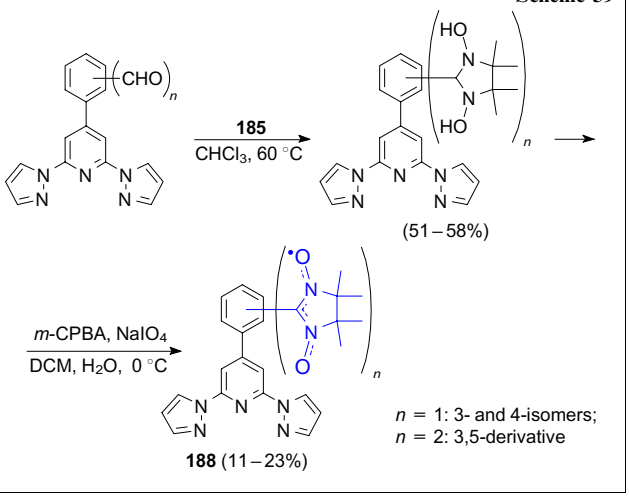


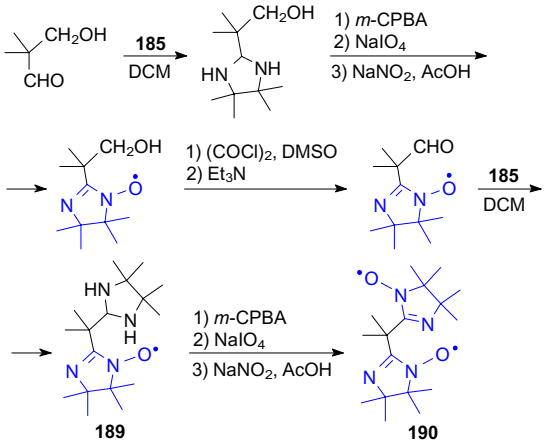
Figure 18. Molecular structure of a fragment of head-to-tail polymer chain complex [$Cu(hfac)_2$(**184e**)] (*a*) and colour of its low-temperature (on the left) and high-temperature (on the right) phases (*b*); temperature dependences of the effective magnetic moment at 0.0001 (*1*), 0.08 (*2*), 0.20 (*3*), 0.28 (*4*), 0.35 (*5*) and 0.48 GPa (*6*) (*c*); and EPR spectrum at 80 (blue line) and 300 K (red line) (*d*).[269] In Fig. *a*, H and F atoms are omitted for simplicity. Published with permission from Royal Society of Chemistry.

Scheme 59



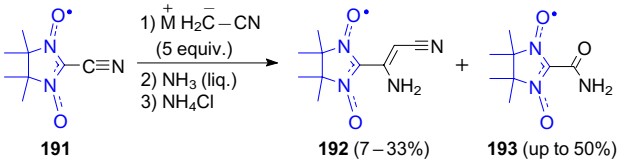
While planning the synthesis of new representatives of nitronyl nitroxides by oxidation of cyclic diamines, it is useful to bear in mind which organic functional groups are tolerant to the used oxidants, *m*-CPBA and $NaIO_4$. Apart from the groups mentioned above, this is true for the hydroxymethyl group and, unexpectedly, the imino nitroxide group. This is indicated by successful synthesis of nitroxide **189** and singlet biradical ($2J/k_B = -144$ K) — dimethylmethylene-bis(imino nitroxide) **190** — from 3-hydroxy-2,2-dimethylpropanal (Scheme 60).[273]

Scheme 60



The discussion of the nitronyl nitroxide chemistry cannot but mention their specific transformation, which is accompanied by retention of the paramagnetic ONCNO moiety. These transformations make it possible to synthesize paramagnetic compounds that cannot be obtained using the approaches considered above. This can be exemplified by multistep transformations of amino-substituted nitronyl nitroxide,[274] resulting in unique paramagnetic acylamides, the structures of which were confirmed by X-ray diffraction analysis. Radical **191** reacts with cyanomethyl anion, which is formed upon treatment of MeCN with MNH_2 (M = K, Na, Li) in liquid ammonia (Scheme 61).[275] Ammonia acts as a competing nucleophile in this reaction; therefore, the formation of the target (*Z*)-3-amino-3-(4,4,5,5-tetramethyl-4,5-dihydro-1*H*-imidazol-2-yl-1-oxyl 3-oxide)acrylonitrile (**192**) is often accompanied by the formation of amide **193**. It is noteworthy that the use of

Scheme 61

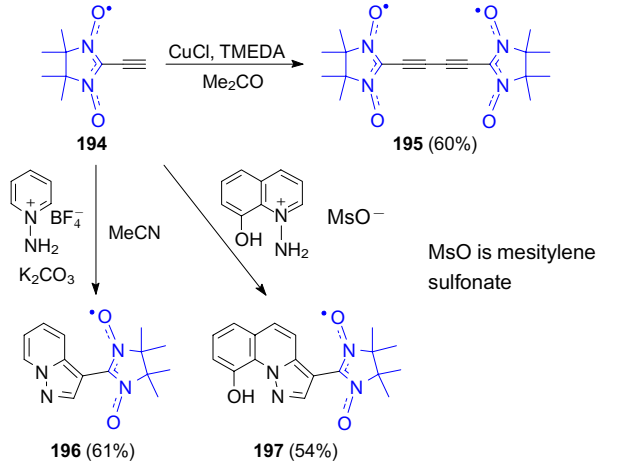


M = Li, Na, K

KNH_2 provides the highest (33%) yield of nitroxide **192**, whereas in the case of $NaNH_2$ or $LiNH_2$, the product yields do not exceed 10%.

One more interesting example is dimerization of ethynyl-substituted nitronyl nitroxide **194**, which yields biradical **195** with a butadiynediyl bridge (Scheme 62). The labile biradical can be obtained in a good yield owing to its low solubility in acetone; therefore, once formed, it rapidly precipitates. Incidentally, the C(8)≡C(9)–C(9′)≡C(8′) diyne moiety (the numbers refer to atoms in the crystallographically independent part of the molecule) has a bent shape: the highest deformation, exceeding 6°, was found for the bond angle at C(8) and C(8′) atoms.[276]

Scheme 62

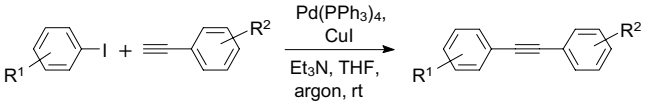


One more recently discovered transformation of nitronyl nitroxide **194** is the reaction with heteroaromatic *N*-imines, resulting in nitronyl nitroxide-substituted pyrazolo[1,5-*a*]pyridine **196** and pyrazolo[1,5-*a*]quinoline **197** (see Scheme 62), which are of interest as paramagnetic ligands.[277]

Postnikov *et al.*[278,279] carried out a systematic study of cross-coupling of iodo and acetylene derivatives of various paramagnetic molecules (Scheme 63). As a result, they synthesized quite a number of verdazyl verdazyl and verdazyl nitronyl nitroxide biradicals, which represented a convenient platform for elucidation of magneto-structural correlations. Furthermore, it was shown that among various paramagnetic blocks, the highest reactivity was inherent in oxoverdazyl iodides, which formed the most thermally stable biradical products.

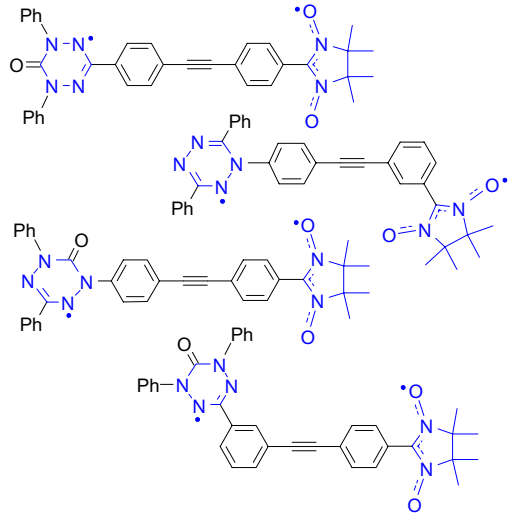
The nitronyl nitroxide group is tolerant to a variety of reagents and reaction conditions, which provides for various transformations in which the paramagnetic moiety is preserved. For example, the reaction of pyrazolyl-substituted nitronyl nitroxide **198** with BrCN resulted in the synthesis of biradical **199** (Scheme 64).[280]

Scheme 63

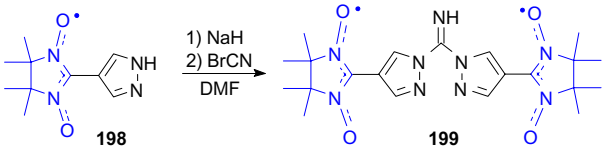


R^1, R^2 — verdazyl or nitroxide radicals

Examples of products



Scheme 64

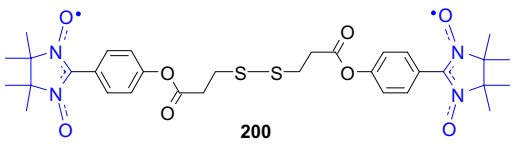


198 **199**

Biradical **200** with a disulfide bridge was obtained by esterification of the appropriate dicarboxylic acid with 4-hydroxyphenyl-substituted nitronyl nitroxide in the presence of dicyclohexylcarbodiimide (DCC) and DMAP.[281] The authors were able to select the optimal conditions for the reaction of paramagnetic disulfide **200** with gold nanoparticles stabilized by tri-n-octylamine and to attain a fairly dense grafting of nitronyl nitroxides on the nanoparticle surface. Gold nanoparticles decorated by paramagnetic groups give rise to an EPR signal at half field ($|\Delta m_s| = 2$) corresponding to the formally forbidden transition from $m_s = -1$ to $m_s = +1$ and indicating the existence of a high-spin state. The intensity of this transition decreases with decreasing temperature, which attests to predominance of antiferromagnetic exchange coupling in the spin-labelled nanoparticles.

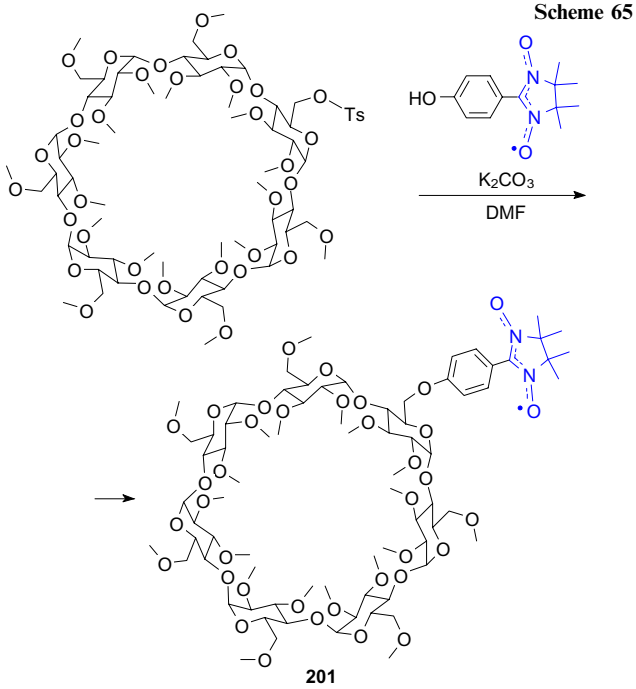
One more useful example of using 4-hydroxyphenyl nitronyl nitroxide is the synthesis of spin-labelled cyclodextrin **201** (Scheme 65).[282] According to electron spin echo envelope modulation (ESEEM) spectrum, compound **201** is

Structure 200



200

Scheme 65

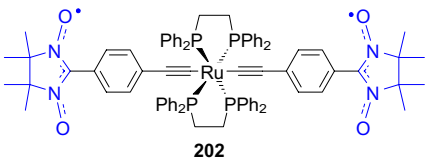


201

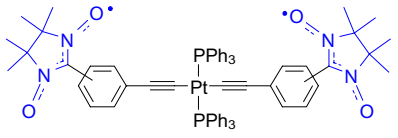
characterized by dynamic equilibrium between the conformation in which the radical moiety closes the cyclodextrin cavity and the conformation in which the radical moiety is located outside the cavity.

Turek and co-workers[283,284] described symmetrical ruthenium and platinum organic complexes **202** and **203**, containing each two nitronyl nitroxide groups. The former was obtained by the reaction of 4-ethynylphenyl-substituted nitronyl nitroxide with the appropriate ruthenium dichloride complex in dichloromethane in the presence of $NaPF_6$ and Et_3N. Platinum-containing biradicals **203** were synthesized using $[Pt(PPh_3)_2Cl_2]$ in the presence of CuI in a THF–Pr^i_2NH mixture (10 : 1). In these biradicals, exchange coupling is weak ($\Delta E_{ST} \leqslant 3$ cm^{-1}) and is antiferromagnetic. It was shown that the oxidation of ruthenium to the paramagnetic state of complex **202** under the action of $KAuCl_4$ in DCM results in disappearance of the exchange between the lateral nitroxide groups.

Structures 202, 203



202

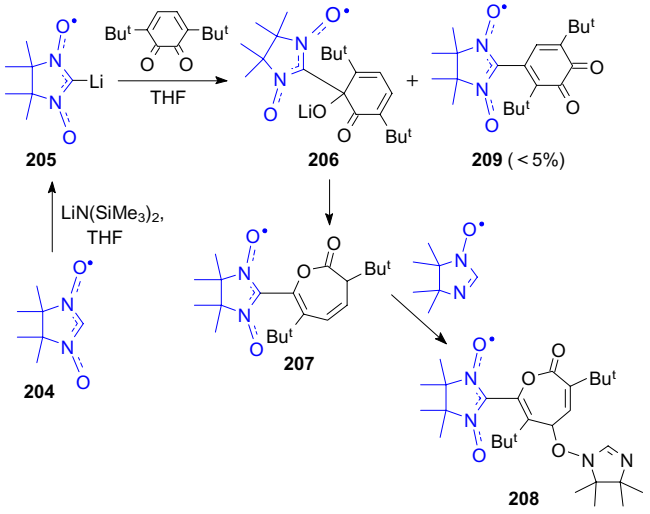


203

The reactions of electrophiles with the lithiated derivative prepared by adding a slight excess (1.1–1.2 equiv.) of $LiN(SiMe_3)_2$ to a solution of nitroxide **204** in THF at a temperature from −80 to −90 °C are fairly important for the nitronyl nitroxide chemistry. 4,4,5,5-Tetramethylimida-

zoline-1-oxyl 3-oxide (**205**) reacts with 3,6-di-*tert*-butyl-*o*-benzoquinone, the reaction proceeding mainly as nucleophilic 1,2-addition to the C=O group and subsequent insertion of the oxygen atom into the ring in lithium salt **206**. Under these conditions, the intermediate 2-(3,6-di-*tert*-butyl-2-oxo-2,3-dihydrooxepin-7-yl)-4,4,5,5-tetramethyl-4,5-dihydro-1*H*-imidazole-1-oxyl 3-oxide (**207**) further reacts with imino nitroxide, which is accumulated during deoxygenation of the starting nitronyl nitroxide, to give 2-[3,6-di-*tert*-butyl-2-oxo-5-(4,4,5,5-tetramethyl-4,5-dihydro-1*H*-imidazol-1-yloxy)-2,5-dihydrooxepin-7-yl]-4,4,5,5-tetramethyl-4,5-dihydro-1*H*-imidazol-1-oxyl 3-oxide (**208**) (Scheme 66).[285] The ratio of dihydrooxepines **207** and **208** depends on the reaction temperature and time. At −80 °C and 2 h reaction time, derivatives **207** and **208** are formed in approximately equal amounts (23 and 26%, respectively), whereas cooling down of the reaction mixture immediately after the reaction followed by stirring for 24 h results in the formation of only compound **208** in 47% yield. It is of interest that lowering the temperature almost to the freezing point of THF (~ −108 °C) results in the formation of not only the product of nucleophilic 1,2-addition, but also the 1,4-addition product — 2-(2,5-di-*tert*-butyl-3,4-dioxocyclohexa-1,5-dienyl)-4,4,5,5-tetramethyl-4,5-dihydro-1*H*-imidazole-1-oxyl 3-oxide (**209**) (< 5%).

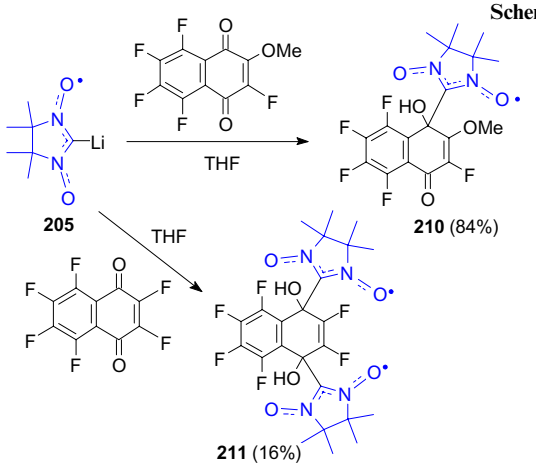
Scheme 66



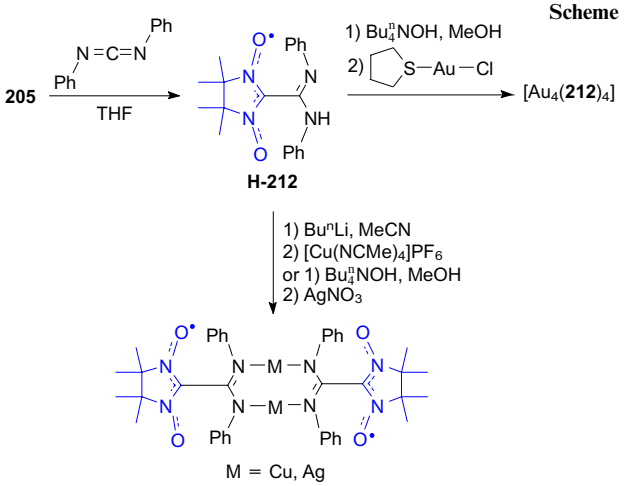
The reaction of lithiated derivative **205** with polyfluoro-1,4-naphthoquinones stops after the formation of carbonyl group adducts.[286] 2-Methoxy-3,5,6,7,8-pentafluoro-1,4-naphthoquinone was converted exclusively to 4,4,5,5-tetramethyl-2-(3,5,6,7,8-pentafluoro-1-hydroxy-2-methoxy-4-oxo-1,4-dihydronaphthalen-1-yl)-4,5-dihydro-1*H*-imidazole-1-oxyl 3-oxide (**210**) in 84% yield; no formation of another isomer was detected (Scheme 67). Hexafluoro-1,4-naphthoquinone was converted to biradical adduct, that is, 1,4-bis(4,4,5,5-tetramethyl-4,5-dihydro-1*H*-imidazol-2-yl-1-oxyl 3-oxide)-2,3,5,6,7,8-hexafluoro-1,4-dihydronaphthalene-1,4-diol (**211**), which formed in a yield of not more than 16%. It is noteworthy that, according to the data of EPR spectroscopy, monoradical **210** and biradical **211** were stable in water; however, in toluene solutions, they were deoxygenated rather rapidly.

The first nitronyl nitroxide amidine **H-212** was prepared by addition of radical **205** to *N*,*N*′-diphenylcarbodiimide

Scheme 67



Scheme 68



(Scheme 68). According to X-ray diffraction data, the crystal structure of paramagnet **H-212** is formed by packing of dimer molecules held by N···H−N pair hydrogen bonds (Fig. 19 *a*).[287] The reaction of amidine **H-212** with $[Cu(NCMe)_4]PF_6$ or $AgNO_3$ in the presence of a base resulted in the formation of binuclear $[Cu_2(\mathbf{H\text{-}212})_2]$ or $[Ag_2(\mathbf{H\text{-}212})_2]$ complexes. Meanwhile, the reaction of deprotonated form **212** with gold(I) derivative in the presence of Bu^n_4NOH in MeOH gave tetranuclear $[Au_4(\mathbf{212})_4]$ complex, as indicated by X-ray diffraction data (Fig. 19 *b*).

Ferrocenyl-substituted *N*,*N*′-diphenylcarbodiimide reacts with radical **205** similarly to parent *N*,*N*′-diphenylcarbodiimide to give polyfunctional amidine (Scheme 69).

The reaction of radical **205** with 2-methyl-2-nitrosopropane gives 2-(*N*-*tert*-butyl-*N*-hydroxylamino)-4,4,5,5-tetramethyl-1*H*-imidazol-1-oxyl 3-oxide, which is oxidized by MnO_2 or PbO_2 to be converted to triplet biradical **18** (see Scheme 69). The reduction of the latter leads to imino nitroxide analogue **213**, which was studied by X-ray diffraction, like biradical **18**.[45,46] The compact biradicals **18** and **213** are stable, highly volatile at reduced pressure and are characterized by strong ferromagnetic exchange ($2J/k_B$ are +780 and +1100 K, respectively).

The unique structural and magnetic characteristics inherent in triplet biradicals **18** and **213** attracted attention of specialists in various fields, including quantum chemists. A systematic evaluation of the adequacy of various models used to calculate zero-field splitting parameters was carried

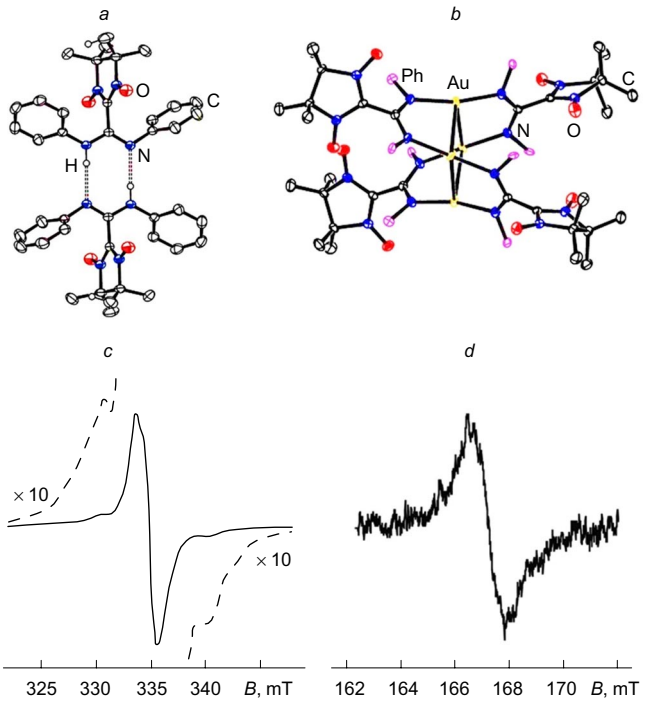
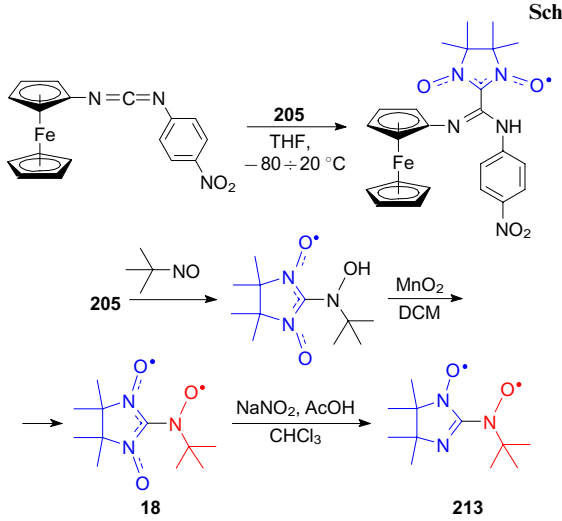


Figure 19. Dimer structure of amidine **212** (*a*), molecular structure of complex [Au_4(**212**)$_4$] (*b*) and EPR spectra of the complex in spin-resolved (*c*) and spin-forbidden (*d*) regions in frozen DCM – Et_2O at 95 K.[287] Published with permission from John Wiley and Sons.

Scheme 69



out.[288] The conformational analysis of biradical **18** revealed only one pair of stable enantiomers in pseudo-eclipsed (PM and MP) conformations (Fig. 20). It was shown that in a solid argon matrix and in racemic crystals, the geometric characteristics of both enantiomers are close to the parameters found by multi-configuration *ab initio* methods: $\theta = 66°$, $\phi = -16.5°$ (Fig. 21).[289]

Since biradicals **18** and **213** have nearly 100% population of the triplet state even at room temperature, it is reasonable to make attempts to use them as spin carriers with $S = 1$ in related fields such as coordination chemistry. It was shown that the reaction of paramagnet **18** with $Mn(hfac)_2$ gives rise to heterospin molecular complex [$Mn(hfac)_2$(**18**)] with chelating coordination of the paramagnetic ligand and strong intramolecular antiferromagnetic exchange ($2J/k_B = -434$ K).[290] The reaction of biradical **18** with $Cu(hfac)_2$ follows a different pathway: in this case, biradical is converted to the paramagnetic anion under the reaction conditions, which results in solid-phase precipitation of complex **214** — [$Cu_2(hfac)_2$(**213′**)$Cu(hfac)_2$]$_n$ (**213′** is paramagnetic anion,

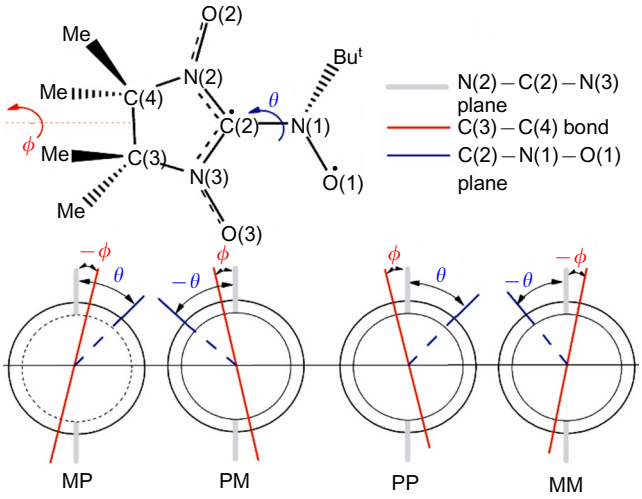


Figure 20. Schematic image of the four possible diastereomers of biradical **18** with pseudo-eclipsed (MP, PM) and pseudo-*anti*-coformations (PP, MM).[289] Published with permission from American Chemical Society.

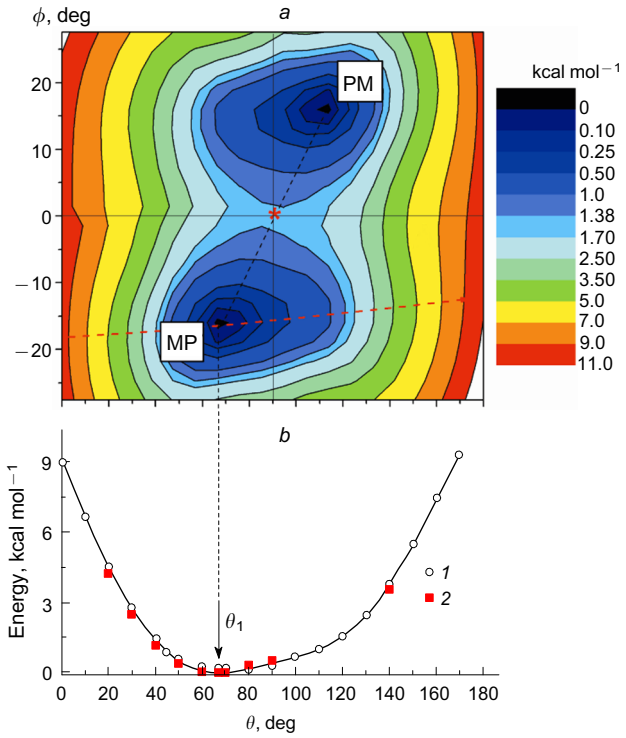
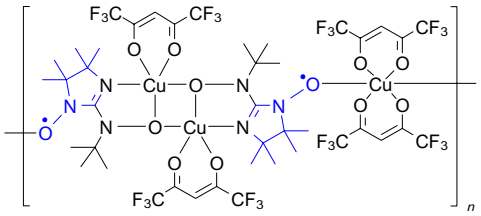


Figure 21. Potential energy surface for biradical **18** in the triplet ground state (the sign * marks the saddle point) (*a*) and calculated energy values depending on the angle θ along the path shown in Fig. *a* by the red dashed line (*b*).[289] The geometry was optimized by DFT (*1*) and CASSCF (*2*) methods. Published with permission from American Chemical Society.

Structure 214

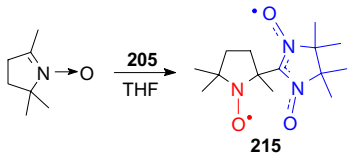


214

the reduced form of biradical **213**). Note that exactly the same complex is formed upon the reaction of $Cu(hfac)_2$ with imino nitroxide derivative **213**. Magnetochemical and quantum chemical investigations of $[Cu_2(hfac)_2(\mathbf{213}')Cu(hfac)_2]_n$ indicate that this complex if composed of virtually isolated clusters {Cu–N=C–NO–Cu–ON–C=N–Cu} and the exchange coupling between the paramagnetic centres within the clusters is ferromagnetic. For Cu–N=C–NO exchange channel, the parameter $2J/k_B$ exceeds 1000 K, whereas for Cu–ON–C=N, it is an order of magnitude lower, being close to 120 K.

The development of the method for the synthesis of lithiated derivative **205** opened up the way to a variety of polyfunctional nitronyl nitroxides. It was shown that compound **205** can add to the multiple bond of cyclic nitrone (2,2,5-trimethyl-3,4-dihydro-2*H*-pyrrole 1-oxidea) to give stable biradical — 2-(4′,4′,5′,5′-tetramethylimidazoline-2′-yl-1′-oxyl 3′-oxide)-2,5,5-trimethylpyrrolidine-1-oxyl (**215**) in a yield of 30% (Scheme 70).[291]

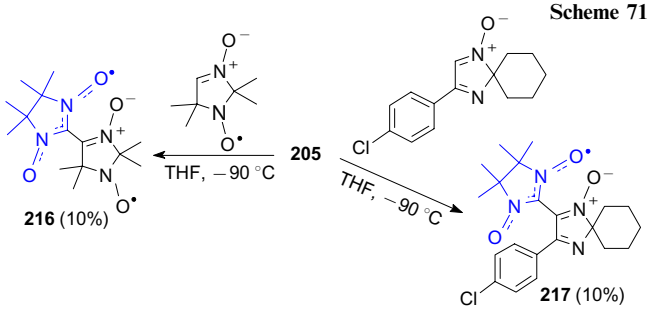
Scheme 70



215

In the case where a hydrogen atom is present at the nitrone double bond, the reaction with Li derivative **205** can be accompanied by substitution. For example, the reaction of compound **205** with 2,2,5,5-tetramethyl-2,5-dihydro-1*H*-imidazol-1-oxyl 3-oxide or 3-(4-chlorophenyl)-1,4-diazaspiro[4.5]deca-1,3-diene 1-oxide affords complex mixtures of products. The α-hydrogen substitution products, 2′,2′,4,4,5,5,5′,5′-octamethyl-2′,4,5,5′-tetrahydro-1*H*,1′*H*-2,4′-biimidazole-1,1′-dioxyl 3,3′-dioxide (**216**) or 4,4,5,5-tetramethyl-2-[1-oxido-3-(4-chlorophenyl)-1,4-diazaspiro[4.5]deca-1,3-dien-2-yl]-4,5-dihydro-1*H*-imidazol-1-oxyl 3-oxide (**217**) were isolated from the product mixtures in moderate yields (Scheme 71).[292] The formation of nitroxides **216** and **217**

Scheme 71

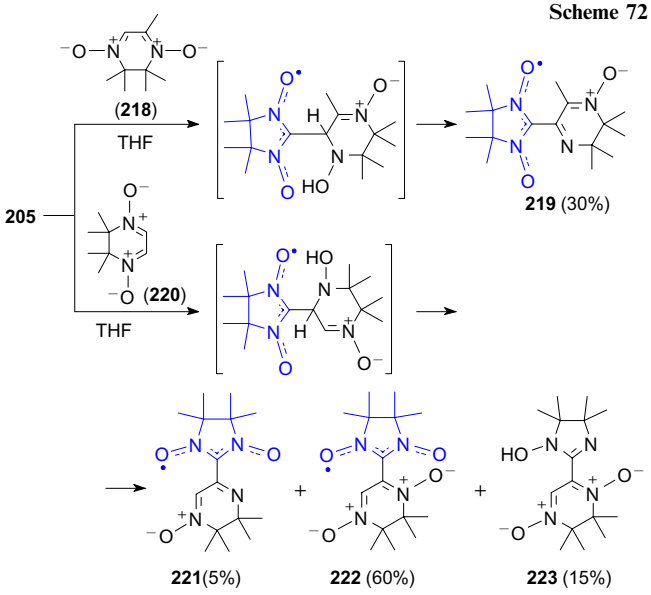


216 (10%) **217** (10%)

implies that the reaction follows the addition–oxidation mechanism; the nitroxide radicals present in the mixture can act as oxidants in this reaction.

The reaction of compound **205** with cyclic dinitrone **218** also gives a complex mixture of products, from which stable 4,4,5,5-tetramethyl-2-(2,2,3,3,6-pentamethyl-1-oxido-2,3-dihydropyrazin-5-yl)-4,5-dihydro-1*H*-imidazol-1-oxyl 3-oxide (**219**) was isolated.[293] Whereas in the reaction of methyl derivative **218**, the yield of the product formed by the addition–elimination mechanism (Scheme 72) was ~30%, in the reaction involving dinitrone **220**, the yield of compound **221** did not exceed 5%. In the latter case, 4,4,5,5-tetramethyl-2-(2,2,3,3-tetramethyl-1,4-dioxido-2,3-dihydropyrazin-5-yl)-4,5-dihydro-1*H*-imidazol-1-oxyl 3-oxide (**222**) was the major reaction product, evidently formed by the addition–oxidation mechanism (see Scheme 72). The presence of hydroxylamine **223** among the reaction products indicates that nitroxide radicals can serve as oxidants in hydrogen substitution reactions.

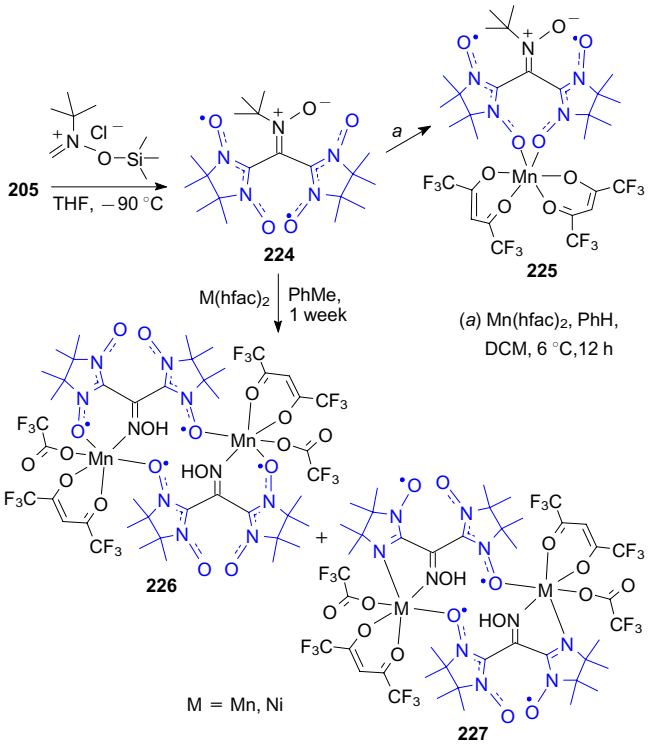
Scheme 72



219 (30%) **221**(5%) **222** (60%) **223** (15%)

A unique reaction is the reaction of Li compound **205** with activated acyclic nitrone derivative, *N*-*tert*-butyl-*N*-methylene-*O*-(trimethylsilyl)hydroxylammonium chloride, which results in displacement of two hydrogen atoms and gives C(sp^2)-bound biradical, *N*-*tert*-butyl-1,1-bis(4,4,5,5-tetramethyl-3-oxido-1-oxyl-4,5-dihydro-1*H*-imidazol-2-yl)-methanimine *N*-oxide, in 20% yield (**224**) (Scheme 73).[294,295] The presence of the bulky bridging group in biradical **224** induces a considerable rotation of the radical moieties relative to each other; this markedly suppresses the intramolecular exchange ($2J/k_B = -14.8$ K). Unexpected results were obtained for reactions of biradical **224** with $M(hfac)_2$. Whereas the molecular complex **225**, obtained by the reaction of $Mn(hfac)_2$ (M = Mn, Ni) with this biradical in a benzene–dichloromethane mixture in 12 h, had the expected composition and structure, complexes **226** and **227**, formed in 2 : 3 ratio upon long-term reaction of biradical **224** with $M(hfac)_2$ in toluene, contained modified ligands. Instead of the *N*-*tert*-butyl nitronyl moiety, which was present in the starting biradical **224**, these products contained considerably less bulky oxime bridging group (C=NOH). This

Scheme 73

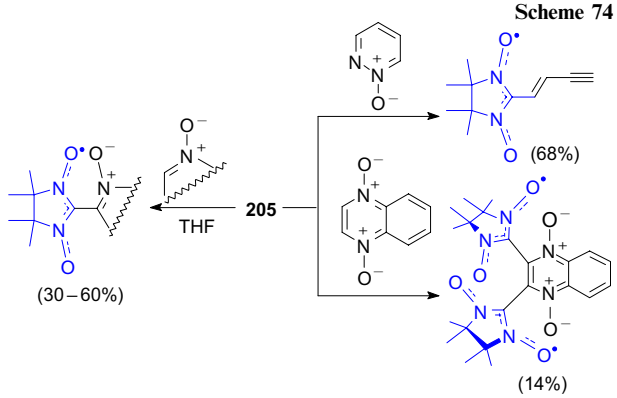


account for the decrease in the rotation angle of the paramagnetic groups relative to each other and, as a consequence, for the change in the type of intraligand exchange from antiferromagnetic to ferromagnetic one.[296]

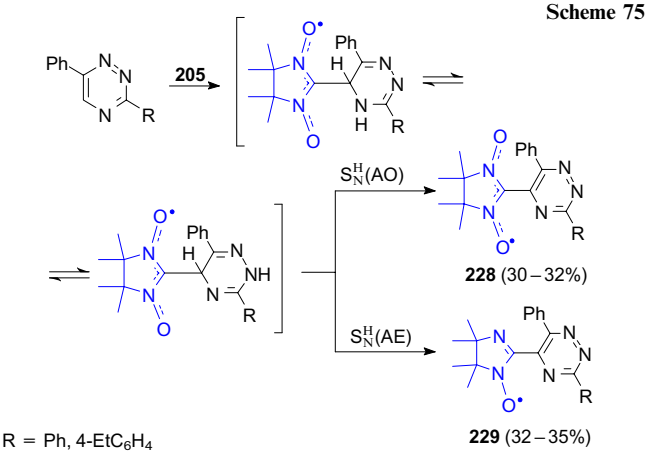
In recent years, development of the chemistry and expansion of the scope of applicability of nitronyl nitroxides are considerably affected by the appearance of methods for direct introduction of the paramagnetic group into the aromatic ring. First of all, mention should be made of the synthetic strategy towards polyfunctional nitronyl nitroxide using nucleophilic aromatic substitution of hydrogen developed by the Ural school of chemists.[297, 298] This can be exemplified by reactions of lithiated paramagnetic compound **205** with azine *N*-oxides, in particular with fluorinated derivatives yielding a family of functionally substituted nitronyl nitroxides, which could not be synthesized previously (Scheme 74).[299–302]

This approach proved to be applicable to a broad range of activated aromatic substrates. It was shown that the reaction of Li compound **205** with 1,2,4-triazine derivatives, particularly with 3,6-diphenyl- and 3-(4-ethylphenyl)-6-phenyl-1,2,4-triazines gives satisfactory yields of two types of products of nucleophilic aromatic substitution of hydrogen: heteroaryl-substituted nitronyl nitroxides **228** and imino nitroxides **229** (Scheme 75).[303] Nitronyl nitroxides **228**, like azine *N*-oxides, are formed by the addition–oxidation (AO) mechanism, whereas imino nitroxides **229** are produced by the addition–elimination (AE) mechanism.

Scheme 74

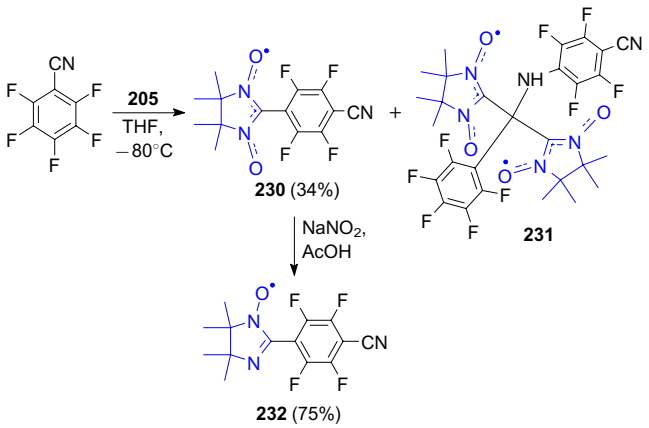


Scheme 75



The second synthetic strategy towards aryl-substituted nitronyl nitroxides implies nucleophilic substitution reaction of polyfluoro(hetero)arenes in which the fluorine atom is displaced on treatment with the lithiated compound **205**.[304] An example is the reaction of **205** with perfluorobenzonitrile, which results in the formation of 2-cyanotetrafluorophenyl derivative — 4,4,5,5-tetramethyl-2-(4-cyano-2,3,5,6-tetrafluorophenyl)-4,5-dihydro-1*H*-imidazol-1-oxyl 3-oxide (**230**) (Scheme 76). A minor amount (~1%) of unusual C(sp^3)-bound biradical **231** was isolated and identified by thorough analysis of the reaction mixture. In the $NaNO_2$–AcOH system, nitronyl nitroxide **230** was easily deoxygenated to give the expected imino nitroxide **232** in a good yield.[305]

Scheme 76



Worthy of note are the results of quantum chemical calculations of the potential energy surface along the coordinates of the possible competing nucleophilic aromatic substitution pathways in which F atoms are substituted under the action of Li derivative **205**, which adds to the CN triple bond (Fig. 22). It was found that F atom is substi-

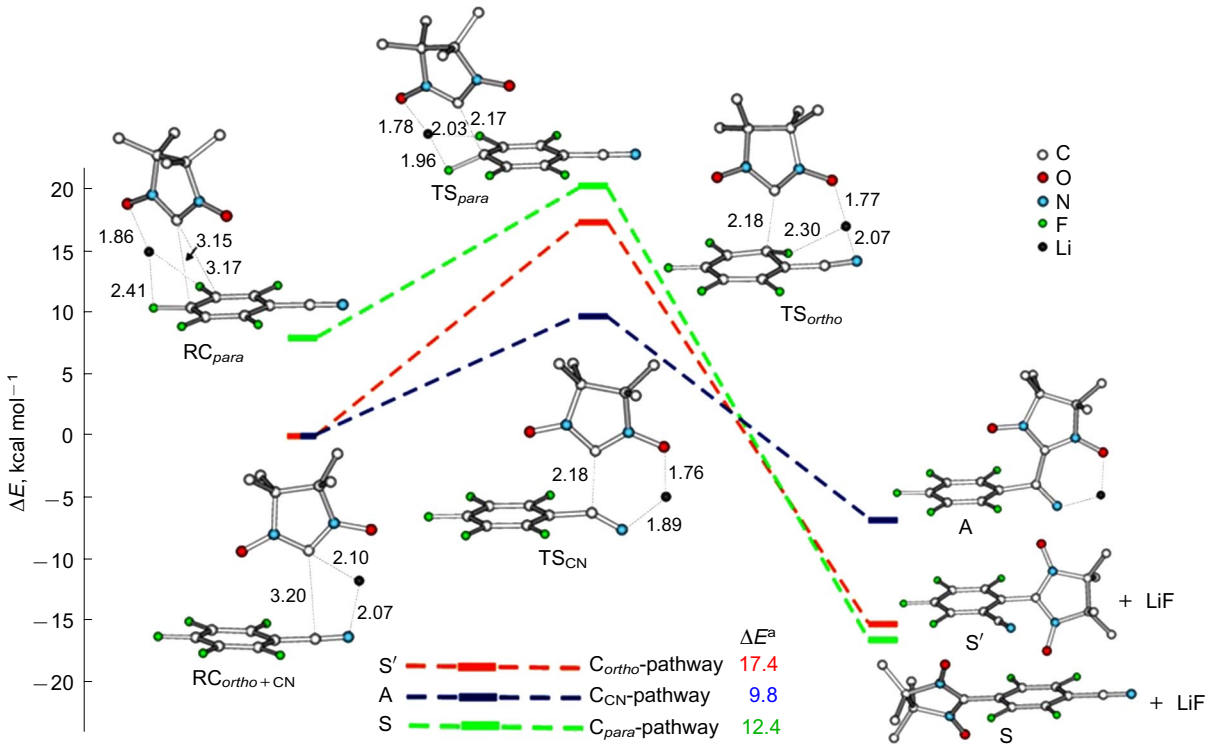


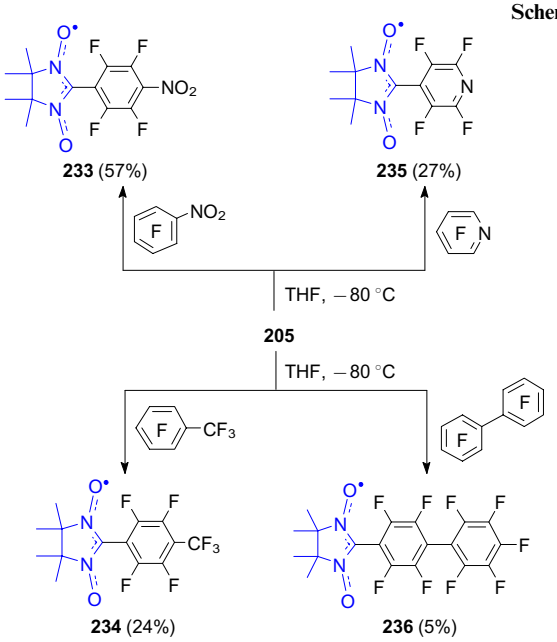
Figure 22. Possible pathways of the reaction of pentafluorobenzonitrile with Li derivative **205** according to CAM-B3LYP/6-31+G* calculation data. The H atoms of the methyl groups are omitted; the numbers at the drawn sructures are bond lengths in Å.[305] RC is the pre-reaction complex, TS is the transition state; the energy is measured in kcal mol^{-1}. Published with permission from American Chemical Society.

tuted in one step without the intermediate formation of the Meisenheimer type anionic intermediate. The *para*-directed substitution (pathway S) provides a pronounced advantage in the activation energy and reaction heat, which is consistent with the formation of nitroxide **230** as the major product. Attention is attracted by the fact that the lowest energy barrier corresponds to the addition of Li derivative **205** to the CN group to give iminium anion (pathway A); however, unlike fluorine substitution (pathways S and S′), this reaction is reversible; therefore, nucleophilic substitution is the preferred mechanism.

Apart from perfluorobenzonitrile, reactions with compound **205** were effected for a range of polyfluorinated substrates to give polyfluoroaryl-substituted nitronyl nitroxides **233**–**236**.[306, 307] It is noteworthy that in all cases, the substitution regioselectively involves the fluorine atom located in the *para*-position relative to the functional group of the polyfluorinated substrate (Scheme 77).

The nucleophilicity of the lithium derivative **205** proved to be insufficient to carry out the reaction with non-activated aromatic compounds to obtain aryl-substituted nitronyl nitroxides. In this case, the third method is used: Pd-catalyzed cross-coupling of organometallic nitronyl nitroxide derivatives **204** with aryl iodides or, more rarely, aryl bromides. An example is the reaction of compound **204** with aryl iodides in the presence of 1 equiv. of Bu^{t}ONa, 10 mol.% $Pd(PPh_3)_4$ and 20 mol.% 2-dicyclohexylphosphino-2′,4′,6′-triisopropylbiphenyl (XPhos) (Scheme 78), which gives cross-coupling products **237** in good yields (Table 1, conditions *a*).[308] High productivity of the reaction was attained using toluene as a solvent and Bu^{t}ONa as a base; when alcohols or THF were used in the presence of

Scheme 77



various bases, cross-coupling did not take place. Other catalysts and phosphine co-ligands also proved to be less efficient. Despite thorough optimization of conditions, aryl bromides and aryl triflates cannot be reacted, which is a considerable limitation of this method.

An alternative method for the synthesis of aryl-substituted nitronyl nitroxides is the cross-coupling of aryl iodides with organozinc derivative **238** (see Scheme 78),

Scheme 78

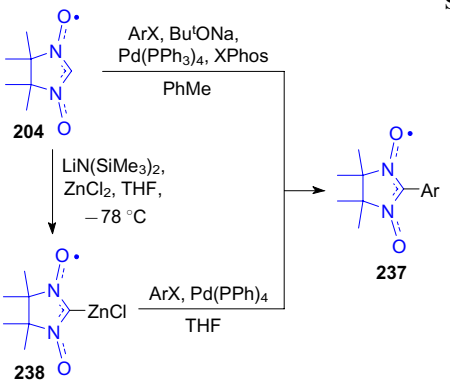
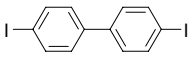
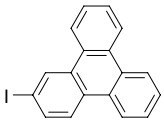
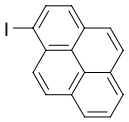


Table 1. Cross-coupling of aryl halides with organometallic derivatives of nitroxide **204**.[308–311]

ArX	Yield of **237** (%)		
	a	*b*	*c*
4-MeOC$_6$H$_4$I	72	65	71
4-MeC$_6$H$_4$I	76	76	–
4-IC$_6$H$_4$I	–	65	–
3-IC$_6$H$_4$I	–	53	–
4-PhC$_6$H$_4$I	78	77	–
4-PhC$_6$H$_4$Br	Traces	Traces	74
PhI	78	85	92
4-AcC$_6$H$_4$I	83	78	80
4-AcC$_6$H$_4$Br	Traces	Traces	83
4-HOCC$_6$H$_4$I	73	72	–
4-O$_2$NC$_6$H$_4$I	84	81	83
C$_6$F$_5$I	–	Traces	–
1-NaphI	60	48	64
2-ThI	61	71	84
	–	71	–
	64	–	–
	–	–	65

Notes. Dash means that the data were not given in the original source. Conditions *a*: Bu^{t}ONa, Pd(PPh$_3$)$_4$ (10 mol.%), XPhos (20 mol.%); conditions *b*: (1) LiN(SiMe$_3$)$_2$; (2) ZnCl$_2$, Pd(PPh$_3$)$_4$; conditions *c*: **246e**, Pd(PPh$_3$)$_4$. Naph is naphthyl, Th is thienyl.

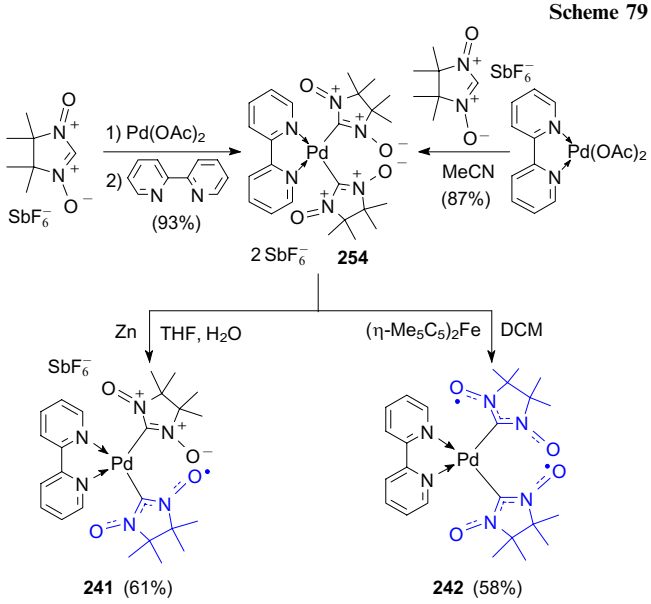
which is obtained by lithiation of compound **204** followed by treatment of the product with ZnCl$_2$ in THF at −78 °C. After that, 2 equiv. of aryl halide and a catalytic amount of Pd(PPh$_3$)$_4$ are added to the formed compound **238** and the reaction mixture is heated for 2 h, which affords the expected nitronyl nitroxides in yields comparable with those attained under conditions *a* (see Table 1, conditions *b*).[309] However, under these conditions, too, aryl bromides and pentafluorophenyl iodide gave only traces of target products.

When reacted with transition metal ions, deprotonated of nitroxide **204** may afford structurally and chemically diverse organometallic compounds. In recent years, a number of compounds **239**–**253** of late transition metals such as Cu, Pd, Ag, Pt, Au and Hg have been isolated in a pure state and structurally characterized. These complexes have various ligand environments of the metal; among them, there is only one carbene gold complex **248** (Fig. 23).

Most organometallic derivatives were synthesized by reactions of halide complexes of ML$_n$Cl type with nitroxide **204** in the presence of a base (NaOH) in MeOH. This method was used to obtain Pt and Hg pincer complexes (**249**–**251**), containing nitronyl nitroxide group, from appropriate chlorides. Gold(II) phosphine complexes **246** were synthesized by the reaction of radical **204** with gold(II) chloride tetrahydrothiophene complex in the presence of NaOH in MeOH followed by the addition of the specified phosphine PR$_3$ (63–94% yields).[318]

Mono- and biradical derivatives **241** and **242** were prepared by the reduction of palladium complex **254** with two oxoammonium cationic ligands on treatment with either zinc dust in a THF–water mixture or decamethylferrocene in dichloromethane (Scheme 79).[313] The starting complex **254** was synthesized by the reaction of oxoammonium hexafluoroantimonate with Pd(OAc)$_2$ with subsequent addition of 2,2′-bipyridine or by the reaction of the same ammonium salt with pre-synthesized palladium complex.

Scheme 79



Palladium derivative **244** was synthesized in a different way, particularly, by the reaction of bromo-substituted nitronyl nitroxide **255** with Pd(PPh$_3$)$_4$ or by the reaction of highly stable mercury derivative **253** with (Bu$^n_4$N)[Pd$_2$Br$_6$] and PPh$_3$ in THF (Scheme 80).[314]

Consider an unusual transformation that takes place for gold nitronyl nitroxide derivative **246e** on treatment with nitric acid. It was shown that stable cyclic triradical **19**, which forms dimeric packing upon crystallization from a mixture of cyclohexane with toluene, is assembled under the reaction conditions (Scheme 81).[47] According to magnetic measurements, the exchange coupling between the paramagnetic centres in symmetrical (space group C_3) triradical

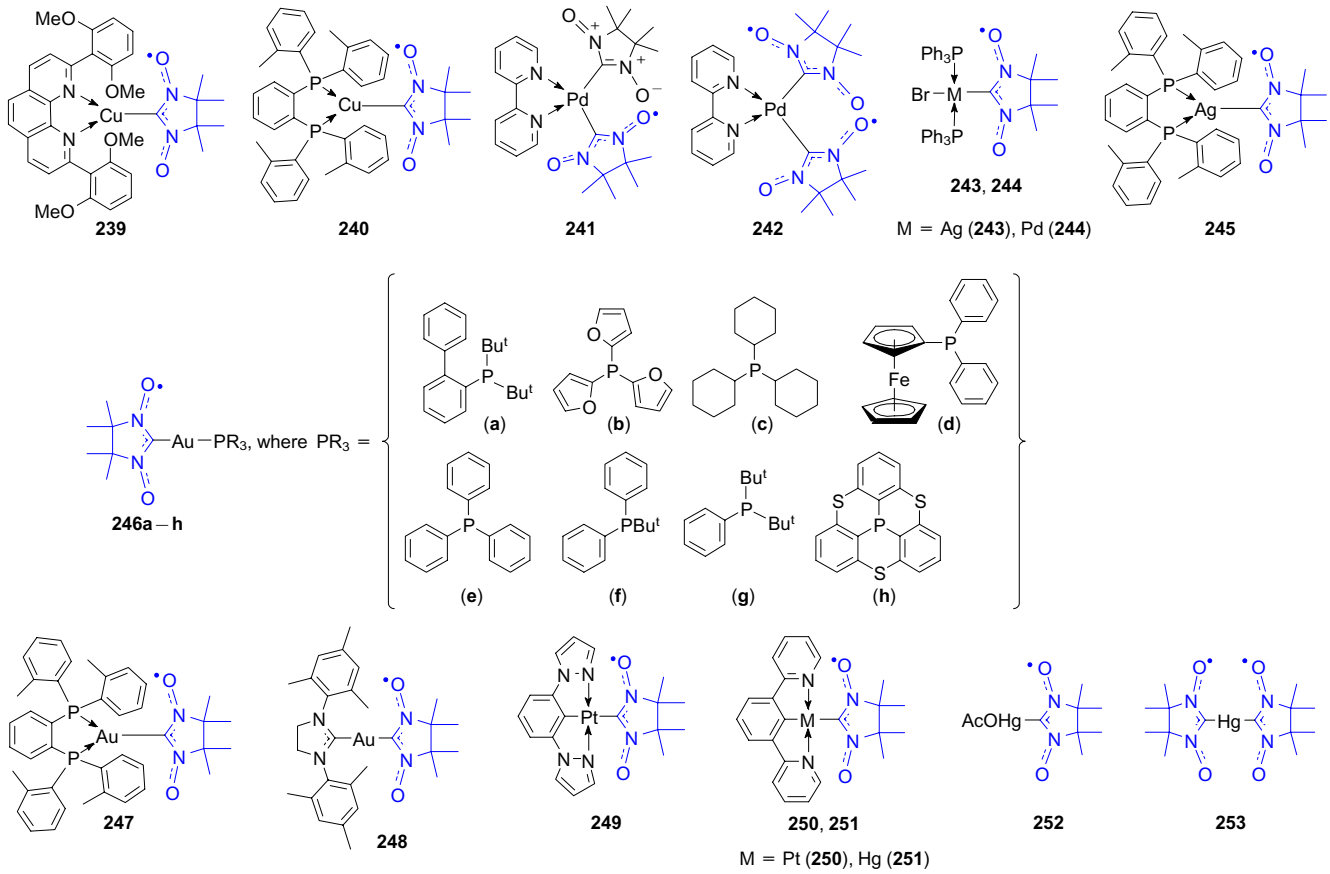
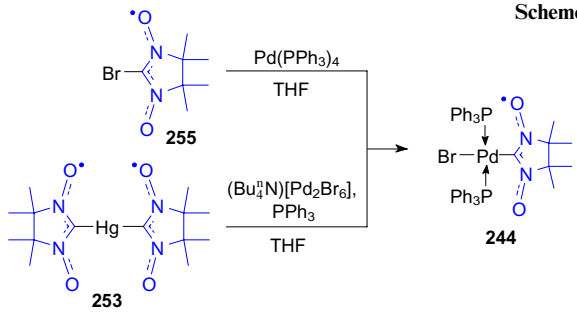
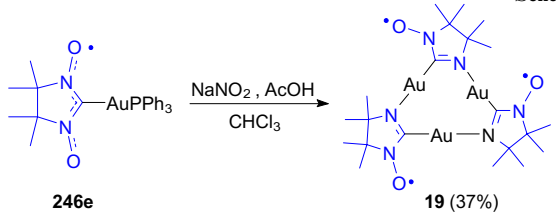


Figure 23. Structures of organocopper nitronyl nitroxides (**239** and **240**),[312] charged and neutral organopalladium and -silver nitronyl nitroxides (**241**–**245**) [313,314] and stable organoplatinum, -gold and -mercury derivatives (**246**–**253**).[315–317]

Scheme 80



Scheme 81



is ferromagnetic ($J/k_B = 29$ K); this accounts for the increase in $\chi_{mol}T$ from 2.461 to ~2.700 cm^3 K mol^{-1} as the temperature is lowered from room temperature to 60 K. Further cooling induces a sharp decrease in $\chi_{mol}T$ due to the antiferromagnetic spin coupling of the triradicals within the {(**19**)·(**19**)} dimer structures ($J/k_B = -12.2$ K). When this triradical reacts with $AgPF_6$ or AgOTf [Tf trifluoromethanesulfonyl (triflyl)] in dichloromethane, stable complexes containing the [(**19**)·Ag·(**19**)]$^+$ cation are formed. According to X-ray diffraction data, [(**19**)·Ag·(**19**)]PF_6 has S_6 symmetry. The distance between the gold and silver ions (2.8095(5) Å) in this complex is smaller than the sum of their van der Waals radii (3.38 Å) (Fig. 24). In [(**19**)·Ag·(**19**)]PF_6, the ferromagnetic exchange energies in derivative **19** ($J/k_B = 25$ K) and antiferromagnetic coupling between the three-spin groups ($J/k_B = -9.7$ K) are virtually equal to those in the {(**19**)·(**19**)} dimer.

The synthesis of organometallic derivatives containing a nitronyl nitroxide group opened a new page in the chemistry of polyfunctional 2-imidazoline-1-oxyl 3-oxides. A very important achievement in this field is the possibility of palladium-catalyzed cross-coupling reactions of compounds like **246** with aryl and vinyl halides. In the case of derivative **246e**, good yields of cross-coupling products were attained by using $Pd(PPh_3)_4$ as the catalyst (see Table 1, conditions *c*), whereas the use of $Pd(PPh_3)_2Cl_2$ or $[Pd_2(dba)_3]\cdot CHCl_3$ (dba is dibenzylideneacetone) resulted in considerably lower yields (Scheme 82).[310,311] Carbene complex **248** was converted, in the presence of $Pd(PPh_3)_4$ and $Pd_2(dba)_3$, into cross-coupling products, the yields of which were comparable with the yields obtained in the **246e**–$Pd(PPh_3)_4$ system.[319] In the case of copper complex **239**, better yields of products were attained with $Pd_2(dba)_3$ in $CHCl_3$ (5 mol.%) or 1,1′-bis(diphenylphosphino)ferrocene (DPPF, 10 mol.%), whereas the reaction conducted in the presence of $Pd(PPh_3)_4$ was accompanied by decomposition of the considerable part of complex **239**.

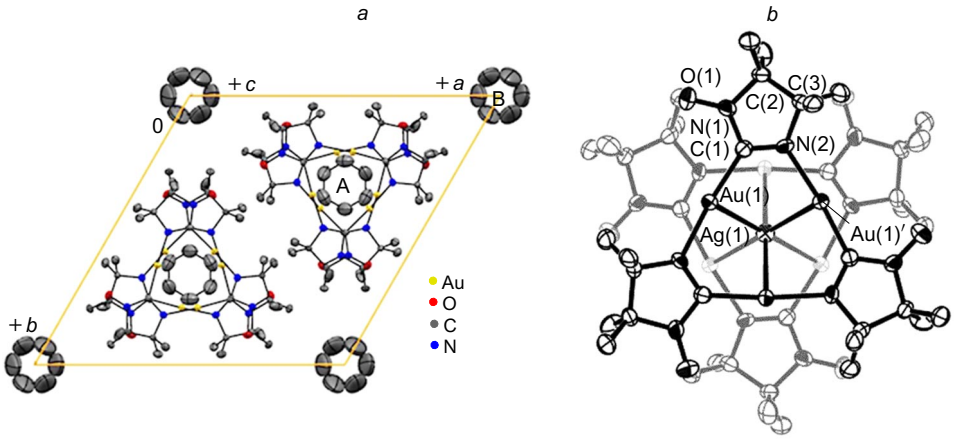
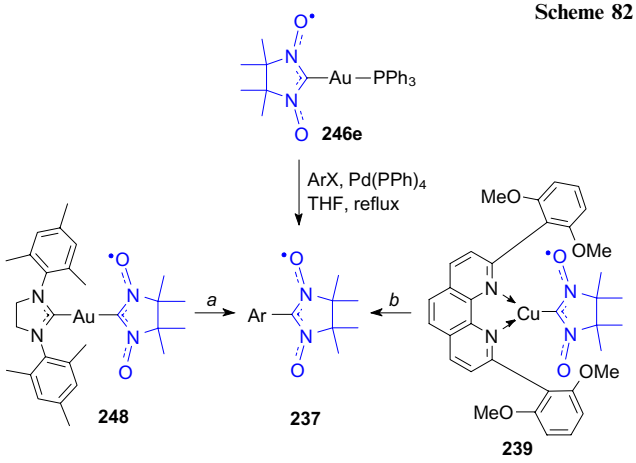


Figure 24. Fragments of packing of gold organic derivative **19** (*a*) and molecular structure of complex [(**19**)·Ag·(**19**)]PF_6 (*b*).[47] A and B are crystallographically independent cyclohexane molecules. Published with permission from John Wiley and Sons.

Scheme 82



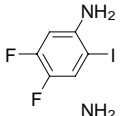
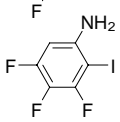
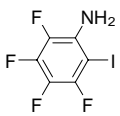
(*a*) ArX, $Pd(PPh)_4$ or $[Pd_2(dba)_3]$, $CHCl_3$, THF, reflux;
(*b*) ArX, DPPF, $[Pd_2(dba)_3]$, $CHCl_3$, THF, reflux; X = I, Br

The yields of the products of cross-coupling of various organometallic derivatives of nitronyl nitroxide **204** with aryl and heteroaryl halides are summarized in Table 2. It is worth noting that these reactions of aryl bromides, especially those containing electron-donating substituents, proceed more slowly and give products in lower yields than the reactions involving aryl iodides; this is correlated with the variation of reactivity of aryl halides in the oxidative addition to PdL_n. Among aryl iodides, lower reactivity is observed for *ortho*-substituted compounds, which is probably caused by steric factors.

Development of methods for the synthesis of metal derivatives of radical **204**, which are reactive towards cross-coupling with aryl iodides, resulted in considerable changes in the function-oriented synthesis of nitronyl nitroxides and design of high-spin systems. It is especially important that these reactions opened up the way to paramagnetic compounds that could not be either obtained by other methods or isolated in acceptable yields. For example, cross-coupling allowed targeted synthesis of phenothiazines **256** and **257**, containing the nitronyl nitroxide substituent in a definite position (Schemes 83 and 84).[309, 320] According to the classical Ullman method, the yields of these paramagnets were low, because not only 1,3-dihydroxyimidazolidine moiety, but also the sulfur atom was oxidized in the final step.

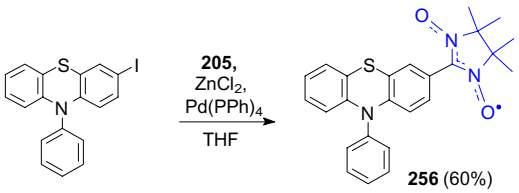
The cross-coupling reaction was used to synthesize nitronyl nitroxide-substituted heterocyclic ensemble **258**,

Table 2. Cross-coupling of organometallic derivatives **246e**, **248** and **239** with aryl and heteroaryl halides.[311, 319]

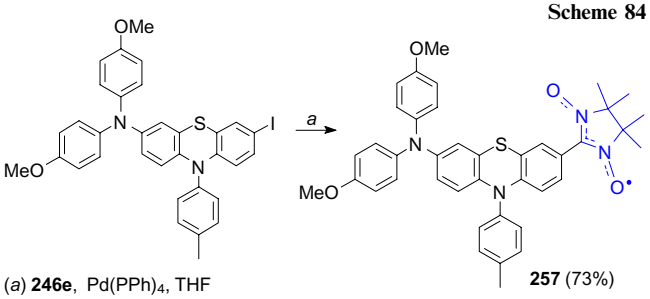
Substrate	Yield of **237** (%) in the reaction of		
	246e	**248**	**239**
4-$Me_2NC_6H_4I$	69	–	–
4-$Me_2NC_6H_4Br$	Traces	–	–
4-$MeOC_6H_4I$	81	73	73
4-$MeOC_6H_4Br$	Traces	34	5
3-$MeOC_6H_4I$	73	79	48
2-$MeOC_6H_4I$	83	53	62
4-PhC_6H_4I	–	91	64
4-PhC_6H_4Br	74	–	–
PhI	92	94	76
PhBr	–	57	6
4-AcC_6H_4I	80	95	71
4-AcC_6H_4Br	83	73	49
3-AcC_6H_4I	86	68	62
2-AcC_6H_4I	85	45	67
4-$F_3CC_6H_4I$	89	–	–
4-$O_2NC_6H_4I$	83	92	74
4-$O_2NC_6H_4Br$	–	85	63
1-NaphI	64	87	66
1-Iodopyrene	65	–	–
2-ThI	84	89	75
4-PyI	88	84	65
3-PyI	83	79	82
2-PyI	50	Traces	Traces
	50	–	–
	65	–	–
	4	–	–

which is oxidized to stable salts **259** and **260** (Scheme 85) characterized by strong ferromagnetic exchange in the cationic biradical part ($2J/k_B \gg 300$ K). A specific feature of salt **260** is that on cooling to 7 K, it undergoes magnetic phase transition to a weakly ferromagnetic state.[321]

Scheme 83

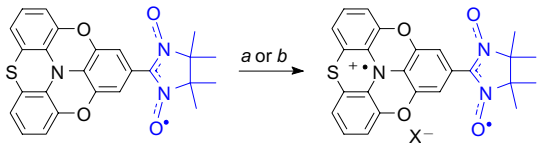


Scheme 84



(*a*) **246e**, $Pd(PPh)_4$, THF

Scheme 85

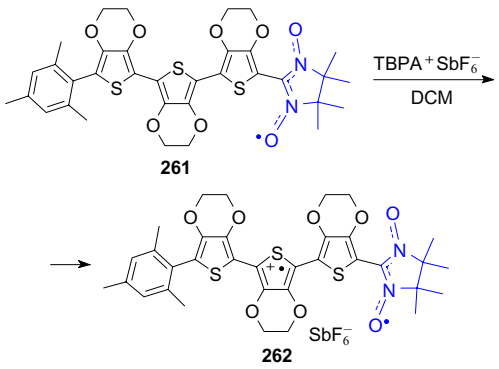


(*a*) tris(4-bromophenyl)ammonium hexafluoroantimonate (1.0 equiv.), DCM;
(*b*) thianthrenium tetrabromoferrate (1.0 equiv.), DCM – MeCN (1 : 1, vol.);
X = SbF_6^- (**259**), $FeBr_4^-$ (**260**)

Unique spin-labelled oligothiophenes (for example, compound **261** in Scheme 86), which are oxidized to biradical cations, were also obtained using this approach.[322, 323] This biradical cation **262** is stable and, according to the results of quantum chemical calculations [BS-UB3LYP/6-31G(d,p)], experiences very strong ferromagnetic exchange ($2J/k_B = +4240$ K), which is confirmed by the absence of the temperature dependence of the EPR signal at half field.[323]

The cross-coupling reaction also proved to be efficient for the synthesis of bi- and polyradicals of systematic structure. As examples, one can consider the transformation of *para*- and *meta*-substituted diodobenzenes into the corresponding stable biradicals **263** and **264**.[310] The reactions

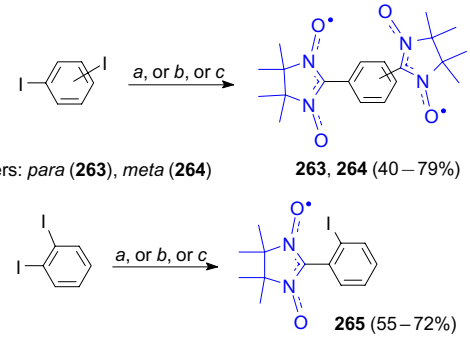
Scheme 86



TBPA is tris(4-bromophenylammonium) hexafluoroantimonate

gave good yields of products; furthermore, it was noticed that the intermediate monoradicals are more reactive towards cross-coupling than the initial diiodides (Scheme 87). A specific feature of the reactions involving *o*-diiodobenzene[310] or 1,8-diiodonaphthalene[324] is that they stop after the formation of the monoradical, *e.g.* **265**, due to steric restrictions.

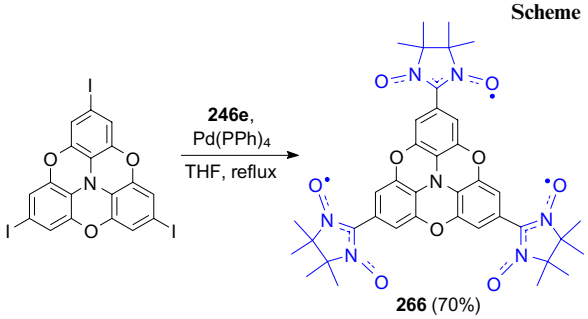
Scheme 87



(*a*) **246e**, $Pd(PPh)_4$; (*b*) **248**, $Pd(PPh)_4$;
(*c*) **239**, $[Pd_2(dba)_3]\cdot CHCl_3$, DPPF, THF, reflux;

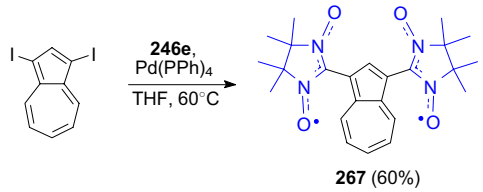
The cross-coupling reactions considered above immediately became an efficient tool that allows the synthesis of previously inaccessible high-spin systems such as triradical **266** with the redox-active core (Scheme 88).[310]

Scheme 88



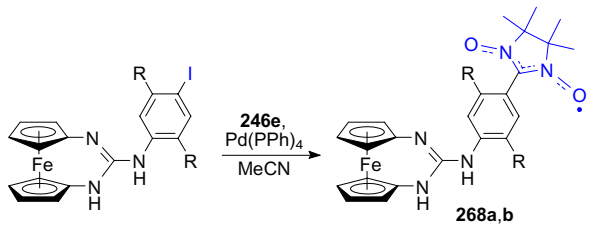
This process is indispensable if the required aldehydes (*e.g.* 1,3-diformylazulene) are available, but cannot be condensed with either bis(hydroxylamine) **145** or its sulfuric acid salt. In this case, it is possible to carry out cross-coupling of 1,3-diodoazulene with paramagnet **246e** to give triplet biradical **267** in a good yield (Scheme 89).[325]

Scheme 89



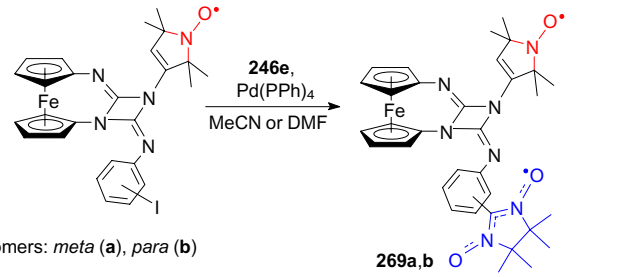
New opportunities for the synthesis of polyfunctional nitroxides are provided by combined approach that implies the use of two types of transformations — intramolecular click-reaction and cross-coupling of aryl iodides with derivative **246e**. This approach made it possible to synthesize a variety of spin-labelled derivatives such as 2-phenylamino-

Scheme 90



R = H (**a**, 34%), F (**b**, 19%)

Scheme 91

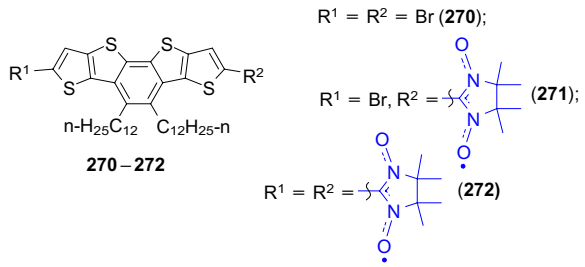


Isomers: *meta* (**a**), *para* (**b**)

1,3-diaza[3]ferrocenophanes **268a**,**b** and 1,3-diazetidine-2,4-diimines **269a**,**b** (Schemes 90 and 91).[326] Biradicals **269a**,**b** serve as convenient model systems, because they have a rigid skeleton and can be tuned towards exchange coupling between spin carriers of different nature.

Usually, aryl bromides are not cross-coupled with nitroxide **246e**. Rare exceptions are 2,2′-dibromo oligothiophene systems, which are able to give the corresponding biradicals in low yields.[327] As an example, consider the reaction of dibromo derivative **270** with nitroxide **246e**, which affords mono- (**271**) and biradical derivatives (**272**).

Structures 270 – 272



270 – 272

According to X-ray diffraction data, the molecules of dibromide **270** are preferably packed in pairs, with the distance between the ring planes being 3.42 Å and the molecules being slightly rotated relative to each other.[328] Monoradical **271** forms centrosymmetric dimers, which are arranged in stacks with a distance of 3.58 Å between the sulfur atoms (Fig. 25).[329] In the crystals of biradical **272**, two independent molecules form the corresponding pairs of centrosymmetric dimers (A···A and B···B), which are then packed into inclined stacks with a shortest distance of 3.58 Å between the sulfur atoms of neighbouring dimers.

The cross-coupling of organometallic derivatives of nitroxide **204** with aryl iodides also proved to be quite efficient in the design of high-spin organic compounds. For example, using this reaction, iodides **273a** – **c** were

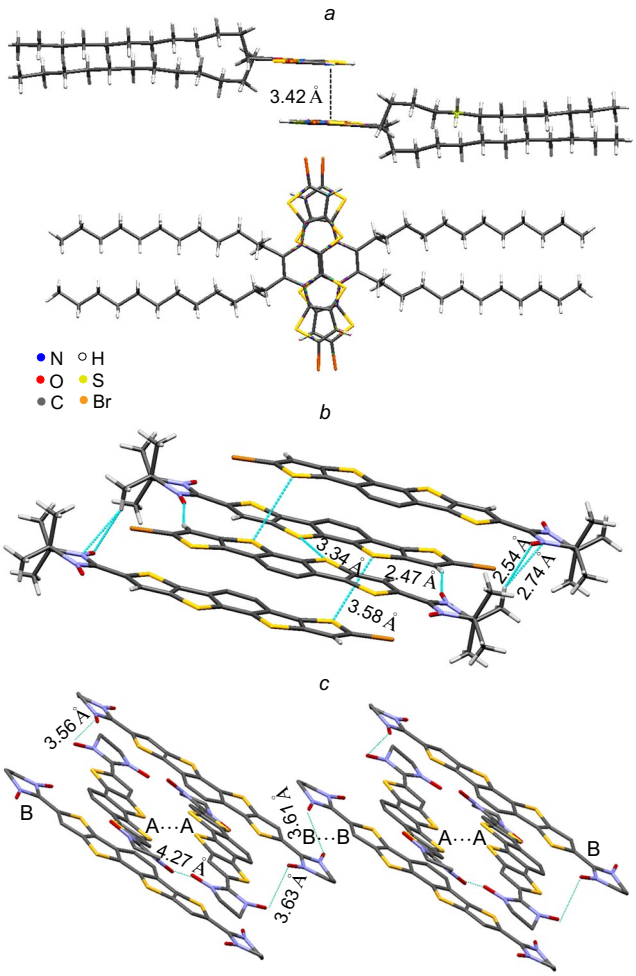
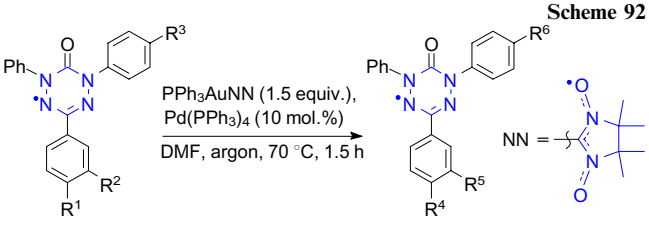


Figure 25. Fragments of packing and characteristic intermolecular contacts in dibromide **270** (*a*),[328] monoradical **271** (*b*) and biradical **272** (*c*).[329] Figure *a* is published with permission from Royal Society of Chemistry, Figs *b* and *c* are published with permission from John Wiley and Sons.

converted to a number of isomeric verdazyl-nitronyl nitroxide biradicals **274a** – **c**, in which the sign and the magnitude of the exchange coupling energy depend on the mode of coupling of two radical moieties (Scheme 92). All biradicals possess a high thermal stability: under inert atmosphere, they do nor decompose up to a temperature of 180 °C. Upon crystallization, biradicals with the triplet ground state form unique one-dimensional exchange-coupled chains with strong intramolecular and weak intermolecular ferromagnetic coupling (Fig. 26).[330]

Scheme 92



273a – c

R1 = I, R2 = R3 = H (**a**);
R1 = R2 = H, R3 = I (**b**);
R1 = R3 = H, R2 = I (**c**)

274a – c (79 – 82%)

R4 = NN, R5 = R6 = H (**a**);
R4 = R5 = H, R6 = NN (**b**);
R4 = R6 = H, R5 = NN (**c**)

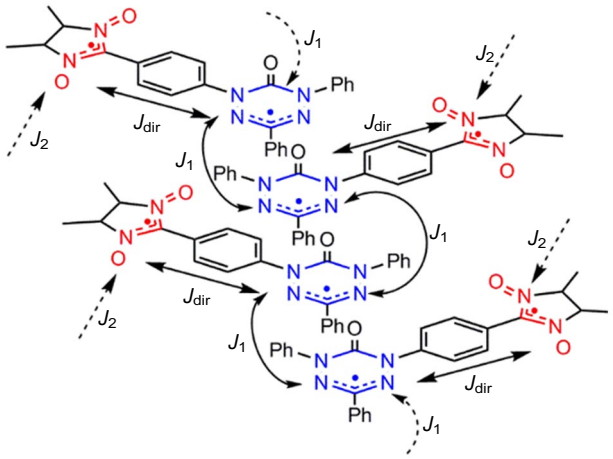
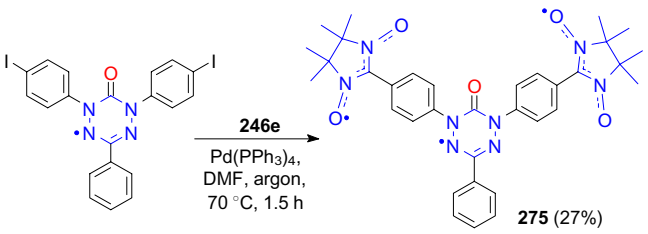


Figure 26. Fragment of chains in the solid phase of biradical **274b**, exchange channels and the corresponding exchange coupling parameters: $J_{dir} = 94 \pm 3$ cm^{-1}, $J_1 = 5.4$ cm^{-1}, $J_2 = -0.8$ cm^{-1}.[330] (J_{dir} and J_n are intra- and intermolecular exchange coupling parameters; the continuous and dashed lines show intra- and interchain exchange coupling channels, respectively). Published with permission from John Wiley and Sons.

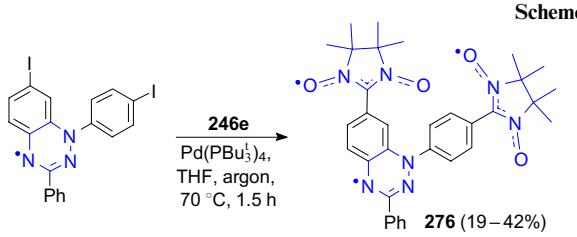
The next step towards the synthesis of polyradicals with the high-spin ground state was the synthesis of quartet triradicals **275**[331] and **276**,[332] containing two nitronyl nitroxide groups and verdazyl or triazinyl moiety (Schemes 93 and 94). Shu *et al.*[332] noted that in the synthesis of triradical **276**, high product yields (19–42%) are attained if the reaction is conducted in the presence of $Pd(PBu^t_3)_4$ rather than $Pd(PPh_3)_4$ (6–17%). Both triradicals possess high thermal stability; under inert atmosphere, they are stable up to a temperature of 160 °C. Moreover, the possibility of vacuum deposition of triradical **276** as molecular beam on the SiO_2/Si(111) surface was demonstrated; on this surface, the paramagnetic molecule remains unchanged for at least 17 h.

The synthesis of spin-labelled graphene nanoribbon **277** and polymeric derivative **278** as a reference compound was a significant event in the nitronyl nitroxide chemistry. The synthesis was accomplished by palladium-catalyzed cross-coupling of polybromides **279**, **280** with nitronyl nitroxide **246e** taken in a large excess (Scheme 95).[333]

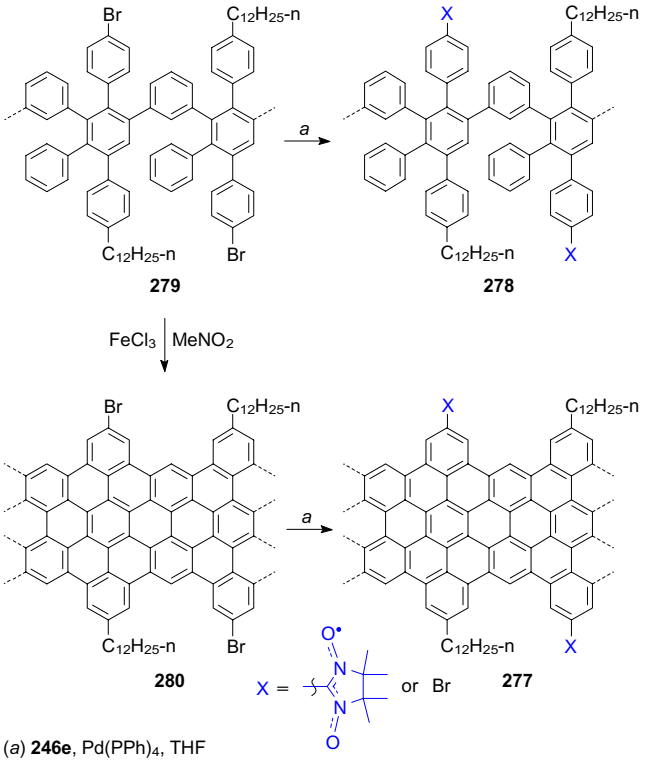
Scheme 93



Scheme 94



Scheme 95



The presence of radical moieties in polyphenylene **278** and in graphene nanoribbon **277** was confirmed by EPR experiments (Fig. 27), including quantitative experiments. It was shown that the degree of replacement of Br atoms by paramagnetic groups in samples of compounds **277** and **278** exceeds 1.3%.[334] Presumably, nitroxide groups in the molecules of polymers **278** and nanoribbons **277** were distributed randomly, but not equally probably, because more lightweight components, polybrominated substrates **279** and **280**, are more soluble in organic solvents; hence, the rate of reaction with organogold compound **246e** is also higher for these components.

In nanoribbon **277**, the parameters of exchange coupling between the unpaired electrons of the paramagnetic groups located on different sides (J_1) or on the same side (J_2) of nanoribbons differ in sign and amount to -25 ± 5 MHz (-8.3×10^{-4} cm^{-1}) and 12 ± 3 MHz (4.0×10^{-4} cm^{-1}), respectively (see Fig. 27). The signs of the exchange parameters are in line with the results of theoretical calculations,[335] but the parameters J_n ($n = 1, 2$) derived from experimental data are markedly smaller in magnitude than those found by quantum chemical calculations of model spin-labelled graphene nanoribbons.[336] Indeed, the calculated values of J_1 for the neighbouring nitroxide groups are in the range from -0.4 to -0.2 cm^{-1}, while J_2 values are close to 0.06 cm^{-1}. The cause behind the fact that the calculated J_n values differ from those derived from experiments by several orders of magnitude is the low content of paramagnetic groups in nanoribbons **277**. Nevertheless, it was possible to carry out an integrated study of compounds **277** and **278** by EPR spectroscopy, which revealed a considerable difference between the magnetic properties of

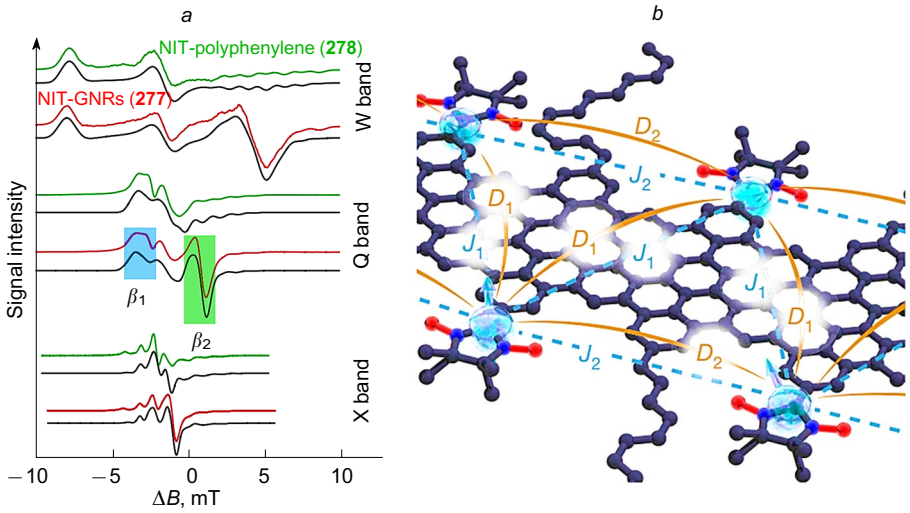


Figure 27. Experimental multifrequency EPR spectra for polymer **278** (green curve) and nanoribbon **277** (red curve) and model spectra (black curves below) plotted against the magnetic field from the edge-state resonance [the DEER pump and probe windows are designated by β_1 and β_2, respectively] (*a*) and pathways for radical spin interactions with indication of exchange (J_1 and J_2, blue dashed lines) and dipole (D_1 and D_2, orange lines) interactions (*b*).[333] Published with permission from Springer Nature.

the spin-labelled nanoribbons and the corresponding polymer.

Apart from the resonance signal of the paramagnetic group, the EPR spectra of nanoribbons **277** exhibit a signal with g-factor components $g_{||} = 2.0024(3)$ and $g_{\perp} = 2.0041(2)$, corresponding to the edge π-electron state of the nanoribbon (see Fig. 27).[337] The transitions between the Zeeman levels in nanoribbon **277** were studied using advanced EPR techniques.[333] The spin–spin (T_2 is the phase memory time of the system) and spin–lattice (T_1 is the time of recovery of the excited spin to the ground state) relaxation times were determined. In paramagnet **277** in the region of room temperatures, the T_1 value was close to ~10 s, which corresponded to theoretical predictions.[338] As the temperature decreased, T_1 increased to reach $10^3 - 10^4$ μs at temperatures <25 K, that is, when the spin–phonon mechanism of spin relaxation started to predominate.[17]

Experiments on determination of the spin echo dephasing time (T_m) in polymer **280** demonstrated that the major contribution to the loss of spin coherence is made by the spin–spin relaxation, which means that the times T_m and T_2 differ little. The T_m value proved to be 0.5 and 1.1 μs at 300 and 85 K, which is several orders of magnitude higher than the times T_m in graphene-based sprintronic devices.[339] However, the main feature of graphene nanoribbon **277** is the presence of two paramagnetic subsystems, the proper nitroxide and edge ones; the electron–electron interactions between the systems were studied using four-pulse double electron–electron resonance (DEER). In the experiment, system excitation and signal detection were carried out at the radical resonance frequency, and perturbation occurred at the edge-state resonance. The DEER spectrum of nanoribbons **277** is a superposition of fast oscillations caused by the dipole–dipole interaction D_1 and D_2 and slow oscillations caused by interactions of the spins of paramagnetic groups and the spins of edge states (Fig. 28 *a*). Fast Fourier transform of the DEER signal gives an electron–electron interaction energy of 1.5 MHz (see Fig. 28 *b*), which corresponds to a characteristic inversion time of spin subsystems of 330 ns. Since this time is markedly shorter than T_m, this opens up the possibility of quantum operations using of graphene edge states and nitroxide spins.[17]

Thus, in recent years, the synthetic chemistry of nitronyl nitroxides made a huge step forward, thus markedly

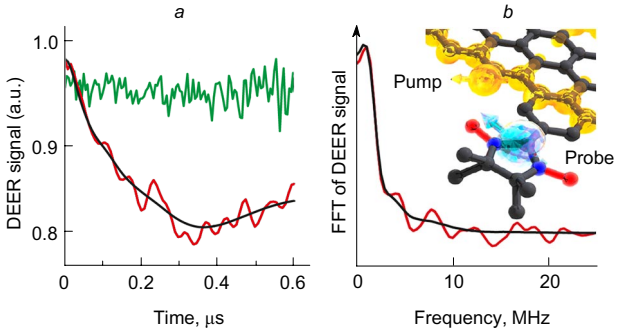


Figure 28. Background-corrected DEER signal for polyphenylene **278** (green curve) and graphene nanoribbon **277** (red curve) and low-frequency component of the DEER signal (black curve) (*a*) and fast Fourier transform (FFT) of the DEER signal for compound **277**, which shows the interaction energy spectrum characteristic of two-spin operations (the black curve singles out the contribution from edge states that interact with localized spins) (*b*).[333] Published with permission from Springer Nature.

expanding the potential of function-oriented synthesis of diverse paramagnetic systems: triplet biradicals and quartet triradicals with high thermal stability, volatile polyfluorinated paramagnets, spin-labelled conjugated polyaromatic compounds, including graphene nanoribbons, and heterospin systems of unusual architecture. The potential of the proposed pathways towards nitronyl nitroxides are far from being exhausted, and their skilled use will open up the way to embodiment of numerous ideas and intentions in the molecular design of magnets.

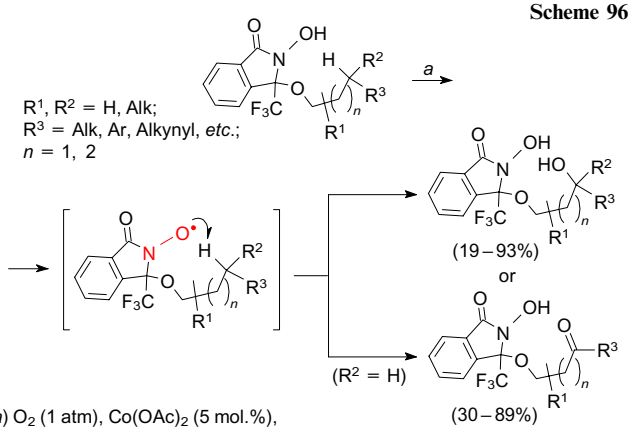
3.5. Phthalimide-*N*-oxyl radicals

Compared with their acyclic analogues, cyclic carbonyl nitroxides are more widely used as *in situ* generated reactive intermediates (or reagents) for CH-functionalization by radical elimination of hydrogen and for radical addition to C=C double bonds. This is apparently caused by the synthetic accessibility of cyclic carbonyl nitroxides and also by their stability against self-decomposition, which provides for the efficiency of targeted functionalization of organic substrates.

The amide-*N*-oxyl radicals generated *in situ* from cyclic arylhydroxamic acids with electron-withdrawing CF_3

groups were used in the intermolecular [340] and intramolecular [341, 342] oxidation reactions of activated [340, 341] and non-activated [341, 342] CH- or CH_2 groups. Scheme 96 shows one of such examples. In the substrate, the hydroxamic acid moiety is covalently linked to diverse alcohols and promotes selective CH oxidation of γ- ($n = 1$) or (more rarely) δ-position ($n = 2$). If there is only one hydrogen atom in this position, a hydroxyl group is formed, while in the presence of two hydrogen atoms, a carbonyl group is generated.[341] When the $Co(OAc)_2 - Me_2S$ system is used, dimethyl sulfide serves for the reduction of intermediate hydroperoxide to alcohol.[341]

Scheme 96

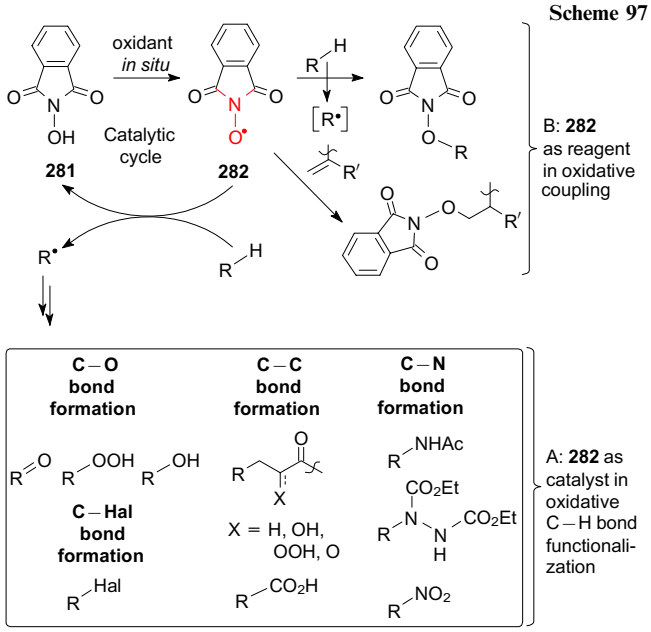


(*a*) O_2 (1 atm), $Co(OAc)_2$ (5 mol.%), $Mn(OAc)_3 \cdot 2H_2O$ (5 mol.%) or $Co(OAc)_2$ (1 mol.%), Me_2S (1.2–3 equiv.), CF_3CH_2OH, rt–50 °C, 0.5–27 h

Imide-*N*-oxyl radicals containing two electron-withdrawing carbonyl groups at the nitrogen atom are more potent oxidants than amide-*N*-oxyl radicals. The available precursor — *N*-hydroxyphthalimide **281** — can be readily converted to phthalimide-*N*-oxyl radical **282**, which is the most widely used imide-*N*-oxyl. The introduction of substituents into the benzene ring of compound **281** changes the O–H bond energy and stability of radicals **282**.[343] Apart from the availability, advantages of radical **281** include generation under mild conditions, slow self-decomposition and high reactivity towards hydrogen atom elimination from organic substrates, including non-activated alkanes. Currently, *N*-hydroxyphthalimide is used in the industrial oxidation of adamantane to hydroxyadamantanes (Daicel, Japan) and is studied as a catalyst for other industrial processes, *e.g.*, oxidation of cyclohexane and alkylarenes and synthesis of carboxylic acids, hydroperoxides, phenols and epoxides.[344]

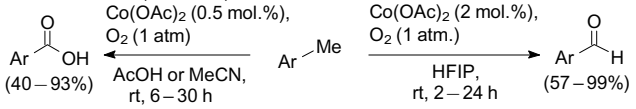
Starting from the 1990s, there have been quite a number of publications on the use of *N*-hydroxyphthalimide (**281**) and its analogues as precursors of catalytically active imide-*N*-oxyl radicals **282**, meant for selective oxidation reactions with the formation of new C–O, C–C, C–N, C–Hal and other bonds (Scheme 97, panel A). These results were summarized earlier in a number of reviews;[344–349] therefore, in this review, we mention only selected examples published mostly after 2010. One more field of application of imide-*N*-oxyl radicals **282** is the synthesis of O-substituted *N*-hydroxyimides *via* oxidative coupling (see Scheme 97, panel B).[350] The development of this field became especially relevant in relation to the developed synthetic applications of these derivatives in selective radical reactions accompanied by N–O bond cleavage.[350–353]

Scheme 97



In the presence of co-catalysts, *N*-hydroxyphthalimide **281** is oxidized with molecular oxygen to give phthalimide-*N*-oxyl radicals **282** even at room temperature; therefore, it serves as the basis for efficient systems for selective liquid-phase aerobic oxidation. An example is the **281**–$Co(OAc)_2$ catalytic system,[354–356] which is active even at room temperature and at atmospheric O_2 partial pressure.[354, 355] Using this system, methylarenes can be oxidized to either aromatic carboxylic acids [354] or aldehydes,[355] depending on the solvent (Scheme 98).

Scheme 98



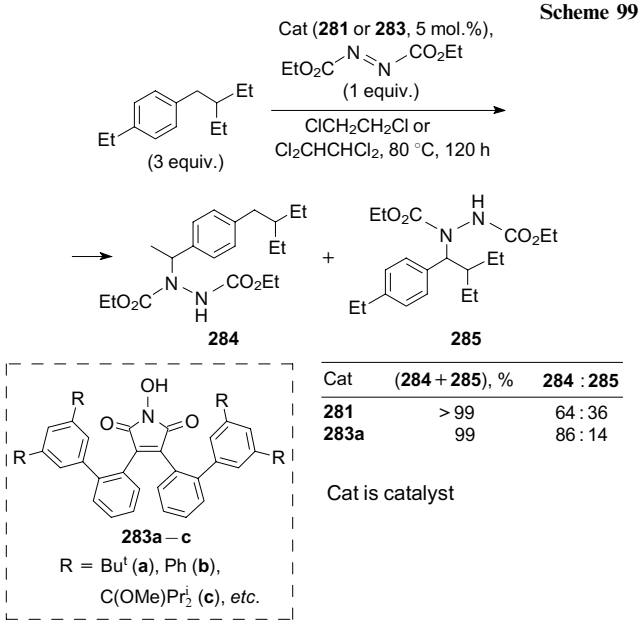
HFIP is 1,1,1,3,3,3-hexafluoropropan-2-ol

Compounds **283**, precursors of imide-*N*-oxyl radicals, with bulky substituents were synthesized with the goal to perform selective functionalization of sterically most accessible C–H groups in the presence of other activated C–H bonds. In relation to CH-amination of 1-ethyl-4-(2-ethylbutyl)benzene, it was shown that the regioselectivity of C–H bond cleavage (ratio of products **284** and **285**) was higher when sterically crowded organocatalyst **283a** was used than in the presence of *N*-hydroxyphthalimide **281** (Scheme 99).[357]

Catalytic systems based on *N*-hydroxyphthalimide **281** or *N*-hydroxysuccinimide **286** in combination with cobalt or copper acetate were successfully used for aerobic oxidation of organosilicon compounds under mild conditions. The developed methods made it possible to prepare silanols [358, 359] and silicon-containing aromatic carboxylic acids difficult to obtain by other methods (Scheme 100).[358]

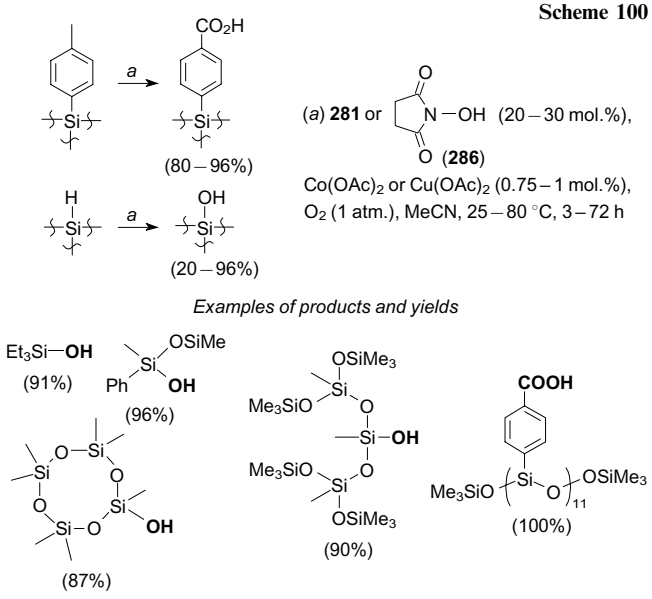
A drawback of catalytic systems for oxidation based on transition metal salts is the tendency of metal ions to complex formation. When substrates or oxidation products have chelating properties, these systems can be deacti-

Scheme 99



Cat	(284 + 285), %	284 : 285
281	> 99	64 : 36
283a	99	86 : 14

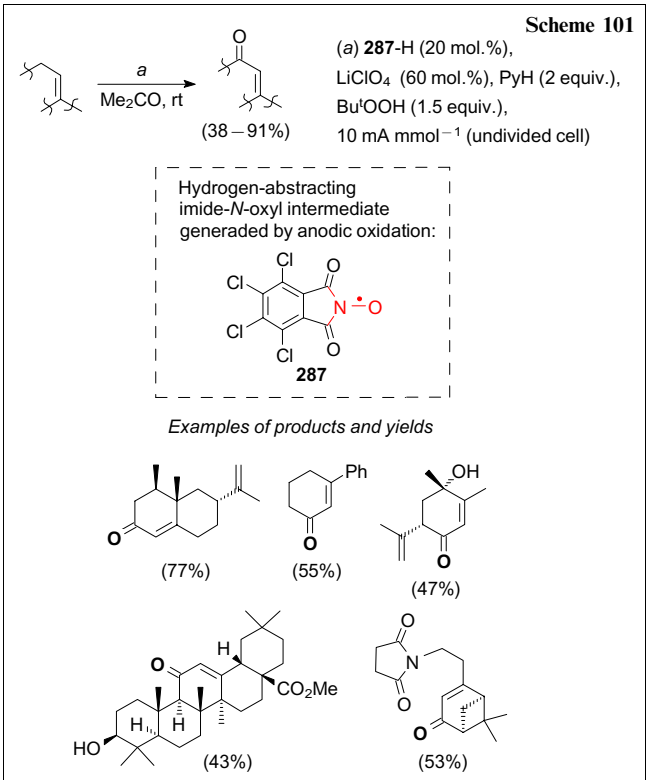
Scheme 100



vated.[356] Together with other factors, this stimulated the search for more reliable and versatile electrochemical oxidation methods in which imide-*N*-oxyl radicals are generated by anodic oxidation of *N*-hydroxyimides.[360] Electrochemical methods were proposed for the synthesis of (hetero)aryl ketones [356, 361] from alkyl-substituted (hetero)arenes, synthesis of iodomethylarenes [362] from methylarenes and synthesis of α,β-unsaturated ketones [363] from alkenes by allylic oxidation.

An example of electrochemical oxidation of alkenes to α,β-unsaturated ketones is depicted in Scheme 101. Tetrachlorophthalimide-*N*-oxyl radical **287** generated at the anode is the active intermediate, which abstracts hydrogen from the allylic position to give allyl radical. In this reaction, *tert*-butyl hydroperoxide should be used apart from the electric current as a co-oxidant to attain high selectivity. This method was found to be applicable, in

Scheme 101

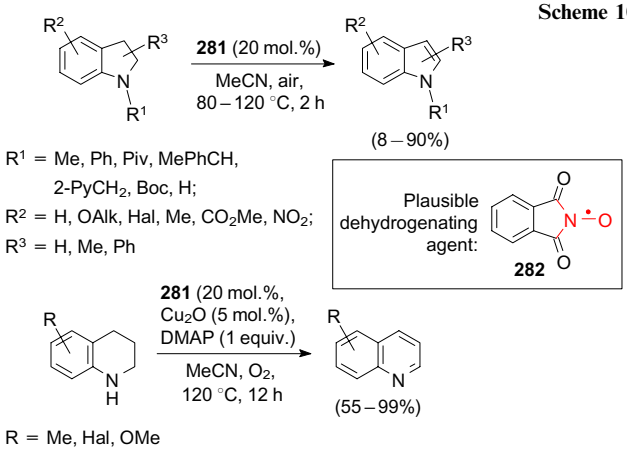


particular, for selective oxidation of complex unsaturated steroids and terpenes.[363]

N-Hydroxyphthalimide **281** was used as the catalyst of aerobic dehydrogenation of *N*-heterocycles (Scheme 102). Apparently, the key step of the process is elimination of a hydrogen atom from the heterocycle by the phthalimide-*N*-oxyl radical **282** generated from *N*-hydroxyphthalimide on heating in air. Dehydrogenation of indolines to indoles proceeds without co-catalyst; however, the product yields can be increased by adding catalytic amounts of $Cu(OAc)_2$.[364] Meanwhile, tetrahydroquinolines and some related heterocycles (tetrahydroisoquinoline, tetrahydroquinoxaline, 2-phenylpiperidine) are dehydrogenated under more drastic conditions in the presence of added Cu_2O and 4-dimethylaminopyridine.

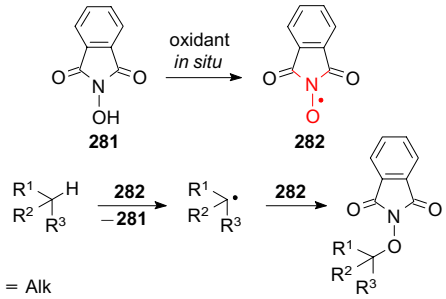
As noted above (see Scheme 97, panel B), imide-*N*-oxyls are used, in some cases, for the radical oxidative C–O coupling. The complexity of these processes lies in the fact that two intermediates prone to side reactions — *N*-oxyl

Scheme 102



and C-centred radicals — are generated simultaneously in the reaction mixture. In order to attain selective formation of the C—O coupling products, it is necessary to rule out the side oxidation of the CH-reagent and decay of *N*-oxyl radicals. This is attained by thorough selection of the oxidative system depending on the structure of the CH- and NOH-reagents. In most studies, *N*-hydroxyimides, most often *N*-hydroxyphthalimide **281**, are used as NOH-reagents. This is due to the fact that phthalimide-*N*-oxyl radical **282** has a sufficiently long lifetime and can abstract a hydrogen atom from the CH-reagent, thus generating C-centred radicals (Scheme 103).

Scheme 103

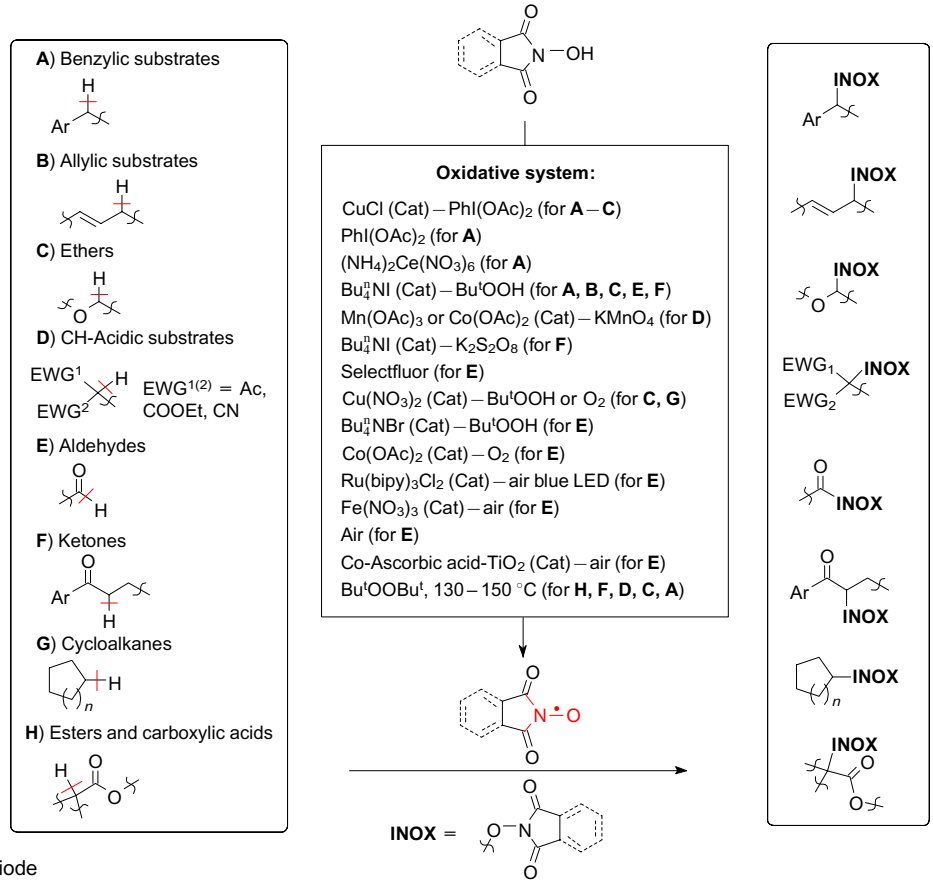


Scheme 104 shows examples of oxidative coupling of *N*-hydroxyimides with various types of substrates such as benzyl- or allyl-containing molecules, ethers, CH-acids, aldehydes, ketones, cycloalkanes, esters and carboxylic acids. Depending on the substrate structure, various oxidants or oxidative systems were proposed: CuCl (Cat) – $PhI(OAc)_2$,[365] $PhI(OAc)_2$,[366] $(NH_4)_2Ce(NO_3)_6$,[175] $Mn(OAc)_3$,[186] Bu^n_4NI (Cat) – Bu^tOOH,[367–371] $Co(OAc)_2$ (Cat) – $KMnO_4$,[186] Bu^n_4NI (Cat) – $K_2S_2O_8$,[372] Selectfluor,[373] $Cu(NO_3)_2$ (Cat) – Bu^tOOH,[374] $Cu(NO_3)_2$ (Cat) – O_2,[374] Bu^n_4NBr – Bu^tOOH,[368] $Co(OAc)_2$ (Cat) – O_2,[375] $Ru(bipy)_3Cl_2$(Cat) – air (bipy is 2,2′-bipyridine) under blue light irradiation,[376] $Fe(NO_3)_3$ (Cat) – air,[377] air without a catalyst,[378] air in the presence of the Co – ascorbic acid – TiO_2 composite,[379] Bu^tOOBu^t.[380]

The oxidative coupling involving *N*-hydroxyimides requires, most often, potent oxidants, which ensure the formation of imide-*N*-oxyl radicals in a higher concentration than it is necessary to carry out the above-considered aerobic oxidation reactions catalyzed by *N*-hydroxyimides. Molecular oxygen, which can compete with the imide-*N*-oxyl radical in the trapping of C-centred radical, is rarely used as the oxidant. An exception is coupling with aldehydes (most often, aromatic aldehydes), for which the largest number of effective oxidative systems were developed. A common drawback of most of the methods shown in the Scheme is the necessity of using an excess of the CH-reagent to suppress side processes. Among the presented examples, attention is drawn by the oxidative coupling involving CH-acidic β-dicarbonyl compounds and their hetero analogues.[186] First, these reactions do not require an excess of CH-reagent and, second, they proceed not only with *N*-hydroxyimides, but also with *N*-hydroxyamides, which are converted to relatively less reactive amide-*N*-oxyl radicals (see Section 2.3).

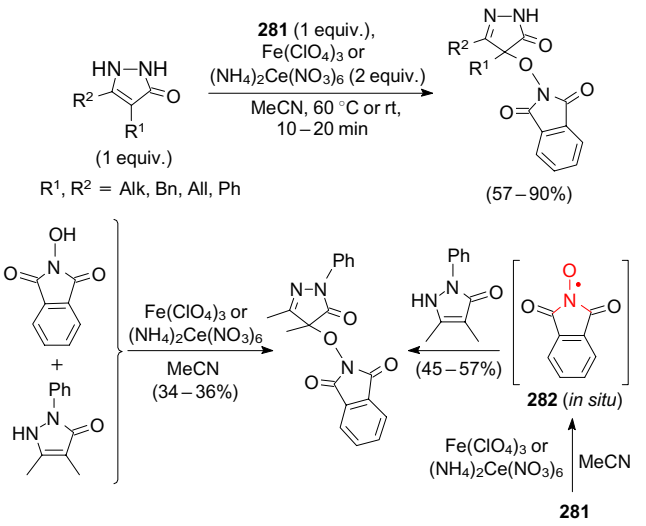
Among the described oxidative C—O coupling reactions using imide-*N*-oxyl radicals, there are no reactions of aromatic compounds. This can be attributed to the greater strength of the $C(sp^2)$—H bonds compared to the

Scheme 104



LED is light-emitting diode

Scheme 105



C(sp^3)–H bonds and the unfavourability of radical addition to the carbon atom of the aromatic ring due to the loss of aromaticity. An example of oxidative coupling of imide-*N*-oxyl radicals with heterocyclic substrates is the reaction of phthalimide **281** with pyrazolones (Scheme 105).[176]

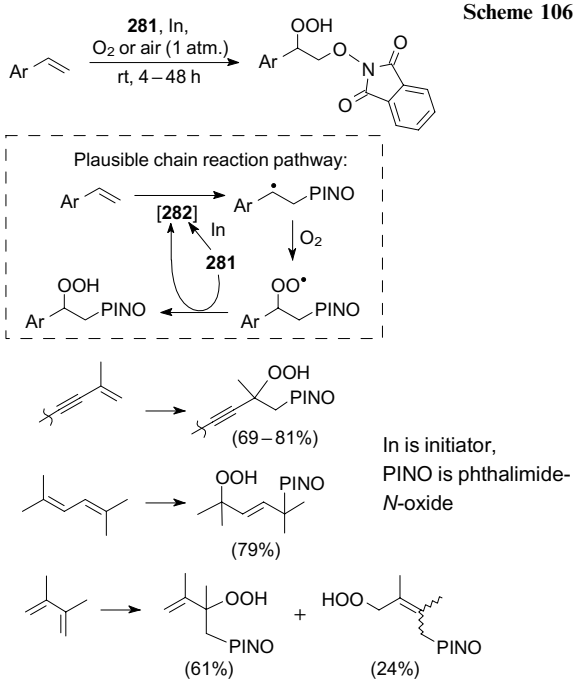
The reaction efficiently proceeds under the action of various oxidants that generate phthalimide-*N*-oxyl radicals *in situ* from *N*-hydroxyphthalimide (**281**). The best results were attained with $Fe(ClO_4)_3$ and $(NH_4)_2Ce(NO_3)_6$ as oxidants. A special place is occupied by phenyl-substituted pyrazolones highly prone to oxidation. When this coupling is carried out with 4,5-dimethyl-2-phenyl-1,2-dihydro-3*H*-pyrazol-3-one by adding an oxidant to a mixture of pyrazolone and *N*-hydroxyphthalimide (**281**), the yield of the C–O coupling product does not exceed 36% and the reaction is accompanied by side oxidative dimerization of pyrazolone. The efficiency of the synthesis of C–O coupling product can be increased by preliminary generation of phthalimide-*N*-oxyl radical **282** before the addition of pyrazolone to the reaction mixture.[176]

While summarizing the discussion of the oxidative C–O coupling involving imide-*N*-oxyl radicals, it should be noted that compounds hard to oxidize (alkanes,[374] non-activated carbonyl compounds[380]) and compounds that are too easily oxidized (*e.g.* some pyrazolones[176]) are both undesirable substrates for these reactions. In the former case, the factor restricting the efficiency of coupling is difficulty of hydrogen atom abstraction from an inert substrate. In the latter case, the excessive tendency of C-components to oxidation results in higher rates of side reactions compared with the rate of generation of imide-*N*-oxyl radicals.

The addition of imide-*N*-oxyl radicals to C=C double bonds is typical for vinylarenes. These substrates tend to add free radicals owing to stabilization of the resulting C-centred radical *via* conjugation with the aryl moiety. In the reactions with imide-*N*-oxyl radicals, non-conjugated alkenes are more prone to hydrogen atom elimination from the allylic position[363,365,367,381] rather than to addition to the C=C bond.

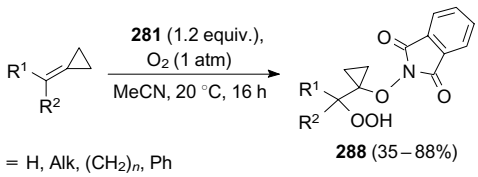
A typical functionalization reaction of vinylarenes involving phthalimide-*N*-oxyl radicals is the chain addition of *N*-hydroxyphthalimide (**281**) and air oxygen to the C=C double bond to give hydroperoxides.[382] The reaction occurs at room temperature and affords products in high (up to nearly quantitative) yields. The reaction can be initiated by Bu^{t}OOH (1 equiv.),[382] blue light irradiation,[383] visible light irradiation in the presence of organic photocatalyst [4,4′-bis(dimethylamino)benzophenone, 2 mol.%],[384] $Mn(acac)_3$ (0.02–0.5 mol.%)[385] (acac is acetylacetonate) or $Fe(NO_3)_3$ (20 mol.%).[386] Unsaturated hydroperoxides were obtained in a similar way from conjugated dienes[385] and enynes (Scheme 106).[385,387]

Scheme 106



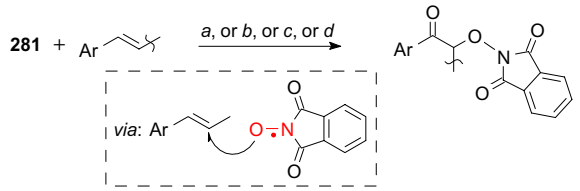
As noted above, non-conjugated alkenes are not prone to selective addition of phthalimide-*N*-oxyl radicals, because hydrogen atom abstraction from the allylic position by this radical predominates. An exception is the reaction of strained methylenecyclopropanes. Apparently, this reaction follows a chain radical mechanism, in which the addition of radical **282** to the C=C bond to give C-centred radical is followed by the addition of an oxygen molecule. The peroxyl radical thus formed abstracts a hydrogen atom from *N*-hydroxyphthalimide (**281**) to afford the final hydroperoxide product **288** and radical **282** (Scheme 107).[388] A similar reaction can be carried out for benzotriazolyl-*N*-oxyl radical generated from *N*-hydroxybenzotriazole.

Scheme 107



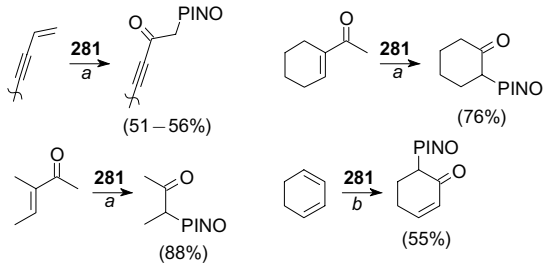
In some cases, the addition of phthalimide-*N*-oxyl radicals **282**, generated *in situ* in the presence of copper and iron salts, to styrenes under similar conditions results in the selective formation of functionalized aryl ketones (Scheme 108). The $Cu(MeCN)_4ClO_4-O_2$,[389] $Cu(OAc)_2$–air,[390] $FeCl_3-O_2$ [391] and $CuBr_2$–Bu^{t}OOBu^t

Scheme 108



(*a*) $Cu(MeCN)_4ClO_4$ (5 mol.%) , O_2, MeCN, rt, 18 h;
(*b*) $Cu(OAc)_2$ (10 mol.%), air, DMF, rt, 5–32 h;
(*c*) $FeCl_3$ (10 mol.%), O_2, MeCN, H_2O, rt, ~72 h;
(*d*) $CuBr_2$ (10 mol.%), Bu^tOOBu^t (3 equiv.), $C_2H_4Cl_2$, air, rt, 12 h

Examples of related reactions



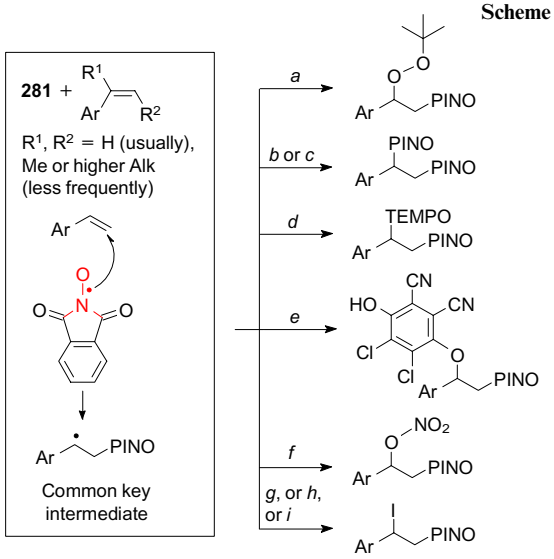
(Ref. 392) systems are suitable as oxidants. A probable pathway to the keto group in the products is the transition metal-catalyzed degradation of the peroxide group, formed as a result of trapping of the benzyl radical by molecular oxygen.[387, 389–391] A similar reaction was carried out with the double bonds of enynes[389] and cyclohexadiene;[390] the product yields were moderate. The addition of phthalimide-*N*-oxyl radicals **282** to α,β-unsaturated ketones is accompanied by deacylation and formation of a new keto group.[389]

By thorough selection of conditions, the benzyl radical formed after the addition of the imide-*N*-oxyl radical to the C=C double bond of vinylarene can be converted to products containing various substituents in the benzylic position (Scheme 109), including $OOBu^t$ group (conditions *a*),[392] PINO moieties (conditions *b* or *c*),[381, 393] 2,2,6,6-tetramethylpiperidine *N*-oxide (TEMPO, conditions *d*),[394] 2,3-dichloro-5,6-dicyano-4-hydroxyphenoxide (conditions *e*),[395] ONO_2 group (conditions *f*)[393] and I atom (conditions *g*, *h* or *i*).[393, 396, 397] Apart from vinylarenes, the radical difunctionalization reactions taking place *via* addition of the phthalimide-*N*-oxyl radical were carried out for norbornene,[394] vinyl acetate[393] and acrylates.[393, 397] Apparently the restricted structural diversity of substrates of molecules containing no aryl substituent at the C=C double bond is associated with the allylic oxidation reactions induced by imide-*N*-oxyl radicals, which take place if the double bond is not activated towards radical addition.[363, 365, 367, 381]

2-Oxoindolines functionalized by an oxyimide moiety were obtained by the addition of phthalimide-*N*-oxyl or succinimide-*N*-oxyl radicals generated *in situ* to the C=C double bond of α,β-unsaturated *N*-arylamides.[372] Presumably, the addition of imide-*N*-oxyl radical to the double bond is followed by cyclization of the resulting C-centred radical *via* attack on the aryl moiety of the substrate by this radical (Scheme 110).[372]

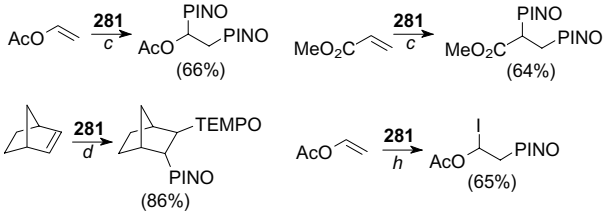
Phthalimide-*N*-oxyl radicals **282** generated by constant-current anodic oxidation of *N*-hydroxyphthalimide **281** in an undivided electrochemical cell add to the C=C bond of

Scheme 109



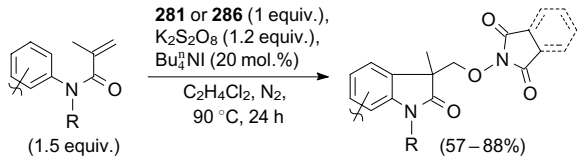
(*a*) CuCl (10 mol.%), 5–6 M Bu^tOOH in decane (5 equiv.), $C_2H_4Cl_2$, air, rt, 12 h;
(*b*) CuCl (10 mol.%), $PhI(OAc)_2$ (2.2 equiv.), $C_2H_4Cl_2$, air, 80 °C, 12 h;
(*c*) $(NH_4)_2CO(NO_3)_6$ (1.5 equiv.), MeOH, rt, ari, 30 min;
(*d*) TEMPO (2 equiv.), 5–6 M Bu^tOOH in decane (3 equiv.), TsOH (10 mol.%), $C_2H_4Cl_2$, 60 °C, air, 4 h;
(*e*) DDQ (0.66 equiv.), $C_2H_4Cl_2$, 60 °C, argon, 5–24 h;
(*f*) $(NH_4)_2Ce(NO_3)_6$ (2 equiv.), MeCN, 0 °C, Ar, 2 h;
(*g*) I_2 (0.5 equiv.), $PhI(OAc)_2$ (0.6 equiv.), $C_2H_4Cl_2$, air, rt, 10 min;
(*h*) I_2 (0.5 equiv.), $(NH_4)_2Ce(NO_3)_6$ (1.5 equiv.), $C_2H_4Cl_2$, H_2O, air, rt, 30 min;
(*i*) I_2 (0.5 equiv.), 70% aq. Bu^tOOH (2 equiv.), $C_2H_4Cl_2$, air, 80 °C, 6 h

Examples of related reactions

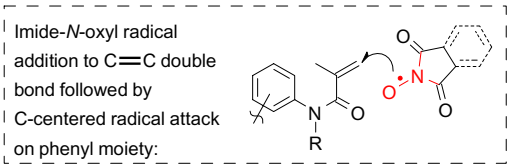


DDQ is 2,3-dichloro-5,6-dicyano-1,4-benzoquinone

Scheme 110

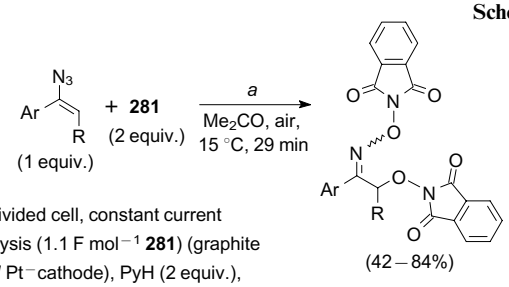


R = Me, Et, Pr^i, Ph, Bn



vinyl azides. The reaction is accompanied by elimination of N_2 from the azide group and addition of a second phthalimide-*N*-oxyl radical **282** to the resulting iminyl radical to give a N–O–N group unusual for organic compounds (Scheme 111).[398]

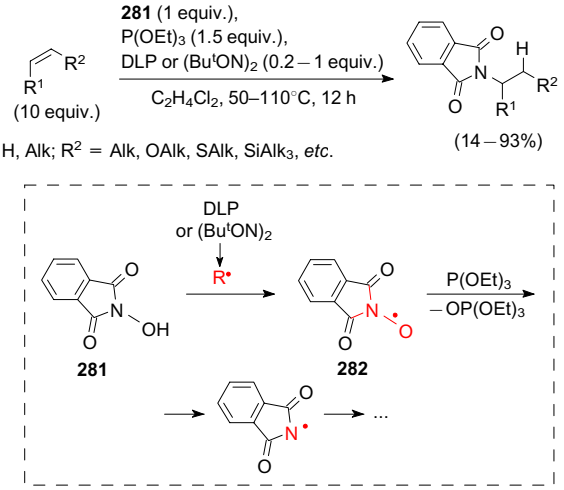
Scheme 111



(*a*) undivided cell, constant current electrolysis (1.1 F mol^{-1} **281**) (graphite anode / Pt$^-$cathode), PyH (2 equiv.), $[PyH_2]ClO_4$ (1 equiv.); R = H, Ph

Special mention should be made of the ability of phthalimide-*N*-oxyl radical **282** to transfer an oxygen atom to the phosphorus(III) atom of triethyl phosphite to give *N*-centred phthalimide radical and triethyl phosphate (Scheme 112).[399] Apparently, this reaction is a key step of the anti-Markovnikov hydroamination of C=C double bonds. In the proposed chain mechanism, phthalimide-*N*-oxyl radicals **282** generated under the action of radical initiators [dilauroyl peroxide or $(Bu^tON)_2$] react with $P(OEt)_3$, being thus converted to phthalimide radicals, which add to the C=C double bond and thus give C-centred radicals. The last step is regeneration of the phthalimide-*N*-oxyl radicals *via* hydrogen atom transfer between *N*-hydroxyphthalimide **281** and C-centred radical.[399]

Scheme 112

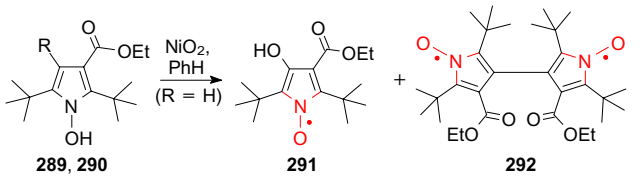


Thus, in recent years, reactions involving the phthalimide-*N*-oxyl radical have become a valuable synthetic tool in organic chemistry. In the future, new discoveries and trends are expected to appear in the chemistry of cyclic acyl nitroxides. Interesting results may be obtained if correlations between the properties and structure of the phthalimide-*N*-oxyl radical are elucidated: for example, the effect of fluorine atoms as substituents, building up a fused aromatic system, *etc*. Of considerable interest for the molecular design of magnets would be successful attempts to stabilize phthalimide-*N*-oxyl radicals and their analogues, isolate these species in a free state and use as planar unpaired electron carriers.

3.6. Pyrrole- and benzimidazole-based aromatic nitroxides

Paramagnetic compounds in which the nitrogen atom of the NO group is incorporated in an aromatic ring form a special group of conjugated nitroxides. The kinetic stability of carbazole-*N*-oxyl mentioned above was increased by surrounding the paramagnetic centre by a cage made of polymethylene units.[195] Similarly, whereas pyrrole-*N*-oxyl and many other its simple derivatives were detected only by EPR in solution,[400] some tetrasubstituted pyrrole-*N*-oxyl radicals can be isolated in a pure state. For example, thermally stable 2,5-di-*tert*-butyl-3,4-diethoxycarbonylpyrrole-*N*-oxyl (**289**)[401] and some its analogues were obtained. The oxidation of *N*-hydroxy derivative **290** on treatment with nickel peroxide gives unexpectedly not only monoradical **291**, but also dimer **292** (Scheme 113). According to X-ray diffraction data, the N–O bond lengths in biradical **292** are 1.279 and 1.281 Å, and the angle between the planes of the aromatic rings 80.77°.[402]

Scheme 113

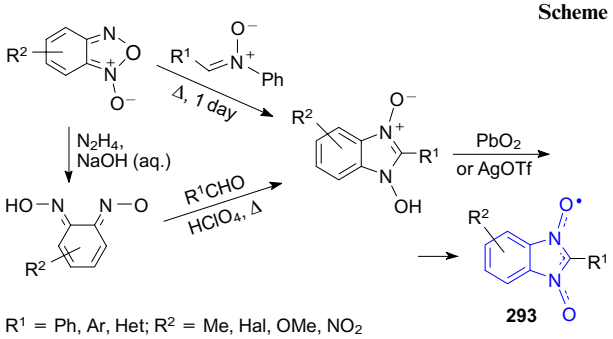


R = CO_2Et (**289**), H (**290**)

Apart from the introduction of bulky and electron-withdrawing substituents, another efficient way to increase the stability of aromatic nitroxides is annulation of aromatic rings and the presence of additional heteroatoms. For example, quite an extensive group of benzimidazole-1-oxyl 3-oxides **293** were isolated in a pure state and fully characterized (Scheme 114).[403–408] According to X-ray diffraction data, the benzimidazole-1-oxyl 3-oxide skeleton is planar, the range of O–N bond lengths is 1.27–1.29 Å, while the N–C(2) bonds are 1.35–1.36 Å long, which corresponds to the ranges of variation of analogous geometric parameters in 2-imidazoline-1-oxyl 3-oxides.[16] It was shown that the planar geometry and spin density delocalization of benzimidazole-1-oxyl 3-oxides **293** may give rise to efficient channels for intermolecular exchange, including ferromagnetic exchange ($2J/k_B$ of -190 to $+130$ K).[407] In addition, it was shown that derivatives **293** containing a 2-thienyl substituent are prone to donor–acceptor interactions, which are manifested as an absorption band in the near-IR range ($\lambda_{max} \approx 1000$ nm) and solvatochromic effects.[409]

It is beyond doubt that aromatic nitroxides would experience a revival, since their planar structure is perfect for implementation of efficient McConnell ferromagnetic exchange. In particular, it would be expedient to concentrate attention on the synthesis of fluoro- and polyfluoro-

Scheme 114



R^1 = Ph, Ar, Het; R^2 = Me, Hal, OMe, NO_2

substituted benzimidazole-1-oxyl 3-oxides and their derivatives containing larger numbers of fused rings. The presence of fluorine atoms in such paramagnets, on the one hand, will enhance their stability, and, on the other hand, will significantly affect their packing in stacks and in the crystal as a whole.

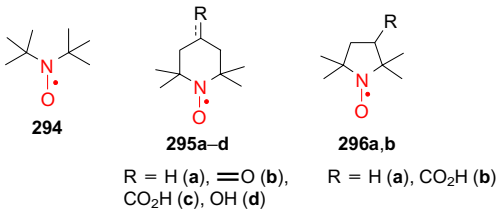
4. Quantum chemistry of nitroxide radicals and biradicals

Along with the synthesis and experimental studies of the properties and reactivity of stable conjugated nitroxide radicals, quantum chemical calculations of the properties of nitroxide radicals and materials based on them have received considerable attention in the literature. Today, computational methods can provide detailed information about the properties and transformations of chemical compounds, including information that cannot be gained by experimental methods.[410] The role of quantum chemistry as an important tool for physicochemical research is continuously increasing. Quantum chemical calculations have long been successfully used to predict and interpret the physicochemical properties of nitroxide radicals, including their EPR,[411–413] electronic absorption and luminescence spectra,[329,414] electrochemical potentials[415,416] and the efficiency of nitroxide formation from their precursors.[417] In recent years, quantum chemistry methods have been used to predict and interpret the magnetic properties of materials based on nitroxide radicals and bi- and polyradicals,[330,418–420] their complexes with metal cations[296] and graphene nanostructures with radical substituents.[336,421] In this Section, attention is focused on published data on the quantum chemical calculations of physicochemical properties of nitroxide radicals and biradicals, including spin Hamiltonian parameters, describing the magnetic properties of polycrystalline samples of conjugated nitroxide radicals and biradicals.

4.1. Parameters of the EPR spectra of nitroxides

Before we proceed to the discussion of the EPR spectra of conjugated nitroxides, it is expedient to consider the EPR spectra of aliphatic nitroxides **294**–**296** and quantum chemical calculations of their parameters.[422–425]

Structures 294–296



294 **295a–d** **296a,b**

R = H (**a**), =O (**b**), CO_2H (**c**), OH (**d**)

R = H (**a**), CO_2H (**b**)

A specific feature of EPR spectra of nitroxides is dependence of the spectral parameters (g-factors and hyperfine coupling constants) on the solvent. When the solvent polarity increases, the nitrogen HFC constants, $a(^{14}N)$, increase, and this increase is more pronounced in the solvents that can be hydrogen-bonded to the NO oxygen atom (Table 3).

Density functional theory calculations (the B3LYP, PBE0 and B1LYP functionals are used most often)[428] taking account of the solvent in the polarized continuum model[429] and by direct inclusion of several solvent molecules lead to a satisfactory agreement between the calculated and experimental hyperfine coupling constants, although the $a(^{14}N)$ value is usually underestimated.[423,426,427,430,431] A good agreement (within 2%) for $a(^{14}N)$ of radicals **295c** and **296b** was attained by using a mixed approach in which two corrections were introduced into the HFC constant determined by DFT. The first correction was equal to the difference between the HFC constants calculated by the configuration interaction method using QCISD and DFT procedures for the $Me_2NO^{\bullet}$ radical with bond lengths and bond angles as in the initial radical. The second correction reflected the degree of pyramidalization of the nitroxide group and was chosen to be 1 G for nitroxides with a five-membered ring and 0 G in the case of the six-membered ring.[427] Thus, the nitrogen hyperfine coupling constant is markedly affected by the solvent in which measurements are carried out (the range is 2–2.5 G). The influence of aliphatic substituents in the nitroxide on the $a(^{14}N)$ value is also moderate: in nonpolar solvents (benzene, dichloromethane), it varies in the range of 13.5–16.0 G, while g-factor varies from 2.0058 to 2.0065.[161]

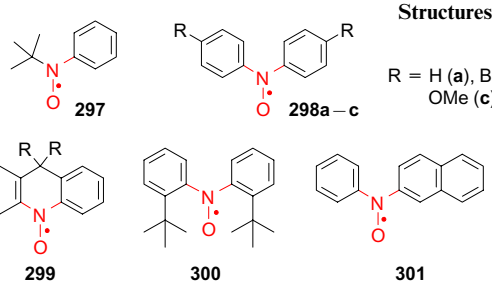
Table 3. Nitrogen hyperfine coupling constants (G) in the EPR spectra of aliphatic nitroxide radicals in various solvents.[426,427]

Radical	Solvent					
	CCl_4	Me_2CO	MeCN	DMSO	MeOH	H_2O
294	–	15.52	15.68	15.74	16.21	17.16
295c	15.45	–	–	15.82	16.25	17.06
296b	14.08	–	–	14.61	15.20	16.06

4.1.1. Alkyl aryl and diaryl nitroxides

The EPR spectral parameters are considerably affected by the chemical structure of conjugated nitroxides. Alkyl, aryl and diaryl nitroxide radicals are well studied classes of conjugated nitroxides. A large contribution to the synthesis of these radicals and studies of their properties, including EPR studies, was made by Forrester *et al.*[161,432,433] The influence of substituents in the benzene ring on the nitrogen and hydrogen HFC constants in alkyl and aryl nitroxides[161,432–435] and in diaryl nitroxides[50,156,436,437] has now been studied in detail. When one *tert*-butyl substituent in radical **294** is replaced by a phenyl group, $a(^{14}N)$ decreases by ~20% (see compound **297** in Table 4), while the introduction of the second phenyl group (radicals **298** and **299**) leads to an even more pronounced decrease in the HFC constant due to delocalization of spin density on the benzene rings. The introduction of electron-donating sub-

Structures 297–301



297 **298a–c**

R = H (**a**), Bu^t (**b**), OMe (**c**)

299 **300** **301**

R = Pr^n, Ph, 4-MeC_6H_4

Table 4. Experimental [50, 156, 161, 426, 432–437] and calculated [50, 426] nitrogen hyperfine coupling constants (G) in the EPR spectra of aryl and diaryl nitroxides in non-polar solvents (xylene and toluene).

Parameter	Radical							
	294	**297**	**298a**	**298b**	**298c**	**299** [a]	**300**	**301**
$a(^{14}N)_{exp}$	15.52 [b]	12.30 [c]	9.66	9.74	10.07	8.82	10.59	9.48
$a(^{14}N)_{cal}$	15.84	–	–	9.53	–	–	11.59	–

[a] R = Pr^n; solvents: [b] acetone, [c] CCl_4.

stituents into the *para*-position relative to the nitroxide group brings about a slight increase in the nitrogen HFC constant. In the presence of bulky substituents in the *ortho*-positions (radical **300**), this constant considerably increases because of deviation from planarity exceeding that in radical **298a**. Conversely, owing to the virtually planar structure of nitroxide **299**, spin density delocalization increases, and the nitrogen HFC constant considerably decreases. The extension of the π-system of the aryl substituent in radical **301** leads to only a slight decrease in $a(^{14}N)$.

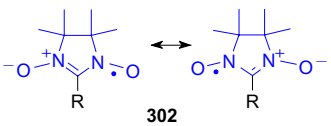
Bogdanov and co-workes [50] calculated the nitrogen, hydrogen and fluorine hyperfine couplung constants for the case of CF_3 substituents (UB1LYP/cc-pVDZ calculations taking account of the solvent in the solvation model based on the solute electron density [438]). Generally, a reasonable agreement with experimental values was attained: the deviation of the calculated constants $a(^{14}N)$ from experimental values did not exceed 9% (on average, ~3%). The calculated and experimental H and F hyperfine coupling constants differed to a larger extent (by a factor of up to two).

4.1.2. Nitronyl nitroxide and imino nitroxides

A specific type of nitroxide radicals are nitronyl nitroxides discovered by Osiecki and Ullman [225] in 1968, which can be easily converted to imino nitroxides. Particularly nitronyl nitroxides and, to a lesser extent, imino nitroxides are widely used as building blocks for the design of molecular magnetic materials.[15, 16, 439] The first purely organic ferromagnet was obtained in 1991 also on the basis of nitronyl nitroxide **302b**.[440]

Soon after the synthesis of the first nitronyl nitroxide **302e**, 4,4,5,5-tetramethyl-4,5-dihydro-1*H*-imidazole-1-oxyl 3-oxide derivatives **302a**–**d**,**f**–**h** with various alkyl, ethynyl, acetylene and aryl substituents in position 2 were synthesized.[226, 413, 441–443] According to EPR spectroscopy data, substituents at the α-carbon atom have a little effect on the g-factor (2.00625 ± 0.00004) and the constant $a(^{14}N)$, which varies in the 7.4–7.6 G range for most of the derivatives; this is approximately a half of the HFC constant of aliphatic nitroxides (Table 5). A substantial decrease in $a(^{14}N)$ is observed when the molecule contains strong electron-withdrawing substituents such as CF_3 (**302b**, 6.9 G) [225] or anthraquinone moiety (7.04 G).[442] For alkyl-substituted nitronyl nitroxides, relatively high HFC constants were also found for the alkyl group proton (3.3 G in radical **302a**) and fluorine nucleus of the CF_3 group (3.5 G in radical **302b**).[226]

Structures 302a–h



302

R = Me (**a**), CF_3 (**b**), CH=CH_2 (**c**), C≡CPh (**d**), Ph (**e**), 4-$O_2NC_6H_4$ (**f**), 4-HOC_6H_4 (**g**), 4-$Me_2NC_6H_4$ (**h**)

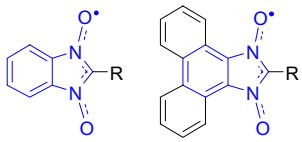
Table 5. Experimental [225, 413, 441] and calculated [411, 413, 445, 446] nitrogen hyperfine coupling constants (G) in the EPR spectra of nitronyl nitroxides **204**, **302a**–**h** in toluene.

Parameter	Radical								
	204	**302a**	**302b**	**302c**	**302d**	**302e**	**302f**	**302g**	**302h**
$a(^{14}N)_{exp}$	7.22	7.4	6.9	7.65	7.25	7.43	7.38	7.53	7.57
$a(^{14}N)_{calc}$	6.94 [a]	6.16 [b]	–	–	–	8.25 [d]	–	–	–
	5.97 [b]	6.98 [c]				5.60 [e]			
	6.70 [c]								

Level of calculations: [a] B3LYP/cc-pVDZ; [b] B3LYP/6-31G(d); [c] B1LYP/6-31G(d); [d] B1LYP/EPRII; [e] B3LYP/EPRII.

In the case of nitronyl nitroxides, the solvent nature considerably influences the HFC constants;[225, 441] for example, replacement of benzene with water results in an increase in $a(^{14}N)$ for radicals **302** by 0.7–0.8 G. A substantial change in the chemical structure, for example, switching from 4,5-dihydro-1*H*-imidazole-1-oxyl 3-oxide derivatives to benzimidazole-1-oxyl 3-oxide derivatives **293a**,**b** and their benzo analogues **303a**,**b**, induces a pronounced delocalization of the unpaired electron and, as a consequence, an almost twofold decrease in $a(^{14}N)$ (Table 6).[444]

Structures 293, 303



293a,**b** **303a**,**b**

R = Bu^t (**a**), Ph (**b**)

Table 6. Experimental [444] and calculated [413] nitrogen hyperfine coupling constants (G) in the EPR spectra of radicals **293a**,**b** and **303a**,**b** in toluene.

Parameter	Radical			
	293a	**293b**	**303a**	**303b**
$a(^{14}N)_{exp}$	4.37	4.38	3.87	3.81
$a(^{14}N)_{calc}$	–	3.63,[a] 4.24 [b]	–	–

Level of calculations: [a] B3LYP/6-31G(d); [b] B1LYP/6-31G(d).

In the 1990s, quantum chemical calculations of the HFC constants of nitronyl nitroxides received particular attention;[411, 413, 445, 446] up to now, the authors of almost every publication on the synthesis and properties of new paramagnets report DFT calculation data.[218, 302] Analysis of these publications indicates that the UB3LYP method is used, most often, to calculate the HFC constants for nitronyl nitroxides; however, the results considerably depend on the used basis set; expansion of the basis set often leads to a poorer agreement with experiment. When B3LYP and B1LYP functionals were used in DFT calculations, the latter provided a better agreement with the experiment. An excellent agreement (~1%) with the experiment was attained for 2-(imidazol-2-yl)-substituted nitronyl nitroxide,[411] as previously for aliphatic nitroxides,[427] using

a combined approach consisting in the calculation of HFC constants by the UB1LYP/EPRIII method and application of a correction equal to the different between the constants calculated for a fragment of this radical by the coupled cluster method with allowance for the single and double (triple) excitations and by DFT with the UB1LYP functional.

Thus, for nitronyl nitroxides, abundant experimental data are available on various HFC constants to various nuclei (N, H, F, Cl), which are determined by the spin density on these nuclei. In addition, polarized neutron diffraction measurements in a strong magnetic field at 5 K made it possible to determine spin populations of atoms in 4,4,5,5-tetramethyl-2-phenyl-4,5-dihydro-1*H*-imidazole-1-oxyl 3-oxide (**302e**).[221] The crystal lattice of this radical was found to contain two forms of the radical slightly differing in properties. The spin populations averaged over the two forms and two NO groups were found to be 0.27 for both N and O atoms. The C atom of the paramagnetic group was found to have a negative spin population of −0.121. The experimental spin populations were compared with the results of quantum chemical calculations using spin-unrestricted HF, MP2, CI and DFT methods. Despite the fact that local spin density approximation was used, the calculated atomic spin populations were in good qualitative agreement with experimental data.

4.2. Electronic absorption spectra of nitroxides

The crystals of nitroxide radicals, including aliphatic ones, are bright-coloured; hence, they absorb visible light. Nevertheless, the data on the UV/Vis spectra of nitroxides are less abundant than the EPR data. The most attention in the literature is paid to the UV/Vis spectra of nitronyl nitroxide radicals and their metal complexes.[447]

4.2.1. Electronic absorption spectra of aliphatic nitroxides

The electronic absorption spectra of aliphatic nitroxide radicals contain a very weak absorption band in the visible region. For example, the spectrum of the well-known TEMPO radical (**295b**) shows two broad bands with λ_{max} of 240 [the extinction coefficient (ε) is 2×10^3 L mol^{-1} cm^{-1}] and 445 nm (ε = 12.6 L mol^{-1} cm^{-1}),[448] with the latter being assigned to nπ* type transition. Similar UV/Vis spectra were recorded for 4-hydroxy derivative **295d** and radical **296**b with long-wavelength band maxima at 430 and 470 nm, respectively (ε_{max} in the range of 10 to 15 L mol^{-1} cm^{-1}).[449] The electron transitions calculated by the time-dependent DFT (TD-B3LYP) for these paramagnets are in excellent agreement with the experimental spectra.

This is exemplified in Fig. 29, which shows the results of calculations of molecular orbitals and transitions between them corresponding to the electronic absorption spectra of the simplest aliphatic nitroxide radical, $Me_2NO^{\bullet}$. The long-wavelength band has a low oscillator strength ($f = 1.31\times10^{-4}$), 99% consists of β-electron transition from n-type orbital to the π-SOMO and corresponds to the maximum at 451 nm, which is in excellent agreement with experimental data for aliphatic nitroxides. The most intense band (209 nm, $f = 0.091$) also mainly (88%) corresponds to β-electron transition from the π- to π*-orbital. One more transition of a lower intensity ($f = 0.012$) mainly corresponds to excitation of the α-electron from the SOMO to the lowest unoccupied molecular orbital (LUMO) (λ = 236 nm).

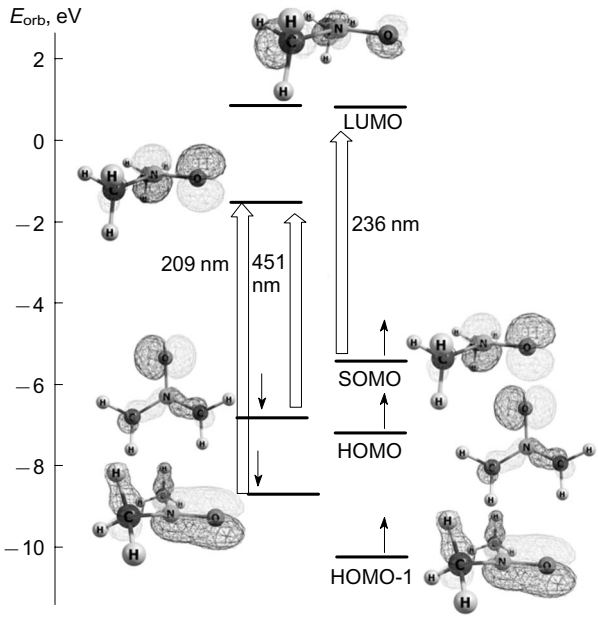


Figure 29. Diagram of α- and β-type molecular orbitals calculated by the UB3LYP/def2-TZVP method for the dimethyl nitroxide radical and electron transitions induced by UV and visible light excitation calculated by the TD-UB3LYP method with the same basis set. HOMO is the highest occupied molecular orbital. Unpublished results of the authors.

Levitskiy *et al.*[50] studied diaryl nitroxides **298b**, **300** and their CF_3-substituted analogues. The electronic absorption spectra of nitroxides showed a very intense band at ~200 nm [$\varepsilon = (1.7-3.4)\times10^4$ L mol^{-1} cm^{-1}], a less intense band in the 270–300 nm range and a weak band at 350–500 nm [$\varepsilon_{max} \approx (500-1500)$ L mol^{-1} cm^{-1}]. In addition, all spectra had an extended tail of the long-wavelength absorption band in the 500–600 nm range, indicating the presence of a long-wavelength transition with $\varepsilon \leqslant 50$ L mol^{-1} cm^{-1}, which can be classified as an nπ*-transition.

Unlike the calculated electronic absorption spectrum of the $Me_2NO^{\bullet}$ radical, the calculated spectrum of diphenyl nitroxide (**298a**) is very complex: 34 electron transitions were predicted in the 200–500 nm range. In addition, each of these excitations corresponds to the sum of single-electron transitions between particular orbitals. For example, the longest-wavelength excitation at 501 nm ($f = 1.4\times10^{-3}$) corresponds to the sum of β-electron transitions (with a contribution from 10 to 45%) from one of the five occupied molecular orbitals (MOs) to the SOMO. For this reason, for radical **298a**, it is very difficult to draw a diagram like the diagram depicted in Fig. 29. The situation can be simplified by using natural transition orbitals (NTOs). The same excitation at 501 nm can be described by one transition between the NTOs (99.3% contribution) shown in Fig. 30 *a*; it can be seen that the transition can be assigned to the nπ* type. The next electron excitation (373 nm, $f = 0.023$) is a superposition of mainly two transitions (Fig. 30 *b*): β-electron to the SOMO and α-electron from the SOMO mainly to the LUMO.

Thus, the longest-wavelength transition for diaryl nitroxides corresponds to the nπ* type, but it is overlapped by the next ππ* type transition and is manifested as an extended absorption tail. This transition is markedly red-

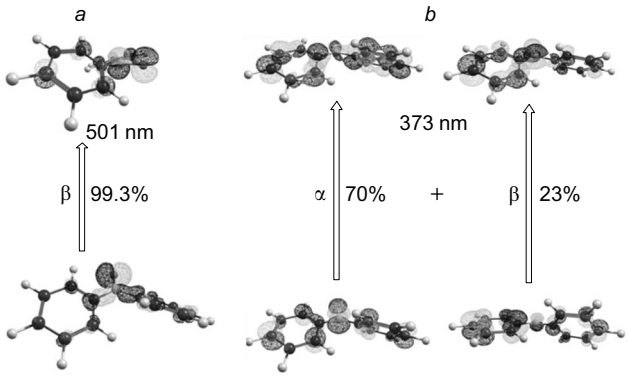
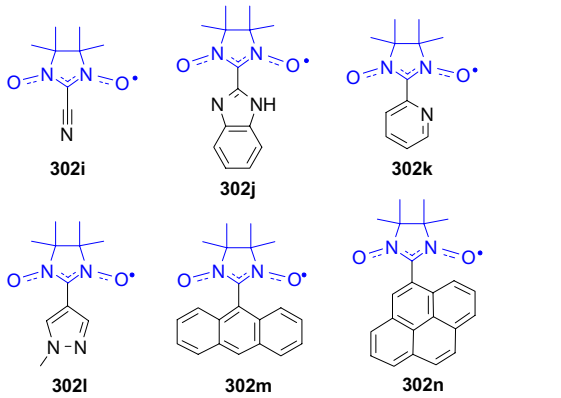


Figure 30. Natural transition orbitals corresponding to two long-wavelength transitions in the calculated absorption spectrum of nitroxide **298a**. For *a*, *b*, see the text. Unpublished results of the authors.

Structures 302i–n



shifted compared to those in the spectra of aliphatic nitroxides, while its oscillator strength is several times greater than those for aliphatic nitroxides

As noted above, the UV/Vis spectra of nitronyl nitroxide radicals received the most attention in the literature.[225,241,329,415,447,450–454] To our knowledge, only the positions of the band maxima and the corresponding extinction coefficients have been determined for 2-alkyl derivatives.[226] These radicals typically exhibit a long-wavelength absorption with two closely located peaks, caused, most likely, by the vibrational structure. For example, the UV/Vis spectrum of radical **302a** in hexane shows bands at λ_{max} = 533 and 563 nm with ε = 1800 L mol^{-1} cm^{-1}. When conjugated substituents are introduced into position 2 (**302c**,**e**), the longest-wavelength maximum is red-shifted (up to 660 and 637 nm, respectively).[226] A number of studies published over the last two decades[329,415,450–454] present detailed information about the UV/Vis spectra of 2-substituted nitronyl nitroxides with aryl and heterocyclic substituents, *e.g.*, compounds **271**, **302j–n**. The spectra of these radicals exhibit a long-wavelength absorption band in the 500–750 nm range with the clear-cut fine structure and a peak at 620–650 nm. Radicals **302m**,**n** with bulky anthranyl and pyrenyl substituents are exceptions: the long-wavelength bands of these radicals (with peaks at 573 and 555 nm, respectively) do not have a fine structure.[241] There is less information about the UV/Vis spectra of imino nitroxides, although it is known that the long-wavelength band of imino nitroxides is significantly blue-shifted: for example, in the case of radical **302j** and its imino nitroxide derivative, the shift is ~60 nm.[447]

Apparently, by analogy with the electronic spectra of aliphatic nitroxides, long-wavelength absorption bands in the spectra of nitronyl nitroxides are often assigned to nπ* type absorption. In our studies,[329,414] on the basis of DFT calculations for radicals **271** and **302l**, the long-wavelength bands in the UV/Vis spectra of these nitronyl nitroxides were assigned to ππ* transitions.

The UV/Vis spectra of radical **302l**, like the spectra of most known radicals of this type with aryl and π-heterocyclic substituents,[447,450–452] exhibit a long-wavelength band in the 500–700 nm range with a pronounced fine

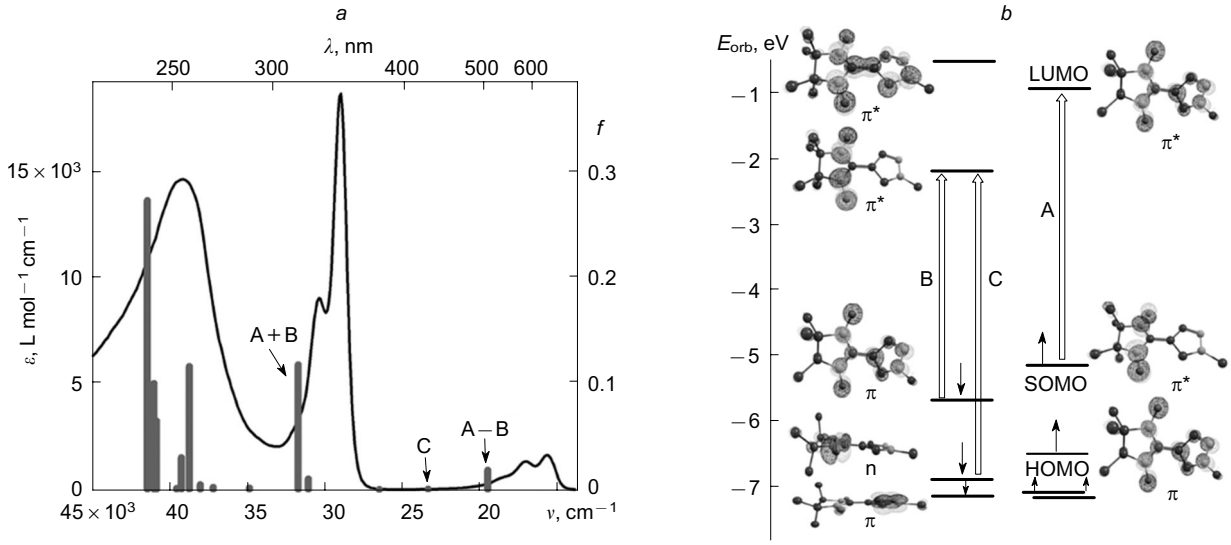


Figure 31. Experimental UV/Vis spectra of the radical (the curve) and TD-UB3LYP/def2-TZVP-calculated oscillator frequencies and strengths for the electron transitions for **302l** in ethanol (*a*); and UB3LYP/def2-TZVP-calculated diagram of α- and β-type molecular orbitals of radical **302l** and electron transitions corresponding to the long-wavelength excitations in its UV/Vis spectra (*b*). Letters A–C designate electron transitions; arrows show the direction of spin. The figure was created by the authors using published data.[414]

structure (Fig. 31 *a*).[414] According to calculations,[414] this band reflects one electron excitation, while the shape of the band reflects the vibrational structure (progression in the stretching mode of the C–C bond between the nitronyl nitroxide and pyrazole moieties), which was calculated using Franck–Condon and Heller's approximations (Fig. 31 *b*).[455] The long-wavelength electronic excitation (λ_{calc} = 510 nm, f = 0.019) corresponds to the difference between α- and β-electron transitions between the highest occupied and lowest unoccupied MOs (transitions A and B in Fig. 31 *a*, respectively); both transitions are of the ππ* type. The two following excitations (λ_{calc} = 432 and 380 nm) correspond to nπ* type transitions; they have low oscillator strength (2×10^{-4} and 8×10^{-5}) and are not manifested in the experimental spectrum. The major contribution to the next experimental absorption band (λ_{max} = 337 nm) is made by the fifth highest-energy excitation, caused by the same two electron transitions A and B, but in this case, as a sum. The third absorption band contains contributions of quite a number of electronic excitations.[414]

Similar calculations were reported for radical **271** containing a complex π-system as a substituent. The long-wavelength band in the UV/Vis spectrum of this radical is also a ππ* type band and reflects one excited state, which corresponds to the difference between α- and β-electron excitations from the HOMO to the LUMO.[329] Note that for radical **302a**, too, calculations (TD-B3LYP/def2-TZVP) predict a ππ* type long-wavelength band, which is consistent with the high extinction coefficient for the maximum of this band in the experimental UV/Vis spectrum (λ_{max} = 563 nm, ε_{max} = 1830 L mol^{-1} cm^{-1}).[225] Thus, it can be concluded that, unlike aliphatic and diaryl-substituted nitroxides, which have nπ* type lowest excited state, nitronyl nitroxides are characterized by ππ* type lowest excited state.

4.3. Vibrational spectra of nitroxides

Quantum chemistry was used to clarify the issue of assignment of IR bands to nitroxide group vibrations. Using a large array of spectral data, Rintoul *et al.*[456] demonstrated that the stretching frequencies of the nitroxide group are in the range of 1450–1340 cm^{-1}. In the case of acyclic and six-membered cyclic nitroxides, the frequencies ν_{N-O} are in the 1400 to 1340 cm^{-1} range, whereas in the case of five-membered cyclic nitroxides, they are shifted to 1435–1400 cm^{-1}. In nitronyl nitroxides, the ν_{N-O} band occurs in the region of 1470 cm^{-1}; isolation of this band without special experiments is difficult due to the pronounced interaction of the N–O stretching modes with aromatic substituent, C–N group and methyl group vibrations.

4.4. Quantum chemical calculations of the properties of nitroxide bi- and triradicals

Apart from nitroxide radicals, considerable attention in the literature is paid to nitroxide bi- and polyradicals.[16,45,46,259,330,457–461] Nitroxide biradicals, like monoradicals, are promising building blocks for the design of molecular magnetic materials. For example, the ferromagnetic transition was first discovered for nitroxide biradical **304**, but, as previously for nitroxide radicals, the transition occurred at a very low Curie temperature (T_C = 1.8 K).[460] This low T_C value is related to very weak exchange coupling both between the radical moieties of the biradical and between the neighbouring biradicals. The exchange coupling parameters are usually derived from analysis of experimental data, but they can also be predicted by quantum chemistry methods. In the case of complex magnetic motifs of magnetically active materials, preliminary quantum chemical calculations can help to choose the correct model for analysis of experimental results. The calculations are often used to establish the magneto-structural correlations.

The multiplicity of the ground state of biradicals in which the radical centres are connected by a conjugated electronic system is usually predicted using the spin alternation rule.[462,463] Generally, this rule operates reasonably well, except for some cases, for example, if heteroatoms are present, if two competing spin polarization pathways exist or, which occurs most often, if the π-conjugated subsystems are not coplanar. Furthermore, this rule does not provide information about the magnitude of singlet–triplet splitting. Therefore, in the theoretical design of building blocks for magnetic materials with desired properties, for example, biradicals with a pronounced exchange coupling between the radical moieties, quantum chemical calculations are utilized to predict the sign and magnitude of ΔE_{ST}. In the vast majority of cases, this is done using the broken-symmetry approach based on spin-unrestricted density functional theory (BS-DFT)[464–466] without testing the accuracy of the obtained results.[259,419,467–472] The accuracy of these calculations can be established by comparing the results with experimental data or with the results of high-level calculations.

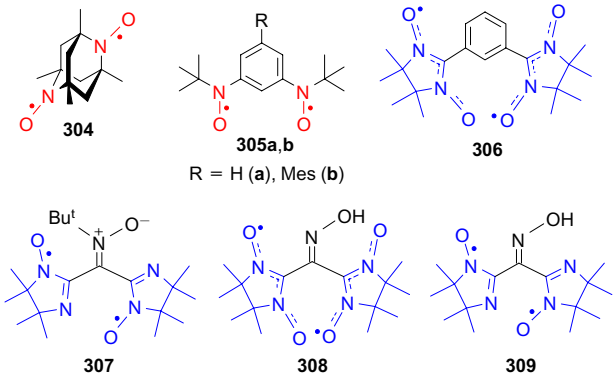
In the last decade, the electronic structures of a series of nitroxide biradicals **18**, **165**, **166**, **224**, **272** and **305**–**309** have been calculated by both the BS-DFT method and the high-level CASSCF/NEVPT2 methods; the calculated exchange coupling parameters have been compared with the values derived from temperature dependences of the magnetic susceptibility.[46,260,292,294,296,325,329,330] It should be noted that, according to the shape of non-bonding molecular orbitals (NBMO) or SOMO, the biradicals in which the radical centres are connected by a conjugated electron system can be divided into two types:[473,474]

— biradicals the NBMO of which can be localized in different regions of the molecule (disjoint),

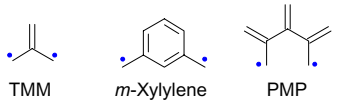
— biradicals the NBMO of which are essentially delocalized (non-disjoint).

Biradicals of the latter type include well-known trimethylenemethane (TMM) and *m*-xylylene and also their nitroxide analogues **18**, **213**, **305a**,**b**, **306** and so on, which typically have a triplet ground state with a relatively high singlet–triplet splitting. Note that the spin alternation rule

Structures 304–309



C-Biradical structures



also predicts a triplet ground state for these species. Meanwhile, 1,1,2,3,3-pentamethylenepropane (PMP) is a well-known biradical of the former type, while **224**, **307**–**309** are its analogues. According to the spin alternation rule, PMP should have a triplet ground state; however, due to its disjoint nature, the singlet–triplet splitting is expected to be low.[473]

We will consider what follows from the theoretical and experimental data for these biradicals. The calculation of ΔE_{ST} for TMM and *m*-xylylene is the subject of numerous publications, which mainly use multiconfiguration methods.[475–482] The singlet–triplet splitting measured by photoelectron spectroscopy ($\Delta E_{ST} = 2J$) proved to be 16.1 ± 0.1 kcal mol^{-1} ($J/k_B = 4060 \pm 30$ K) for TMM[483] and 9.6 ± 0.2 kcal mol^{-1} ($J/k_B = 2420 \pm 50$ K) for *m*-xylylene.[484] Table 7 summarizes the calculation results only for optimized geometries of the singlet and triplet states, since the values derived from experimental data are adiabatic energy differences. It can be seen that the BS-DFT calculations result in satisfactory prediction of the singlet–triplet splitting energy for TMM and *m*-xylylene and for their nitroxide analogues **18**, **213**, **305a**,**b** and **306**. The prediction accuracy for TMM and *m*-xylylene is ~20%. In the case of *m*-xylylene, both the geometry optimization and ΔE_{ST} calculations were carried out using different functionals, with the results being in reasonably good agreement.[482]

As noted above, the ground triplet state of PMP is expected to have small ΔE_{ST}. Indeed, for the planar C_{2v}-symmetric structure, the calculations predicted the ground triplet state with $J/k_B = 78$ K. However, the optimized structure is non-planar (the symmetry is close to C_2) and its ground state is singlet ($J/k_B = -142$ K). Nitronyl nitroxide and imino nitroxide analogues of PMP — biradicals **224**, **307**–**309** — also have non-planar structures; their parameters *J* are very low (Table 8) and can be either positive (**308**, **309**)[296] or negative (**224**, **307**).[294] It is noteworthy that for all PMP analogues, the BS-UB3LYP calculations predict the ground triplet state and *J* parameters that exceed the absolute experimental values by an order of magnitude or more. Meanwhile, the CASSCF/NEVPT2 calculations with relatively large active space are in excellent agreement with the experiment. Table 8 presents the results of calculations for two more disjoint type nitronyl nitroxide biradicals (**166**, **272**) and one imino nitroxide biradical (**165**). In this case, BS-UB3LYP calculations correctly predict the ground singlet state; however, the absolute magnitudes of *J* are considerably (by a factor of 4 or more) greater than those found experimentally or calculated by higher-level methods.

In recent years, a series of mixed biradicals (with verdazyl or triazinyl and nitronyl nitroxide moieties) with the ground triplet state have been synthesized.[259, 330] According to preliminary BS-UB3LYP calculations, these biradicals were expected to have relatively large singlet–triplet splittings: 3.5 kcal mol^{-1} ($J/k_B = 880$ K) for radical **159**[43] and 1.36 and 0.37 kcal mol^{-1} for compounds **274b**,**c**

Table 7. Experimental [a] and calculated exchange coupling parameters (J/k_B, K; $\Delta E_{ST} = 2J$) for a series of non-disjoint hydrocarbon radicals and their nitroxide analogues.

Method	Biradical					
	TMM [b]	**18** (see [c])	**213**	*m*-Xylylene [d]	**305a**,**b**	**306** (see [e])
BS-DFT	4830	439	–	2970	–	30
MCSCF	3030	–	–	3220	–	–
NEV(CAS)PT2	3060	–	–	3060	220 [f]	–
Experiment	4060	390	550	2420	~500	~18

[a] Experimental *J* values were derived from photoelectron spectroscopy data for TMM[483] and *m*-xylylene;[484] from analysis of the temperature dependence of the EPR signal for radical **306**;[485] from analysis of the temperature dependences of magnetic susceptibility for radicals **18** and **213**,[45] **305a**,[486] **305b**.[487] [b] Calculated by the BS-BP86/cc-pVDZ, MCSCF(10,10)/cc-pVTZ and CASPT2N(10,10)/cc-pVTZ methods for the optimized structures of the singlet and triplet states.[488] [c] Calculated by BS-UB3LYP/TZV for the experimental geometry.[46] [d] Calculated by the BS-UB3LYP/6-311++G(d,p), CASSCF(8,8)/6-31G(d,p) and CAS(8,8)MP2 methods for the optimized geometries of the singlet and triplet states.[482] [e] Calculated by BS-UB3LYP/6-311+G(d,p).[467] [f] Calculated by DDCI for the optimized triplet state geometry.[489]

Table 8. Experimental (derived from analysis of the temperature dependences of magnetic susceptibility)[260, 294, 296] and calculated exchange coupling parameters (J/k_B, K; $\Delta E_{ST} = 2J$) for PMP and a series of disjoint type nitronyl nitroxide biradicals.

Method	PMP [a]		**224** (see [a])	**307** (see [a])	**308** (see [b])	**309** (see [b])	**272** (see [c])	**166** (see [d])	**165** (see [d])
	C_{2v}	~C_2							
BS-DFT	171	−162	159	34	95	66	−76	−414	−127
MCSCF	114	−94	−1.4	−0.6	34	27	−4	−167	−68
NEV(CAS)PT2	78	−142	−6.8	−3.4	27	4.3	−6	−138	−45
Experiment	–	–	−7.4	−6.0	–	5.0	–	−111	−32

[a] Calculated by the BS-UB3LYP/def2-TZVP, CASSCF(8,8)/def2-SVP and CASSCF(8,8)/NEVPT2/def2-SVP methods for the PMP geometry optimized in the triplet state and experimental geometry for radicals **224** and **307**.[294] [b] Calculated by the BS-UB3LYP/def2-TZVP, CASSCF(16,12)/def2-SVP and CASSCF(16,12)/NEVPT2/def2-SVP methods for the experimental geometry of radicals **308** and **309**.[296] [c] Calculated by the BS-UB3LYP/def2-TZVP, CASSCF(10,10)/def2-SVP and CAS(10,10)/NEVPT2/def2-SVP methods for the experimental geometry of radical **272**.[329] [d] Calculated by the BS-UB3LYP/6-3111+G(d,p), CASSCF(20,15)/def2-TZVP and CAS(20,15)/NEVPT2/def2-TZVP methods for the experimental geometry of radical **166** and CASSCF(16,13)/def2-TZVP, CAS(16,13)/NEVPT2/def2-TZVP for radical **165**.[260]

respectively (J/k_B = 342 and 93 K).[330] Substantially lower J/k_B were found from analysis of the temperature dependences of the molar magnetic susceptibility: 438, 72 and 18 K for nitroxides **159**, **274b** and **274c** respectively.[43, 330] Note that the results of most accurate calculations [CASSCF(18,15)/NEVPT2] for radicals **274b**,**c** are in good agreement with experiment (J/k_B = 72 and 26 K respectively).[330]

It is worth noting that the crystal of biradical **159** consists of one-dimensional antiferromagnetically coupled chains of biradicals with the intermolecular exchange coupling parameter J/k_B of −14 K (estimated from experimental data); this is consistent with the results of BS-UB3LYP calculation for dimeric biradicals.[259] In the crystals of compounds **274b**,**c**, one-dimensional chains of biradicals are also formed; the exchange coupling between the most proximate radical groups in them was calculated by the BS-UB3LYP method.[330] For biradical **274b**, the calculations showed a significant ferromagnetic (FM) coupling between the verdazyl moieties (J/k_B = 11 K), while in the case of biradical **274c**, FM coupling of the verdazyl moiety with verdazyl and nitronyl nitroxide moieties was detected (J/k_B = 17 and 11 K, respectively). These calculated values are in satisfactory agreement with those derived from approximation of the experimental dependences $\chi_{mol}(T)T$.[330]

For some crystalline samples of nitroxide radicals or biradicals with a very weak intramolecular exchange coupling, the intermolecular exchange parameters were found from approximation of the experimental dependences $\chi_{mol}(T)T$. The parameters found by the BS-UB3LYP calculations were in all cases in satisfactory agreement with the experiment, including the situation where ferromagnetic intermolecular exchange predominated.[292, 490, 491]

Thus, the use of the BS-DFT method for evaluation of intermolecular exchange coupling is legitimate. Comparison of the calculation results with experimental data showed that for non-disjoint type biradicals, the BS-DFT method predicts singlet–triplet splitting with a satisfactory accuracy. In the case of disjoint biradicals, the BS-DFT method considerably overestimates the magnitude of singlet–triplet splitting and even may result in a wrong prediction of the nature of the ground state. The multiconfiguration CASSCF method with a relatively large active space and additional inclusion of dynamic electron correlation by, *e.g.*, NEVPT2 (or CASPT2, CASCI) method is able to predict the singlet–triplet splitting in biradicals with a good accuracy. However, these methods require very large computational resources. It is also necessary to appropriately choose the active space, and it is desirable to analyze the effect of extension of this space and the effect of basis set on the calculation results. Only this labour-consuming procedure makes it possible to predict the exchange coupling parameters with an acceptable accuracy.

5. Potential of practical application of conjugated nitroxides

Roald Hoffmann, Nobel Prize winner in chemistry (1981), noted in one of his publications[492] that molecules perform tasks. Indeed, chemists usually invent and synthesize new molecules with a particular purpose. The synthesis of such molecules may be of theoretical interest (*e.g.*, to verify some scientific hypothesis and so on) or may help to solve purely practical problems, including development of new materials, which meet increasing demands of the mankind.

The targeted design and synthesis of molecules possessing specified properties forms the basis for the design of new materials to be used in various fields. The interest in stable nitroxide radicals persisting for many decades is due to a wide range of their practical applications. Numerous papers and reviews have been published, in particular in recent years, discussing the traditional aspects of the use of nitroxide radicals as spin traps and spin labels,[424, 493] catalysts and mediators of oxidation reactions,[360, 494–496] organic conductors,[497] organic magnets,[209, 210, 498–501] redox-active materials,[502–504] radical polymerization initiators[505] and so on. However, due to development of new synthetic approaches, the fabrication of combined materials that function *via* a combination of properties of the nitroxide group and an additional moiety is now attracting increasing interest. This approach requires targeted molecular design of organic polyfunctional compounds containing nitroxide groups.

As the additional structural moiety, it is possible to use, for example, redox(or photo)-active group, or another functional group that responds to a certain external stimulus. This approach gives rise to molecular systems the properties of which (magnetic, coordination, antioxidant, sensory, *etc.*) can be tuned (switched). One more nitroxide moiety can also be used as the additional function. In this case, the molecule should acquire new properties based on the cooperative action of several functional groups.

In some cases, the functional properties of the nitroxide radical itself are changed under an external stimulus, and it can thus perform different tasks. Examples are ambipolar nitroxides, which are able to exist in three stable redox states depending on the applied potential (*i.e.*, they can be stable in the cationic, radical and anionic forms). Such compounds can be used as anode and cathode materials for the design of new-generation symmetric (pole-less) batteries containing the same compound in the anode and cathode compartments, but the compound exists in different redox states.

This part of the review addresses examples of molecules containing unsaturated nitroxide moieties and meant for the development of combined materials. The attention is focused on the redox activity of nitroxides and their photo(thermo, redox)-dependent properties. The information given here does not claim to cover all publications on this topic; the aim of the authors is to show the new opportunities offered by the use of bifunctional nitroxides. This approach is mainly illustrated by recent publications; however, whenever necessary, most characteristic earlier studies are also considered. To the best of our knowledge, no reviews on bifunctional unsaturated nitroxide radicals have been published so far .

The range of practical application of combined nitroxide-containing systems is very broad, which is largely due to the diversity of properties of nitroxide radicals. Figure 32 shows the areas of practical application of compounds that are addressed in this Section.

It should be noted that most publications devoted to the design and synthesis of nitroxide-containing materials consider alkyl nitroxides (TEMPO and the like), because they are less expensive and more available, and, in some cases, they are more stable than aromatic derivatives. However, the diversity of structural types of unsaturated nitroxides that appeared in recent years and development of synthetic

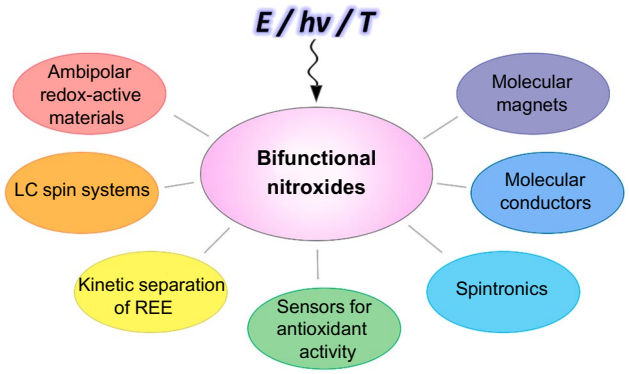


Figure 32. Examples of practical application of switchable nitroxides. LC are liquid crystals. The figure was created by the authors.

routes to these nitroxides make them more and more in-demand for practical applications. Unsaturated nitroxide radicals, in particular aryl nitroxides, offer more opportunities for the structural tuning of properties to a particular task and are more easily functionalized. In addition, the benzene ring may become a part of photosensitive polyaromatic or cross-conjugated system, which creates conditions for the photo(redox) activation of the molecule.

5.1. Redox switchable molecular systems based on unsaturated nitroxides

The design of molecular structures the electronic properties of which can be controlled by external stimuli is of paramount interest for the design of molecular switches, memory storage devices, *etc*. Depending on which functional groups are integrated into a common system and what is the nature of the linker binding them, the properties (or functions) of the molecular system and the choice of the external (controlling) stimulus change. Since the properties of the proper nitroxides are quite diverse, the range of their practical applications is very broad.

Nitroxides are stable compounds with open electron shell; therefore, development of single-molecule magnets is an important area of their practical use. The properties of these systems are determined by intra- and intermolecular exchange couplings of neighbouring spins. If the exchange coupling parameter is positive ($J > 0$), the neighbouring spins are aligned parallel to one another. If such spin–spin interaction involves a macroscopic number of spins (*i.e.*, on going from single molecules to matter), a ferromagnetic material is formed. Otherwise, when the exchange coupling parameter is negative ($J < 0$), the neighbouring spins are ordered in the antiparallel fashion, which results in the formation of an antiferromagnetic macroscopic material. If the parameter J is close to zero (in practice, if it is significantly lower than the energy of thermal motion, $|J| \ll k_B T$), the exchange coupling is not strong enough to align the spins, and the resulting material is paramagnetic. Here two remarks are relevant. The first one concerns the sign of J: the opposite convention of this sign is also encountered in the literature ($J < 0$ for the ferromagnetic coupling [506–508]). As noted above, in this review we adhere to the convention that is more commonly used in the literature on single-molecule magnets and corresponds to the Heisenberg Hamiltonian (see p. 9).

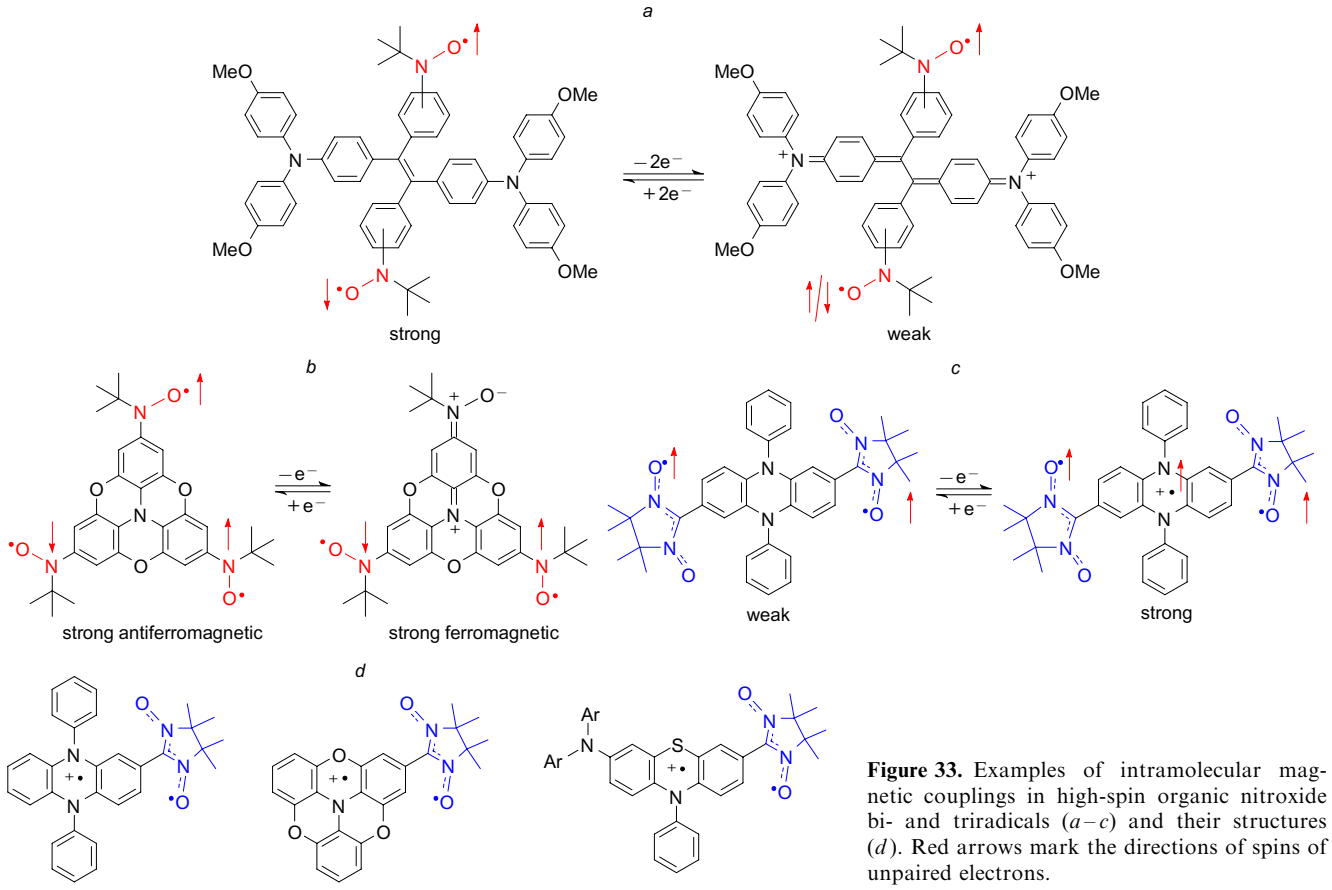


Figure 33. Examples of intramolecular magnetic couplings in high-spin organic nitroxide bi- and triradicals (*a*–*c*) and their structures (*d*). Red arrows mark the directions of spins of unpaired electrons.

Second, spin orientation should not be confused with the orientation of the molecular moiety on which the unpaired electron is localized. Molecules can be arranged in space in an arbitrary way, while the spin of the unpaired electron is quantized with respect to the direction of the external magnetic field and, in the simplest case of weakly interacting spins, it can have one of two directions, either along the external magnetic field or opposite to the field.

The multispin molecular systems in which the intramolecular exchange couplings can be controlled by external stimuli are of considerable interest as a base for the design of diverse spin magnetic devices. However, only few such structures have been described to date. The cause is that most of these molecules are unstable at room temperature, which restricts their practical application.

The molecular design of the indicated systems is based on the introduction of radical groups into the π-electron system. The distance between the spin centres should not be too great to ensure a significant intramolecular exchange energy. As a convenient model, one can consider cross-conjugated systems in which switching from one π-conjugated system to another one can be induced by redox action (Fig. 33). The design of such a structure requires the presence of a relatively extended π-system that is oxidized at lower anode potentials than the nitroxide group. Ito and co-workers [509, 510] used for this purpose a tetraarylene moiety connecting two aryl alkyl nitroxide radicals. The oxidation (reduction) made it possible to switch off (on) the intramolecular interaction between two spin centres, which occurred by the π-conjugation mechanism (see Fig. 33 *a*).

A stable multispin system based on aryl alkyl nitroxide was reported by Suzuki *et al.*[511] (see Fig. 33 *b*). It is interest that the multispin system in the trinitroxide-substituted trioxyphenylamine is preserved both in neutral (triradical in the doublet state) and in oxidized forms (triplet biradical cation). Strong intramolecular exchange couplings were observed in both states, but their nature changed from negative (in the neutral state, $J/k_B = -200$ K) to positive (in the oxidized state, $J/k_B = +300$ K). It should be emphasized that the introduction of oxygen bridges significantly stabilized the oxidized form in comparison with the previously studied analogue in which three nitroxide centres were located in the *para*-positions of triphenylamine (the right-hand part of Fig. 33 *b*).[512] The radical cation was even characterized by X-ray diffraction, which confirmed its nearly planar quinoid structure.

The introduction of two nitronyl nitroxide groups into the *N*,*N*-diphenylphenazine skeleton gave a stable redox-controlled multispin system (see Fig. 33 *c*).[513] In neutral form, this is a triplet biradical with a weak positive exchange coupling, while the oxidation of the phenazine moiety gives a triradical (the ground state is a quartet) and involves strong (differing by two orders of magnitude) exchange couplings.

Stable multispin systems based on phenazine,[514] phenoxazine [54] and phenothiazine [320] containing a nitronyl nitroxide moiety were obtained by single-electron oxidation (see Fig. 33 *d*). These biradical cations have a triplet ground state with strong exchange coupling ($2J/k_B > +300$ K). A phenothiazine derivative [320] the radical cation of which is stable at room temperature in air in the solid state and in solution proved to be most stable. It can undergo three reversible redox transitions both in the anodic and cathodic regions, *i.e.*, it is an ambipolar molecule. If the diamagnetic $GaBr_4^-$ serves as the counter-ion, the salt experiences strong intramolecular ferromagnetic coupling between the phenothiazine radical cation and nitronyl nitroxide ($J_1/k_B = +320$ K) and weak intermolecular antiferromagnetic coupling ($J_2/k_B = -2$ K). The replacement of the counter-ion with paramagnetic $FeBr_4^-$ gives rise to weak additional interactions ($J_3/k_B = -7$ K and $J_4/k_B = -4$ K).

Examples of multispin molecular systems in which localized and delocalized spins occur in one molecule are shown in Fig. 34. They were obtained *via* single-electron oxidation of oligo(triarylamine) carrying a nitroxide group in the *meta*-position (see Fig. 34 *a*) [515] or bis-nitroxide containing a *p*-phenylenediamine linker (see Fig. 34 *b*).[516] These derivatives of aromatic amines can be reversibly oxidized at moderate anode potentials; therefore, they are often used in the molecular design of combined redox systems. A voltammetric study of oligo(triarylamine) showed the presence of three successive oxidation peaks: the first two reversible redox transitions correspond to oxidation of the linker, while the third one is due to oxidation of the nitroxide moiety. It is important to emphasize that the choice of a suitable linker is always preceded by a detailed electrochemical study of parts of the molecule: the linker should be oxidized more easily than the nitroxide radicals. For exam-

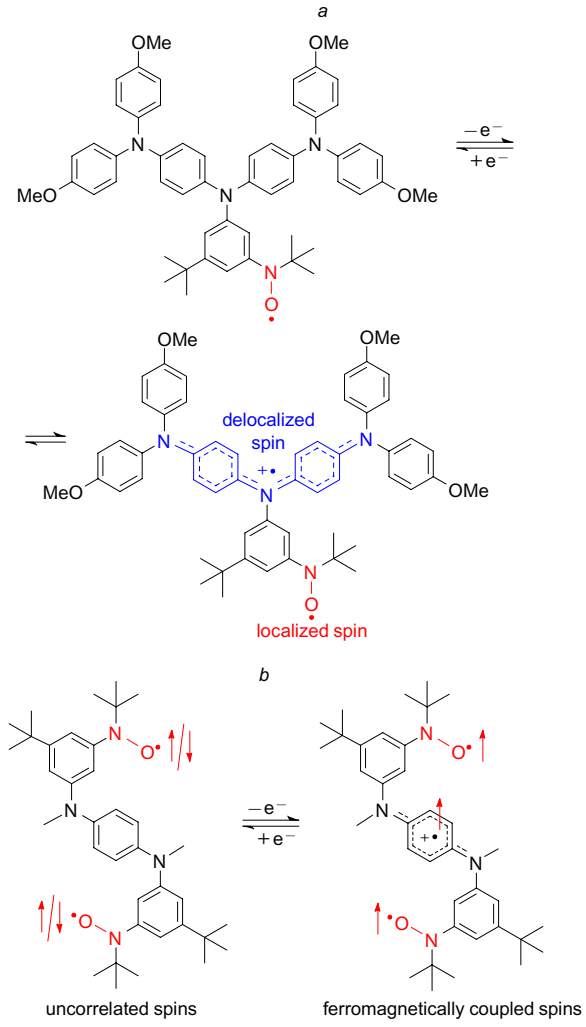


Figure 34. Multispin systems based on triarylamine (*a*) and *p*-phenylenediamine (*b*) in which localized and delocalized spins are present in one molecule.

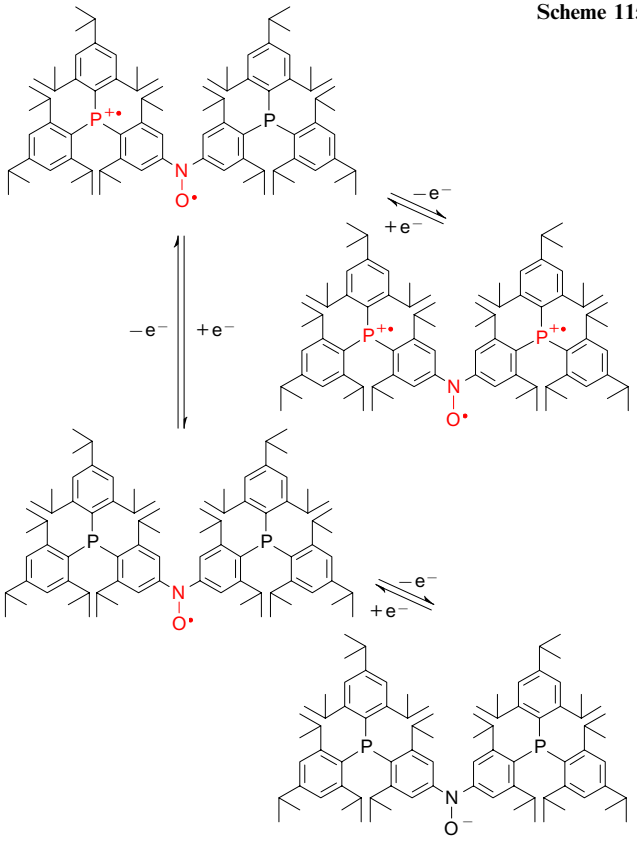
ple, in the bis-nitroxide shown in Fig. 34 *b*, oxidation of the *p*-phenylenediamine moiety proceeds ~400 mV more readily than oxidation of phenyl *tert*-butyl nitroxides. This also accounts for the fact that an electron-donating group is usually introduced into the linker during the molecular design of redox-switchable multispin systems.

Multispin systems containing localized and delocalized spin centres are of interest for molecular electronics. The biradical cation depicted in Fig. 34 *a* can be considered as the minimum structural unit of molecular conductors for spin polarization [284, 517, 518] that experience redox-controlled intramolecular magnetic couplings between localized spin centres.

The triradical cation proposed by Ito *et al.*[516] (see Fig. 34 *b*) is the first example of a multispin system in which the delocalized spin induces parallel arrangement of the spins of two localized stable nitroxide radicals. In the starting neutral structure, the large torsion angle between the amino group and the phenylene moiety results in almost complete disappearance of the spin–spin exchange coupling. The quinoid system formed upon oxidation gives rise to ferromagnetic properties in the triradical cation. It was shown [519] that the ferromagnetic coupling between the localized and delocalized spins accounts for the spin-polarized state.

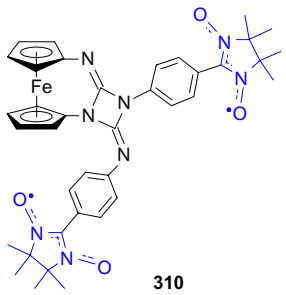
An unusual diaryl nitroxide containing two sterically crowded triarylphosphine moieties (Scheme 115) was synthesized [73] in order to study the interactions between the nitroxide radical and the phosphorus atoms in neutral and oxidized states. Due to distortion of the tetrahedral geometry, the lone electron pair of phosphorus acquires a greater π-character, which provides for spin delocalization on the phosphorus atom in the neutral form. Voltammetric analysis demonstrated that the electrochemical oxidation includes two reversible transitions corresponding to the successive oxidation of two phosphorus atoms. This attests to the presence of intramolecular interaction between the remote phosphine moieties, which occurs *via* the nitroxide moiety. Thus, an unusual molecular system was designed; it may be a part of a longer chain in which the electron effects could be transferred over large distances.

Scheme 115



The interaction of nitroxide radicals with metal ions has been studied in sufficient detail, but mainly in the context of magnetic properties of complexes.[100, 150, 499, 520] An interesting example of the design of dual-function molecules was reported by Gurskaya *et al.*[326] The authors used intramolecular click-reactions to obtain for the first time and fully characterize metallocenophanes **268** and **269** (see Schemes 90, 91) and their analogue **310**, which contained one or two nitroxide moieties. In these compounds, the redox-active ferrocenyl moiety can serve as a redox switch that modulates the properties of nitroxide radicals, in particular, magnetic interactions.[517] Voltammetric study of nitroxides **268**, **269** and **310** showed the presence of a reversible redox transition in the anodic potential region; however, the magnetic properties of the oxidized form of the complex have not yet been studied.

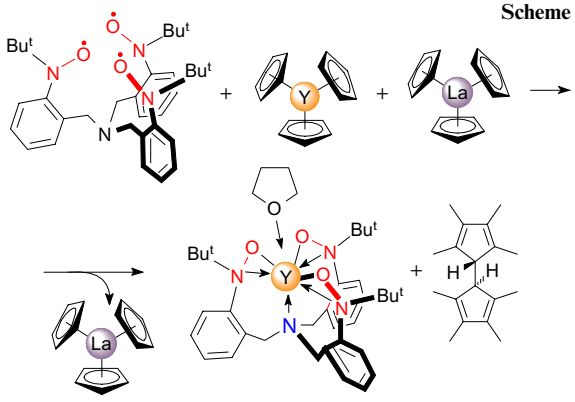
Structure 310



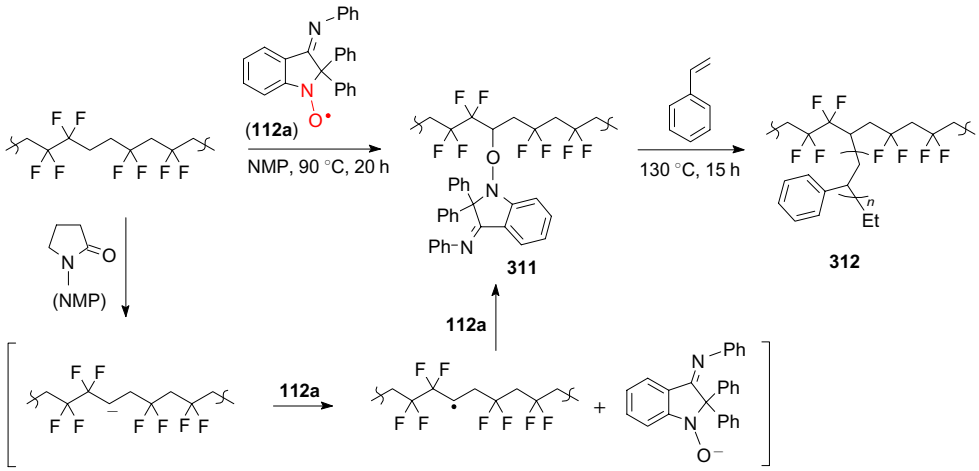
310

One more fairly unexpected application of trinitroxides is redox-activated kinetic separation of rare earth elements.[521–523] This method is based on the dual function of nitroxides, which combine redox and coordination properties. The proligand containing three aryl alkyl nitroxide moieties can be reduced by cyclopentadienyl lanthanide complexes to the corresponding aminoxyl anions. The cooperative effect of three NO^- groups coordinated to the metal ion can be used for the kinetic separation of lanthanides (Scheme 116). The complex formation rate strongly depended on the nature of the metal: for example, the La–Y separation factor reached 26.

Scheme 116



Scheme 117



The idea of using redox-activated thermally superstable indoline nitroxide radical **112a** in an elegant synthesis of fluorinated graft copolymers under mild polymerization conditions proved to be no less interesting.[524] Nitroxide moieties can be grafted to the polyvinylidene fluoride (PVDF) in solution without preliminary activation of the polymer. The resulting derivatives **311** can act as efficient macroinitiators of styrene polymerization, resulting in the formation of graft copolymers **312** containing 17 to 40 mass.% styrene with molecular masses of 1000 to 1500 g mol^{-1}. According to Lienafa *et al.*,[524] the crucial role in this process is played by the choice of the appropriate basic solvent, in this case, *N*-methylpyrrolidone (NMP), in which PVDF is converted to the anion, which is then oxidized with nitroxide **112a** to the (PVDF)$^{\bullet}$ radical. Recombination of this radical with nitroxide **112a** yields modified polymer **311** (Scheme 117). The attempts to use other solvents and other radical polymerization mediators (*e.g.*, TEMPO) in this reaction did not meet with success.

5.2. Complex formation of metal ions with conjugated nitroxides: an approach to the molecular design of magnets

The complex formation of paramagnetic metal ions with conjugated nitroxides to give heterospin systems opened up a new area in the molecular design of magnets,[525, 526] which has been intensively developed in recent years.[499, 520, 527–530] Often, these heterospin systems not only have unusual magnetic properties, but also provide additional opportunities for the control of the magnetic behaviour of the complex, which is important for the creation of innovative materials. Some examples illustrating the main trends of these studies are considered below.

The first trend that deserves attention is the design of magnetoactive materials,[131, 531] including chiral ones,[75] which, like classical magnets, are able to switch to ferro-, ferri- and antiferromagnetic ordered states as temperature drops below the critical value. Among transition metal complexes with nitroxides, the best magnetic ordering temperatures were attained for coordination compounds of manganese(II) with deprotonated imidazol-2-yl- (**313**) and benzimidazol-2-yl-substituted (**314**) nitronyl nitroxide moieties. These compounds react with Mn^{II} acetate in the presence of NaAn salts [An (anion) = ClO_4, BF_4, PF_6, *etc.*] to give coordination polymers $[Mn_2(\mathbf{313})_3]An$ and $[Mn_2(\mathbf{314})_3]An$, respectively, which have a lamellar structure with a honeycomb motif and contain alternating chiral (Λ and Δ) moieties formed by metal ions (Fig. 35).[530]

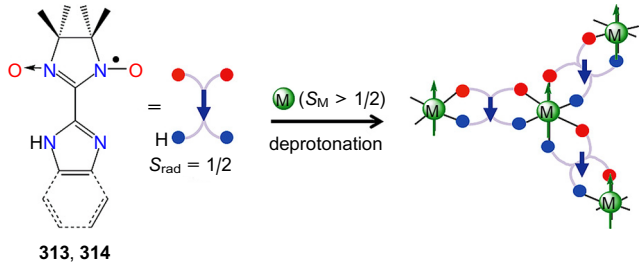


Figure 35. Schematic diagram of formation of coordination polymers (M = Mn, Co) based on (benzo)imidazole-substituted nitronyl nitroxides.[530] The arrows mark the directions of electron spins. Published with permission from John Wiley and Sons.

The critical temperatures characteristic of these heterospin polymers considerably depend on the structure of the paramagnetic ligand and the nature of outer-sphere anions (An). The highest T_C value was found for $\{[Mn_2(\mathbf{314})_3](ClO_4)\}_n$, which switched to a magnetically ordered state below 50 K (Fig. 36). A specific feature of the whole series of compounds $[Mn_2(\mathbf{314})_3]An$ is that their magnetizations (M) at the point where their field dependences saturate are different and are always lower than the theoretical 7 μ_B value expected for $S = 7/2$ of the $[Mn_2(\mathbf{314})_3]$ moiety. Thus, in the magnetic properties, the coordination polymers represent a case of weak ferromagnetism resulting from the Dzyaloshinskii–Moriya interaction in the chiral crystal structure.[530]

The second type of designed heterospin systems is characterized by structural phase transitions accompanied by a change in the geometry of the N–O–M groups, which, in turn, can significantly affect the magnetic susceptibility. A classical example is the family of transition metal complexes with nitronyl nitroxides or aryl *tert*-butyl nitroxides with a molecular or polymer chain structure. Structural phase transitions in these compounds induce magnetic anomalies similar to the spin-crossover in the temperature dependence of the effective magnetic moment [$\mu_{eff}(T)$].[520, 532, 533] The vast majority of complexes of this type are coordination compounds of $Cu(hfac)_2$ with nitroxides, in which the nitroxides act as mono- or bidentate bridging ligands.[534] The reaction of $Cu(hfac)_2$ with spin-labelled pyrazoles **52** [R = Me (**a**), Et (**b**), Pr^n (**c**)] gives rise to head-to-head polymer complexes [$Cu(hfac)_2$(**52a–c**)]

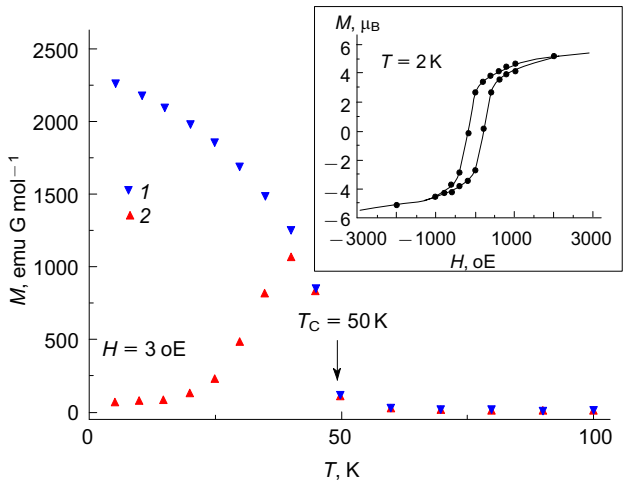


Figure 36. Temperature dependences of magnetization of $\{[Mn_2(\mathbf{314})_3](ClO_4)\}_n$ during cooling without magnetic field (*1*) and in a 3 Oe magnetic field (*2*) with a hysteresis loop (in the inset).[530] Published with permission from John Wiley and Sons.

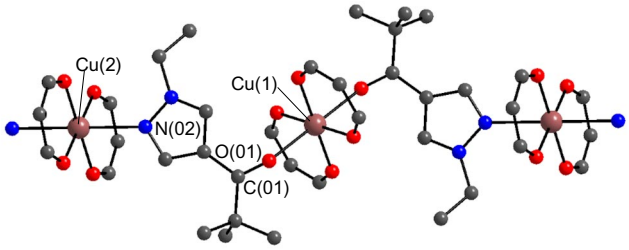


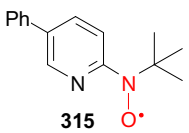
Figure 37. Molecular structure of a chain fragment of the complex [Cu(hfac)$_2$(**52b**)] at high temperatures.[134] Published with permission from American Chemical Society.

(Fig. 37). A decrease in the temperature induces a rearrangement of the coordination sphere of the metal ion in which the nitroxide group migrates from the axial to equatorial coordination. The global structural changes lead to changes in the spectral characteristics and a considerable decrease in μ_{eff} (Fig. 38).[134] The latter circumstance serves as an indicator of strong antiferromagnetic interaction between the unpaired electron of the copper ion and the paramagnetic ligand, which is the driving force of transitions in copper nitroxide complexes.[134, 535]

Transitions in the Cu(hfac)$_2$ complexes with nitronyl nitroxides or aryl *tert*-butyl nitroxides are induced not only by temperature changes, but also by irradiation.[133, 536–538] Furthermore, the photoswitching between the low-temperature and high-temperature magnetic states is very fast, taking place within a nanosecond.[539] In addition, the phase transition temperature in the copper nitroxide complexes is fairly sensitive to the applied pressure; the sensitivity reaches $\sim 290 \pm 15$ K GPa^{-1}, *i.e.*, it is several times higher than analogous characteristics of conventional iron complexes in which spin transitions take place.[269, 540]

One more type of spin-crossover is observed in copper(II) complexes with nitroxides in which the NO group is involved in the formation of chelate metallacycles.[541] As an example, one can consider the molecular copper complex with *tert*-butyl 5-phenyl-2-pyridyl nitroxide (**315**) (Fig. 39 *a*).

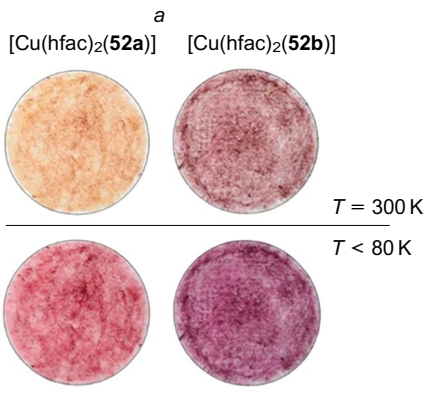
Structure 315



315

On cooling to 175 K, the complex undergoes a reversible phase transition accompanied by change in the space group from $C222_1$ to $P2_12_12_1$ and by a sharp change in $\chi_{mol}T$ (Fig. 39 *b*). This is caused by the increase in one Cu–O–N–C_{2Py} dihedral angle (ϕ_2) from 3.3 to 31.1° during the phase transition, thus changing the overlap of the magnetic orbitals and, as a consequence, inducing switching from strong ferromagnetic ($2J/k_B = +312$ K) to antiferromagnetic ($2J/k_B = -463$ K) exchange coupling.[542]

It was shown that the spin-crossover-like magnetic behaviour can be observed not only in copper nitroxide coordination compounds, but also in nickel(II) nitroxide complexes.[543–546] An interesting feature of the latter compounds is that the phase transition in them is gradual and is not accompanied by a change in the space group. For example, according to X-ray diffraction data, the space group of [Ni(**315**)$_2$Cl$_2$] remains invariable, $P2_1/c$, in the range from 85 to 400 K (Fig. 40). The Ni–O–N–C_{2Py} dihedral angles change gradually and, in fact, insignificantly, and this is accompanied by a decrease in $\chi_{mol}T$ from 2.38 cm^3 K mol^{-1} ($S = 2$) to virtually zero ($S = 0$).[543] This high sensitivity of magnetic properties to the molecular geometry inherent in [Ni(**315**)$_2$Cl$_2$] and, generally, in the whole group of metal nitroxide systems[547] became the



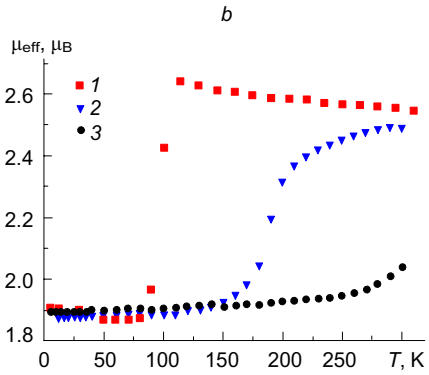


Figure 38. Colour change of complexes [Cu(hfac)$_2$(**52a**,**b**)] following temperature variation (*a*) and temperature dependences of the effective magnetic moment $\mu_{eff}(T)$ for [Cu(hfac)$_2$(**52a**)] (*1*), [Cu(hfac)$_2$(**52b**)] (*2*) and [Cu(hfac)$_2$(**52c**) (*3*).[134] Published with permission from American Chemical Society.

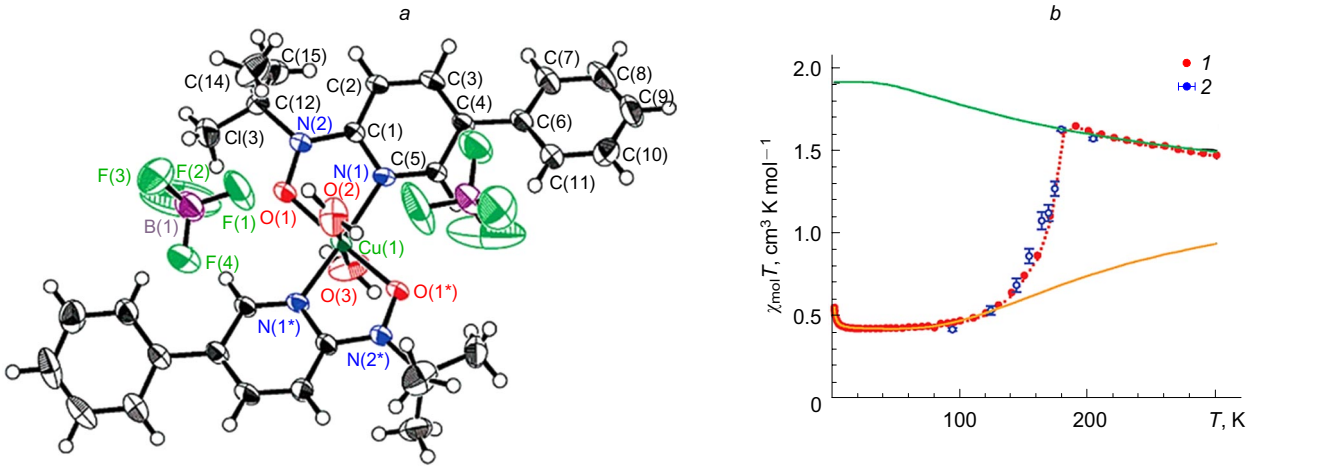


Figure 39. Molecular structure of $[Cu(\mathbf{315})_2(H_2O)_2](BF_4)_2$ (*a*) and temperature dependence $\chi_{mol}T(T)$ for this complex in a 500 Oe magnetic field [(*1*) experimental data, (*2*) values calculated using the geometric parameters of the Cu–O–N–C_{2Py} moiety] (*b*).[542] The orange and green curves show approximations of the experimental data measured at temperatures of >180 and <120 K, respectively. Published with permission from American Chemical Society.

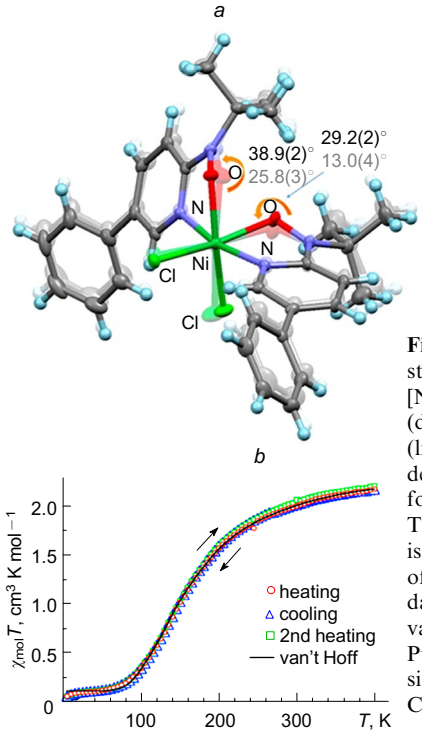


Figure 40. Molecular structure of the complex $[Ni(\mathbf{315})_2Cl_2]$ at 85 K (dark tone) and 400 K (light tone) (*a*) and dependence $\chi_{mol}T(T)$ fot this complex (*b*).[543] The black line in Fig. *b* is the approximation of the experimental data according to the van't Hoff equation. Published with permission from American Chemical Society.

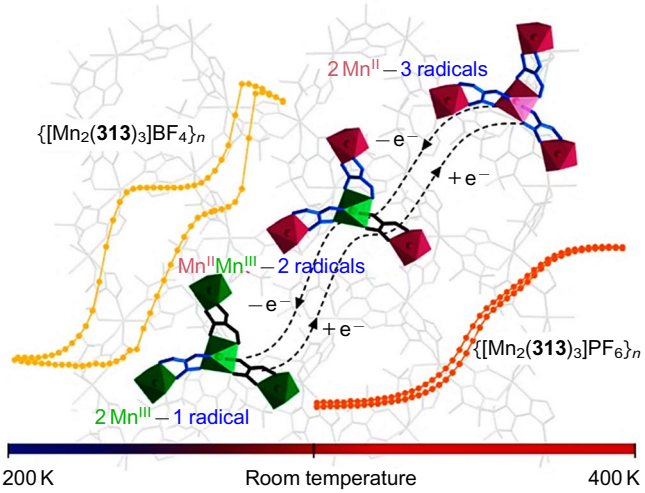


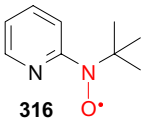
Figure 41. Thermally induced valence tautomerism in nitronyl nitroxide-containing coordination polymers $\{[Mn_2(\mathbf{313})_3]X\}_n$, where X = PF_6, BF_4.[550] Published with permission from Royal Society of Chemistry.

hallmark of heterospin systems of this type. The use of these compounds as sensors for external stimuli is only a matter of time.[548]

The third, virtually unexplored, type of metal nitroxide derivatives demonstrating magnetic anomalies includes complexes that undergo thermally induced valence tautomeric conversions.[549, 550] It was shown that layered polymeric compounds $\{[Mn^{II}_{2-y}Mn^{III}_y(\mathbf{313})_{3-y}(\mathbf{313}^{Red})_y]X\}_n$ ($\mathbf{313}^{Red}$ is the reduced dianionic form of **313**; X = PF_6, BF_4) undergo a two-step reversible transition between three valence isomers, accompanied by hysteresis (Fig. 41). At high temperature, $y = 0$, and all paramagnetic centres are coupled by strong antiferromagnetic exchange. In the temperature ranges of 280–220 K (for X = BF_4) and 380–330 K (for X = PF_6), successive reversible transfer of two electrons takes place; as a result, a half of Mn^{II} ions are oxidized to Mn^{III} by reducing a third of nitroxide radicals (for X = BF_4 at 252 K). As the temperature is further decreased, all Mn^{II} ions are converted to Mn^{III}, while 2/3 of radicals are transformed into the reduced diamagnetic state (see Fig. 41). Surprisingly, considering the redox potentials of $Mn^{3+/2+} = 1.54$ V [*versus* the standard hydrogen electrode (SHE)] and (H-**313**$^-$)/(H-**313**) = –0.25 V (*versus* SHE), the conversion of Mn^{2+}-**313** to Mn^{3+}-$\mathbf{313}^{Red}$ is thermodynamically impossible. In the opinion of Lecourt *et al.*,[550] the situation changes for honeycomb type charged structures such as $[Mn_2(\mathbf{313})_3]^+$, in which the cooperative effect is manifested.

The fourth group of metal nitroxide systems includes complexes with single-molecule magnetism effect. The search for such structures among thousands of synthesized coordination compounds can be described by a famous quote from V.V.Mayakovsky: is like getting at radium.

Structure 316



316

The profit in grams, but the work in years. Only highly qualified research of persistent scientists did result in the preparation and reliable verification of a number of single-molecule [81, 551–560] and single-chain [561–564] magnets. An example is the complex [Tb(hfac)$_3$(**316**)], in which the barriers to magnetization reversal ($\Delta^{(n)}$) for two independent molecules in the lattice, according to magnetic measurements, are $\Delta^{(1)}/k_B = 39.2(3)$ K for $\tau_0(1) = 4.2(4) \times 10^{-8}$ s and $\Delta^{(2)}/k_B = 36(2)$ K for $\tau_0(2) = 4.1(12) \times 10^{-7}$ s, where τ_0 is the pre-exponential factor in the Arrhenius equation (Fig. 42).[122]

Upon variation of the lanthanide ion and structure of the paramagnetic ligand and analysis of the obtained structural and magnetic data, researchers made several fundamental conclusions. First of all, when the paramagnetic ligand with the magnetization reversal barrier $\Delta/k_B = 21.1(8)$ K [$\tau_0 = 1.7(6) \times 10^{-9}$ s] in [Tb(hfac)$_3$(**316**)] is replaced by the diamagnetic analogue, the molecular magnetism completely disappears.[565] Analysis of the magneto-structural correlations showed that for complexes with direct coordination of the nitroxide group, the spin of the ligand $S = 1/2$ should be taken into account while determining the spin parity. In this case, the design of Kramers molecules — potential molecular magnets — may be more successful.[566]

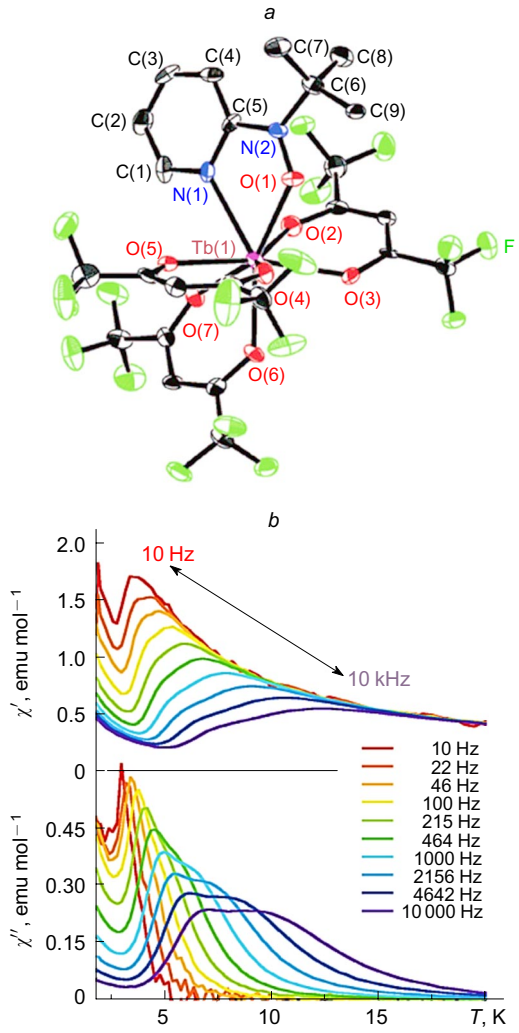
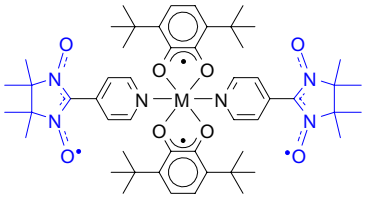


Figure 42. Molecular structure of one of independent molecules of [Tb(hfac)$_3$(**316**)] (*a*) and temperature dynamics of in-phase (χ') and out-of-phase (χ'') portions of magnetic susceptibility of this complex (*b*).[122] Published with permission from Royal Society of Chemistry.

The number of publications in which researchers try to introduce as more as possible diverse spin carriers into the solid phase has markedly increased in recent years. Here, two actively developed approaches can be distinguished. One approach includes the synthesis of complexes that contain paramagnetic transition metal ions or simultaneously transition metal and lanthanide ions, apart from nitroxide radicals.[500] The essence of the other approach is to synthesize complexes containing paramagnetic ligands of various types or biradical heterospin structures. This approach can be illustrated by publications describing the synthesis and properties of complexes **317a**,**b**, containing nitronyl nitroxide and semiquinolate ligands around the metal centre.[567–570]

Structures 317

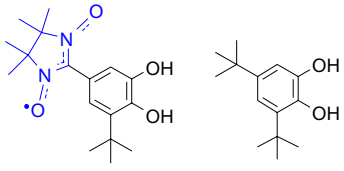


317a,**b** M = Ni (**a**), Mn (**b**)

A large contribution to the design of metal complexes with heterospin triplet anions was made by Shultz and co-workers.[571–575] This American research team carried out systematic study of a large number of high-spin systems consisting of a coordinated semiquinolate moiety and nitronyl nitroxide radical, elucidated the effect of linker structure on the intramolecular exchange, studied spin polarization and dynamics of photoexcited states and constructed numerous magneto-structural correlations. This is illustrated by one of the most recent studies,[576] in which the authors elucidated the effect of the structure of the bridging moiety, more precisely, the angle of rotation of the bridge relative to spin carriers on the triplet–singlet splitting in the biradical ligand **318** (Fig. 43).

There are still a lot of unexplored areas in the series of metal nitroxide systems. Among other issues, mention should be made of spin-crossover complexes containing paramagnetic ligands. Only in 2015, Tichnell *et al.*[577] described the catecholate iron complex [(TPA)Fe^{III}(**319a**)]BPh$_4$ [TPA is tris(2-pyridylmethyl)-

Structures 319



H$_2$-**319a** H$_2$-**319b**

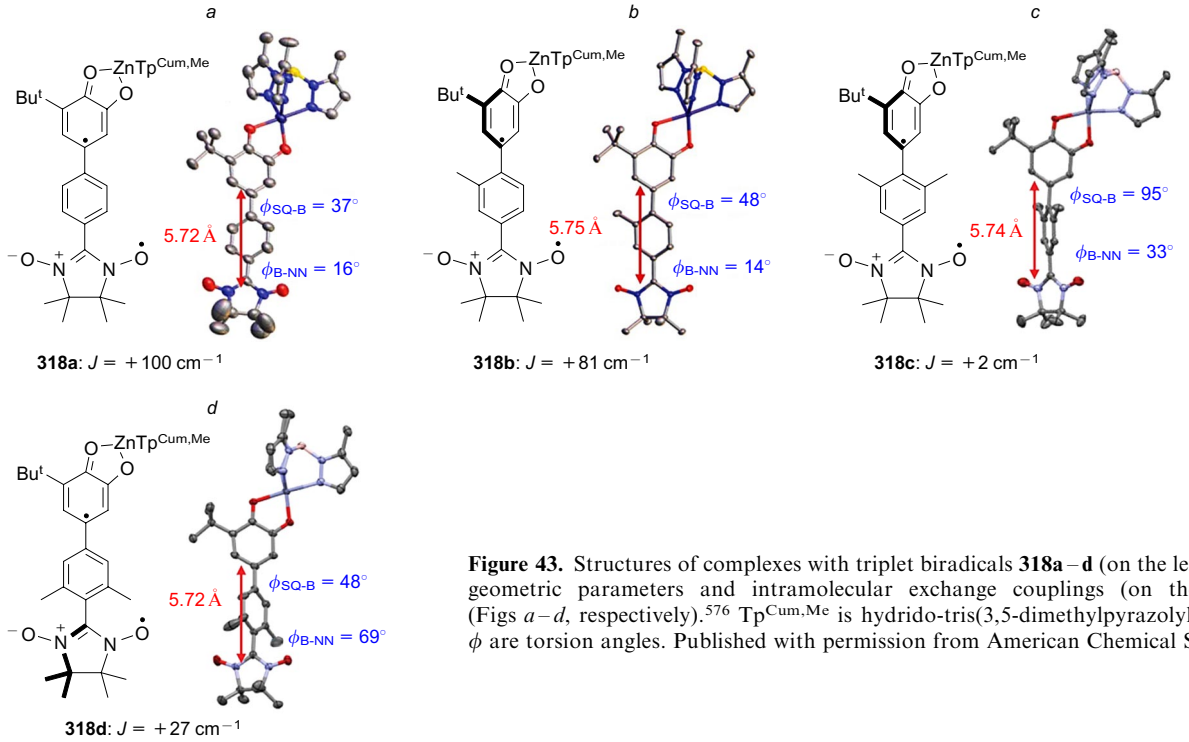


Figure 43. Structures of complexes with triplet biradicals **318a**–**d** (on the left), their geometric parameters and intramolecular exchange couplings (on the right) (Figs *a*–*d*, respectively).[576] $Tp^{Cum,Me}$ is hydrido-tris(3,5-dimethylpyrazolyl)borate, ϕ are torsion angles. Published with permission from American Chemical Society.

amine] and its analogue with ligand **319b** containing a *tert*-butyl group instead of the nitronyl nitroxide group (Fig. 44).

According to Mössbauer spectroscopy and magnetic measurements, classical spin transition takes place in both complexes [(TPA)Fe^{III}(**319**)]BPh_4. Although no noticeable effect of paramagnetic substituents on the spin-crossover and photophysical properties were found in either of these complexes, the necessity to design new iron complexes with nitroxides and other organic radicals characterized by

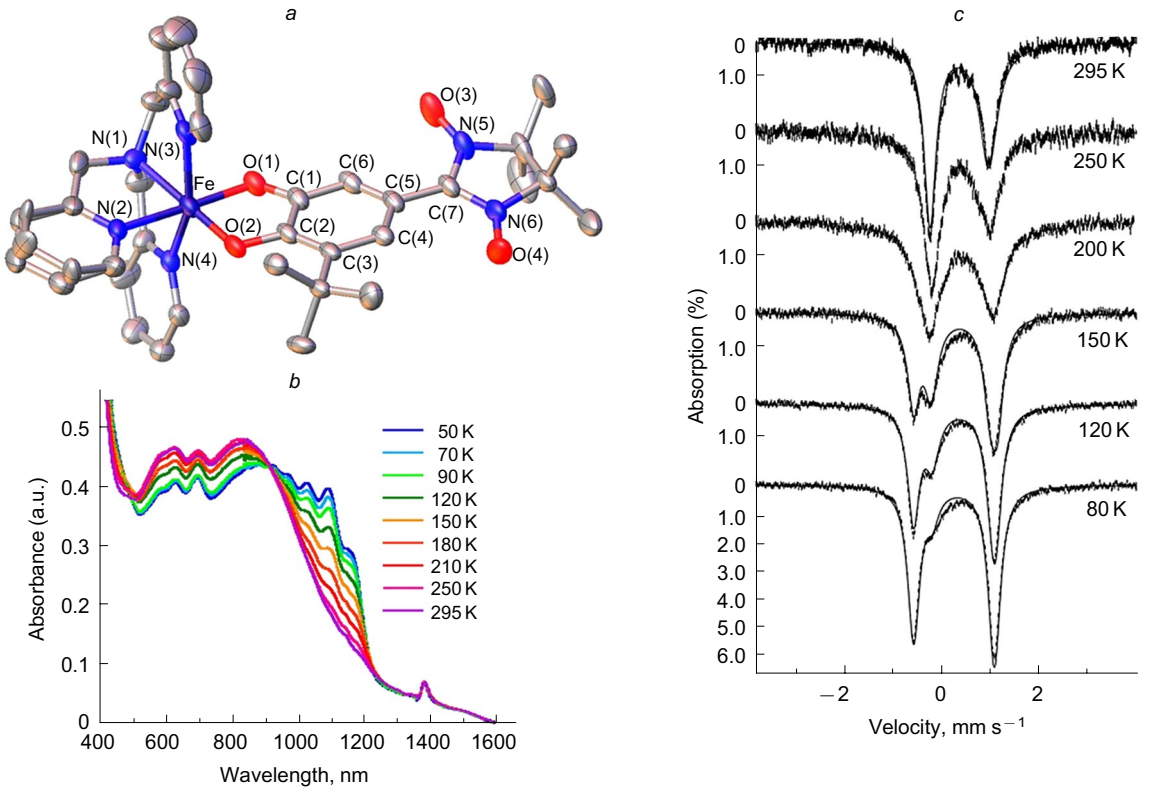


Figure 44. Molecular structure of the complex cation [(TPA)Fe^{III}(**319b**)]$^+$ (*a*), temperature dynamics of optical (*b*) and Mössbauer spectra of [(TPA)Fe^{III}(**319b**)]BPh_4 (*c*).[577] Published with permission from American Chemical Society.

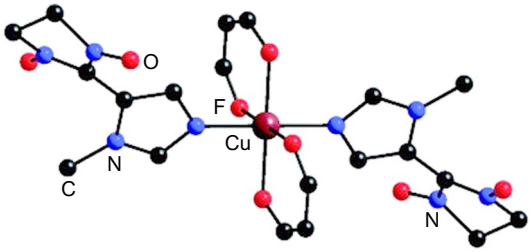
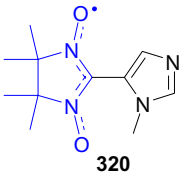


Figure 45. Molecular structure of the complex $[Cu(hfac)_2(\mathbf{320})_2]$. The figure was created by the authors using published data.[578]

Structure 320



320

strong exchange between the paramagnetic centres is obvious.

The metal nitroxide research is not devoid of occasional, so-called intuitive discoveries. For example, while examining the crystals of $Cu(hfac)_2$ with nitronyl nitroxide **320** under a microscope (Fig. 45), we noticed that they behave in a fairly specific way: experience a jet propulsion as a result of detachment of small, rapidly scattering pieces from the surface. This scene was so fascinating that the process was video recorded and the video was enclosed to the original manuscript.[578] The essence of the effect was also unique: this was due to accumulation of photogenerated molecular oxygen inside the crystal; the increasing oxygen pressure in the surface layers induces ejection of crystalline fragments, which are scattered from the main crystal at a high velocity. The recoil force thus arising results in the observable movement and rotation of the crystals.[579–581]

Selected examples described in this Section give a general idea of the main approaches to the molecular design of magnets using metal complexes with nitroxides. They are worth paying attention to, since these complexes can serve as platforms for the construction of magnetically ordered and bifunctional systems with enhanced characteristics.

5.3. Photoswitchable molecular systems based on nitroxides

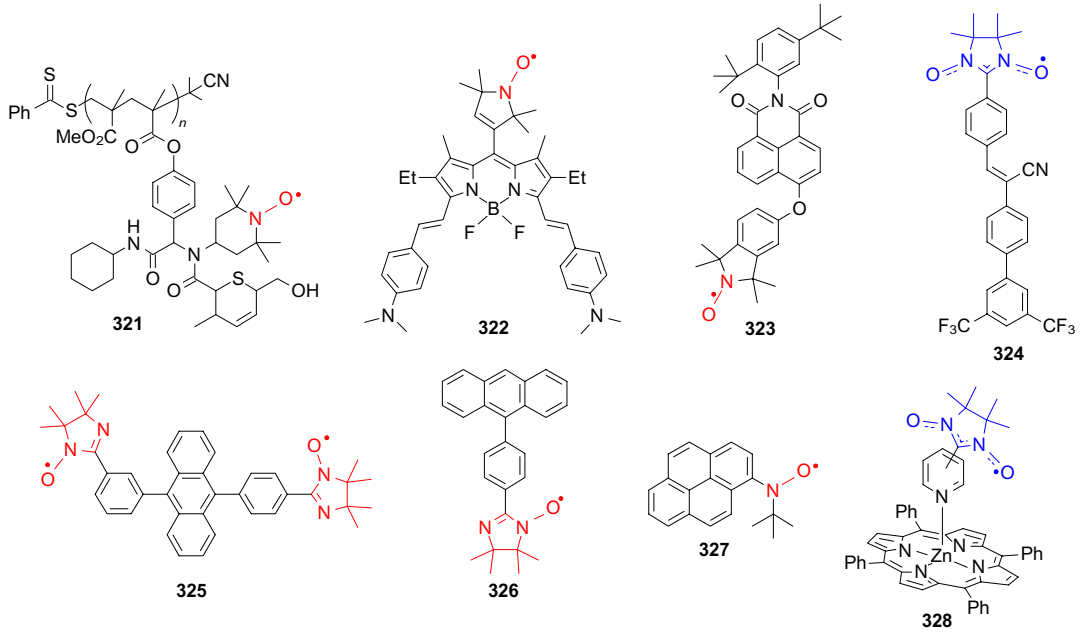
Combination of the nitroxide–fluorophore moiety in one molecule is one more trend of fabrication of bifunctional systems. These compounds are used for highly sensitive rapid tests for the redox state of the sample and for determining the sample antioxidant activity and sensitivity to oxidative stress, *etc*. They can provide a lot of information for studying the molecular dynamics and intermolecular charge transfer or fluorescence quenching and can be used used as photoswitches or analytical reagents.

The numerous applications of the nitroxide–fluorophore systems are based on the following three effects:[582] the nitroxide moiety is able to quench fluorescence; the chemical, electro- or photoreduction of the radical leads to a sharp decrease in the EPR signal, but simultaneously to fluorescence enhancement; and the reduction kinetics appreciably depends on the molecular-dynamic properties of the medium. These effects form the basis for the quantitative study of the molecular dynamic processes and redox reactions (including biochemical reactions).

Development along this line involved the synthesis of compounds containing not only traditionally used aliphatic nitroxides (*e.g.*, TEMPO and its analogues **321**–**323**[583, 584]), but also unsaturated nitroxides of various types — **150**, **324**–**328**. The molecular design of these bifunctional systems, which implies a definite combination of fluorophore–linker–nitroxide moieties, allows relatively fine tuning of the system properties to particular task.[585–590]

Nitronyl nitroxide **150** covalently bound to an organic fluorophore, pyrene, was used to detect superoxide radicals and to quantitatively estimate the antioxidant activity of biomolecules with different redox potentials (quercetin, ascorbic acid, *etc*.).[591] The reduction of the nitroxide group with organic radical is accompanied by a decrease in

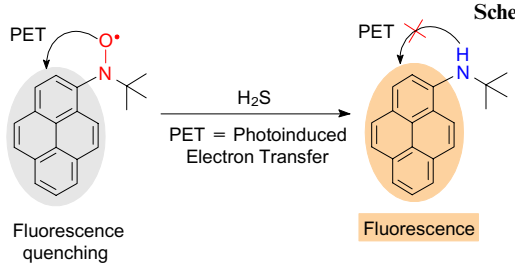
Structures 321–328



the EPR response and a sharp increase in the fluorescence intensity (by three orders of magnitude). This allows detection of submicromolar concentrations of the antioxidant, *i.e.*, sensitivity of the method is very high. Nitronyl nitroxide **324**[592] showed good results in the detection of ascorbic acid over a broad concentration range (1 μM – 2 mM). Owing to the 4,4-difluoro-4-bora-3a,4a-diaza-s-indacene (BODIPY) moiety, compound **322** is capable of fluorescence in the near-IR range, which makes it suitable for being detected in living organisms.[593]

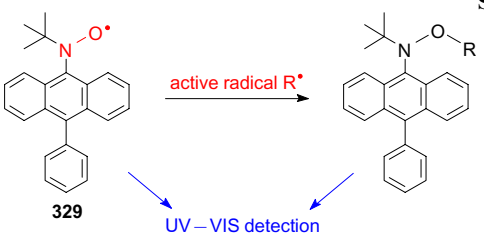
Nitroxide **327** was used to propose the first test for determining exogenous H_2S, which is a potent environmental toxicant, in living organisms. The electron exchange coupling between the radical and the fluorophore in the excited state leads to fluorescence quenching, presumably, by the photoinduced electron transfer mechanism. However, in the presence of H_2S, the nitroxide radical is reduced to the corresponding amine, which leads to fluorescence enhancement (Scheme 118).[594]

Scheme 118



The reactive radicals formed in chemical and biochemical processes can be trapped and studied by stable nitroxides containing a photoactive organic moiety suitable for detection. For example, 9-phenylanthryl nitroxide derivative **329** was tested as a scavenger for reactive radicals (Scheme 119).[4]

Scheme 119



The presence of polyaromatic system, first, stabilizes this nitroxide (efficient detection requires a certain balance between the radical stability and reactivity) and, second, serves as the fluorophore suitable for UV detection (when the adduct is formed, the absorption band shifts to longer wavelengths).[4] Examples of the design of fluorescent sensors for reactive organic radicals were reported by Lederhose *et al.*[595]

The introduction of nitroxide radical centres into photochromic fluorophores is used to obtain photosensitive organic magnets, the magnetic properties of which markedly change upon irradiation. Examples of such compounds have been reported (see structures **325**, **326**, **328**).[55, 596, 597] The nitroxide – fluorophore type bifunctional systems are often used as convenient models for studying the mechanisms of photophysical processes related to exchange coupling in paramagnetic particles, including hybrid particles, *e.g.*, spin-labelled cadmium selenide nanoparticles.[598] One more possible mechanism of quenching of the excited state of the chromophore in the presence of a nitroxide radical is based on the fact that the spin-forbidden $S_1 \rightarrow T_1$ and $T_1 \rightarrow S_0$ transitions become allowed in the excited chromophore because of the spin of the radical, in particular, they become the transitions between the doublet states of the whole molecule. Interesting models of this type were considered by Likhtenstein *et al.*[599]

An unusual relaxation pathway consists in the photoinduced deoxygenation of coordinated radicals in copper nitroxide complexes, which induces jet propulsion of the crystals as they eject small pieces — so-called jumping crystals (see above and Refs 578 and 579).

It should be emphasized that the functional properties of the combined radical – fluorophore systems far exceed a mere superposition of the properties of their components. These systems provide more possibilities for real-time monitoring of redox processes, for example, to analyze the antioxidant activity, or biochemical processes such as the generation of NO, superoxide and other reactive radicals in real time. It is known that fluorescent methods are 2 – 3 orders of magnitude more sensitive than the EPR spectroscopy or optical spectroscopy. For this reason, these systems can serve as the basis for photosensitive and photoswitchable organic magnets and are convenient for analysis of intramolecular exchange couplings.

5.4. Nitroxide radicals as ambipolar redox-active materials

Recently, the development of alternative energy sources based on renewable organic raw materials has been among the most hot areas of research; this is due to deterioration of the environmental situation and gradual depletion of mineral resources. Therefore, a relevant problem is the molecular design of new redox-active molecules that could be used to invent new-generation organic batteries.[600 – 603] Nitroxide radicals are promising candidates for the design of these products.[604]

In the examples described above, the bifunctional nature of combined nitroxides was attained by combining their properties and additional possibilities offered by the other structural moiety. This symbiosis opens up new prospects for the design of controllable materials. This brings out the question of whether it is possible to change the functionality of the proper nitroxide under an external stimulus. For example, whether one and the same compound can act as an efficient redox-active material for both anode and cathode upon application of cathodic and anodic potentials, respectively (to generate one or another charged state)

For this purpose, it is necessary that the compound (in our case, nitroxide radical) be able to exist in three redox states (cation, radical and anion), which should be sufficiently stable. Such molecules are called ambipolar, and they are in great demand as redox-active components for symmetric all-organic batteries; creation of these devices is highly relevant for the development of new energy storage devices. The benefits of symmetric (pole-less) batteries is obvious:[605] they are safe on storage, because in the discharged state, one and the same compound is present at the cathode and at the anode. For the same reason, the requirements to the nature of the separating membrane are less stringent. Pole-less batteries can change the polarity at intervals, which increases the operation time. Thus, these batteries are most easy-to-maintain, cost-efficient and envi-

ronmentally benign (if renewable organic raw materials are used). Meanwhile, their wide practical use is largely delayed by the absence of a suitable redox-active material.

Stable organic radicals, in particular nitroxides, which are characterized by fast kinetics of electrode processes, are promising candidates for this application. However, stabilization of three redox states of one molecule is a challenging task requiring fine tuning of the molecular structure.[606, 607] Dialkyl nitroxides, such as TEMPO, the most well-known and well-studied nitroxide radical, form a reversible redox pair only in the anodic potential region; therefore, they are suitable only as cathode materials. TEMPO was tested for the first time for this function in a Li-ion battery in 2004,[608] and since then, the number of publications on this subject has been steadily increasing. In order to make the electroactive material more convenient for handling, TEMPO was immobilized on various carbon and polymer supports.[603, 609–611] More recent studies demonstrated the applicability of TEMPO as a cathodic material for not only portable devices, but also for flow batteries,[612, 613] including all-organic [614, 615] and Zn–organic batteries.[603, 616]

Unsaturated nitroxides, particularly aryl alkyl nitroxides, have an important advantage over dialkyl derivatives: aromatic radicals offer more opportunities for structural tuning of the molecule to stabilize opposite redox states.[617] For example, modification of the aromatic ring in aryl alkyl nitroxides by introduction of electron-withdrawing substituents resulted in the synthesis of redox-active molecules **330**–**332** (Fig. 46), which were used as n-type anode materials in organic batteries.[24, 618] It should be emphasized that organic redox-active molecules of n-type (suitable for the manufacture of anode materials) are encountered much more rarely than p-type cathode materials. It was shown that aryl alkyl nitroxide radicals can be converted to n- or p-type molecules by introducing electron-withdrawing or -donating substituents, respectively.[619]

Unsaturated nitroxides **333**, **334** were also tested as cathode materials. In 2019, Yeşilot *et al.*[620] reported the preparation of a polymer containing four nitroxide groups, which proved to be efficient as a cathode material (capable of transferring four electrons) in a rechargeable Li-ion battery. The battery demonstrated high power characteristics with a discharge capacity of 100 mA h g^{-1} at $C/2$ discharge rate (corresponds to the current needed for full charge–discharge of the electrode in 2 h) during 500 cycles. Nitronyl nitroxides were also fairly efficient as cathode materials in Zn-ion batteries and demonstrated characteristics exceeding those of not only organic, but also inorganic materials.[602, 621, 622]

Stabilization of both oxidized (cationic) and reduced (anionic) forms sufficient for practical application was so far attained only for nitronyl nitroxides. The presence of the electron-withdrawing iminium moiety in the close vicinity of

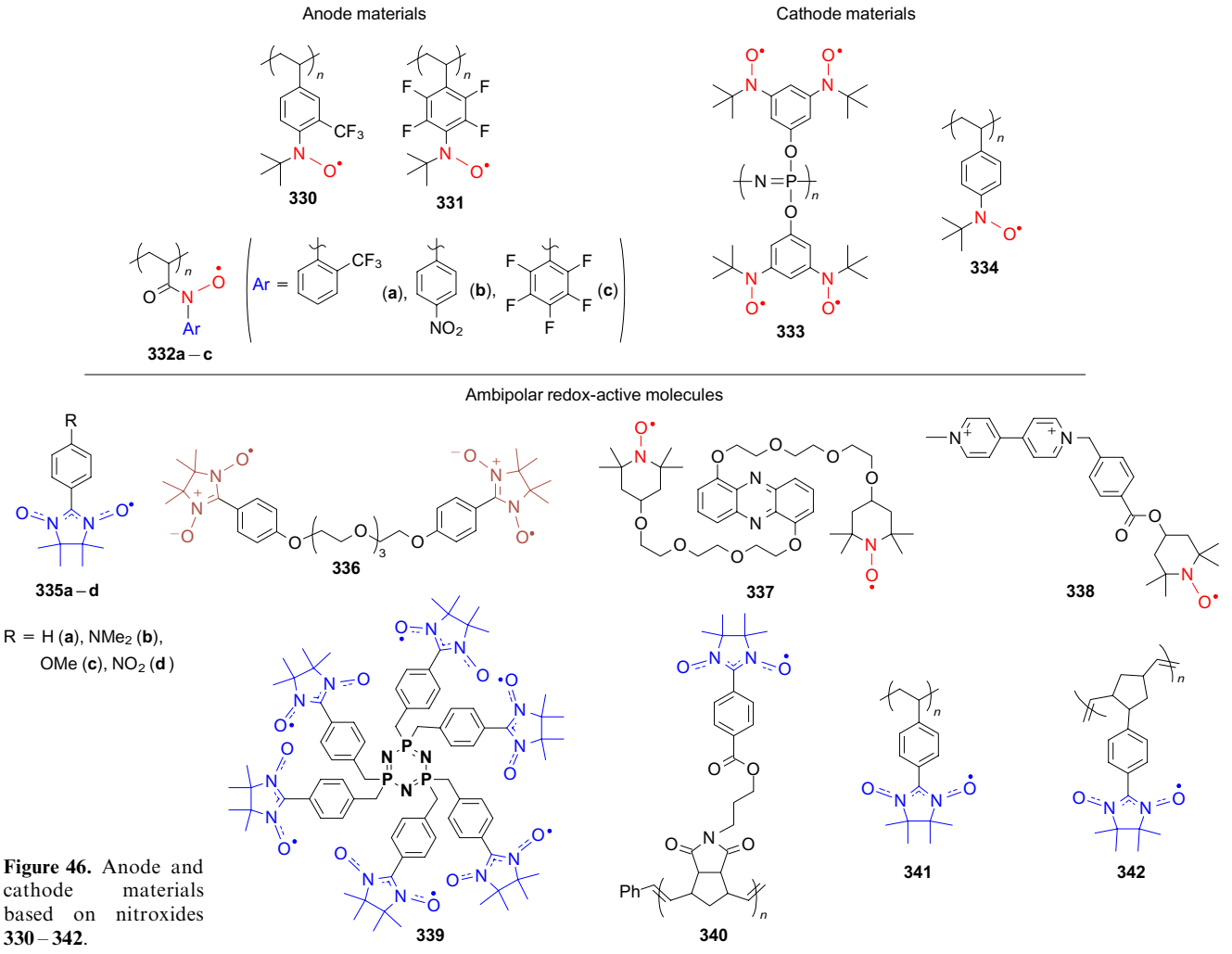
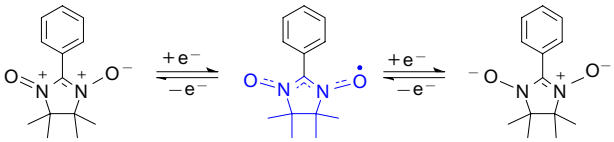


Figure 46. Anode and cathode materials based on nitroxides **330**–**342**.

Scheme 120



335a

the NO group stabilizes the reduced form of the radical, but does not affect significantly the stability of the cationic (oxidized) form, which was stabilized by conjugation with the nitrogen electron pair (Scheme 120). This double stabilization gives rise to bifunctional (redox-amphoteric) properties for compounds of this type.

The first ambipolar device based on nitronyl nitroxide **341** immobilized on polystyrene was designed in 2011 by Nishide and co-workers.[623] Although characteristics of the battery were quite modest, the authors demonstrated the conceptual possibility of creating an ambipolar device based on nitronyl nitroxides. Later, nitronyl nitroxide ambipolar moieties were also immobilized on other macromolecular compounds, for example isoleucine-based gelator[624] or on polymers — polyacetylene,[625] norbornene (**342**)[626] and so on.[627] In the case of norbornene, the monomer forms classical reversible redox pairs both in cathodic and anodic potential regions. However, during the repeated potential scanning in solution, the redox response in the cathodic potential region is not reproduced in the polymer, which was attributed[627] to partial passivation of the electrode surface.

In 2016–2018, the first symmetric redox flow battery involving nitroxide **335** was designed;[504,628] the battery had reasonably good characteristics: cell voltage of 1.73 V, current and voltage efficiency of ~90% and charge and discharge energy density of 9 and 5 W L^{-1}, respectively. Later, some of these characteristics were improved using biradical **336** with tetraethylene glycol linkers between the nitronyl nitroxide moieties.[629]

Tkacheva *et al.*[630] showed that paramagnet **335a** and its derivatives substituted with NMe_2, OMe or NO_2 in the *para*-position of the aromatic ring (**335b–d**) can act as redox mediators in Li–O_2 batteries. These paramagnets efficiently catalyze the charging process, which is important for practical purposes, but have almost no effect on the discharge (Fig. 47).[630]

Another formal strategy was proposed to design symmetric all-organic redox flow batteries. In this case, the anodic and cathodic activity of the ambipolar material was achieved by introducing, into one molecule, two different redox-active moieties connected by a non-conducting linker. As a rule, TEMPO was used as the cathodic component, while the anodic redox activity (nitroxides **337**, **338**) was due to the presence of another moiety such as phenazine,[631] viologen[632] and so on. In both cases, the attained voltage was ~1.2 V.

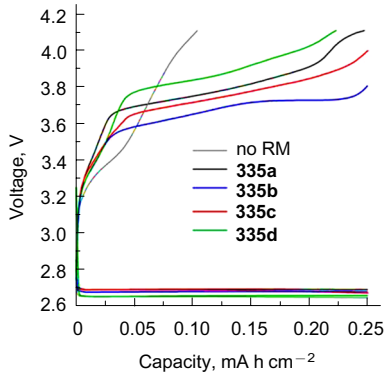


Figure 47. Galvanostatic discharge/charge curves in nitroxides **335a–d** (concentration of 10^{-3} mol L^{-1}) in a LiTFSI–diglyme mixture (first cycle).[630] TFSI is bis(trifluoromethanesulfonyl)imide. Published with permission from American Chemical Society.

Fidan *et al.*[633] synthesized an unusual polyradical structure **339**, which contained several nitronyl nitroxide moieties covalently bound to the cyclotriphosphazene core. The authors did not test this compound in model devices, but according to a voltammetric study, it could be reversibly oxidized and reduced, *i.e.*, the cationic and anionic forms were relatively stable.

As can be seen from the above discussion, despite certain progress, the structural design of ambipolar nitroxide radicals is still a problem to be solved. These compounds are in-demand not only for the design of modern energy devices, but also in organic electronics, as active components of transistors[634] and so on.

Among all types of nitroxide radicals, diaryl nitroxides offer the greatest opportunities for structural modification towards a specific practical task. A systematic approach to address the problem of stabilization of opposite charge states (anion and cation) has been implemented in a number of studies by Magdesieva and co-workers.[50,156,635,636] The tools used for structural tuning included not only the traditional introduction of electron-donating and -withdrawing substituents into different benzene rings (two aromatic rings with substituents of the opposite nature form a cross-conjugated system with the functional group), but also dynamic stabilization methods. In the latter case, the molecule adjusts its geometry in such a way that stabilizing effects on the reaction centre are enhanced and destabilizing interactions are minimized. This can be attained by varying the torsion angles between the aromatic ring and the NO group plane, for example, by introducing a bulky substituent into the *ortho*-position of one of the rings or a linker connecting the benzene rings. The removal of one of the rings from the conjugated plane weakens π-binding between this ring and the NO group. This minimizes the mutual cancellation of the electron-donating and electron-withdrawing effects on the functional group and facilitates the variation of the dihedral angle between the ring and the functional group: an increase in the case of adverse effect of the substituent on stabilization of charged particles and a decrease if it promotes stabilization of the charged state. Thus, it is possible to obtain three redox forms for the same nitroxide radical (Fig. 48).

The possibility of varying the rotation angle of the benzene ring upon the change in the nitroxide redox state was confirmed both theoretically (DFT calculations) and experimentally (voltammetric measurements).[157,416,636] There is a linear dependence between the experimental values of $^{1/2}[E_{1/2}(\mathrm{Ox}) + E_{1/2}(\mathrm{Red})]$, where $E_{1/2}(\mathrm{Ox})$ and $E_{1/2}(\mathrm{Red})$ are the anodic and cathodic half-wave potentials, respectively, and the sum of substituent constants (adjusted for including the DFT-calculated C–C–N–O dihedral angles). This confirms the variability of contributions of D–A rings to the stabilization of redox states.

The second way to stabilize the opposite charge states of diaryl nitroxide radicals is to introduce chameleonic groups,[637] which are capable of changing their donor-acceptor properties upon rotation relative to the benzene ring, thus enhancing stabilization of the oppositely charged redox states. An example of such group is α-methylcyclo-

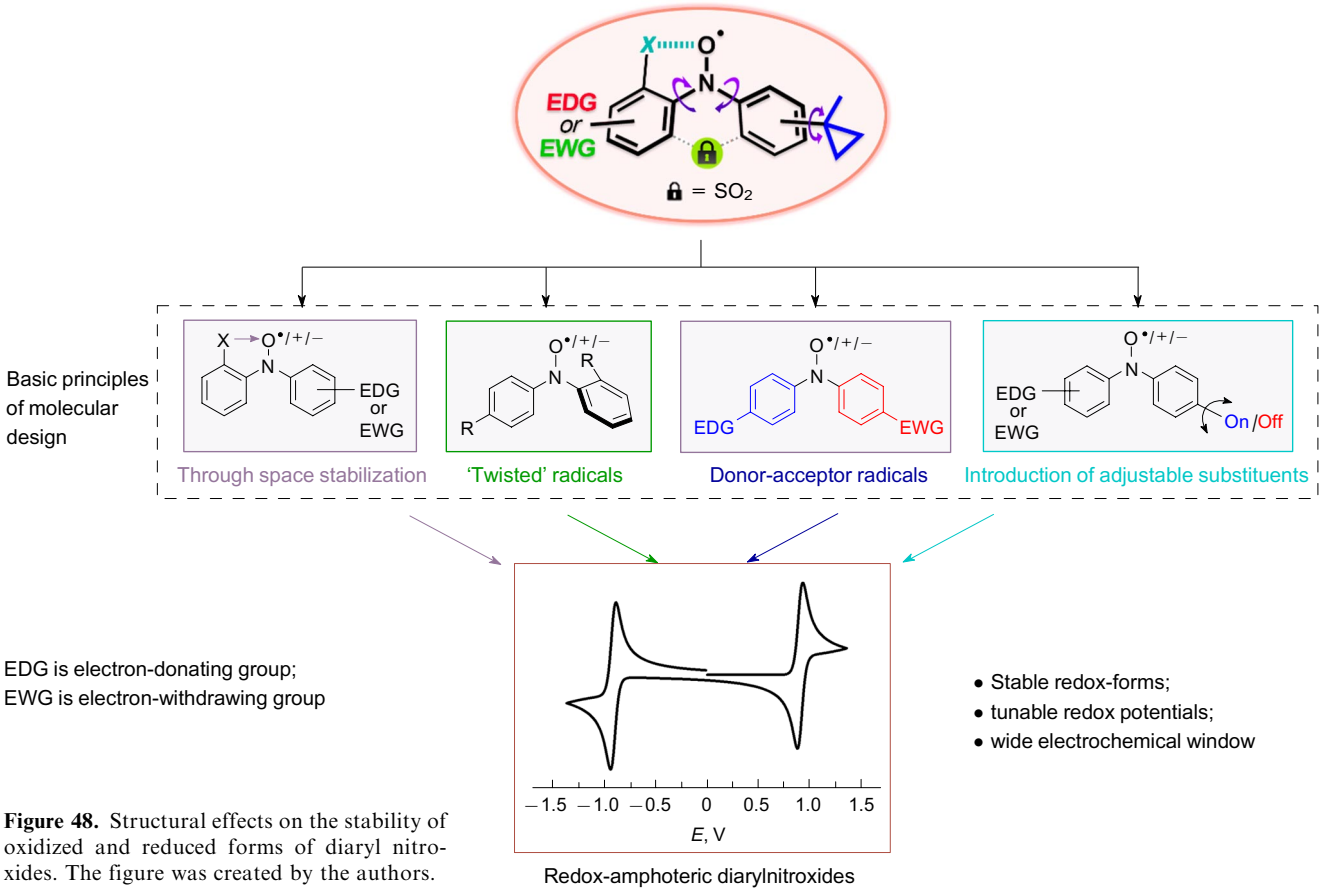


Figure 48. Structural effects on the stability of oxidized and reduced forms of diaryl nitroxides. The figure was created by the authors.

propyl. The rotation of the chameleonic MCP substituent in the benzene ring on going from the cationic to the anionic state was proved by both quantum chemical calculations and experimental methods (X-ray diffraction and voltammetric measurements).[157] The orientations of the *para*-MCP group relative to the benzene ring are different for cations, anions and radicals. The cations exist only in the conformation that enables π-stabilization, although it is more sterically crowded. The π-interaction with the vacant orbital of cyclopropane is less significant for stabilization of the anionic form (because of the pronounced difference between the orbital energies) and cannot counterbalance the increasing steric repulsion. As a result, the cyclopropane moiety rotates through 90° (see Fig. 48). For the radical, the energy difference between the two conformations is much less pronounced, although the conformation ensuring the π-conjugation with the ring prevails. In the crystal cell of 2,4′-bis(α-methylcyclopropylphenyl) nitroxide, there are molecules in two conformations differing in the rotation angle of the *para*-MCP group relative to the benzene ring.[157]

The third approach is introduction of structural moieties capable of stabilizing the redox states by through-space non-covalent interactions (see Fig. 48). The through-space stabilization was observed for diaryl nitroxides containing α-methylcyclopropyl and/or 2-pyridyl substituent in the *ortho*-position. The donation of the σ_{C-C} orbital of the MCP group or the nitrogen p orbital of the pyridine moiety to the π*-orbital of the N—O bond substantially stabilizes the oxoammonium cation.[157]

This approach based on the fabrication of self-adjusting redox-active molecules proved to be very useful. The application of the above structural design methods resulted in the preparation of new nitroxides that have unique stability in solutions among diaryl nitroxides[157,638] ($\tau_{1/2}$ in benzene solutions at room temperature reaches 2310 h, *i.e.* >3 months for some compounds)[157] and that are able to form relatively stable oxidized and reduced forms (the examples are shown in Fig. 48).

The efficiency of methods for stabilization of opposite redox states (aminoxyl anions and oxoammonium cations) was confirmed by voltammetric study of new diaryl nitroxides, most of which show reversible redox pairs both in the cathodic and anodic regions.[157,636] This effect could not be attained in the case alkyl derivatives. New highly stable radicals have not yet been tested in model devices; however, presumably, the developed approaches to the molecular design of ambipolar bifunctional nitroxides will be used in various technologies.

6. Conclusion

The chemistry of conjugated nitroxide radicals started to be developed owing to the studies of organic paramagnetic compounds, in particular to the fundamental discoveries of E.Fremi, O.Piloty, B.G.Schwerin, H.Wieland and M.Offenbacher.[55] Having gone a long way starting with the works of the 1970–1990s and having formed the principles of molecular design of magnets, it diveloped into a large interdisciplinary fundamental research area and a useful tool for solving applied problems. This was facilitated by advancement of the existing and development of new high-tech methods for studying paramagnets and high-spin systems including both long-lived and short-life-

time ones. First of all, these are steady-state and pulsed EPR techniques; SQUID magnetometry and nano-SQUID magnetometry; X-ray diffraction analysis, including the techniques using synchrotron radiation sources; and in special cases, also multimode scanning electron and force microscopy, magneto-structural analysis *via* polarized neutron diffraction; and super-strong magnetic field experiments. Owing to increase in the capacity of available computing systems and progress in the used software packages, calculation methods made a huge step forward and became an efficient tool for the chemical modelling and prediction of the magnetic properties of magnetically active systems.

Meanwhile, the development of chemistry of conjugated nitroxides resulted in the synthesis of a unique series of open electron shell compounds meant for materials science, molecular design of magnets, elucidation of the fundamental trends in the physics of magnetism and evolution of spin systems. Potential applications of functionalized nitroxide radicals can be found virtually in any related field of science. Conjugated nitroxides are in fairly high demand in organic, analytical and coordination chemistry. They are of interest as reagents and components of catalytic systems; organic radicals are actively used to study mechanisms of catalytic redox processes.[639] The design principles were formulated and molecular machines based on organic paramagnets were devised.[640] Fundamental research associated with the development of spin manipulation techniques requiring special multispin systems is carried out.[641] The development of magnetochemistry of magnetically active single molecules is in progress. This opens up the way to the design of molecular parts of electronics and spintronics: spin filters, molecular transistors, quantum dots, magneto-optical switches, *etc*.

In all practical applications of nitroxides, the possibility of varying the structure of stable spin carriers over rather wide limits will always serve as the main source of new ideas and goals for exploratory research.

This review was written with the financial support of the Russian Foundation for Basic Research (Project No. 20-13-50016).

7. List of acronyms and designations

$a(^{14}N)$ hyperfine coupling constant,
A — acceptor,
Am — amyl (pentyl),
B — magnetic induction,
Boc — *tert*-butyloxycarbonyl,
BS-DFT — broken symmetry density functional theory,
C — chromophore,
Cat — catalyst,
D — donor,
DCC — dicyclohexylcarbodiimide,
DCM — dichloromethane,
DEER — double electron–electron resonance,
DFT — density functional theory,
DLP — lauroyl peroxide,
DMAP — 4-dimethylaminopyridine,
DPPF — 1,1′-bis(diphenylphosphino)ferrocene,
ee — enantiomeric excess,
$E_{1/2}$ — half-wave potential,
ΔE_{ST} — singlet–triplet splitting,
ESEEM — electron spin echo envelope modulation,
EWG — electron-withdrawing group,
f — oscillator strength,
Fc — ferrocenyl,
FM — ferromagnetic (coupling),
GC — graft copolymers,
hfac — hexafluoroacetylacetonate,
HFC — hyperfine coupling,
HOMO — highest occupied molecular orbital,
J — exchange coupling parameter,
In — initiator,
k_B — Boltzmann constant,
LDA — lithium diisopropylamide,
LED — light-emitting diode,
LUMO — lowest unoccupied molecular orbital,
M — magnetization,
m-CPBA — *m*-chloroperoxybenzoic acid,
m_s — spin quantum number,
MCP — α-methylcyclopropyl,
MEM — 2-methoxyethoxymethyl,
MO — molecular orbital,
Naph — naphthyl,
NMO — *N*-methylmorpholine *N*-oxide,
NMP — *N*-methylpyrrolidone,
NTOs — natural transition orbitals,
Ox — oxidants,
pin — pinacolate,
PINO — phthalimide *N*-oxide,
PMP — 1,1,2,3,3-pentamethylenepropane,
PVDF — polyvinylidene fluoride
Py — pyridyl,
Red — reducing agent,
rt — room temperature,
SHE — standard hydrogen electrode,
SOMO — singly occupied molecular orbital,
T_C — Curie temperature,
T_1 — spin–spin relaxation time,
T_2 — spin–lattice relaxation time,
T_m — spin echo dephasing time,
TBA — tetra-n-butylammonium,
TBDMS — *tert*-butyldimethylsilyl,
TEMPO — (2,2,6,6-tetramethylpiperidin-1-yl)oxyl,
Tf — trifluoromethanesulfonyl (triflyl),
TFSI — bis(trifluoro methanesulfonyl)imide,
Th — thienyl,
TMEDA — tetramethylethylenediamine,
TMM — trimethylenemethane,
T_N — Néel temperature,
TPAP — tetra-n-propylammonium perruthenate,
TREPR — time-resolved electron paramagnetic resonance,
Ts — *p*-toluenesulfonyl (tosyl),
U_{eff} — effective activation barrier,
XPhos — 2-dicyclohexylphosphino-2′,4′,6′-triisopropylbiphenyl,
$\Delta^{(n)}$ — magnetization reversal barriers,
ε — extinction coefficient,
μ_{eff} — effective magnetic moment,
τ_0 — pre-exponential factor of the Arrhenius equation,
χ — magnetic susceptibility.

8. References

1. H.Iwamura. *Polyhedron*, **66**, 3 (2013)
2. M.Gomberg. *J. Am. Chem. Soc.*, **22**, 757 (1900)
3. *Stable Radicals: Fundamentals and Applied Aspects of Odd-Electron Compounds*. (Ed. R.G.Hicks). (Chichester: Wiley, 2010)

4. R.Toba, H.Gotoh, K.Sakakibara. *Org. Lett.*, **16**, 3868 (2014)
5. R.Amorati, M.Lucarini, V.Mugnaini, G.F.Pedulli, F.Minisci, F.Recupero, F.Fontana, P.Astolfi, L.Greci. *J. Org. Chem.*, **68**, 1747 (2003)
6. N.Zhang, S.R.Samanta, B.M.Rosen, V.Percec. *Chem. Rev.*, **114**, 5848 (2014)
7. D.Gigmes, S.R.A.Marque. In *Encyclopedia of Radicals in Chemistry, Biology and Materials*. (Eds C.Chatgilialoglu, A.Studer). (Chichester: Wiley, 2012). P. 1813
8. C.J.Hawker, A.W.Bosman, E.Harth. *Chem. Rev.*, **101**, 3661 (2001)
9. M.V.Edeleva, S.R.A.Marque, E.G.Bagryanskaya. *Russ. Chem. Rev.*, **87**, 328 (2018)
10. H.V.-T.Nguyen, Q.Chen, J.T.Paletta, P.Harvey, Y.Jiang, H.Zhang, M.D.Boska, M.F.Ottaviani, A.Jasanoff, A.Rajca, J.A.Johnson. *ACS Cent. Sci.*, **3**, 800 (2017)
11. V.V.Khramtsov. *Antioxid. Redox Signal.*, **28**, 1365 (2018)
12. D.Gatteschi. *Adv. Mater.*, **6**, 635 (1994)
13. W.Fujita. *Science*, **286**, 261 (1999)
14. *Magnetic Properties of Organic Materials*. (Ed. P.M.Lahti). (New York: Marcel Dekker, 1999)
15. *Magnetism: Molecules to Materials*. Vols 1 – 5. (Eds J.S.Miller, M.Drillon). (Weinheim: Wiley-VCH, 2001 – 2005)
16. E.V.Tretyakov, V.I.Ovcharenko. *Russ. Chem. Rev.*, **78**, 971 (2009)
17. Yu.A.Ten, N.M.Troshkova, E.V.Tretyakov. *Russ. Chem. Rev.*, **89**, 693 (2020)
18. W.L.Hubbell, A.Gross, R.Langen, M.A.Lietzow. *Curr. Opin. Struct. Biol.*, **8**, 649 (1998)
19. G.Fanucci, D.Cafiso. *Curr. Opin. Struct. Biol.*, **16**, 644 (2006)
20. G.Jeschke, Y.Polyhach. *Phys. Chem. Chem. Phys.*, **9**, 1895 (2007)
21. E.G.Bagryanskaya, O.A.Krumkacheva, M.V.Fedin, S.R.A.Marque. *Methods Enzymol.*, **563**, 365 (2015)
22. G.Audran, S.R.A.Marque, P.Mellet. *Acc. Chem. Res.*, **53**, 2828 (2020)
23. T.Janoschka, M.D.Hager, U.S.Schubert. *Adv. Mater.*, **24**, 6397 (2012)
24. T.Suga, H.Ohshiro, S.Sugita, K.Oyaizu, H.Nishide. *Adv. Mater.*, **21**, 1627 (2009)
25. R.Gaudenzi, E.Burzurí, D.Reta, I.de P.R.Moreira, S.T.Bromley, C.Rovira, J.Veciana, H.S.J.van der Zant. *Nano Lett.*, **16**, 2066 (2016)
26. R.Frisenda, R.Gaudenzi, C.Franco, M.Mas-Torrent, C.Rovira, J.Veciana, I.Alcon, S.T.Bromley, E.Burzurí, H.S.J.van der Zant. *Nano Lett.*, **15**, 3109 (2015)
27. D.Maspoch, D.Ruiz-Molina, J.Veciana. *J. Mater. Chem.*, **14**, 2713 (2004)
28. D.Maspoch, N.Domingo, D.Ruiz-Molina, K.Wurst, G.Vaughan, J.Tejada, C.Rovira, J.Veciana. *Angew. Chem., Int. Ed.*, **43**, 1828 (2004)
29. A.Rajca, S.Utamapanya. *J. Org. Chem.*, **57**, 1760 (1992)
30. H.Mei, J.Han, S.White, G.Butler, V.A.Soloshonok. *J. Fluorine Chem.*, **227**, 109370 (2019)
31. K.Goto, T.Kubo, K.Yamamoto, K.Nakasuji, K.Sato, D.Shiomi, T.Takui, M.Kubota, T.Kobayashi, K.Yakusi, J.Ouyang. *J. Am. Chem. Soc.*, **121**, 1619 (1999)
32. Y.Morita, T.Ohba, N.Haneda, S.Maki, J.Kawai, K.Hatanaka, K.Sato, D.Shiomi, T.Takui, K.Nakasuji. *J. Am. Chem. Soc.*, **122**, 4825 (2000)
33. V.Tormyshev, A.Chubarov, O.Krumkacheva, D.Trukhin, O.Rogozhnikova, A.Spitsina, A.Kuzhelev, V.Koval, M.Fedin, T.Godovikova, M.Bowman, E.G.Bagryanskaya. *Chem. – Eur. J.*, **26**, 2705 (2020)
34. M.R.Geraskina, A.T.Buck, A.H.Winter. *J. Org. Chem.*, **79**, 7723 (2014)
35. J.Back, J.Park, Y.Kim, H.Kang, Y.Kim, M.J.Park, K.Kim, E.Lee. *J. Am. Chem. Soc.*, **139**, 15300 (2017)
36. K.Kato, K.Furukawa, A.Osuka. *Angew. Chem., Int. Ed.*, **57**, 9491 (2018)
37. G.P.Yong, C.F.Li, Y.Z.Li, S.W.Luo. *Chem. Commun.*, **46**, 3194 (2010)
38. K.Lekin, H.Phan, S.M.Winter, J.W.L.Wong, A.A.Leitch, D.Laniel, W.Yong, R.A.Secco, J.S.Tse, S.Desgreniers, P.A.Dube, M.Shatruk, R.T.Oakley. *J. Am. Chem. Soc.*, **136**, 8050 (2014)
39. D.Gatteschi, P.Carretta, A.Lascialfari. *Physica B: Condens. Matter*, **289 – 290**, 94 (2000)
40. Patent WO 2010121900 (2010)
41. H.Quast, G.Philipp, K.-H.Ross, U.M.Doht. *Eur. J. Org. Chem.*, 1891 (2011)
42. P.Kaszynski. *Molecules*, **9**, 716 (2004)
43. N.M.Gallagher, J.J.Bauer, M.Pink, S.Rajca, A.Rajca. *J. Am. Chem. Soc.*, **138**, 9377 (2016)
44. Y.Homma, A.Okazawa, T.Ishida. *Tetrahedron Lett.*, **54**, 3120 (2013)
45. S.Suzuki, T.Furui, M.Kuratsu, M.Kozaki, D.Shiomi, K.Sato, T.Takui, K.Okada. *J. Am. Chem. Soc.*, **132**, 15908 (2010)
46. E.V.Tretyakov, S.E.Tolstikov, G.V.Romanenko, A.S.Bogomyakov, D.V.Stass, A.G.Maryasov, N.P.Gritsan, V.I.Ovcharenko. *Russ. Chem. Bull., Int. Ed.*, **60**, 2608 (2011)
47. S.Suzuki, T.Wada, R.Tanimoto, M.Kozaki, D.Shiomi, K.Sugisaki, K.Sato, T.Takui, Y.Miyake, Y.Hosokoshi, K.Okada. *Angew. Chem., Int. Ed.*, **55**, 10791 (2016)
48. W.Wang, L.Wang, S.Chen, W.Yang, Z.Zhang, X.Wang. *Sci. China Chem.*, **61**, 300 (2018)
49. W.Wang, C.Chen, C.Shu, S.Rajca, X.Wang, A.Rajca. *J. Am. Chem. Soc.*, **140**, 7820 (2018)
50. O.A.Levitskiy, D.B.Eremin, A.V.Bogdanov, T.V.Magdesieva. *Eur. J. Org. Chem.*, 4726 (2017)
51. G.M.Coppinger. *J. Am. Chem. Soc.*, **79**, 501 (1957)
52. N.O.Chalkov, V.K.Cherkasov, G.A.Abakumov, A.G.Starikov, V.A.Kuropatov. *Beilstein J. Org. Chem.*, **12**, 2450 (2016)
53. N.O.Chalkov, V.K.Cherkasov, G.A.Abakumov, G.V.Romanenko, S.Yu.Ketkov, I.V.Smolyaninov, A.G.Starikov, V.A.Kuropatov. *Eur. J. Org. Chem.*, 4571 (2014)
54. M.Kuratsu, S.Suzuki, M.Kozaki, D.Shiomi, K.Sato, T.Takui, T.Kanzawa, Y.Hosokoshi, X.Lan, Y.Miyazaki, A.Inaba, K.Okada. *Chem. – Asian J.*, **7**, 1604 (2012)
55. G.I.Likhtenshtein. *Nitroxides. Brief History, Fundamentals, and Recent Developments*. (Switzerland: Springer Nature, 2020); https://doi.org/10.1007/978-3-030-34822-9
56. J.Naganuma, Y.Yamazaki, H.Gotoh. *Struct. Chem.*, **30**, 2085 (2019)
57. Y.Yamazaki, J.Naganuma, H.Gotoh. *Sci. Rep.*, **9**, 20339 (2019)
58. F.Troiani, M.Affronte. *Chem. Soc. Rev.*, **40**, 3119 (2011)

59. Z.Wang, J.Zhao, A.Barbon, A.Toffoletti, Y.Liu, Y.An, L.Xu, A.Karatay, H.G.Yaglioglu, E.A.Yildiz, M.Hayvali. *J. Am. Chem. Soc.*, **139**, 7831 (2017)
60. J.Zhao, W.Wu, J.Sun, S.Guo. *Chem. Soc. Rev.*, **42**, 5323 (2013)
61. S.V.Chapyshev, D.V.Korchagin, E.Ya.Misochko. *Russ. Chem. Rev.*, **90**, 39 (2021)
62. A.Rajca. In *Nitroxides: Synthesis, Properties and Applications*. (Eds O.Ouari, D.Gigmes). (London: Royal Society of Chemistry, 2021). P. 359
63. H.G.Aurich, K.Hahn, K.Stork. *Angew. Chem., Int. Ed. Engl.*, **14**, 551 (1975)
64. H.G.Aurich, O.Bubenheim, W.Kessler, K.D.Mogendorf. *J. Org. Chem.*, **53**, 4997 (1988)
65. A.Studer, T.Vogler. In *Science of Synthesis*. (Ed. D.Enders). (Stuttgart: Georg Thieme Verlag, 2009). P. 845
66. A.V.Gushchin, O.S.Kalistratova, A.I.Maleeva, V.A.Dodonov, D.Yu.Kosov, D.N.Emel'yanov, V.A.Kuropatov. *Russ. J. Gen. Chem.*, **87**, 1547 (2017)
67. J.A.Pedersen, K.Torssell, J.Roustesuo, J.Virtanen, J.Koskikallio, S.Kachi. *Acta Chem. Scand.*, **25**, 3151 (1971)
68. J.Goldman, T.E.Petersen, K.Torssell, J.Becher. *Tetrahedron*, **29**, 3833 (1973)
69. M.Baskett, P.M.Lahti, A.Paduan-Filho, N.F.Oliveira. *Inorg. Chem.*, **44**, 6725 (2005)
70. N.Roques, P.Gerbier, U.Schatzschneider, J.-P.Sutter, P.Guionneau, J.Vidal-Gancedo, J.Veciana, E.Rentschler, C.Guérin. *Chem. – Eur. J.*, **12**, 5547 (2006)
71. T.Shimada, T.Ishida, T.Nogami. *Polyhedron*, **24**, 2593 (2005)
72. T.Sawai, K.Sato, T.Ise, D.Shiomi, K.Toyota, Y.Morita, T.Takui. *Angew. Chem., Int. Ed.*, **47**, 3988 (2008)
73. S.Sasaki, K.Kato, M.Yoshifuji. *Bull. Chem. Soc. Jpn.*, **80**, 1791 (2007)
74. C.Uerpmann, B.J.L.Henner, C.Guérin, F.Carré. *J. Organomet. Chem.*, **690**, 197 (2005)
75. Y.Numata, K.Inoue, N.Baranov, M.Kurmoo, K.Kikuchi. *J. Am. Chem. Soc.*, **129**, 9902 (2007)
76. L.Marx, A.Rassat. *Tetrahedron Lett.*, **56**, 1762 (2015)
77. K.Osanai, A.Okazawa, T.Nogami, T.Ishida. *J. Am. Chem. Soc.*, **128**, 14008 (2006)
78. M.Baskett, P.M.Lahti. *Polyhedron*, **24**, 2645 (2005)
79. O.B.Borobia, P.Guionneau, H.Heise, F.H.Köhler, L.Ducasse, J.Vidal-Gancedo, J.Veciana, S.Golhen, L.Ouahab, J.-P.Sutter. *Chem. – Eur. J.*, **11**, 128 (2005)
80. Y.Miyazaki, A.Inaba, M.Sorai, P.S.Taylor, P.M.Lahti. *J. Phys. Chem. B*, **112**, 8144 (2008)
81. T.Kanetomo, M.Yasui, T.Ishida. *Polyhedron*, **136**, 30 (2017)
82. S.Karasawa, D.Yoshihara, N.Watanabe, M.Nakano, N.Koga. *Dalton Trans.*, 1418 (2008)
83. A.Okazawa, T.Nogami, T.Ishida. *Polyhedron*, **28**, 1917 (2009)
84. F.Iwahori, T.Suzuki, K.Kato. *Heterocycles*, **87**, 2031 (2013)
85. A.Okazawa, Y.Nagaichi, T.Nogami, T.Ishida. *Inorg. Chem.*, **47**, 8859 (2008)
86. N.Roques, P.Gerbier, I.Imaz, P.Guionneau, J.-P.Sutter. *Acta Crystallogr., Sect. C*, **62**, m386 (2006)
87. N.Koizumi, T.Ishida. *Tetrahedron Lett.*, **58**, 2804 (2017)
88. T.Sadhukhan, S.Hansda, I.A.Latif, S.N.Datta. *J. Phys. Chem. A*, **117**, 13151 (2013)
89. E.Ali, A.S.Roy, S.N.Datta. *J. Phys. Chem. A*, **111**, 5523 (2007)
90. M.Jung, A.Sharma, D.Hinderberger, S.Braun, U.Schatzschneider, E.Rentschler. *Inorg. Chem.*, **48**, 7244 (2009)
91. T.Yoshitake, T.Ishida. *Chem. Lett.*, **45**, 391 (2016)
92. Z.Delen, P.M.Lahti. *J. Org. Chem.*, **71**, 9341 (2006)
93. K.Das, M.Pink, S.Rajca, A.Rajca. *J. Am. Chem. Soc.*, **128**, 5334 (2006)
94. Z.An, J.Zhang, R.Wang, N.Koga. *Polyhedron*, **26**, 2126 (2007)
95. K.Takeda, Y.Yoshida, Y.Inanaga, T.Kawae, D.Shiomi, T.Ise, M.Kozaki, K.Okada, K.Sato, T.Takui. *Phys. Rev. B*, **72**, 024435 (2005)
96. H.Murata, M.Baskett, H.Nishide, P.M.Lahti. *Langmuir*, **30**, 4026 (2014)
97. Y.Teki, S.Miyamoto, K.Koide. *Phys. Chem. Chem. Phys.*, **17**, 31646 (2015)
98. M.T.Colvin, A.L.Smeigh, E.M.Giacobbe, S.M.M.Conron, A.B.Ricks, M.R.Wasielewski. *J. Phys. Chem. A*, **115**, 7538 (2011)
99. A.Ueda, K.Ogasawara, S.Nishida, K.Fukui, K.Sato, T.Takui, K.Nakasuji, Y.Morita. *Aust. J. Chem.*, **63**, 1627 (2010)
100. P.Ravat, T.Marszalek, W.Pisula, K.Müllen, M.Baumgarten. *J. Am. Chem. Soc.*, **136**, 12860 (2014)
101. E.M.Giacobbe, Q.Mi, M.T.Colvin, B.Cohen, C.Ramanan, A.M.Scott, S.Yeganeh, T.J.Marks, M.A.Ratner, M.R.Wasielewski. *J. Am. Chem. Soc.*, **131**, 3700 (2009)
102. D.M.Gardner, H.-F.Chen, M.D.Krzyaniak, M.A.Ratner, M.R.Wasielewski. *J. Phys. Chem. A*, **119**, 8040 (2015)
103. H.Nishimaki, S.Mashiyama, M.Yasui, T.Nogami, T.Ishida. *Chem. Mater.*, **18**, 3602 (2006)
104. H.Nishimaki, T.Ishida. *J. Am. Chem. Soc.*, **132**, 9598 (2010)
105. T.Konno, H.Kudo, T.Ishida. *J. Mater. Chem. C*, **3**, 7813 (2015)
106. G.Spagnol, K.Shiraishi, S.Rajca, A.Rajca. *Chem. Commun.*, 5047 (2005)
107. S.Osada, N.Hirosawa, T.Ishida. *Tetrahedron*, **68**, 6193 (2012)
108. P.Ravat, M.Baumgarten. *Phys. Chem. Chem. Phys.*, **17**, 983 (2015)
109. P.Ravat, Y.Teki, Y.Ito, E.Gorelik, M.Baumgarten. *Chem. – Eur. J.*, **20**, 12041 (2014)
110. P.Ravat, M.Baumgarten. *J. Phys. Chem. B*, **119**, 13649 (2015)
111. X.Hu, Y.Li, H.Yang, Y.Luo. *Tetrahedron Lett.*, **47**, 7463 (2006)
112. A.Rajca, M.Pink, T.Rojsajjakul, K.Lu, H.Wang, S.Rajca. *J. Am. Chem. Soc.*, **125**, 8534 (2003)
113. L.Kröck, A.Shivanyuk, D.B.Goodin, J.Rebek Jr. *Chem. Commun.*, 272 (2004)
114. T.Sawai, K.Sato, D.Shiomi, K.Toyota, Q.Wang, J.-S.Wang, Y.Li, G.-S.Wu, T.Takui. *Appl. Magn. Reson.*, **41**, 337 (2011)
115. X.Hu, H.Yang, Y.Li. *Spectrochim. Acta, Part A*, **70**, 439 (2008)
116. A.Rajca, S.Mukherjee, M.Pink, S.Rajca. *J. Am. Chem. Soc.*, **128**, 13497 (2006)
117. A.Olankitwanit, V.Kathirvelu, S.Rajca, G.R.Eaton, S.S.Eaton, A.Rajca. *Chem. Commun.*, **47**, 6443 (2011)

118. Y.Omokawa, S.Hatano, M.Abe. *J. Phys. Org. Chem.*, **28**, 116 (2015)
119. A.Okazawa, T.Nogami, T.Ishida. *Chem. Mater.*, **19**, 2733 (2007)
120. Z.Zhu, S.Karasawa, N.Koga. *Inorg. Chem.*, **44**, 6004 (2005)
121. S.Kanegawa, S.Karasawa, M.Nakano, N.Koga. *Bull. Chem. Soc. Jpn.*, **79**, 1372 (2006)
122. R.Murakami, T.Ishida, S.Yoshii, H.Nojiri. *Dalton Trans.*, **42**, 13968 (2013)
123. K.Koide, T.Ishida. *Inorg. Chem. Commun.*, **14**, 194 (2011)
124. K.Koide, T.Ishida. *Polyhedron*, **30**, 3034 (2011)
125. T.Konno, K.Koide, T.Ishida. *Chem. Commun.*, **49**, 5156 (2013)
126. Y.Numata, K.Inoue. *J. Magn. Magn. Mater.*, **310**, 1847 (2007)
127. S.Ito, T.Ishida. *Chem. Lett.*, **49**, 1062 (2020)
128. P.M.Lahti, M.Baskett, L.M.Field, M.C.Morón, F.Palacio, A.Paduan-Filho, N.F.Oliveira. *Inorg. Chim. Acta*, **361**, 3697 (2008)
129. M.Baskett, A.Paduan-Filho, N.F.Oliveira, A.Chandrasekaran, J.T.Mague, P.M.Lahti. *Inorg. Chem.*, **50**, 5060 (2011)
130. L.M.Field, M.C.Morón, P.M.Lahti, F.Palacio, A.Paduan-Filho, N.F.Oliveira. *Inorg. Chem.*, **45**, 2562 (2006)
131. H.Ogawa, K.Mori, K.Murashima, S.Karasawa, N.Koga. *Inorg. Chem.*, **55**, 717 (2016)
132. M.V.Fedin, I.Yu.Drozdyuk, E.V.Tretyakov, S.E.Tolstikov, V.I.Ovcharenko, E.G.Bagryanskaya. *Appl. Magn. Reson.*, **41**, 383 (2011)
133. I.Yu.Drozdyuk, S.E.Tolstikov, E.V.Tretyakov, S.L.Veber, V.I.Ovcharenko, R.Z.Sagdeev, E.G.Bagryanskaya, M.V.Fedin. *J. Phys. Chem. A*, **117**, 6483 (2013)
134. E.V.Tretyakov, S.E.Tolstikov, A.O.Suvorova, A.V.Polushkin, G.V.Romanenko, A.S.Bogomyakov, S.L.Veber, M.V.Fedin, D.V.Stass, E.Reijerse, W.Lubitz, E.M.Zueva, V.I.Ovcharenko. *Inorg. Chem.*, **51**, 9385 (2012)
135. J.A.Bogart, H.B.Lee, M.A.Boreen, M.Jun, E.J.Schelter. *J. Org. Chem.*, **78**, 6344 (2013)
136. A.Okazawa, T.Nogami, T.Ishida. *Polyhedron*, **26**, 1965 (2007)
137. A.Okazawa, Y.Terakado, T.Ishida, N.Kojima. *New J. Chem.*, **42**, 17874 (2018)
138. H.Kawakami, A.Tonegawa, T.Ishida. *Dalton Trans.*, **45**, 1306 (2016)
139. Z.Zhu, M.Mikuriya. *Chem. Lett.*, **37**, 400 (2008)
140. M.Aso, T.Ikeno, K.Norihisa, M.Tanaka, N.Koga, H.Suemune. *J. Org. Chem.*, **66**, 3513 (2001).
141. T.Kaneko, M.Aso, N.Koga, H.Suemune. *Org. Lett.*, **7**, 303 (2005)
142. M.Aso, Y.Matsui, B.Yang, M.Sasagaki, D.Okado, K.Usui, N.Koga, H.Suemune. *Tetrahedron*, **71**, 5414 (2015)
143. M.Aso, J.W.Mirc, M.Kurita, N.Koga, H.Suemune. *Nucleic Acids Symp. Ser.*, **51**, 163 (2007)
144. M.Aso, M.Kurita, J.W.Mirc, T.Kaneko, Y.Higuchi, N.Koga, H.Suemune. *Nucleic Acids Symp. Ser.*, **52**, 151 (2008)
145. M.Kurita, Y.Higuchi, J.Mirc, S.Matsumoto, K.Usui, H.Suemune, M.Aso. *ChemBioChem*, **17**, 2346 (2016)
146. H.Murata, P.M.Lahti, S.Aboaku. *Chem. Commun.*, 3441 (2008)
147. K.-M.Liu, F.Zhang, X.-F.Duan. *Eur. J. Org. Chem.*, 6152 (2013)
148. C.Agawa, K.Otsuka, M.Minoura, Y.Mazaki, G.Yamamoto. *Bull. Chem. Soc. Jpn.*, **77**, 2273 (2004)
149. G.Yamamoto, K.Kuwahara, K.Inoue. *Chem. Lett.*, **24**, 351 (1995)
150. E.Tretyakov, P.Fedyushin, E.Panteleeva, L.Gurskaya, T.Rybalova, A.Bogomyakov, E.Zaytseva, M.Kazantsev, I.Shundrina, V.Ovcharenko. *Molecules*, **24**, 4493 (2019)
151. Patent RU 2736262 (2020)
152. P.Fedyushin, T.Rybalova, N.Asanbaeva, E.Bagryanskaya, A.Dmitriev, N.Gritsan, M.Kazantsev, E.Tretyakov. *Molecules*, **25**, 2701 (2020)
153. L.V.Politanskaya, P.A.Fedyushin, T.V.Rybalova, A.S.Bogomyakov, N.B.Asanbaeva, E.V.Tretyakov. *Molecules*, **25**, 5427 (2020)
154. A.R.Forrester, R.H.Thomson. *Nature (London)*, **203**, 74 (1964)
155. A.Calder, A.R.Forrester. *J. Chem. Soc., Chem. Commun.*, 682 (1967)
156. T.V.Magdesieva, O.A.Levitskiy. *Russ. Chem. Rev.*, **87**, 707 (2018)
157. O.A.Levitskiy, D.A.Dulov, A.V.Bogdanov, Y.K.Grishin, S.E.Nefedov, T.V.Magdesieva. *Chem. – Eur. J.*, **26**, 6793 (2020)
158. S.Kanaya, M.Kozaki, D.Shiomi, K.Sato, T.Takui, K.Okada. *Synth. Met.*, **121**, 1808 (2001)
159. S.Kanegawa, S.Karasawa, M.Maeyama, M.Nakano, N.Koga. *J. Am. Chem. Soc.*, **130**, 3079 (2008)
160. E.Flesia, J.-M.Surzur, P.Tordo. *Org. Magn. Reson.*, **11**, 123 (1978)
161. A.R.Forrester. In *Organic N-Centered Radicals and Nitroxide Radicals*. (Eds H.Fischer, K.-H.Hellwege). (*Subvol. C1 of Vol. 9 Magnetic Properties of Free Radicals of Landolt-Börnstein — Group II Molecules and Radicals*). (Berlin, Heidelberg: Springer-Verlag, 1979). Pt. 1
162. I.B.Krylov, M.O.Kompanets, K.V.Novikova, I.O.Opeida, O.V.Kushch, B.N.Shelimov, G.I.Nikishin, D.O.Levitsky, A.O.Terent'ev. *J. Phys. Chem. A*, **120**, 68 (2016)
163. C.Annunziatini, M.F.Gerini, O.Lanzalunga, M.Lucarini. *J. Org. Chem.*, **69**, 3431 (2004)
164. F.R.Stermitz, D.W.Neiswander. *J. Am. Chem. Soc.*, **95**, 2630 (1973)
165. R.Braslau, J.R.Axon, B.Lee. *Org. Lett.*, **2**, 1399 (2000)
166. P.F.Alewood, S.A.Hussain, T.C.Jenkins, M.J.Perkins, A.H.Sharma, N.P.Y.Siew, P.Ward. *J. Chem. Soc., Perkin Trans. 1*, 1066 (1978)
167. P.F.Alewood, I.C.Calder, R.L.Richardson. *Synthesis*, 121 (1981)
168. M.G.Capraro, P.Franchi, O.Lanzalunga, A.Lapi, M.Lucarini. *J. Org. Chem.*, **79**, 6435 (2014)
169. D.Griller, M.J.Perkins. *J. Am. Chem. Soc.*, **102**, 1354 (1980)
170. J.Kulys, H.-J.Deussen, K.Krikstopaitis, R.Lolck, P.Schneider, A.Ziemys. *Eur. J. Org. Chem.*, 3475 (2001)
171. M.Nechab, D.N.Kumar, C.Philouze, C.Einhorn, J.Einhorn. *Angew. Chem., Int. Ed.*, **46**, 3080 (2007)
172. C.Einhorn, J.Einhorn, C.Marcadal-Abbadi, J.-L.Pierre. *J. Org. Chem.*, **64**, 4542 (1999)
173. D.J.Brooks, M.J.Perkins, S.L.Smith, D.M.Goodall, D.K.Lloyd. *J. Chem. Soc., Perkin Trans. 2*, 393 (1992)
174. M.J.Perkins, C.Berti, D.J.Brooks, L.Grierson, J.A.-M.Grimes, T.C.Jenkins, S.L.Smith. *Pure Appl. Chem.*, **62**, 195 (1990)

175. A.O.Terent'ev, I.B.Krylov, M.Yu.Sharipov, Z.M.Kazanskaya, G.I.Nikishin. *Tetrahedron*, **68**, 10263 (2012)
176. I.B.Krylov, S.A.Paveliev, B.N.Shelimov, B.Lokshin, I.A.Garbuzova, V.A.Tafeenko, V.V.Chernyshev, A.S.Budnikov, G.I.Nikishin, A.O.Terent'ev. *Org. Chem. Front.*, **4**, 1947 (2017)
177. S.A.Hussain, T.C.Jenkins, M.J.Perkins, N.P.Y.Siew. *J. Chem. Soc., Perkin Trans. 1*, 2803 (1979)
178. V.A.Schmidt, E.J.Alexanian. *Angew. Chem., Int. Ed.*, **49**, 4491 (2010)
179. V.A.Schmidt, E.J.Alexanian. *Chem. Sci.*, **3**, 1672 (2012)
180. V.A.Schmidt, E.J.Alexanian. *J. Am. Chem. Soc.*, **133**, 11402 (2011)
181. R.K.Quinn, V.A.Schmidt, E.J.Alexanian. *Chem. Sci.*, **4**, 4030 (2013)
182. B.C.Giglio, E.J.Alexanian. *Org. Lett.*, **16**, 4304 (2014)
183. B.C.Giglio, V.A.Schmidt, E.J.Alexanian. *J. Am. Chem. Soc.*, **133**, 13320 (2011)
184. Q.Lu, Z.Liu, Y.Luo, G.Zhang, Z.Huang, H.Wang, C.Liu, J.T.Miller, A.Lei. *Org. Lett.*, **17**, 3402 (2015)
185. B.Wei, D.Xie, S.Lai, Y.Jiang, H.Fu, D.Wei, B.Han. *Angew. Chem., Int. Ed.*, **133**, 3219 (2021)
186. A.O.Terent'ev, I.B.Krylov, V.P.Timofeev, Z.A.Starikova, V.M.Merkulova, A.I.Ilovaisky, G.I.Nikishin. *Adv. Synth. Catal.*, **355**, 2375 (2013)
187. V.A.Reznikov, I.V.Ovcharenko, N.V.Pervukhina, V.N.Ikorskii, A.Grand, V.I.Ovcharenko. *Chem. Commun.*, 539 (1999)
188. V.A.Reznikov, L.B.Volodarsky, T.V.Rybalova, Yu.V.Gatilov. *Russ. Chem. Bull., Int. Ed.*, **49**, 106 (2000)
189. V.A.Reznikov, L.A.Vishnivetskaya, L.B.Volodarskii. *Russ. Chem. Bull., Engl. Transl.*, **42**, 1547 (1993)
190. V.A.Reznikov, L.B.Volodarsky. *Russ. Chem. Bull.*, **45**, 1699 (1996)
191. E.V.Tretyakov, A.V.Tkachev, T.V.Rybalova, Yu.V.Gatilov, D.W.Knight, S.F.Vasilevsky. *Tetrahedron*, **56**, 10075 (2000)
192. D.G.Mazhukin, A.Ya.Tikhonov, V.A.Reznikov, L.B.Volodarsky. *Mendeleev Commun.*, 69 (2000)
193. E.V.Tretyakov, G.V.Romanenko, D.V.Stass, A.V.Mareev, A.S.Medvedeva, V.I.Ovcharenkoa. *Russ. Chem. Bull.*, **57**, 601 (2008)
194. V.A.Reznikov, G.I.Roshchupkina, D.G.Mazhukin, P.A.Petrov, S.A.Popov, S.V.Fokin, G.V.Romanenko, T.V.Rybalova, Yu.V.Gatilov, Yu.G.Shvedenkov, I.G.Irtegova, L.A.Shundrin, V.I.Ovcharenko. *Eur. J. Org. Chem.*, 749 (2004)
195. H.Hashimoto, Y.Inagaki, H.Momma, E.Kwon, W.Setaka. *J. Org. Chem.*, **84**, 11783 (2019)
196. A.Rajca, M.Takahashi, M.Pink, G.Spagnol, S.Rajca. *J. Am. Chem. Soc.*, **129**, 10159 (2007)
197. A.Rajca, K.Shiraishi, S.Rajca. *Chem. Commun.*, 4372 (2009)
198. C.Berti, M.Colonna, L.Greci, L.Marchetti. *Tetrahedron.*, **31**, 1745 (1975)
199. P.Astolfi, L.Greci, P.Stipa, C.Rizzoli, C.Ysacco, M.Rollet, L.Autissier, A.Tardy, Y.Guillaneuf, D.Gigmes. *Polym. Chem.*, **4**, 3694 (2013)
200. G.Tommasi, P.Bruni, L.Greci, P.Sgarabotto, L.Righi, R.Petrucci, *J. Chem. Soc., Perkin Trans. 2*, 2123 (1999)
201. M.Beyer, J.Fritscher, E.Feresin, O.Schiemann. *J. Org. Chem.*, **68**, 2209 (2003)
202. M.Nakagawa, T.Ishida, M.Suzuki, D.Hashizume, M.Yasui, F.Iwasaki, T.Nogami. *Chem. Phys. Lett.*, **302**, 125 (1999)
203. H.Oka, H.Kouno, H.Tanaka. *J. Mater. Chem.*, **17**, 1209 (2007)
204. R.Suzuki, R.Tada, Y.Miura, N.Yoshioka. *J. Mol. Struct.*, **1106**, 399 (2016)
205. O.A.Levitskiy, D.A.Dulov, A.V.Bogdanov, T.V.Magdesieva. *Eur. J. Org. Chem.*, 6225 (2019)
206. A.Rajca, K.Shiraishi, P.J.Boratyński, M.Pink, M.Miyasaka, S.Rajca. *J. Org. Chem.*, **76**, 8447 (2011)
207. M.Ooishi, M.Seino, R.Imachi, T.Ishida, T.Nogami. *Tetrahedron Lett.*, **43**, 5521 (2002)
208. T.Ishida, M.Ooishi, N.Ishii, H.Mori, T.Nogami. *Polyhedron*, **26**, 1793 (2007)
209. T.Kanetomo, K.Ichihashi, M.Enomoto, T.Ishida. *Org. Lett.*, **21**, 3909 (2019)
210. K.Ichihashi, T.Kanetomo, M.Enomoto, T.Ishida. *Tetrahedron Lett.*, **61**, 152428 (2020)
211. P.Astolfi, P.Stipa. *J. Org. Chem.*, **76**, 9253 (2011)
212. M.Yao, H.Inoue, N.Yoshioka. *Chem. Phys. Lett.*, **402**, 11 (2005)
213. M.Yao, S.Asakura, M.Abe, H.Inoue, N.Yoshioka. *Cryst. Growth Des.*, **5**, 413 (2005)
214. S.M.Winter, A.R.Balo, R.J.Roberts, K.Lekin, A.Assoud, P.A.Dube, R.T.Oakley. C*hem. Commun.*, **49**, 1603 (2013)
215. J.W.LWong, A.Mailman, K.Lekin, S.M.Winter, W.Yong, J.Zhao, S.V.Garimella, J.S.Tse, R.A.Secco, S.Desgreniers, Y.Ohishi, F.Borondics, R.T.Oakley. *J. Am. Chem. Soc.*, **136**, 1070 (2014)
216. P.Vasko, J.Hurmalainen, A.Mansikkamäki, A.Peuronen, A.Mailman, H.M.Tuononen. *Dalton Trans.*, **46**, 16004 (2017)
217. E.Zaytseva, D.Shiomi, Yu.Ten, Yu.V.Gatilov, A.Lomanovich, D.Stass, A.Bogomyakov, A.Yu, K.Sugisaki, K.Sato, T.Takui, E.Bagryanskaya, D.Mazhukin. *J. Phys. Chem. A*, **124**, 2416 (2020)
218. S.A.Amitina, E.V.Zaytseva, N.A.Dmitrieva, A.V.Lomanovich, N.V.Kandalintseva, Yu.A.Ten, I.A.Artamonov, A.F.Markov, D.G.Mazhukin. *Molecules*, **25**, 3118 (2020)
219. Yu.A.Ten, O.G.Salnikov, S.A.Amitina, D.V.Stass, T.V.Rybalova, M.S.Kazantsev, A.S.Bogomyakov, E.A.Mostovich, D.G.Mazhukin. *RSC Adv.*, **8**, 26099 (2018)
220. A.Yu, Yu.Ten, Yu.Gatilov, D.Mazhukin. In *Book of Abstracts of the 3rd International Conference Spin Physics, Spin Chemistry and Spin Technology (SPCT-2018)*. (Novosibirsk, 2018). P. 129
221. A.Zheludev, V.Barone, M.Bonnet, B.Delley, A.Grand, E.Ressouche, P.Rey, R.Subra, J.Schweizer. *J. Am. Chem. Soc.*, **116**, 2019 (1994)
222. F.M.Romero, R.Ziessel, M.Bonnet, Y.Pontillon, E.Ressouche, J.Schweizer, B.Delley, A.Grand, C.Paulsen. *J. Am. Chem. Soc.*, **122**, 1298 (2000)
223. K.Awaga, T.Inabe, U.Nagashima, Y.Maruyama. *J. Chem. Soc., Chem. Commun.*, 1617 (1989)
224. J.Veciana, H.Iwamura. *MRS Bull.*, **25**, 41 (2000)
225. J.H.Osiecki, E.F.Ullman. *J. Am. Chem. Soc.*, **90**, 1078 (1968)
226. E.F.Ullman, J.H.Osiecki, D.G.B.Boocock, R.Darcy. *J. Am. Chem. Soc.*, **94**, 7049 (1972)
227. Patent US 3927019 (1975)

228. K.Doi, T.Ishida, T.Nogami. *Chem. Lett.*, **32**, 544 (2003)
229. A.Paun, I.Zarafu, M.T.Caproiu, P.Ionita. *ARKIVOC*, (iv), 144 (2013)
230. E.Önal, Y.Yerli, B.Cosut, G.Pilet, V.Ahsen, D.Luneau, C.Hirel. *New J. Chem.*, **38**, 4440 (2014)
231. H.Douib, M.Puget, Y.Suffren, F.Pointillart, K.Bernot, B.L.Guennic, O.Cador, A.Gouasmia, L.Ouahab. *Dyes Pigm.*, **145**, 285 (2017)
232. E.Önal, I.Fidan, D.Luneau, C.Hirel. *J. Porphyrins. Phthalocyanines*, **23**, 584 (2019)
233. I.Fidan, D.Luneau, V.Ahsen, C.Hirel. *Chem. – Eur. J.*, **24**, 5359 (2018)
234. L.Gorini, A.Caneschi, S.Menichetti. *Synlett*, 948 (2006)
235. L.Poggini, A.Lunghi, A.Collauto, A.Barbon, L.Armelao, A.Magnani, A.Caneschi, F.Totti, L.Sorace, M.Mannini. *Nanoscale*, **13**, 7613 (2021)
236. R.Kakavandi, S.-A.Savu, A.Caneschi, M.B.Casu. *J. Phys. Chem. C*, **117**, 26675 (2013)
237. S.-A.Savu, I.Biswas, L.Sorace, M.Mannini, D.Rovai, A.Caneschi, T.Chassé, M.B.Casu. *Chem. – Eur. J.*, **19**, 3445 (2013)
238. J.Lee, E.Lee, S.Kim, G.S.Bang, D.A.Shultz, R.D.Schmidt, M.D.E.Forbes, H.Lee. *Angew. Chem., Int. Ed.*, **50**, 4414 (2011)
239. K.Kolanji, M.Baumgarten. *Chem. – Eur. J.*, **26**, 3626 (2020)
240. H.Komatsu, M.M.Matsushita, S.Yamamura, Y.Sugawara, K.Suzuki, T.Sugawara. *J. Am. Chem. Soc.*, **132**, 4528 (2010)
241. H.Han, M.Wang, H.Wang. *New J. Chem.*, **38**, 914 (2014)
242. D.Shiomi, Y.Kanzaki, S.Okada, R.Arima, Y.Miyazaki, A.Inaba, R.Tanaka, K.Sato, T.Takui. *J. Phys. Chem. Lett.*, **2**, 3036 (2011)
243. E.Badetti, V.Lloveras, F.A.Scaramuzzo, K.Wurst, J.Veciana, J.Vidal-Gancedo, G.Licini, C.Zonta. *Dalton Trans.*, **49**, 10011 (2020)
244. M.De Zotti, K.Wright, E.d'Aboville, A.Toffoletti, C.Toniolo, G.Longhi, G.Mazzeo, S.Abbate, F.Formaggio. *J. Org. Chem.*, **82**, 10033 (2017)
245. R.Tanimoto, S.Suzuki, M.Kozaki, D.Shiomi, K.Sato, T.Takui, K.Okada. *Bull. Chem. Soc. Jpn.*, **87**, 314 (2014)
246. X.-Y.Qin, G.-R.Ding, X.-W.Wang, J.Tan, G.-Z.Guo, X.-L.Sun. *J. Chem. Res.*, **2009**, 511 (2009)
247. X.Qin, G.Xiong, Y.Sun, M.-Y.Guo, Y.Ma, Q.Wang, P.Liu, P.Gao, X.Sun. *J. Mol. Struct.*, **989**, 10 (2011)
248. E.V.Tretyakov, A.V.Mareev, M.M.Demina, G.V.Romanenko, D.V.Stass, A.S.Medvedeva, V.I.Ovcharenko. *Russ. Chem. Bull.*, **58**, 1915 (2009)
249. E.Mostovich, Yu.Borozdina, V.Enkelmann, K.Remović-Langer, B.Wolf, M.Lang, M.Baumgarten. *Cryst. Growth Des.*, **12**, 54 (2012)
250. Yu.B.Borozdina, E.Mostovich, V.Enkelmann, B.Wolf, P.T.Cong, U.Tutsch, M.Lang, M.Baumgarten. *J. Mater. Chem. C*, **2**, 6618 (2014)
251. N.Amaya, T.Ono, Y.Oku, H.Yamaguchi, A.Matsuo, K.Kindo, H.Nojiri, F.Palacio, J.Campo, Y.Hosokoshi. *J. Phys. Soc. Jpn.*, **86**, 074706 (2017)
252. P.Ravat, Y.Ito, E.Gorelik, V.Enkelmann, M.Baumgarten. *Org. Lett.*, **15**, 4280 (2013)
253. H.Akpinar, J.A.Schlueter, R.A.A.Cassaro, J.R.Friedman, P.M.Lahti. *Cryst. Growth Des.*, **16**, 4051 (2016)
254. K.Kolanji, L.Postulka, B.Wolf, M.Lang, D.Schollmeyer, M.Baumgarten. *J. Org. Chem.*, **84**, 140 (2019)
255. Z.-X.Xiao, H.Miao, D.Shao, H.-Y.Wei, Y.-Q.Zhang, X.-Y.Wang. *Dalton Trans.*, **47**, 7925 (2018)
256. X.Li, T.Li, L.Tian, Z.Y.Liu, X.G.Wang. *RSC Adv.*, **5**, 74864 (2015)
257. Y.Huang, Z.Xu, S.Jin, C.Li, K.Warncke, F.A.Evangelista, T.Lian, E.Egap. *Chem. Mater.*, **30**, 7840 (2018)
258. D.Wang, Y.Ma, B.Wolf, A.I.Kokorin, M.Baumgarten. *J. Phys. Chem. A*, **122**, 574 (2018)
259. N.Gallagher, H.Zhang, T.Junghoefer, E.Giangrisostomi, R.Ovsyannikov, M.Pink, S.Rajca, M.B.Casu, A.Rajca. *J. Am. Chem. Soc.*, **141**, 4764 (2019)
260. E.Tretyakov, A.Tkacheva, G.Romanenko, A.Bogomyakov, D.Stass, A.Maryasov, E.Zueva, B.Trofimov, V.Ovcharenko. *Molecules*, **25**, 1503 (2020)
261. A.Shimizu, A.Ito, Y.Teki. *Chem. Commun.*, **52**, 2889 (2016)
262. A.Rajca, M.Pink, S.Mukherjee, S.Rajca, K.Das. *Tetrahedron*, **63**, 10731 (2007)
263. E.V.Tretyakov, V.G.Vasil'ev, A.S.Bogomyakov, G.V.Romanenko, M.V.Fedin, I.S.Antipin, S.E.Solov'eva, A.I.Konovalov, R.Z.Sagdeev, V.I.Ovcharenko. *Russ. Chem. Bull.*, **62**, 543 (2013)
264. I.Fidan, E.Önal, Y.Yerli, D.Luneau, V.Ahsen, C.Hirel. *Inorg. Chem.*, **55**, 11447 (2016)
265. K.Maekawa, D.Shiomi, T.Ise, K.Sato, T.Takui. *Org. Biomol. Chem.*, **5**, 1641 (2007)
266. K.Kolanji, P.Ravat, A.S.Bogomyakov, V.I.Ovcharenko, D.Schollmeyer, M.Baumgarten. *J. Org. Chem.*, **82**, 7764 (2017)
267. N.A.Artiukhova, K.Yu.Maryunina, S.V.Fokin, E.V.Tretyakov, G.V.Romanenko, A.V.Polushkin, A.S.Bogomyakov, R.Z.Sagdeev, V.I.Ovcharenko. *Russ. Chem. Bull.*, **62**, 2132 (2013)
268. S.E.Tolstikov, N.A.Artiukhova, G.V.Romanenko, A.S.Bogomyakov, E.M.Zueva, I.Y.Barskaya, M.V.Fedin, K.Yu.Maryunina, E.V.Tretyakov, R.Z.Sagdeev, V.I.Ovcharenko. *Polyhedron*, **100**, 132 (2015)
269. N.A.Artiukhova, G.V.Romanenko, A.S.Bogomyakov, I.Yu.Barskaya, S.L.Veber, M.V.Fedin, K.Yu.Maryunina, K.Inoue, V.I.Ovcharenko. *J. Mater. Chem. C*, **4**, 11157 (2016)
270. V.I.Ovcharenko, S.K.Fokin, G.K.Romanenko, L.V.Korobkov, P.Rey. *Russ. Chem. Bull.*, **48**, 1519 (1999)
271. C.Hirel, K.E.Vostrikova, J.Pécaut, V.I.Ovcharenko, P.Rey. *Chem. – Eur. J.*, **7**, 2007 (2001)
272. P.Hui, K.Arif, R.Chandrasekar. *Org. Biomol. Chem.*, **10**, 2439 (2012)
273. S.Suzuki, N.Itoh, K.Furuichi, M.Kozaki, D.Shiomi, K.Sato, T.Takui, H.Ohi, S.Itoh, K.Okada. *Chem. Lett.*, **40**, 22 (2011)
274. E.V.Tretyakov, G.V.Romanenko, S.E.Tolstikov, V.I.Ovcharenko. *J. Struct. Chem.*, **54**, 560 (2013)
275. E.V.Tretyakov, R.Yu.Peshkov, E.V.Panteleeva, A.S.Scrypnik, D.V.Stass, G.V.Romanenko, V.I.Ovcharenko. *Tetrahedron Lett.*, **57**, 2327 (2016)
276. E.V.Tretyakov, S.E.Tolstikov, G.V.Romanenko, A.S.Bogomyakov, D.V.Stass, M.K.Kadirov, K.V.Holin, O.G.Sinyashin, V.I.Ovcharenko. *Polyhedron*, **30**, 3232 (2011)
277. V.Romanov, A.Vorob'ev, I.Bagryanskaya, D.Parkhomenko, E.Tretyakov. *Aust. J. Chem.*, **70**, 1317 (2017)

278. D.E.Votkina, P.V.Petunin, S.I.Zhivetyeva, I.Yu.Bagryanskaya, M.N.Uvarov, M.S.Kazantsev, M.E.Trusova, E.V.Tretyakov, P.S.Postnikov. *Eur. J. Org. Chem.*, 1996 (2020)
279. P.V.Petunin, T.V.Rybalova, M.E.Trusova, M.N.Uvarov, M.S.Kazantsev, E.A.Mostovich, L.Postulka, P.Eibisch, B.Wolf, M.Lang, P.S.Postnikov, M.Baumgarten. *ChemPlusChem*, **85**, 159 (2020)
280. S.E.Tolstikov, E.V.Tretyakov, G.V.Romanenko, A.S.Bogomyakov, R.Z.Sagdeev, V.I.Ovcharenko. *Russ. Chem. Bull.*, **62**, 223 (2013)
281. V.Lloveras, E.Badetti, J.Veciana, J.Vidal-Gancedo. *Nanoscale*, **8**, 5049 (2016)
282. R.K.Strizhakov, E.V.Tretyakov, A.S.Medvedeva, V.V.Novokshonov, V.G.Vasiliev, V.I.Ovcharenko, O.A.Krumkacheva, M.V.Fedin, E.G.Bagryanskaya. *Appl. Magn. Reson.*, **45**, 1087 (2014)
283. C.Stroh, M.Mayor, C.von Hanisch, P.Turek. *Chem. Commun.*, 2050 (2004)
284. E.D.Piazza, A.Merhi, L.Norel, S.Choua, P.Turek, S.Rigaut. *Inorg. Chem.*, **54**, 6347 (2015)
285. E.V.Tretyakov, S.E.Tolstikov, G.V.Romanenko, A.S.Bogomyakov, V.K.Cherkasov, D.V.Stass, V.I.Ovcharenko. *Russ. Chem. Bull.*, **60**, 2325 (2011)
286. S.I.Zhivetyeva, I.A.Zayakin, I.Yu.Bagryanskaya, E.V.Zaytseva, E.G.Bagryanskaya, E.V.Tretyakov. *Tetrahedron*, **74**, 3924 (2018)
287. R.Tanimoto, S.Suzuki, M.Kozaki, Y.Kanzaki, D.Shiomi, K.Sato, T.Takui, R.Tanaka, K.Okada. *ChemistrySelect*, **5**, 11170 (2020)
288. S.S.R.R.Perumal. *Chem. Phys. Lett.*, **501**, 608 (2011)
289. E.Ya.Misochko, D.V.Korchagin, A.V.Akimov, A.A.Masitov, S.E.Tolstikov, E.V.Tretyakov, V.I.Ovcharenko. *J. Phys. Chem. A*, **117**, 8065 (2013)
290. T.Furui, S.Suzuki, M.Kozaki, D.Shiomi, K.Sato, T.Takui, K.Okada, E.V.Tretyakov, S.E.Tolstikov, G.V.Romanenko, V.I.Ovcharenko. *Inorg. Chem.*, **53**, 802 (2014)
291. H.Tsujimoto, S.Suzuki, M.Kozaki, D.Shiomi, K.Sato, T.Takui, K.Okada. *Chem. – Asian J.*, **14**, 1801 (2019)
292. S.E.Tolstikov, E.V.Tretyakov, D.E.Gorbunov, I.F.Zhurko, M.V.Fedin, G.V.Romanenko, A.S.Bogomyakov, N.P.Gritsan, D.G.Mazhukin. *Chem. – Eur. J.*, **22**, 14598 (2016)
293. M.V.Varaksin, E.V.Tretyakov, I.A.Utepova, G.V.Romanenko, A.S.Bogomyakov, D.V.Stass, R.Z.Sagdeev, V.I.Ovcharenko, O.N.Chupakhin. *Russ. Chem. Bull.*, **61**, 1469 (2012) 1454 (2012)]
294. S.Tolstikov, E.Tretyakov, S.Fokin, E.Suturina, G.Romanenko, A.Bogomyakov, D.Stass, A.Maryasov, M.Fedin, N.Gritsan, V.Ovcharenko. *Chem. – Eur. J.*, **20**, 2793 (2014)
295. L.A.Shundrin, I.G.Irtegova, N.V.Vasilieva, E.V.Tretyakov, E.M.Zueva, V.I.Ovcharenko. *Tetrahedron Lett.*, **56**, 1207 (2015)
296. E.M.Kadilenko, N.P.Gritsan, E.V.Tretyakov, S.V.Fokin, G.V.Romanenko, A.S.Bogomyakov, D.E.Gorbunov, D.Schollmeyer, M.Baumgarten, V.I.Ovcharenko. *Dalton Trans.*, **49**, 16916 (2020)
297. O.N.Chupakhin, V.N.Charushin, H.C.van der Plas. *Nucleophilic Aromatic Substitution of Hydrogen*. (San Diego, CA: Academic Press, 1994)
298. V.N.Charushin, O.N.Chupakhin. *Pure Appl. Chem.*, **76**, 1621 (2004)
299. V.I.Ovcharenko, O.N.Chupakhin, I.S.Kovalev, E.V.Tretyakov, G.V.Romanenko, D.V.Stass. *Russ. Chem. Bull.*, **57**, 2227 (2008)
300. O.N.Chupakhin, I.A.Utepova, M.V.Varaksin, E.V.Tretyakov, G.V.Romanenko, D.V.Stass, V.I.Ovcharenko. *J. Org. Chem.*, **74**, 2870 (2009)
301. O.N.Chupakhin, E.V.Tretyakov, I.A.Utepova, M.V.Varaksin, G.V.Romanenko, A.S.Bogomyakov, S.L.Veber, V.I.Ovcharenko. *Polyhedron*, **30**, 647 (2011)
302. L.Gurskaya, T.Rybalova, I.Beregovaya, E.Zaytseva, M.Kazantseva, E.Tretyakov. *J. Fluorine Chem.*, **237**, 109613 (2020)
303. E.V.Tretyakov, I.A.Utepova, M.V.Varaksin, S.E.Tolstikov, G.V.Romanenko, A.S.Bogomyakov, D.V.Stass, V.I.Ovcharenko, O.N.Chupakhin. *ARKIVOC*, (viii), 76 (2011)
304. L.V.Politanskaya, G.A.Selivanova, E.V.Panteleeva, E.V.Tretyakov, V.E.Platonov, P.V.Nikul'shin, A.S.Vinogradov, Yu.V.Zonov, V.M.Karpov, T.V.Mezhenkova, A.V.Vasilyev, A.B.Koldobskii, O.S.Shilova, S.M.Morozova, Ya.V.Burgart, E.V.Shchegolkov, V.I.Saloutin, V.B.Sokolov, A.Yu.Aksinenko, V.G.Nenajdenko, M.Yu.Moskalik, V.V.Astakhova, B.A.Shainyan, A.A.Tabolin, S.L.Ioffe, V.M.Muzalevskiy, E.S.Balenkova, A.V.Shastin, A.A.Tyutyunov, V.E.Boiko, S.M.Igumnov, A.D.Dilman, N.Yu.Adonin, V.V.Bardin, S.M.Masoud, D.V.Vorobyeva, S.N.Osipov, E.V.Nosova, G.N.Lipunova, V.N.Charushin, D.O.Prima, A.G.Makarov, A.V.Zibarev, B.A.Trofimov, L.N.Sobenina, K.V.Belyaeva, V.Ya.Sosnovskikh, D.L.Obydennov, S.A.Usachev. *Russ. Chem. Rev.*, **88**, 425 (2019)
305. E.V.Tretyakov, P.A.Fedyushin, E.V.Panteleeva, D.V.Stass, I.Yu.Bagryanskaya, I.V.Beregovaya, A.S.Bogomyakov. *J. Org. Chem.*, **82**, 4179 (2017)
306. P.Fedyushin, E.Panteleeva, I.Bagryanskaya, K.Maryunina, K.Inoue, D.Stass, E.Tretyakov. *J. Fluorine Chem.*, **217**, 1 (2019)
307. P.Fedyushin, L.Gurskaya, E.Panteleeva, B.Koshcheev, A.Maksimov, T.V.Rybalova, E.Zaytseva, E.Tretyakov. *Fluorine Notes*, **123** (2), 7 (2019)
308. S.Suzuki, F.Nakamura, T.Naota. *Org. Lett.*, **22**, 1350 (2020)
309. S.Suzuki, F.Nakamura, T.Naota. *Mater. Chem. Front.*, **2**, 591 (2018)
310. R.Tanimoto, S.Suzuki, M.Kozaki, K.Okada. *Chem. Lett.*, **43**, 678 (2014)
311. E.V.Tretyakov, T.V.Makhneva, L.V.Politanskaya, I.Yu.Bagryanskaya, D.V.Stass. *J. Struct. Chem.*, **59**, 689 (2018)
312. R.Tanimoto, K.Yamada, S.Suzuki, M.Kozaki, K.Okada. *Eur. J. Inorg. Chem.*, 1198 (2018)
313. S.Suzuki, H.Yokoi, M.Kozaki, Y.Kanzaki, D.Shiomi, K.Sato, T.Takui, K.Okada. *Eur. J. Inorg. Chem.*, 4740 (2014)
314. G.V.Romanenko, S.V.Fokin, A.S.Bogomyakov, V.I.Ovcharenko. *J. Struct. Chem.*, **61**, 1952 (2020)
315. X.Zhang, S.Suzuki, M.Kozaki, K.Okada. *J. Am. Chem. Soc.*, **134**, 17866 (2012)
316. Patent US 3697535 (1969)
317. I.Zayakin, I.Bagryanskaya, D.Stass, M.Kazantsev, E.Tretyakov. *Crystals*, **10**, 770 (2020)

318. S.Suzuki, S.Kira, M.Kozaki, M.Yamamura, T.Hasegawa, T.Nabeshima, K.Okada. *Dalton Trans.*, **46**, 2653 (2017)
319. K.Yamada, X.Zhang, R.Tanimoto, S.Suzuki, M.Kozaki, R.Tanaka, K.Okada. *Bull. Chem. Soc. Jpn.*, **91**, 1150 (2018)
320. T.Tahara, S.Suzuki, M.Kozaki, D.Shiomi, K.Sugisaki, K.Sato, T.Takui, Y.Miyake, Y.Hosokoshi, H.Nojiri, K.Okada. *Chem. – Eur. J.*, **25**, 7201 (2019)
321. N.Yokoyama, N.Tanaka, N.Fujimoto, R.Tanaka, S.Suzuki, D.Shiomi, K.Sato, T.Takui, M.Kozaki, K.Okada. *Chem. – Asian J.*, **16**, 72 (2021)
322. T.Nishinaga, Y.Kanzaki, D.Shiomi, K.Matsuda, S.Suzuki, K.Okada. *Chem. – Eur. J.*, **24**, 11717 (2018)
323. T.Tahara, S.Suzuki, M.Kozaki, T.Nishinaga, K.Okada. *Bull. Chem. Soc. Jpn.*, **91**, 1193 (2018)
324. E.V.Tretyakov, K.A.Lomanovich, E.G.Bagryanskaya, G.V.Romanenko, A.S.Bogomyakov, E.M.Zueva, M.M.Petrova, A.A.Dmitriev, N.P.Gritsan. *Eur. J. Org. Chem.*, 2355 (2021)
325. M.Haraguchi, E.Tretyakov, N.Gritsan, G.Romanenko, D.Gorbunov, A.Bogomyakov, K.Maryunina, S.Suzuki, M.Kozaki, D.Shiomi, K.Sato, T.Takui, S.Nishihara, K.Inoue, K.Okada. *Chem. – Asian J.*, **12**, 2929 (2017)
326. L.Gurskaya, I.Bagryanskaya, E.Amosov, M.Kazantsev, L.Politanskaya, E.Zaytseva, E.Bagryanskaya, A.Chernonosov, E.Tretyakov. *Tetrahedron*, **74**, 1942 (2018)
327. E.Tretyakov, K.Okada, S.Suzuki, M.Baumgarten, G.Romanenko, A.Bogomyakov, V.Ovcharenko. *J. Phys. Org. Chem.*, **29**, 725 (2016)
328. A.Keerthi, C.An, M.Li, T.Marszalek, A.G.Ricciardulli, B.Radha, F.D.Alsewailem, K.Müllen, M.Baumgarten. *Polym. Chem.*, **7**, 1545 (2016)
329. E.Tretyakov, A.Keerthi, M.Baumgarten, S.Veber, M.Fedin, D.Gorbunov, I.Shundrina, N.Gritsan. *Chemistry Open*, **6**, 642 (2017)
330. E.V.Tretyakov, S.I.Zhivetyeva, P.V.Petunin, D.E.Gorbunov, N.P.Gritsan, I.Yu.Bagryanskaya, A.S.Bogomyakov, P.S.Postnikov, M.S.Kazantsev, M.E.Trusova, I.K.Shundrina, E.V.Zaytseva, D.A.Parkhomenko, E.G.Bagryanskaya, V.I.Ovcharenko. *Angew. Chem., Int. Ed.*, **59**, 20704 (2020)
331. E.V.Tretyakov, P.V.Petunin, S.I.Zhivetyeva, D.E.Gorbunov, N.P.Gritsan, M.V.Fedin, D.V.Stass, R.I.Samoilova, I.Yu.Bagryanskaya, I.K.Shundrina, A.S.Bogomyakov, M.S.Kazantsev, P.S.Postnikov, M.E.Trusova, V.I.Ovcharenko. *J. Am. Chem. Soc.*, **143**, 8164 (2021)
332. C.Shu, M.Pink, T.Junghoefer, E.Nadler, S.Rajca, M.B.Casu, A.Rajca. *J. Am. Chem. Soc.*, **143**, 5508 (2021)
333. M.Slota, A.Keerthi, W.K.Myers, E.Tretyakov, M.Baumgarten, A.Ardavan, H.Sadeghi, C.J.Lambert, A.Narita, K.Müllen, L.Bogani. *Nature (London)*, **557**, 691 (2018)
334. D.Stass, E.Tretyakov. *Magnetochemistry*, **5**, 32 (2019)
335. M.Golor, S.Wessel, M.J.Schmidt. *Phys. Rev. Lett.*, **112**, 046601 (2014)
336. V.Morozov, E.Tretyakov. *J. Mol. Model.*, **25**, 58 (2019)
337. S.S.Rao, A.Stesmans, J.van Tol, D.V.Kosynkin, A.Higginbotham-Duque, W.Lu, A.Sinitskii, J.M.Tour. *ACS Nano*, **6**, 7615 (2012)
338. P.R.Struck, G.Burkard. *Phys. Rev. B*, **82**, 125401 (2010)
339. M.Drögeler, C.Franzen, F.Volmer, T.Pohlmann, L.Banszerus, M.Wolter, K.Watanabe, T.Taniguchi, C.Stampfer, B.Beschoten. *Nano Lett.*, **16**, 3533 (2016)
340. Y.Kadoh, K.Oisaki, M.Kanai. *Chem. Pharm. Bull.*, **64**, 737 (2016)
341. J.Ozawa, M.Tashiro, J.Ni, K.Oisaki, M.Kanai. *Chem. Sci.*, **7**, 1904 (2016)
342. J.Ni, J.Ozawa, K.Oisaki, M.Kanai. *Org. Biomol. Chem.*, **14**, 4378 (2016)
343. O.Kushch, I.Hordieieva, K.Novikova, Y.Litvinov, M.Kompanets, A.Shendrik, I.Opeida. *J. Org. Chem.*, **85**, 7112 (2020)
344. L.Melone, C.Punta. In *Liquid Phase Aerobic Oxidation Catalysis: Industrial Applications and Academic Perspectives*. (Eds S.S.Stahl, P.L.Alsters). (Weinheim: Wiley-VCH, 2016). P. 253
345. F.Recupero, C.Punta. *Chem. Rev.*, **107**, 3800 (2007)
346. S.Coseri. *Catal. Rev.*, **51**, 218 (2009)
347. L.Melone, C.Punta. *Beilstein J. Org. Chem.*, **9**, 1296 (2013)
348. S.Wertz, A.Studer. *Green Chem.*, **15**, 3116 (2013)
349. K.Chen, P.Zhang, Y.Wang, H.Li. *Green Chem.*, **16**, 2344 (2014)
350. A.S.Budnikov, I.B.Krylov. *Chem. Heterocycl. Compd.*, **56**, 36 (2020)
351. Y.Li, L.Ge, M.Muhammad, H.Bao. *Synthesis*, **49**, 5263 (2017)
352. K.Jia, Y.Chen. *Chem. Commun.*, **54**, 6105 (2018)
353. S.Murarka. *Adv. Synth. Catal.*, **360**, 1735 (2018)
354. Y.Yoshino, Y.Hayashi, T.Iwahama, S.Sakaguchi, Y.Ishii. *J. Org. Chem.*, **62**, 6810 (1997)
355. E.Gaster, S.Kozuch, D.Pappo. *Angew. Chem., Int. Ed.*, **56**, 5912 (2017)
356. D.P.Hruszkewycz, K.C.Miles, O.R.Thiel, S.S.Stahl. *Chem. Sci.*, **8**, 1282 (2017)
357. T.Kato, K.Maruoka. *Angew. Chem., Int. Ed.*, **59**, 14261 (2020)
358. I.K.Goncharova, K.P.Silaeva, A.V.Arzumanyan, A.A.Anisimov, S.A.Milenin, R.A.Novikov, P.N.Solyev, Ya.V.Tkachev, A.D.Volodin, A.A.Korlyukov, A.M.Muzafarov. *J. Am. Chem. Soc.*, **141**, 2143 (2019)
359. A.V.Arzumanyan, I.K.Goncharova, R.A.Novikov, S.A.Milenin, K.L.Boldyrev, P.N.Solyev, Ya.V.Tkachev, A.D.Volodin, A.F.Smol'yakov, A.A.Korlyukov, A.M.Muzafarov. *Green Chem.*, **20**, 1467 (2018)
360. J.E.Nutting, M.Rafiee, S.S.Stahl. *Chem. Rev.*, **118**, 4834 (2018)
361. Y.Mo, K.F.Jensen. *Chem. – Eur. J.*, **24**, 10260 (2018)
362. M.Rafiee, F.Wang, D.P.Hruszkewycz, S.S.Stahl. *J. Am. Chem. Soc.*, **140**, 22 (2018)
363. E.J.Horn, B.R.Rosen, Y.Chen, J.Tang, K.Chen, M.D.Eastgate, P.S.Baran. *Nature (London)*, **533**, 77 (2016)
364. W.Chen, H.Tang, W.Wang, Q.Fu, J.Luo. *Adv. Synth. Catal.*, **362**, 3905 (2020)
365. J.M.Lee, E.J.Park, S.H.Cho, S.Chang. *J. Am. Chem. Soc.*, **130**, 7824 (2008)
366. P.-C.Qian, Y.Liu, R.-J.Song, M.Hu, X.-H.Yang, J.-N.Xiang, J.-H.Li. *Eur. J. Org. Chem.*, 1680 (2015)
367. L.Dian, S.Wang, D.Zhang-Negrerie, Y.Du. *Adv. Synth. Catal.*, **357**, 3836 (2015)
368. B.Tan, N.Toda, C.F.Barbas. *Angew. Chem., Int. Ed.*, **51**, 12538 (2012)
369. Y.Siddaraju, K.R.Prabhu. *Org. Biomol. Chem.*, **13**, 11651 (2015)

370. Y.Lv, K.Sun, T.Wang, G.Li, W.Pu, N.Chai, H.Shen, Y.Wu. *RSC Adv*., **5**, 72142 (2015)
371. Y.Zhou, J.Chen, A.A.Elsayed, Z.Zhang, Z.Bao, Q.Yang, Y.Yang, Q.Ren. *Catal. Lett*., **149**, 574 (2019)
372. M.-Z.Zhang, N.Luo, R.-Y.Long, X.-T.Gou, W.-B.Shi, S.-H.He, Y.Jiang, J.-Y.Chen, T.Chen. *J. Org. Chem*., **83**, 2369 (2018)
373. Y.Lv, K.Sun, W.Pu, S.Mao, G.Li, J.Niu, Q.Chen, T.Wang. *RSC Adv*., **6**, 93486 (2016)
374. X.Xu, J.Sun, Y.Lin, J.Cheng, P.Li, Y.Yan, Q.Shuai, Y.Xie. *Org. Biomol. Chem*., **15**, 9875 (2017)
375. H.Yao, K.Yamamoto. *Chem. – Asian J*., **7**, 1542 (2012)
376. M.Dinda, C.Bose, T.Ghosh, S.Maity. *RSC Adv*., **5**, 44928 (2015)
377. X.Xu, J.Sun, Y.Lin, J.Cheng, P.Li, X.Jiang, R.Bai, Y.Xie. *Eur. J. Org. Chem*., 7160 (2017)
378. X.Xu, P.Li, Y.Huang, C.Tong, Y.Yan, Y.Xie. *Tetrahedron Lett*., **58**, 1742 (2017)
379. F.Feizpour, M.Jafarpour, A.Rezaeifard. *New J. Chem*., **42**, 807 (2018)
380. I.B.Krylov, E.R.Lopat'eva, A.S.Budnikov, G.I.Nikishin, A.O.Terent'ev. *J. Org. Chem*., **85**, 1935 (2020)
381. X.-F.Xia, S.-L.Zhu, D.Zhang. *Tetrahedron*, **71**, 8517 (2015)
382. I.B.Krylov, A.S.Budnikov, A.V.Lastovko, Ya.A.Ibatov, G.I.Nikishin, A.O.Terent'ev. *Russ. Chem. Bull*., **68**, 1454 (2019)
383. S.Samanta, C.Ravi, A.Joshi, V.Pappula, S.Adimurthy. *Tetrahedron Lett*., **58**, 721 (2017)
384. J.Luo, J.Zhang. *J. Org. Chem*., **81**, 9131 (2016)
385. D.Yamamoto, M.Soga, H.Ansai, K.Makino. *Org. Chem. Front*., **3**, 1420 (2016)
386. R.Bag, D.Sar, T.Punniyamurthy. *Org. Biomol. Chem*., **14**, 3246 (2016)
387. M.R.Miner, K.A.Woerpel. *Eur. J. Org. Chem*., 1860 (2016)
388. T.E.Anderson, K.A.Woerpel. *Org. Lett*., **22**, 5690 (2020)
389. A.A.Andia, M.R.Miner, K.A.Woerpel. *Org. Lett*., **17**, 2704 (2015)
390. R.Bag, D.Sar, T.Punniyamurthy. *Org. Lett*., **17**, 2010 (2015)
391. J.Zhang, Y.Tang. *Adv. Synth. Catal*., **358**, 752 (2016)
392. X.-F.Xia, S.-L.Zhu, Z.Gu, H.Wang, W.Li, X.Liu, Y.-M.Liang. *J. Org. Chem*., **80**, 5572 (2015)
393. I.B.Krylov, S.A.Paveliev, O.K.Matveeva, A.O.Terent'ev. *Tetrahedron*, **75**, 2529 (2019)
394. X.-F.Xia, S.-L.Zhu, Y.-N.Niu, D.Zhang, X.Liu, H.Wang. *Tetrahedron*, **72**, 3068 (2016)
395. T.-S.Zhang, Y.-J.Xiong, W.-J.Hao, X.-T.Zhu, S.-L.Wang, G.Li, S.-J.Tu, B.Jiang. *J. Org. Chem*., **81**, 9350 (2016)
396. I.B.Krylov, S.A.Paveliev, M.A.Syroeshkin, A.A.Korlyukov, P.V.Dorovatovskii, Ya.V.Zubavichus, G.I.Nikishin, A.O.Terent'ev. *Beilstein J. Org. Chem*., **14**, 2146 (2018)
397. X.Li, K.Chen, Y.Tang, H.Zhu, F.Chen, X.Yan, X.Xu. *Synlett*, **29**, 1634 (2018)
398. S.A.Paveliev, A.I.Churakov, L.S.Alimkhanova, O.O.Segida, G.I.Nikishin, A.O.Terent'ev. *Adv. Synth. Catal*., **362**, 3864 (2020)
399. S.W.Lardy, V.A.Schmidt. *J. Am. Chem. Soc*., **140**, 12318 (2018)
400. J.A.Crayston, C.Kakouris, J.C.Walton. *Magn. Reson. Chem*., **30**, 77 (1992)
401. R.Ramasseul, A.Rassat. *Bull. Soc. Chim. France*, 4330 (1970)
402. C.Riplinger, J.P.Y.Kao, G.M.Rosen, V.Kathirvelu, G.R.Eaton, S.S.Eaton, A.Kutateladze, F.Neese. *J. Am. Chem. Soc*., **131**, 10092 (2009)
403. P.R.Serwinski, B.Esat, P.M.Lahti, Y.Liao, R.Walton, J.Lan. *J. Org. Chem*., **69**, 5247 (2004)
404. B.M.Dooley, S.E.Bowles, T.Storr, N.L.Frank. *Org. Lett*., **9**, 4781 (2007)
405. Y.Kusaba, M.Tamura, Y.Hosokoshi, H.Sawa, R.Kato, H.Kobayashi. *J. Mater. Chem*., **7**, 1377 (1997)
406. E.V.Tretyakov, G.V.Romanenko, V.N.Ikorskii, E.V.Gorelik, D.V.Stas', V.I.Ovcharenko, R.Z.Sagdeev. *Russ. J. Phys. Chem*., **81**, 2064 (2007)
407. A.Zakrassov, V.Shteiman, Y.Sheynin, B.Tumanskii, M.Botoshansky, M.Kapon, A.Keren, M.Kaftory, T.E.Vos, J.S.Miller. *J. Mater. Chem*., **14**, 1827 (2004)
408. B.Esat, I.Fidan, S.Bahceci, Y.Yerli, L.Sari. *Magn. Reson. Chem*., **47**, 641 (2009)
409. S.E.Bowles, B.M.Dooley, J.B.Benedict, W.Kaminsky, N.L.Frank. *Polyhedron*, **28**, 1704 (2009)
410. *Frontiers of Quantum Chemistry*. (Eds M.J.Wójcik, H.Nakatsuji, B.Kirtman, Y.Ozaki). (Singapore: Springer Nature, 2018)
411. C.Adamo, A.di Matteo, P.Rey, V.Barone. *J. Phys. Chem. A*, **103**, 3481 (1999)
412. R.Improta, A.di Matteo, V.Barone. *Theor. Chem. Acta*, **104**, 273 (2000)
413. A.Zakrassov, M.Kaftory. *J. Solid State Chem*., **169**, 75 (2002)
414. I.Yu.Barskaya, S.L.Veber, E.A.Suturina, P.S.Sherin, K.Yu.Maryunina, N.A.Artiukhova, E.V.Tretyakov, R.Z.Sagdeev, V.I.Ovcharenko, N.P.Gritsan, M.V.Fedin. *Dalton Trans*., **46**, 13108 (2017)
415. M.Shibuya, F.Pichierri, M.Tomizawa, S.Nagasawa, I.Suzuki, Y.Iwabuchi. *Tetrahedron Lett*., **53**, 2070 (2012)
416. O.A.Levitskiy, T.V.Magdesieva. *Mendeleev Commun*., **28**, 187 (2018)
417. D.A.Parkhomenko, M.V.Edeleva, V.G.Kiselev, E.G.Bagryanskaya. *J. Phys. Chem. B*, **118**, 5542 (2014)
418. J.P.Malrieu, R.Caballol, C.J.Calzado, C.de Graaf, N.Guihery. *Chem. Rev*., **114**, 429 (2014)
419. M.Song, X.Song, Y.Bu. *ChemPhysChem*, **18**, 2487 (2017)
420. V.E.Romanov, I.Yu.Bagryanskaya, D.E.Gorbunov, N.P.Gritsan, E.V.Zaytseva, D.Luneau, E.V.Tretyakov. *Crystals*, **8**, 334 (2018)
421. V.I.Minkin, A.G.Starikov, A.A.Starikova, O.A.Gapurenko, R.M.Minyaev, A.I.Boldyrev. *Phys. Chem. Chem. Phys*., **22**, 1288 (2020)
422. O.E.Lebedev, M.I.Khidekel', G.A.Razuvaev. *Dokl. Akad. SSSR*, **140**, 1327 (1961)
423. H.Karoui, F.Le Moigne, O.Ouari, P.Tordo. In *Stable Radicals. Fundamentals and Applied Aspects of Odd-Electron Compounds*. (Ed. R.G.Hicks). (Chichester: Wiley, 2010). P. 173
424. M.M.Haugland, J.E.Lovett, E.A.Anderson. *Chem. Soc. Rev*., **47**, 668 (2018)
425. B.Bognára, G.Úra, C.Sára, O.H.Hankovszkya, K.Hideg, T.Kálai. *Curr. Org. Chem*., **23**, 480 (2019)
426. S.M.Mattar, A.D.Stephens. *Chem. Phys. Lett*., **347**, 189 (2001)
427. G.A.A.Saracino, A.Tedeschi, G.D'Errico, R.Improta, L.Franco, M.Ruzzi, C.Corvaia, V.Barone. *J. Phys. Chem. A*, **106**, 10700 (2002)

428. J.P.Perdew, M.Ernzerhof, K.Burke. *J. Chem. Phys.*, **105**, 9982 (1996)
429. J.Tomasi, B.Mennucci, R.Cammi. *Chem. Rev.*, **105**, 2999 (2005)
430. P.Cimino, A.Pedone, E.Stendardoc, V.Barone. *Phys. Chem. Chem. Phys.*, **12**, 3741 (2010)
431. L.N.Ikryannikova, L.Yu.Ustynyuk, A.N.Tikhonov. *J. Phys. Chem. A*, **108**, 4759 (2004)
432. A.R.Forrester, S.P.Hepburn. *J. Chem. Soc. C*, 1277 (1970)
433. A.R.Forrester, S.P.Hepburn. *J. Chem. Soc., Perkin Trans. 1*, 2208 (1974)
434. A.R.Forrester, J.Henderson, S.P.Hepburn. *J. Chem. Soc., Perkin Trans. 1*, 1165 (1981)
435. H.B.Stegmann, F.-M.Schaber, P.Schuler, K.Schemer. *Magn. Res. Chem.*, **27**, 887 (1989)
436. P.H.H.Fischer, F.A.Neugebauer. *Z. Naturforsch., Sect. A*, **19**, 1514 (1964)
437. P.Astolfi, P.Carloni, E.Damiani, L.Greci, M.Marini, C.Rizzoli, P.Stipa. *Eur. J. Org. Chem.*, 3279 (2008)
438. A.V.Marenich, C.J.Cramer, D.G.Truhlar. *J. Phys. Chem. B*, **113**, 6378 (2009)
439. P.Turek. In *Electron Paramagnetic Resonance Spectroscopy. Applications*. (Ed. P.Bertrand). (Switzerland: Springer Nature, 2020). P. 247
440. M.Kinoshita, P.Turek, M.Tamura, K.Nozawa, D.Shiomi, Y.Nakazawa, M.Ishikawa, M.Takahashi, K.Awaga, T.Inabe, Y.Maruyama. *Chem. Lett.*, **20**, 1225 (1991)
441. J.A.D'Anna, J.H.Wharton. *J. Chem. Phys.*, **53**, 4047 (1970)
442. H.Akpinar, J.A.Schlueter, P.M.Lahti. *Chem. Commun.*, **49**, 3345 (2013)
443. O.Jurgens, J.Cirujeda, M.Mas, I.Mata, A.Cabrero, J.Vidal-Gancedo, C.Rovira, E.Molins, J.Veciana. *J. Mater. Chem.*, **7**, 1723 (1997)
444. D.Shiomi, K.Sato, T.Takui, K.Itoh, M.Tamura, Y.Nishio, K.Kajita, M.Nakagawa, T.Ishida, T.Nogami. *Mol. Cryst. Liq. Cryst.*, **335**, 359 (1999)
445. J.Cirujeda, J.Vidal-Gancedo, O.Jurgens, F.Mota, J.J.Novoa, C.Rovira, J.Veciana. *J. Am. Chem. Soc.*, **122**, 11393 (2000)
446. A.di Matteo, C.Adamo, M.Cossi, V.Barone, P.Rey. *Chem. Phys. Lett.*, **310**, 159 (1999)
447. G.Bussiere, R.Beaulac, H.Belisle, C.Lescop, D.Luneau, P.Rey, C.Reber. *Top. Curr. Chem.*, **241**, 97 (2004)
448. In *Atlas Spektrov Aromaticheskikh i Geterotsiklicheskikh Soedinenii. Spektry Pogloshcheniya Nitroksil'nykh Radikalov Proizvodnykh 3-Imidazolina, Pirrolina, Pirrolidina, Piperidina i Diazepina i ikh Predshestvennikov v Infrakrasnoi, Ul'trafioletovoi i Vidimoi Oblastyakh. (Atlas of Spectra of Aromatic and Heterocyclic Compounds. Absorption Spectra of Nitroxyl Radicals of 3-Imidazoline Derivatives, Pyrroline, Pyrrolidine, Piperidine and Deazepine and Their Precursors in the Infrared, Ultraviolet and Visible Regions)*. No. 24. (Ed. V.A.Koptyug). (Novosibirsk: Nauka, Sib. Otd., 1982). P. 105
449. Y.Kawahashi, G.Maruta, S.Takeda. *Polyhedron*, **28**, 2063 (2009)
450. G.Zoppellaro. PhD Thesis. Johnnes Gutenberg-Universität in Mainz, Mainz, 2004; https://pure.mpg.de/rest/items/item_1418381/component/file_1418380/content (last access 21.01.2022)
451. G.Zoppellaro, A.Ivanova, V.Enkelmann, A.Geies, M.Baumgarten. *Polyhedron*, **22**, 2099 (2003)
452. C.Rajadurai, A.Ivanova, V.Enkelmann, M.Baumgarten. *J. Org. Chem.*, **68**, 9907 (2003)
453. R.Beaulac, G.Bussiere, C.Reber, C.Lescop, D.Luneau. *New J. Chem.*, **27**, 1200 (2003)
454. K.Wright, E.d'Aboville, J.Scola, T.Margola, A.Toffoletti, M.De Zotti, M.Crisma, F.Formaggio, C.Toniolo. *Eur. J. Org. Chem.*, 1741 (2014)
455. T.Petrenko, F.Neese. *J. Chem. Phys.*, **127**, 164319 (2007)
456. L.Rintoul, A.S.Micallef, S.E.Bottle. *Spectrochim. Acta, Part A*, **70**, 713 (2008)
457. H.Iwamura. *Adv. Phys. Org. Chem.*, **26**, 179 (1990)
458. A.Rajca. *Chem. Rev.*, **94**, 871 (1994)
459. A.Rajca. *Adv. Phys. Org. Chem.*, **40**, 153 (2005)
460. R.Chiarelli, M.A.Novak, A.Rassat, J.L.Tholence. *Nature (London)*, **363**, 147 (1993)
461. N.M.Gallagher, A.Olankitwanit, A.Rajca. *J. Org. Chem.*, **80**, 1291 (2015)
462. C.Trindle, S.N.Datta, B.Mallik. *J. Am. Chem. Soc.*, **119**, 12947 (1997)
463. D.Bhattacharya, A.Misra. *J. Phys. Chem. A*, **113**, 5470 (2009)
464. L.Noodleman. *J. Chem. Phys.*, **74**, 5737 (1981)
465. L.Noodleman, C.Y.Peng, D.A.Case, J.-M.Mouesca. *Coord. Chem. Rev.*, **144**, 199 (1995)
466. H.Nagao, M.Nishino, Y.Shigeta, T.Soda, Y.Kitagawa, T.Onishi, Y.Yoshioka, K.Yamaguchi. *Coord. Chem. Rev.*, **198**, 265 (2000)
467. E.Ali, S.N.Datta. *J. Phys. Chem. A*, **110**, 2776 (2006)
468. P.Sarbadhikary, S.Shil, A.Panda, A.Misra. *J. Org. Chem.*, **81**, 5623 (2016)
469. A.K.Pal, S.N.Datta. *Chem. Phys. Lett.*, **67**6, 70 (2017)
470. S.Sato, R.Hirao, I.Timofeev, O.Krumkacheva, E.Zaytseva, O.Rogozhnikova, V.M.Tormyshev, D.Trukhin, E.Bagryanskaya, T.Gutmann, V.Klimavicius, G.Buntkowsky, K.Sugisaki, S.Nakazawa, H.Matsuoka, K.Toyota, D.Shiomi, T.Takui. *J. Phys. Chem. A*, **123**, 7507 (2019)
471. M.M.Petrova, S.I.Zhivetyeva, E.V.Tretyakov. *J. Comput. Chem. Mol. Model.*, **2**, 172 (2018)
472. F.K.B.Burnea, Y.Nam, J.Y.Lee. *J. Mater. Chem. C*, **8**, 3402 (2020)
473. W.T.Borden, E.R.Davidson. *J. Am. Chem. Soc.*, **99**, 4587 (1977)
474. T.Stuyver, B.Chen, T.Zeng, P.Geerlings, F.DeProft, R.Hoffmann. *Chem. Rev.*, **119**, 11291 (2019)
475. L.V.Slipchenko, A.I.Krylov. *J. Chem. Phys.*, **117**, 4694 (2002)
476. L.V.Slipchenko, A.I.Krylov. *J. Chem. Phys.*, **118**, 6874 (2003)
477. S.N.Datta, P.Mukherjee, P.P.Jha. *J. Phys. Chem. A*, **107**, 5049 (2003)
478. X.Li, J.Paldus. *J. Chem. Phys.*, **129**, 174101 (2008)
479. D.H.Ess, E.R.Johnson, X.Hu, W.Yang. *J. Phys. Chem. A*, **115**, 76 (2011)
480. R.C.Fort, S.J.Getty, D.A.Hrovat, P.M.Lahti, W.T.Borden. *J. Am. Chem. Soc.*, **114**, 7549 (1992)
481. M.Mitani, H.Mori, Y.Takano, D.Yamaki, Y.Yoshioka, K.Yamaguchi. *J. Chem. Phys.*, **113**, 4035 (2000)
482. D.R.Mañeru, A.K.Pal, I.de P.R.Moreira, S.N.Datta, F.Illas. *J. Chem. Theory Comput.*, **10**, 335 (2014)
483. P.G.Wenthold, J.Hu, R.R.Squires, W.C.Lineberger. *J. Am. Chem. Soc.*, **118**, 475 (1996)
484. P.G.Wenthold, J.B.Kim, W.C.Lineberger. *J. Am. Chem. Soc.*, **119**, 1354 (1997)

485. L.Catala, J.Le Moigne, N.Kyritsakas, P.Rey, J.J.Novoa, P.Turek. *Chem. – Eur. J.*, **7**, 2466 (2001)
486. T.Ishida, H.Iwamura. *J. Am. Chem. Soc.*, **113**, 4238 (1991)
487. H.Sekine, T.Ishida. *AIP Conf. Proc.*, **1929**, 020022 (2018)
488. C.J.Cramer, B.A.Smith. *J. Phys. Chem.*, **100**, 9664 (1996)
489. V.Barone, I.Cacelli, A.Ferretti, S.Monti, G.Prampolini. *J. Chem. Theory Comput.*, **7**, 699 (2011)
490. V.Romanov, I.Bagryanskaya, N.Gritsan, D.Gorbunov, Yu.Vlasenko, M.Yusubov, E.Zaytseva, D.Luneau, E.Tretyakov. *Crystals*, **9**, 219 (2019)
491. Y.Naoki, I.Munetoshi, M.Yuichiro, K.Takanari, I.Hidenari, O.Shigeru. *Chem. Lett.*, **26**, 251 (1997)
492. R.Hoffmann. *Am. Sci.*, **96**, 372 (2008)
493. H.V.-T.Nguyen, A.Detappe, N.M.Gallagher, H.Zhang, P.Harvey, C.Yan, C.Mathieu, M.R.Golder, Y.Jiang, M.F.Ottaviani, A.Jasanoff, A.Rajca, I.Ghobrial, P.P.Ghoroghchian, J.A.Johnson. *ACS Nano*, **12**, 11343 (2018)
494. K.Iwasaki, Y.Yudai, H.Gotoh. *Asian J. Chem.*, **31**, 2107 (2019)
495. R.A.Sheldon, I.W.C.E.Arends. *Adv. Synth. Catal.*, **346**, 1051 (2004)
496. M.Griesser, R.Shah, A.T.Van Kessel, O.Zilka, E.A.Haidasz, D.A.Pratt. *J. Am. Chem. Soc.*, **140**, 3798 (2018)
497. T.Kurata, K.Koshika, F.Kato, J.Kido, H.Nishide. *Chem. Commun.*, 2986 (2007)
498. T.Sugawara, H.Komatsu, K.Suzuki. *Chem. Soc. Rev.*, **40**, 3105 (2011)
499. X.Meng, W.Shi, P.Cheng. *Coord. Chem. Rev.*, **378**, 134 (2019)
500. M.G.F.Vaz, M.Andruh. *Coord. Chem. Rev.*, **427**, 213611 (2021)
501. S.J.Blundell, T.Lancaster, P.J.Baker, F.L.Pratt, D.Shiomi, K.Sato, T.Takui. *Magnetochemistry*, **7**, 71 (2021)
502. D.A.Wilcox, V.Agarkar, S.Mukherjee, B.W.Boudouris. *Annu. Rev. Chem. Biomol. Eng.*, **9**, 83 (2018)
503. Y.Xie, K.Zhang, Y.Yamauchi, K.Oyaizu, Z.Jia. *Mater. Horiz.*, **8**, 803 (2021)
504. C.G.Armstrong, K.E.Toghill. *Electrochem. Commun.*, **91**, 19 (2018)
505. H.R.Lamontagne, B.H.Lessard. *ACS Appl. Polym. Mater.*, **2**, 5327 (2020)
506. G.R.Luckhurst, G.F.Pedulli. *Mol. Phys.*, **20**, 1043 (1971)
507. S.S.Eaton, L.B.Woodcock, G.R.Eaton. *Concepts Magn. Reson., Part A*, **47A**, e21426 (2018)
508. A.V.Bogdanov, B.Y.Mladenova-Kattnig, A.K.Vorobiev, G.Grampp, A.I.Kokorin. *J. Phys. Chem. B*, **124**, 11007 (2020)
509. A.Ito, Y.Nakano, T.Kato, K.Tanaka. *Chem. Commun.*, 403 (2005)
510. Y.Nakano, A.Ito, K.Tanaka. *Polyhedron*, **30**, 3106 (2011)
511. S.Suzuki, A.Nagata, M.Kuratsu, M.Kozaki, R.Tanaka, D.Shiomi, K.Sugisaki, K.Toyota, K.Sato, T.Takui, K.Okada. *Angew. Chem., Int. Ed.*, **51**, 3193 (2012)
512. T.Itoh, K.Matsuda, H.Iwamura, K.Hori. *J. Solid State Chem.*, **159**, 428 (2001)
513. A.Nagata, S.Hiraoka, S.Suzuki, M.Kozaki, D.Shiomi, K.Sato, T.Takui, R.Tanaka, K.Okada. *Chem. – Eur. J.*, **26**, 3166 (2020)
514. Y.Masuda, H.Takeda, M.Kuratsu, S.Suzuki, M.Kozaki, D.Shiomi, K.Sato, T.Takui, K.Okada. *Pure Appl. Chem.*, **82**, 1025 (2010)
515. A.Ito, R.Kurata, Y.Noma, Y.Hirao, K.Tanaka. *J. Org. Chem.*, **81**, 11416 (2016)
516. A.Ito, Y.Nakano, M.Urabe, T.Kato, K.Tanaka. *J. Am. Chem. Soc.*, **128**, 2948 (2006)
517. S.Shil, C.Herrmann. *Inorg. Chem.*, **54**, 11733 (2015)
518. M.Souto, V.Lloveras, S.Vela, M.Fumanal, I.Ratera, J.Veciana. *J. Phys. Chem. Lett.*, **7**, 2234 (2016)
519. A.Ito, M.Urabe, K.Tanaka. *Polyhedron*, **22**, 1829 (2003)
520. M.V.Fedin, S.L.Veber, E.G.Bagryanskaya, V.I.Ovcharenko. *Coord. Chem. Rev.*, **289 – 290**, 341 (2015)
521. B.E.Cole, T.Cheisson, R.F.Higgins, E.Nakamaru-Ogiso, B.C.Manor, P.J.Carroll, E.J.Schelter. *Inorg. Chem.*, **59**, 172 (2020)
522. H.Fang, B.E.Cole, Y.Qiao, J.A.Bogart, T.Cheisson, B.C.Manor, P.J.Carroll, E.J.Schelter. *Angew. Chem., Int. Ed.*, **56**, 13450 (2017)
523. B.E.Cole, T.Cheisson, J.J.M.Nelson, R.F.Higgins, M.R.Gau, P.J.Carroll, E.J.Schelter. *ACS Sustain. Chem. Eng.*, **8**, 14786 (2020)
524. L.Lienafa, S.Monge, Y.Guillaneuf, B.Ameduri, D.Siri, D.Gigmes, J.-J.Robin. *Eur. Polym. J.*, **109**, 55 (2018)
525. J.S.Miller, D.Gatteschi. *Chem. Soc. Rev.*, **40**, 3065 (2011)
526. A.Caneschi, D.Gatteschi, R.Sessoli, P.Rey. *Acc. Chem. Res.*, **22**, 392 (1989)
527. V.I.Ovcharenko. In *Stable Radicals: Fundamentals and Applied Aspects of Odd-Electron Compounds*. (Ed. R.G.Hicks). (Chichester: Wiley, 2010). P. 461
528. S.Demir, I.-R.Jeon, J.R.Long, T.D.Harris. *Coord. Chem. Rev.*, **289 – 290**, 149 (2015)
529. J.Ferrando-Soria, J.Vallejo, M.Castellano, J.Martínez-Lillo, E.Pardo, J.Cano, I.Castro, F.Lloret, R.Ruiz-García, M.Julve. *Coord. Chem. Rev.*, **339**, 17 (2017)
530. D.Luneau. *Eur. J. Inorg. Chem.*, 597 (2020)
531. S.V.Fokin, S.E.Tolstikov, E.V.Tretyakov, G.V.Romanenko, A.S.Bogomyakov, S.L.Veber, R.Z.Sagdeev, V.I.Ovcharenko. *Russ. Chem. Bull.*, **60**, 2470 (2011)
532. R.A.Allão Cassaro, M.Baskett, P.M.Lahti. *Polyhedron*, **64**, 231 (2013)
533. V.I.Ovcharenko, S.V.Fokin, E.T.Kostina, G.V.Romanenko, A.S.Bogomyakov, E.V.Tretyakov. *Inorg. Chem.*, **51**, 12188 (2012)
534. V.Ovcharenko, S.Fokin, E.Chubakova, G.Romanenko, A.Bogomyakov, Z.Dobrokhotova, N.Lukzen, V.Morozov, M.Petrova, M.Petrova, E.Zueva, I.Rozentsveig, E.Rudyakova, G.Levkovskaya, R.Sagdeev. *Inorg. Chem.*, **55**, 5853 (2016)
535. E.V.Tretyakov, G.V.Romanenko, S.L.Veber, M.V.Fedin, A.V.Polushkin, A.O.Tkacheva, V.I.Ovcharenko. *Aust. J. Chem.*, **68**, 970 (2015)
536. M.Fedin, V.Ovcharenko, R.Sagdeev, E.Reijerse, W.Lubitz, E.Bagryanskaya. *Angew. Chem., Int. Ed.*, **47**, 6897 (2008)
537. M.V.Fedin, E.G.Bagryanskaya, H.Matsuoka, S.Yamauchi, S.L.Veber, K.Yu.Maryunina, E.V.Tretyakov, V.I.Ovcharenko, R.Z.Sagdeev. *J. Am. Chem. Soc.*, **134**, 16319 (2012)
538. X.Dong, M.Lorenc, E.V.Tretyakov, V.I.Ovcharenko, M.V.Fedin. *J. Phys. Chem. Lett.*, **8**, 5587 (2017)
539. W.Kaszub, A.Marino, M.Lorenc, E.Collet, E.G.Bagryanskaya, E.V.Tretyakov, V.I.Ovcharenko, M.V.Fedin. *Angew. Chem., Int. Ed.*, **53**, 10636 (2014)

540. G.V.Romanenko, G.A.Letyagin, K.Yu.Maryunina, A.S.Bogomyakov, S.Nishihara, K.Inoue, V.I.Ovcharenko. *Russ. Chem. Bull.*, **69**, 1530 (2020)
541. A.Okazawa, D.Hashizume, T.Ishida. *J. Am. Chem. Soc.*, **132**, 11516 (2010)
542. A.Okazawa, T.Ishida. *Inorg. Chem.*, **49**, 10144 (2010)
543. Y.Homma, T.Ishida. *Chem. Mater.*, **30**, 1835 (2018)
544. Y.Kyoden, Y.Homma, T.Ishida. *Inorg. Chem.*, **58**, 10743 (2019)
545. Y.Kyoden, T.Ishida. *RSC Adv.*, **10**, 16009 (2020)
546. Y.Kyoden, T.Ishida. *Molecules*, **25**, 3790 (2020)
547. E.M.Zueva, E.V.Tretyakov, S.V.Fokin, G.V.Romanenko, A.O.Tkacheva, A.S.Bogomyakov, O.V.Petrova, B.A.Trofimov, R.Z.Sagdeev, V.I.Ovcharenko. *Russ. Chem. Bull.*, **65**, 666 (2016)
548. A.A.Starikova, V.I.Minkin. *New J. Chem.*, **41**, 6497 (2017)
549. A.Lannes, Y.Suffren, J.B.Tommasino, R.Chiriac, F.Toche, L.Khrouz, F.Molton, C.Duboc, I.Kieffer, J.L.Hazemann, C.Reber, A.Hauser, D.Luneau. *J. Am. Chem. Soc.*, **138**, 16493 (2016)
550. C.Lecourt, Y.Izumi, L.Khrouz, F.Toche, R.Chiriac, N.Bélanger-Desmarais, C.Reber, O.Fabelo, K.Inoue, C.Desroches, D.Luneau. *Dalton Trans.*, **49**, 15646 (2020)
551. F.Pointillart, K.Bernot, G.Poneti, R.Sessoli. *Inorg. Chem.*, **51**, 12218 (2012)
552. J.Wang, H.Miao, Z.-X.Xiao, Y.Zhou, L.-D.Deng, Y.-Q.Zhang, X.-Y.Wang. *Dalton Trans.*, **46**, 10452 (2017)
553. A.A.Patrascu, M.Briganti, S.Soriano, S.Calancea, R.A.Allão Cassaro, F.Totti, M.G.F.Vaz, M.Andruh. *Inorg. Chem.*, **58**, 13090 (2019)
554. A.Lannes, M.Intissar, Y.Suffren, C.Reber, D.Luneau. *Inorg. Chem.*, **53**, 9548 (2014)
555. P.Y.Chen, M.Z.Wu, Z.Y.Liu, L.Tian, Y.Q.Zhang. *Dalton Trans.*, **48**, 558 (2019)
556. E.V.Tretyakov, S.V.Fokin, E.M.Zueva, A.O.Tkacheva, G.V.Romanenko, A.S.Bogomyakov, S.V.Larionov, S.A.Popov, V.I.Ovcharenko. *Russ. Chem. Bull.*, **63**, 1459 (2014)
557. J.Sun, Z.Sun, L.Li, J.-P.Sutter. *Inorg. Chem.*, **57**, 7507 (2018)
558. L.Xi, H.Li, J.Sun, Y.Ma, J.Tang, L.Li. *Inorg. Chem.*, **59**, 443 (2020)
559. E.Coronado, C.Giménez-Saiz, A.Recuenco, A.Tarazón, F.M.Romero, A.Camón, F.Luis. *Inorg. Chem.*, **50**, 7370 (2011)
560. J.Y.Shi, M.Z.Wu, P.Y.Chen, T.Li, L.Tian, Y.Q.Zhang. *Inorg. Chem.*, **58**, 14285 (2019)
561. M.G.F.Vaz, R.A.A.Cassaro, H.Akpinar, J.A.Schlueter, P.M.Lahti, M.A.Novak. *Chem. – Eur. J.*, **20**, 5460 (2014)
562. X.Liu, Y.Zhang, W.Shi, P.Cheng. *Inorg. Chem.*, **57**, 13409 (2018)
563. C.Li, J.Sun, M.Yang, G.Sun, J.Guo, Y.Ma, L.Li. *Cryst. Growth Des.*, **16**, 7155 (2016)
564. R.A.A.Cassaro, S.G.Reis, T.S.Araujo, P.M.Lahti, M.A.Novak, M.G.F.Vaz. *Inorg. Chem.*, **54**, 9381 (2015)
565. T.Kanetomo, S.Yoshii, H.Nojiri, T.Ishida. *Inorg. Chem. Front.*, **2**, 860 (2015)
566. T.Ishida. *IOP Conf. Ser.: Mater. Sci. Eng.*, **202**, 012001 (2017)
567. E.Yu.Fursova, O.V.Kuznetsova, E.V.Tretyakov, G.V.Romanenko, A.S.Bogomyakov, V.I.Ovcharenko, R.Z.Sagdeev, V.K.Cherkasov, M.P.Bubnov, G.A.Abakumov. *Russ. Chem. Bull.*, **60**, 809 (2011)
568. M.P.Bubnov, I.A.Teplova, E.A.Kopylova, K.A.Kozhanov, A.S.Bogomyakov, M.V.Petrova, V.A.Morozov, V.I.Ovcharenko, V.K.Cherkasov. *Inorg. Chem.*, **56**, 2426 (2017)
569. M.Bubnov, A.Cherkasova, I.Teplova, E.Kopylova, G.Fukin, M.Samsonov, A.Bogomyakov, S.Fokin, G.Romanenko, V.Cherkasov, V.Ovcharenko. *Polyhedron*, **119**, 317 (2016)
570. M.Bubnov, I.Teplova, K.Kozhanov, R.Rumyantcev, G.Fukin, A.Bogomyakov, V.Cherkasov. *Inorg. Chim. Acta*, **486**, 113 (2019)
571. M.L.Kirk, D.A.Shultz, E.C.Depperman, D.Habel-Rodriguez, R.D.Schmidt. *J. Am. Chem. Soc.*, **134**, 7812 (2012)
572. M.L.Kirk, D.A.Shultz. *Coord. Chem. Rev.*, **257**, 218 (2013)
573. M.L.Kirk, D.A.Shultz, D.E.Stasiw, D.Habel-Rodriguez, B.Stein, P.D.Boyle. *J. Am. Chem. Soc.*, **135**, 14713 (2013)
574. M.L.Kirk, D.A.Shultz, D.E.Stasiw, G.F.Lewis, G.Wang, C.L.Brannen, R.D.Sommer, P.D.Boyle. *J. Am. Chem. Soc.*, **135**, 17144 (2013)
575. B.W.Stein, C.R.Tichnell, J.Chen, D.A.Shultz, M.L.Kirk. *J. Am. Chem. Soc.*, **140**, 2221 (2018)
576. D.A.Shultz, M.L.Kirk, J.Zhang, D.E.Stasiw, G.Wang, J.Yang, D.Habel-Rodriguez, B.W.Stein, R.D.Sommer. *J. Am. Chem. Soc.*, **142**, 4916 (2020)
577. C.R.Tichnell, D.A.Shultz, C.V.Popescu, I.Sokirniy, P.D.Boyle. *Inorg. Chem.*, **54**, 4466 (2015)
578. V.I.Ovcharenko, S.V.Fokin, E.Yu.Fursova, O.V.Kuznetsova, E.V.Tretyakov, G.V.Romanenko, A.S.Bogomyakov. *Inorg. Chem.*, **50**, 4307 (2011)
579. V.I.Ovcharenko, E.V.Tretyakov, S.V.Fokin, E.Yu.Fursova, O.V.Kuznetsova, S.E.Tolstikov, G.V.Romanenko, A.S.Bogomyakov, R.Z.Sagdeev. *Russ. Chem. Bull.*, **60**, 2457 (2011)
580. E.V.Tretyakov, S.V.Fokin, E.Yu.Fursova, O.V.Kuznetsova, G.V.Romanenko, R.Z.Sagdeev, V.I.Ovcharenko. *Russ. Chem. Bull.*, **62**, 1803 (2013)
581. R.Z.Sagdeev, S.E.Tolstikov, S.V.Fokin, I.V.Obsharova, S.V.Tumanov, S.L.Veber, G.V.Romanenko, A.S.Bogomyakov, M.V.Fedin, E.V.Tretyakov, M.Halcrow, V.I.Ovcharenko. *Russ. Chem. Bull.*, **66**, 222 (2017)
582. I.M.Bystryak, G.I.Likhtenshtein, A.I.Kotelnikov, O.H.Hankovsky, K.Hideg. *Russ. J. Phys. Chem.*, **60**, 1679 (1986)
583. M.Eing, B.T.Tuten, J.P.Blinco, C.Barner-Kowollik. *Chem. – Eur. J.*, **24**, 12246 (2018)
584. V.C.Lussini, J.P.Blinco, K.E.Fairfull-Smith, S.E.Bottle. *Chem. – Eur. J.*, **21**, 18258 (2015)
585. A.G.Coman, C.C.Paraschivescu, A.Paun, A.Diac, N.D.Hădade, L.Jouffret, A.Gautier, M.Matache, P.Ionita. *New J. Chem.*, **41**, 7472 (2017)
586. K.-A.Hansen, K.E.Fairfull-Smith, S.E.Bottle, J.P.Blinco. *Macromol. Chem. Phys.*, **217**, 2330 (2016)
587. V.C.Lussini, J.M.Colwell, K.E.Fairfull-Smith, S.E.Bottle. *Sens. Actuators, B*, **241**, 199 (2017)
588. B.A.Chalmers, S.Saha, T.Nguyen, J.McMurtrie, S.T.Sigurdsson, S.E.Bottle, K.S.Masters. *Org. Lett.*, **16**, 5528 (2014)
589. M.Barzegar Amiri Olia, A.Zavras, C.H.Schiesser, S.A.Alexander. *Org. Biomol. Chem.*, **14**, 2272 (2016)
590. S.Sato, S.Endo, Y.Kurokawa, M.Yamaguchi, A.Nagai, T.Ito, T.Ogata. *Spectrochim. Acta, Part A*, **169**, 66 (2016)

591. N.Medvedeva, V.V.Martin, A.L.Weis, G.I.Likhtenshten. *J. Photochem. Photobiol.*, **163**, 45 (2004)
592. H.Nam, J.E.Kwon, M.W.Choi, J.Seo, S.Shin, S.Kim, S.Y.Park. *ACS Sens.*, **1**, 392 (2016)
593. J.P.Allen, M.C.Pfrunder, J.C.McMurtrie, S.E.Bottle, J.P.Blinco, K.E.Fairfull-Smith. *Eur. J. Org. Chem.*, 476 (2017)
594. J.Nie, D.Yang, X.Tang, L.Zhang, Z.Ni, X.Gui. *Dyes Pigm.*, **170**, 107644 (2019)
595. P.Lederhose, N.L.Haworth, K.Thomas, S.E.Bottle, M.L.Coote, C.Barner-Kowollik, J.P.Blinco. *J. Org. Chem.*, **80**, 8009 (2015)
596. Y.Teki, T.Toichi, S.Nakajima. *Chem. – Eur. J.*, **12**, 2329 (2006)
597. S.Nakatsuji, M.Fujino, S.Hasegawa, H.Akutsu, J.I.Yamada, V.S.Gurman, A.K.Vorobiev. *J. Org. Chem.*, **72**, 2021 (2007)
598. C.Mi, M.Saniepay, R.Beaulac. *Chem. Mater.*, **30**, 5714 (2018)
599. G.I.Likhtenstein, K.Ishii, S.Nakatsuji. *Photochem. Photobiol.*, **83**, 871 (2007)
600. P.Poizot, F.Dolhem, J.Gaubicher. *Curr. Opin. Electrochem.*, **9**, 70 (2018)
601. J.Winsberg, T.Hagemann, T.Janoschka, M.D.Hager, U.S.Schubert. *Angew. Chem., Int. Ed.*, **56**, 686 (2017)
602. F.Zhong, M.Yang, M.Ding, C.Jia. *Front. Chem.*, **8**, 451 (2020)
603. J.Xie, Q.Zhang. *Mater. Today Energy*, **18**, 100547 (2020)
604. N.Dardenne, X.Blase, G.Hautier, J.-C.Charlier, G.-M.Rignanese. *J. Phys. Chem. C*, **119**, 23373 (2015)
605. R.A.Potash, J.R.McKone, S.Conte, H.D.Abruña. *J. Electrochem. Soc.*, **163**, A338 (2016)
606. V.V.Sentyurin, O.A.Levitskiy, T.V.Magdesieva. *Curr. Opin. Electrochem.*, **24**, 15 (2020)
607. V.V.Sentyurin, O.A.Levitskiy, T.V.Magdesieva. *Curr. Opin. Electrochem.*, **24**, 6 (2020)
608. H.Nishide, S.Iwasa, Y.J.Pu, T.Suga, K.Nakahara, M.Satoh. *Electrochim. Acta*, **50**, 827 (2004)
609. H.Itoi, H.Hasegawa, H.Iwata, Y.Ohzawa. *Sustain. Energy Fuels*, **2**, 558 (2018)
610. L.Xu, L.Ji, G.Wang, C.Zhang, C.Su. *Ionics (Kiel)*, **22**, 1377 (2016)
611. P.O.Schwartz, M.Pejic, M.Wachtler, P.Bäuerle. *Synth. Met.*, **243**, 51 (2018)
612. X.Wei, W.Xu, M.Vijayakumar, L.Cosimbescu, T.Liu, V.Sprenkle, W.Wang. *Adv. Mater.*, **26**, 7649 (2014)
613. J.Winsberg, T.Janoschka, S.Morgenstern, T.Hagemann, S.Muench, G.Hauffman, J.-F.Gohy, M.D.Hager, U.S.Schubert. *Adv. Mater.*, **28**, 2238 (2016)
614. Z.Li, S.Li, S.Liu, K.Huang, D.Fang, F.Wang, S.Peng. *Electrochem. Solid-State Lett.*, **14**, A171 (2011)
615. S.Perticarari, E.Grange, T.Doizy, Y.Pellegrin, E.Quarez, K.Oyaizu, A.J.Fernandez-Ropero, D.Guyomard, P.Poizot, F.Odobel, J.Gaubicher. *Chem. Mater.*, **31**, 1869 (2019)
616. Z.Tie, Z.Niu. *Angew. Chem., Int. Ed.*, **59**, 21293 (2020)
617. L.Marx, B.Schoellhorn. *New J. Chem.*, **30**, 430 (2006)
618. T.Jähnert, T.Janoschka, M.D.Hager, U.S.Schubert. *Eur. Polym. J.*, **61**, 105 (2014)
619. T.Suga, Y.J.Pu, S.Kasatori, H.Nishide. *Macromolecules*, **40**, 3167 (2007)
620. S.Yeşilot, F.Hacivelioğlu, S.Küçükköylü, E.Demir, K.B.Çelik, R.Demir-Cakan. *Polym. Adv. Technol.*, **30**, 2977 (2019)
621. C.Friebe, U.S.Schubert. *Top. Curr. Chem.*, **375**, 1 (2017)
622. Y.Luo, F.Zheng, L.Liu, K.Lei, X.Hou, G.Xu, H.Meng, J.Shi, F.Li. *ChemSusChem*, **13**, 2239 (2020)
623. T.Suga, S.Sugita, H.Ohshiro, K.Oyaizu, H.Nishide. *Adv. Mater.*, **23**, 751 (2011)
624. D.Yamaguchi, H.Eimura, M.Yoshio, T.Kato. *Chem. Lett.*, **45**, 863 (2016)
625. K.Oyaizu, T.Sukegawa, H.Nishide. *Chem. Lett.*, **40**, 184 (2011)
626. T.Sukegawa, A.Kai, K.Oyaizu, H.Nishide. *Macromolecules*, **46**, 1361 (2013)
627. M.Anghel, F.Magnan, S.D.Catingan, M.A.McCready, E.Aawani, V.Wong, D.Singh, G.Fanchini, J.B.Gilroy. *J. Polym. Sci.*, **58**, 309 (2020)
628. W.Duan, R.S.Vemuri, J.D.Milshtein, S.Laramie, R.D.Dmello, J.Huang, L.Zhang, D.Hu, M.Vijayakumar, W.Wang, J.Liu, R.M.Darling, L.Thompson, K.Smith, J.S.Moore, F.R.Brushett, X.Wei. *J. Mater. Chem. A*, **4**, 5448 (2016)
629. T.Hagemann, J.Winsberg, B.Häupler, T.Janoschka, J.J.Gruber, A.Wild, U.S.Schubert. *NPG Asia Mater.*, **9**, 340 (2017)
630. A.Tkacheva, B.Sun, J.Zhang, G.Wang, A.M.McDonagh. *J. Phys. Chem. C*, **125**, 2824 (2021)
631. J.Winsberg, C.Stolze, S.Muench, F.Liedl, M.D.Hager, U.S.Schubert. *ACS Energy Lett.*, **1**, 976 (2016)
632. T.Janoschka, C.Friebe, M.D.Hager, N.Martin, U.S.Schubert. *Chemistry Open*, **6**, 216 (2017)
633. I.Fidan, E.Önal, Y.Yerli, D.Luneau, V.Ahsen, C.Hirel. *ChemPlusChem*, **82**, 1384 (2017)
634. Y.Ren, X.Yang, L.Zhou, J.Mao, S.Han, Y.Zhou. *Adv. Funct. Mater.*, **29**, 1902105 (2019)
635. O.A.Levitskiy, V.V.Sentyurin, A.V.Bogdanov, T.V.Magdesieva. *Mendeleev Commun.*, **26**, 535 (2016)
636. O.A.Levitskiy, V.V.Sentyurin, T.V.Magdesieva. *Electrochim. Acta*, **260**, 459 (2018)
637. S.Z.Vatsadze, Yu.D.Loginova, G.dos Passos Gomes, I.V.Alabugin. *Chem. – Eur. J.*, **23**, 3225 (2017)
638. A.Bogdanov, O.Levitskiy, A.Vorobiev, T.Magdesieva. *Tetrahedron Lett.*, **59**, 3124 (2018)
639. O.R.Luca, R,H.Crabtree. *Chem. Soc. Rev.*, **42**, 1440 (2013)
640. Y.Wang, M.Frasconi, J.F.Stoddart. *ACS Cent. Sci.*, **3**, 927 (2017)
641. K.Ayabe, K.Sato, S.Nakazawa, S.Nishida, K.Sugisaki, T.Ise, Y.Morita, K.Toyota, D.Shiomi, M.Kitagawa, S.Suzuki, K.Okada, T.Takui. *Mol. Phys.*, **111**, 2767 (2013)